



# **Molecular *in vitro* analysis of the human ABC transporter MDR3**

Inaugural-Dissertation

zur Erlangung des Doktorgrades  
der Mathematisch-Naturwissenschaftlichen Fakultät  
der Heinrich-Heine-Universität Düsseldorf

vorgelegt von

**Marianne Kluth**

aus

Neuss

Düsseldorf, Oktober 2014





# **Molecular *in vitro* analysis of the human ABC transporter MDR3**

Inaugural-Dissertation

zur Erlangung des Doktorgrades  
der Mathematisch-Naturwissenschaftlichen Fakultät  
der Heinrich-Heine-Universität Düsseldorf

vorgelegt von

**Marianne Kluth**

aus

Neuss

Düsseldorf, Oktober 2014





aus dem Institut für Biochemie  
der Heinrich-Heine-Universität Düsseldorf

Gedruckt mit der Genehmigung der  
Mathematisch-Naturwissenschaftlichen Fakultät der  
Heinrich-Heine-Universität Düsseldorf

Referent: Prof. Dr. rer. nat. Lutz Schmitt  
Korreferent: PD Dr. med. Verena Keitel-Anselmino

Tag der mündlichen Prüfung: 29. Januar 2015



## Abstract

The ATP-dependent secretion of phosphatidylcholine into the liver bile canaliculi is an important process of bile formation and is mediated by the multidrug resistance protein 3 (MDR3), also called ATP-binding cassette subfamily B member 4 (ABCB4). Dysfunction of MDR3 causes liver diseases from the range of gallstones to serious cholestasis. Interestingly, MDR3 shares 86% homology with the multidrug resistance (MDR) mediating ABC transporter MDR1 (ABCB1) in the amino acid sequences. However, due to the difficulty to express and purify human ABC transporters in sufficient quantities for biochemical analysis the molecular mechanism of MDR3 is still poorly understood.

In this thesis the expression in *Pichia pastoris* and the purification of MDR3 was established. For this purpose, over 100 different detergents were analysed with respect to the efficacy to solubilize MDR3 from membrane vesicles. The monodispersity of detergent-soluble GFP-fusion protein of MDR3 was investigated using fluorescence-detected size exclusion chromatography. The best result was obtained with the zwitterionic detergent Fos-choline-16, which was subsequently used to purify wild type MDR3 and mutants investigated in this study. The ATPase activity of wild type MDR3 in detergent solution was analyzed in terms of kinetic parameters, substrate spectrum and effects of phosphate analogs. The presence of phosphatidylcholine induced a two-fold stimulation, while phosphatidylethanolamine (PE), phosphatidylserine (PS) and sphingomyelin (SM) lipids did not stimulate the ATPase activity of MDR3. Furthermore, the crosslinking of MDR3 with a thiol-reactive fluorophore abolished PC-induced and basal ATPase activity. The substrate-induced ATPase activity of MDR3 provides the foundation to investigate the clinically relevant Q1174E mutation at the functional level. The substitution of glutamine to glutamate within the extended X-loop of the nucleotide-binding domain 2 (NBD2) abolished substrate-induced ATPase activity, but not basal activity. In addition, the analysis of the homology model of MDR3 suggested that the glutamine participated in the transduction of the conformational change as a result of binding and hydrolysis of ATP at the nucleotide-binding site (NBS) to the transmembrane domain (TMD) and consequently plays an essential role in the communication between NBD and TMD.

In a previous study, it was demonstrated that MDR3 transports cytotoxic drugs with low-level rate. However, up to date MDR3 shows no phenotype with respect to MDR. In this thesis, the drug-modulated ATPase activity was analyzed. None of the tested drugs stimulated the basal ATPase activity of MDR3. Contrary, ATP hydrolysis was inhibited by cyclosporin A, verapamil, paclitaxel, zosuquidar and itraconazole indicating that drug binding blocks MDR3.

Furthermore, the regulation of the cell surface expression of MDR3 was investigated. For MDR3 function, the localization of the transporter at the canalicular membrane is indispensable. Radixin was identified as new adaptor protein mediating the interaction of MDR3 with the cytoskeleton.

In summary, this thesis highlights new insights into the mode of action of the human ABC transporter MDR3.



## Zusammenfassung

Die ATP-abhängige Sekretion von Phosphatidylcholin in die Gallenkanälchen der Leber ist ein wichtiger Prozess bei der Gallenbildung und wird durch das *multidrug resistance protein 3* (MDR3), das auch als *ATP-binding cassette subfamily B member 4* (ABCB4) bezeichnet wird, vermittelt. Die Fehlfunktion von MDR3 führt von der Gallensteinbildung bis hin zu schwerwiegenden Lebererkrankungen. Interessanterweise weist MDR3 eine 86%ige Sequenzhomologie mit dem Multi-Drogenresistenz-vermittelnden ABC-Transporter MDR1 (ABCB1) auf. Jedoch ist die molekulare Funktionsweise von MDR3, aufgrund der Schwierigkeit humane ABC Transporter in ausreichenden Mengen für biochemische Analysen zu exprimieren und zu reinigen, bis heute noch weitgehend unverstanden.

Im Rahmen dieser Arbeit wurde die Expression in *Pichia Pastoris* und die Reinigung von MDR3 etabliert. Zu diesem Zweck wurden über 100 verschiedene Detergenzien in Bezug auf ihre Fähigkeit MDR3 aus der Membran zu extrahieren analysiert und die Monodispersität des im Detergenz gelösten MDR3-GFP-Fusionsproteins mittels Fluoreszenz-basierter Größenausschlusschromatographie untersucht. Das beste Resultat wurde mit dem zwitterionischen Detergenz Fos-Cholin-16 erhalten, das für die weitere Reinigung von wildtypischem MDR3 und die, in dieser Arbeit untersuchten Mutanten, verwendet wurde. Die ATPase Aktivität von wildtypischem MDR3 wurde bezüglich kinetischer Parametern, Substratspektrum und die Inhibition durch Phosphatanaloga untersucht. Die Anwesenheit von Phosphatidylcholin (PC) führte zu einer zweifachen Stimulation, während die Lipide Phosphatidylethanolamin (PE), Phosphatidylserin (PS) und Sphingomyelin (SM) die ATPase Aktivität von MDR3 nicht stimulierten. Des Weiteren hemmte die Quervernetzung von MDR3 mit einem thiol-reaktiven Fluorophor die PC-stimulierte und basale ATPase Aktivität von MDR3. Auf Basis der substratstimulierten ATPase Aktivität von MDR3 war es nun möglich, die klinisch relevante Mutation Q1174E auf funktioneller Ebene zu untersuchen. Die Substitution des Glutamins zu Glutamat im erweiterten X-Loop Motiv führte zur Aufhebung der substratstimulierten ATPase Aktivität, während die basale ATPase Aktivität erhalten blieb. Darüber hinaus zeigte die Analyse des Strukturmodells von MDR3, dass das Glutamin an der Weiterleitung der durch die Bindung und Hydrolyse von ATP an der Nukleotid-Bindestelle (NBS) resultierenden Konformationsänderung zur Transmembrandomäne (TMD) beteiligt ist und somit eine wichtige Rolle in der Kommunikation zwischen der Nukleotid-bindende Domäne (NBD) und der TMD spielt.

In einer vorangegangenen Studie wurde gezeigt, dass MDR3 eine Anzahl von zytotoxisch Pharmazeutika mit niedriger Rate transportiert, aber bis heute wurde ein Beitrag von MDR3 an der Multi-Drogenresistenz von Krebszellen nicht nachgewiesen. In dieser Arbeit wurde die ATPase Aktivität von MDR3 bezüglich der Modulation durch Pharmazeutika untersucht. Keines der ausgewählten Pharmazeutika stimulierte die ATPase Aktivität von MDR3. Im Gegenteil, die ATP

Hydrolyse wurde durch Cyclosporin A, Verapamil, Paclitaxel, Zosuquidar und Itraconazol inhibiert. Dieses Ergebnis deutet darauf hin, dass das Pharmakon die Funktion von MDR3 blockiert.

Im Weiterem befasste sich diese Arbeit mit der Regulation der Zelloberflächenexpression von MDR3. Für die Funktion von MDR3 ist die Lokalisation des Transporters an der kanalikulären Membran unabdingbar. Radixin wurde als neuer Interaktionspartner identifiziert, der die Interaktion von MDR3 mit dem Zytoskelett vermittelt.

Zusammenfassend lieferte diese Arbeit neue Einblicke in die Wirkungsweise des menschlichen ABC-Transporter MDR3.

## Table of contents

<b>ABSTRACT .....</b>	<b>I</b>
<b>ZUSAMMENFASSUNG.....</b>	<b>III</b>
<b>TABLE OF CONTENTS .....</b>	<b>V</b>
<b>LIST OF FIGURES.....</b>	<b>VII</b>
<b>ABBREVIATIONS.....</b>	<b>IX</b>
<b>1 INTRODUCTION .....</b>	<b>1</b>
1.1 BIOLOGICAL MEMBRANES .....	1
1.2 LIPID TRANSBILAYER MOVEMENT.....	2
1.2.1 <i>Energy-independent lipid translocases</i> .....	2
1.2.2 <i>Energy-dependent lipid translocases</i> .....	4
1.3 GENERAL FEATURES OF THE ABC PROTEIN SUPERFAMILY .....	5
1.3.1 <i>The core architecture of ABC transporters</i> .....	5
1.3.2 <i>The nucleotide-binding domains – the motor domains</i> .....	7
1.3.3 <i>The transmembrane domains</i> .....	9
1.3.4 <i>The transmission interface</i> .....	10
1.4 ABC TRANSPORTERS MEDIATED LIPID TRANSPORT – THE HUMAN ABCB FAMILY .....	12
1.4.1 <i>The multidrug resistance protein 1</i> .....	13
1.4.2 <i>The multidrug resistance protein 3</i> .....	15
1.4.2.1 MDR3 and its role in bile formation.....	16
1.4.2.2 Regulation of MDR3 function .....	17
1.5 MECHANISMS OF LIPID TRANSBILAYER TRANSPORT BY ABC TRANSPORTERS .....	18
<b>2 AIMS AND OBJECTIVES.....</b>	<b>21</b>
<b>3 RESULTS.....</b>	<b>23</b>
CHAPTER I – STRUCTURE AND FUNCTION OF HEPATIC ABC TRANSPORTERS .....	23
CHAPTER II – OPTIMIZATION OF THE EXPRESSION AND PURIFICATION OF MDR3 .....	49
CHAPTER III – DETERGENT SCREENING AND PURIFICATION OF BSEP AND MDR3 .....	65
CHAPTER IV – <i>IN VITRO</i> ATPASE ACTIVITY OF WILD TYPE MDR3 AND MUTANTS .....	91
CHAPTER V – DRUG-MODULATED ATPASE ACTIVITY OF MDR3.....	117
CHAPTER VI – INTERACTIONS OF MDR3 WITH SCAFFOLD PROTEINS.....	137

<b>4</b>	<b>GENERAL DISCUSSION .....</b>	<b>155</b>
4.1	HETEROLOGOUS EXPRESSION AND PURIFICATION OF HUMAN MDR3 .....	156
4.2	FUNCTIONAL ANALYSIS OF MDR3 .....	160
4.3	THE X-LOOP OF MDR3 – COUPLING THE ENGINE TO THE GATE.....	162
4.4	MDR3 – A MULTIDRUG PUMP? .....	165
4.5	INTRACELLULAR TRAFFIC AND ITS ROLE IN MDR3 FUNCTION .....	166
<b>5</b>	<b>LITERATURE .....</b>	<b>169</b>
<b>6</b>	<b>ACKNOWLEDGMENT / DANKSAGUNG .....</b>	<b>187</b>
<b>7</b>	<b>CURRICULUM VITAE.....</b>	<b>189</b>
<b>8</b>	<b>ERKLÄRUNG ZUR DISSERTATION .....</b>	<b>191</b>



## List of Figures

FIGURE 1 TRANSBILAYER LIPID MOVEMENT IN BIOLOGICAL MEMBRANES. ....	2
FIGURE 2 PROTEIN-MEDIATED TRANSBILAYER MOVEMENT .....	3
FIGURE 3 CRYSTAL STRUCTURES OF FOUR DIFFERENT CLASSES OF ABC TRANSPORTERS. ....	6
FIGURE 4 NBD OF THE ABC TRANSPORTER HAEMOLYSIN B. ....	7
FIGURE 5 DIMER OF THE NBD. ....	8
FIGURE 6 CRYSTAL STRUCTURE OF SAV1866 FROM <i>S. AUREUS</i> . ....	10
FIGURE 7 TRANSMISSION INTERFACE BETWEEN NBDs AND TMDs. ....	11
FIGURE 8 CRYSTAL STRUCTURES OF P-GLYCOPROTEIN. ....	14
FIGURE 9 LOCALIZATION OF TRANSPORTERS IN THE HEPATOCYTES. ....	16
FIGURE 10 BILE FORMATION AT THE CANALICULAR MEMBRANE OF HEPATOCYTES. ....	17
FIGURE 11 SCHEME OF THE ATP SWITCH MODEL FOR ABC TRANSPORTER. ....	19
FIGURE 12 MODELS FOR ABC TRANSPORTER MEDIATED LIPID TRANSPORT. ....	20
FIGURE 13 TRANSMISSION INTERFACE OF MDR3 .....	163
FIGURE 14 MODEL OF HUMAN MDR3. ....	163
FIGURE 15 ADAPTER PROTEINS OF MDR3 MEDIATING THE INTERACTION OF MDR3 WITH THE CYTOSKELETON. ....	167



## Abbreviations

aa	Amino acid
ABC	ATP binding cassette
ABCB	ATP binding cassette subfamily B
ADP	Adenosine-5'-diphosphate
ATP	Adenosine-5'-triphosphate
bp	Base pair
BRIC	Benign recurrent intrahepatic cholestasis
BSEP	Bile salt export pump
CBP	Calmodulin binding peptide
cDNA	Complementary DNA
<i>C. elegans</i>	<i>Caenorhabditis elegans</i>
Cer	Ceramide
CFTR	Cystic fibrosis transmembrane regulator
cmc	Critical micellar concentration
<i>C. merolae</i>	<i>Cyanidioschyzom merolae</i>
cpm	Counts per minute
Da	Dalton
$\beta$ -DDM	n-Dodecyl $\beta$ -D-maltoside
$\beta$ -DM	n-Decyl $\beta$ -D-maltoside
DNA	Deoxyribonucleic acid
dsDNA	Double-stranded DNA
DTT	Desthiothreitol
ECF	Energy-coupling factor
<i>E. coli</i>	<i>Escherichia coli</i>
e.g.	exempli gratia
ER	Endoplasmatic reticulum
FC-16	Fos-choline-16
FIC-1	Familial intrahepatic cholestasis-1
FRAP	Fluoresence recovery after photobleaching
FSEC	Fluorescence-detection size exclusion chromatography
FXR	Farnesoid-X receptor
GlcCer	Glucosylceramide
HEK293	Human embryonic kidney 293 cells
His <sub>6</sub> -tag	Hexahistidinistidine-tag

## Abbreviations

---

HR	Homologous recombination
ICL	Intracellular loop
ICP	Intrahepatic cholestasis during pregnancy
IMAC	Immobilized metal ion affinity chromatography
$K_M$	Michaelis-Menten constant
<i>L. lactis</i>	<i>Lactococcus lactis</i>
LLC-PK1	Pig kidney epithelial cells
LPAC	Low phospholipid associated cholestasis
MDR	Multidrug resistance
MDR1/3	Chimera protein of MDR1 TMDs and MDR3 NBDs
MRP	Multidrug resistance related protein
NBD	Nucleotide-binding domain
$Ni^{2+}$ -IDA	Nickel(2+)- iminodiacetic acid
nt	Nucleotide
NTCP	sodium-taurocholate cotransporting polypeptide
$P_i$	Inorganic phosphate
PC	Phosphatidylcholine
PCR	Polymerase chain reaction
PE	Phosphatidylethanolamine
PFIC	Proressive familial intrahepatic cholestasis
P-glycoprotein	Permeability glycoprotein 1
PI	Phosphatidylinositol
PL	Phospholipid
P-loop	Phosphate-binding loop
PM	Plasma membrane
<i>P. pastoris</i>	<i>Pichia pastoris</i>
PS	Phosphatidylserine
RNA	Ribonucleic acid
SBP	Substrate-binding protein
<i>S. cerevisiae</i>	<i>Saccharomyces cerevisiae</i>
SDR	Structural diverse region
SERCA	Sarcoendoplasmic reticulum $Ca^{2+}$ -ATPase
<i>Sf9</i>	<i>Spodoptera frugiperda</i> 9
SM	Spinghomyelin
SNP	Single nucleotide polymorphism
TAP1/2	Transporter associated with antigen processing
TC	Taurocholic acid

---

TCDC	Taurochenodeoxycholic acid
TMD	Transmembrane domain
TMH	Transmembrane helix
UDCA	Ursodeoxycholate
wcw	Wet cell weight

Amino acid	Three/One letter code	Amino acid	Three/One letter code
alanine	Ala / A	leucine	Leu / L
arginine	Arg / R	lysine	Lys / K
asparagine	Asn / N	methionine	Met / M
aspartic acid	Asp / D	phenylalanine	Phe / F
cysteine	Cys / C	proline	Pro / P
glutamic acid	Glu / E	serine	Ser / S
glutamine	Gln / Q	threonine	Thr / T
glycine	Gly / G	tryptophan	Trp / W
histidine	His / H	tyrosine	Tyr / Y
isoleucine	Ile / I	valine	Val / V



# 1 Introduction

## 1.1 Biological membranes

Biological membranes of prokaryotes and eukaryotes are lipid bilayers, which define the boundary between the intracellular space and the environment surrounding a cell or a cell compartment (1). Because of the amphipathic nature of the lipid bilayer, this boundary prevents the diffusion of ions, polar molecules, and macromolecules and is responsible for obtaining the electrochemical gradient, which is fundamental for a number of cellular processes such as ATP synthesis. However, the movement of molecules across the membrane allowing cells to import nutrients or export toxic compounds and the transduction of signals are indispensable for cell survival. Thus, membrane proteins are essential to mediate the selective permeability of the membrane. The functional characteristics of membranes strongly depend on their protein content, which consists of integral and peripherally associated membrane proteins and can be up to 80% of the biological membrane (2).

In 1972, Singer and Nicolson postulated the fluid mosaic model and proposed that biological membranes are not rigid and static structures and that membrane proteins and lipids distribute randomly by lateral diffusion (1). This would result in a uniform composition for all membranes. However, various organelles display different protein and lipid compositions (3). Membranes of the late secretory pathway and the endocytic pathway are enriched in sphingolipids and cholesterol (4) and the endoplasmatic reticulum (ER) is highly enriched in unsaturated phospholipids (5). Many eukaryotic membranes are polarized and exhibit lateral inhomogenities, e.g. the basolateral and apical plasma membrane of polarized epithelial cells. Furthermore, the lipid bilayer is asymmetrically distributed in the eukaryotic plasma membrane (6). The plasma membrane of mammalian erythrocytes was extensively investigated. Phosphatidylcholine (PC) and sphingomyelin (SM) are mainly located in the outer leaflet, while the phospholipids phosphatidylserine (PS), phosphatidylethanolamine (PE) and phosphatidylinositol (PI) in the inner leaflet (6-8). The lipid asymmetry is involved in numerous cellular processes, such as signal transduction, cell morphology, cell movement, regulation of membrane protein activity, and vesicle formation in the secretory and endocytotic pathways (9-13). Contrary, phospholipid randomization has been related to processes like blood coagulation, macrophage recognition and apoptosis (9,14,15). Hence, lipid bilayer asymmetry is crucial for the cell and raises the question about the biological mechanism by which membrane asymmetry is generated.

## 1.2 Lipid transbilayer movement

The symmetric and asymmetric distribution of biological membranes requires the flip-flop from one leaflet to the other leaflet of the lipid bilayer. Lipids and membrane proteins move spontaneously in lateral motion, a process called lateral diffusion (Figure 1) (1,16). The dynamic of lateral lipid movement has been demonstrated with several techniques, for instance fluorescence recovery after photobleaching (FRAP) using fluorescence microscopy to measure the diffusion of fluorescently labeled lipids from non-bleached areas into a bleached spot (17,18). Devaux and McConnell demonstrated that lipids diffuse very fast laterally with a diffusion rate of  $10^7$  lipids per second (19). In contrast, the transverse diffusion, so-called flip-flop, depends explicitly on the lipid structure and the environment (13). In general, the transverse diffusion is a slow process and shows half-times of seconds or minutes for uncharged lipids such as cholesterol to hours or days in case of lipids with polar headgroups (13,20-22). In addition, a high content of cholesterol in the plasma membrane drastically reduces the transverse diffusion of phospholipids. A number of lipid translocators have been identified to fulfill a role in phospholipid flip-flop, which can be classified into two categories: (i) the energy-independent and (ii) the energy-dependent lipid translocases (Figure 2) (23).

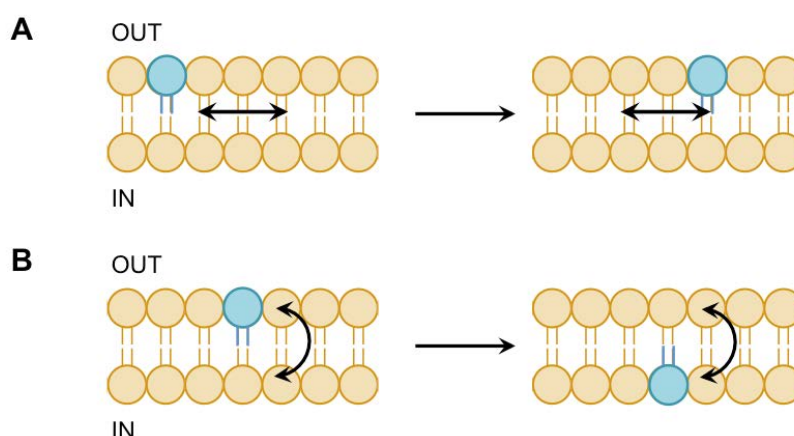


**Figure 1** Transbilayer lipid movement in biological membranes. (A) Lateral diffusion of lipids through the membrane leaflet. (B) Transversal diffusion (flip-flop) of lipids from the inner to the outer leaflet of the membrane.

### 1.2.1 Energy-independent lipid translocases

Two protein families, the biogenic membrane flippases and scramblases, facilitate the energy-independent bidirectional transport of lipids across the lipid bilayer.



Phospholipids are synthesized exclusively in the cytoplasmic leaflet of the ER revealing an asymmetrical membrane. To maintain the balance of lipid molecules in the ER, flippases are required (24). In order to understand how new symmetrically membranes are synthesized to facilitate cell growing and division, bionic membrane flippases were identified in the ER, Golgi and bacterial cytoplasmic membranes. They are characterized by a rapid and rather non-specific, energy-independent and bidirectional transport of newly synthesized phospholipids (13,25-32).

Similarly, energy-independent and bidirectional rapid transversal diffusion of all major phospholipids were observed for the scramblase protein family. Scramblases are conserved in eukaryotic organisms and are located in the plasma membrane. In response to signals for cell activation, apoptosis or blood coagulation, the concentration of intracellular calcium ions increases and activates the scramblase, which facilitates the transversal diffusion of phospholipids and destroys the phospholipid asymmetry of the plasma membrane (33-35). While energy-independent lipid translocases equilibrate rapidly lipids between the two bilayer leaflets, energy-dependent lipid translocases are responsible to form asymmetrical membranes.

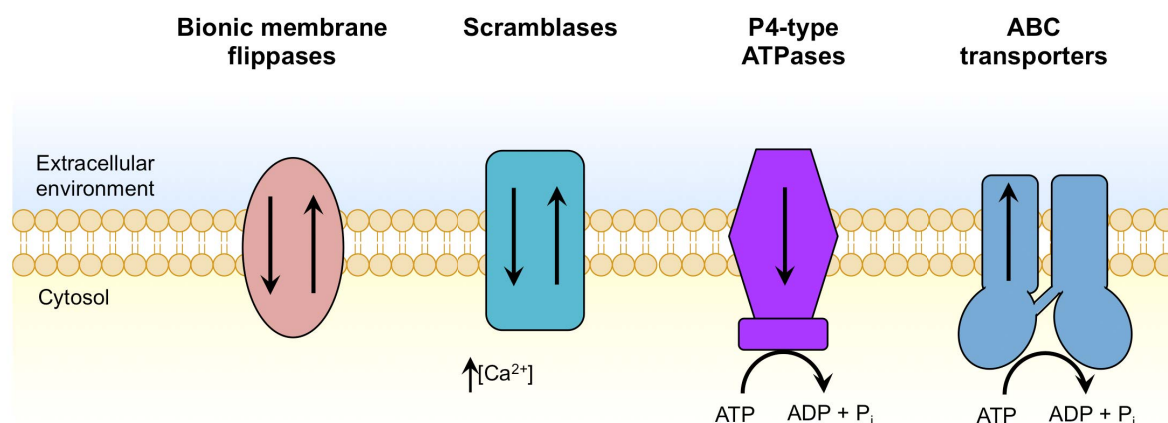


**Figure 2** Protein-mediated transbilayer movement. Bionic membrane flippases and scramblases flip lipids energy-independent and bidirectional across the membrane. Energy-dependent lipid transport is mediated by P4-type ATPases from the exoplasmic to the cytoplasmic leaflet and by ATP-binding cassette (ABC) transporter in opposite direction.

### 1.2.2 Energy-dependent lipid translocases

In the plasma membrane spontaneous flip-flop of phospholipids is limited, allowing the generation of a stable asymmetric lipid bilayer. To maintain the asymmetry of the plasma membrane, two classes of protein families, the P4-type ATPases family and the ATP binding-cassette (ABC) transporter family, actively transport phospholipids from one leaflet to the other leaflet of the lipid bilayer (Figure 2).

P-type ATPases are divided into five subfamilies (P1-P5) and share the common feature of forming a phosphorylated intermediate during their catalytical cycle (36,37). P1-P3 are cation transporters and found in prokaryotes, archaea and eukaryotes. The best structurally studied P-type ATPase are the sarcoendoplasmic reticulum  $\text{Ca}^{2+}$ -ATPase (SERCA, P2-ATPase), which transports calcium ions into the sarcoendoplasmic reticulum, and the plasma membrane  $\text{Na}^+/\text{K}^+$ -ATPase (P2-ATPase), which generates the membrane potential in cells.

P4-ATPases are only present in eukaryotes and are involved in lipid homeostasis in most cases of PC, PE and PS lipids (38). They are so-called flippases and transport specific lipids from the exoplasmic to the cytoplasmic leaflet of the membrane against a concentration gradient energized by ATP hydrolysis. Furthermore, P4-ATPases require an interaction with protein subunits of the cell division cycle (CDC50)/ligand effect modulator (LEM) family to be released from the ER and for targeting to the proper membrane (39-41). In mammals, 14 P4-ATPases were found based on amino acid sequence similarity. The most prominent and best studied member is ATP8B1, also called familial intrahepatic cholestasis 1 (FIC-1). ATP8B1 is, amongst others, located in the canalicular membrane of hepatocytes and translocates PS from the exoplasmic to the cytoplasmic leaflet of the canalicular membrane (39,42). Paulusma *et al.* demonstrated that ATP8B1-mediated PS translocation was increased by the co-expression of CDC50 (39). The lipid asymmetry build up by ATP8B1 activity protects the canalicular membrane. Thus, mutations of ATP8B1 results in hereditary liver diseases such as progressive familial intrahepatic cholestasis type 1 (PFIC-1) and benign recurrent intrahepatic cholestasis (BRIC-1) (43-45), which are described in more detail in section 1.4.2.

The second family of energy-dependent lipid translocators is the ATP-binding cassette (ABC) transporter family. The PC floppase multidrug resistance protein 3 (MDR3/ABCB4) is one member of this family and the next sections give an in-depth overview of ABC transporters and their mode of action.

### 1.3 General features of the ABC protein superfamily

ATP-binding cassette (ABC) proteins are divided into two classes of subfamilies. On the one hand ABC proteins are soluble ATPases, which utilize the free energy of ATP hydrolysis to drive cellular processes such as regulation of gene expression (46), chromatin organization (47), DNA repair (48-50) and mRNA trafficking through the nuclear pore (51). On the other hand the majority of ABC proteins are associated to a membrane subunit wherefore they are termed ABC transporters. ABC transporters are one of the largest families of membrane proteins and are found in all kingdoms of life. For example, almost 5% of the *Escherichia coli* genome codes for ABC transporters, corresponding to 52-83 ABC transporters (52,53), the genome of *Saccharomyces cerevisiae* contains 31 (54) and the human genome 48 ABC transporters (55). These transporters bind and hydrolyze ATP to power the translocation of a diverse range of substrates from inorganic ions to macromolecules across biological membranes, often against a concentration gradient (56). ABC transporters function either as importers, which transport nutrients and trace elements into the cell, or as exporters, which play crucial roles in export of bacterial toxins or signal molecules, conferring resistance against toxic drugs and homeostasis of the asymmetry of lipid bilayer. Importers are exclusively present in prokaryotes and archaea, whereas exporters are found also in eukaryotic organism. In humans, ABC transporters feature a clinically important role since they are involved in cholesterol and lipid transport, antigen presentation, mitochondrial iron homeostasis and the ATP-dependent regulation of ion channels (57-59). Mutations have been associated with a range of hereditary diseases, for instance cystic fibrosis, a number of eye diseases and liver cholestasis (60,61). In contrast, expression of ABC transporters in tumor cells is responsible in extruding cytotoxic drugs, leading to multidrug resistance (MDR) (62).

#### 1.3.1 The core architecture of ABC transporters

Despite the high diversity of substrates, ABC transporters have a characteristic modular architecture of at least four domains. The core ABC transporter is composed of two kinds of units, the cytoplasmatic nucleotide-binding domain (NBD) and a transmembrane domain (TMD) (56). In general, a fully assembled and functional ABC transporter consists of two NBDs and two TMDs, organized in four distinct polypeptides or fused in various combinations (52,63). Beyond these domains additional units can be fused to the TMDs or NBDs of the transporter and probably have regulatory functions (63). To date, 14 structures of ABC transporters have been solved by X-ray crystallography. Based on these structures four

different classes of ABC transporters have been discovered (Figure 3): type I importer, type II importer, energy-coupling factor (ECF) importer and exporter.

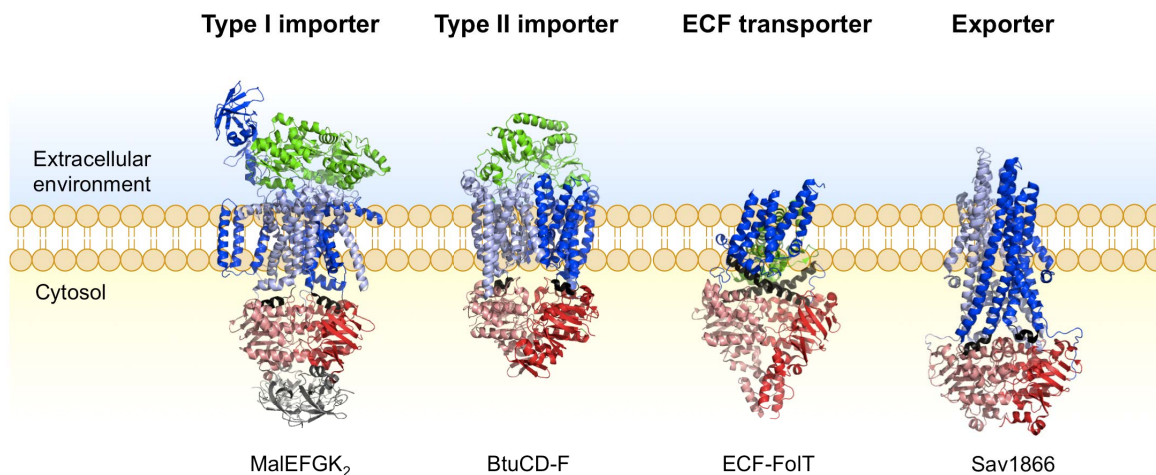


**Figure 3** Crystal structures of four different classes of ABC transporters. The type I importers are exemplified by the maltose transporter MalEFGK<sub>2</sub> from *Escherichia coli* (Protein Data Bank (PDB) accession number 2R6G) (64-66), type II importers exemplified by the vitamin B12 transporter BtuCD-F from *E. coli* (PDB accession number 4FI3) (67-69), energy-coupling factor (ECF) importer exemplified by the folate transporter ECF-FolT from *Lactobacillus brevis* (PDB accession number 4HUQ) (70) and ABC exporters exemplified by multidrug transporter Sav1866 from *Staphylococcus aureus* (PDB accession number 2HYD) (71,72). The nucleotide-binding domains (NBDs) are shown in red and light red, the transmembrane domains (TMDs) are represented in blue and light blue and the substrate-binding proteins (SBPs) of the ABC importers are colored in green. The coupling helices, which are involved in TMD:NBD communication, are highlighted in black. Figure adapted from (73).

Type I and II importers require an additional exoplasmatic substrate-binding protein (SBP), which binds the extracellular substrate and delivers it to the transport domain. SBPs are either soluble proteins in the periplasmic space of Gram-negative bacteria, or cell-surfaced associated in Gram-positive bacteria (74). The recently discovered ECF importers use one of the integral membrane subunits, the S-component (EcfS), instead of a classical SBP to provide substrate specification to the ECF importer (73,75). The two NBDs (EcfA and the EcfA') and the transmembrane domain EcfT form the energizing EcF module (76).

In ABC exporters, it is common that one NBD is fused to one TMD, which is called half-size transporter, or that all four domains are synthesized on a single polypeptide. This is called full-size transporter. The half-size transporters assemble as homo- or heterodimers to form a functional transporter (56).

### 1.3.2 The nucleotide-binding domains – the motor domains

The nucleotide-binding domains (NBDs) are the motors of ABC transporters. These domains bind and hydrolyze ATP to provide mechanical energy for the transport of the substrate. Biochemical and structural analysis of several isolated NBDs and ABC transporters revealed insights into ATP binding and hydrolysis. The first structure solved was the NBD monomer of the histidine permease HisP from *Salmonella typhimurium* in 1998 (77). The NBD has an L-shaped form, which is divided into a catalytical anti-parallel beta-roll subdomain and a more structurally diverse  $\alpha$ -helical subdomain (Figure 4) (78). The catalytical subdomain contains the highly conserved Walker A (P-loop; GXXGXXGKS/T, where X can be any amino acid residue) and Walker B motifs ( $\phi\phi\phi\phi$ D, where  $\phi$  can be any hydrophobic residue), which are characteristic for the large family of P-loop NTPases (79). The  $\alpha$ -helical subdomain harbors the hallmark of ABC transporters, the ABC signature motif or C-loop (LSGGQ) (78). These two subdomains are connected by the Q-loop and the Pro-loop. Further highly conserved motifs are the H-loop, the D-loop (SALD) and the A-loop.

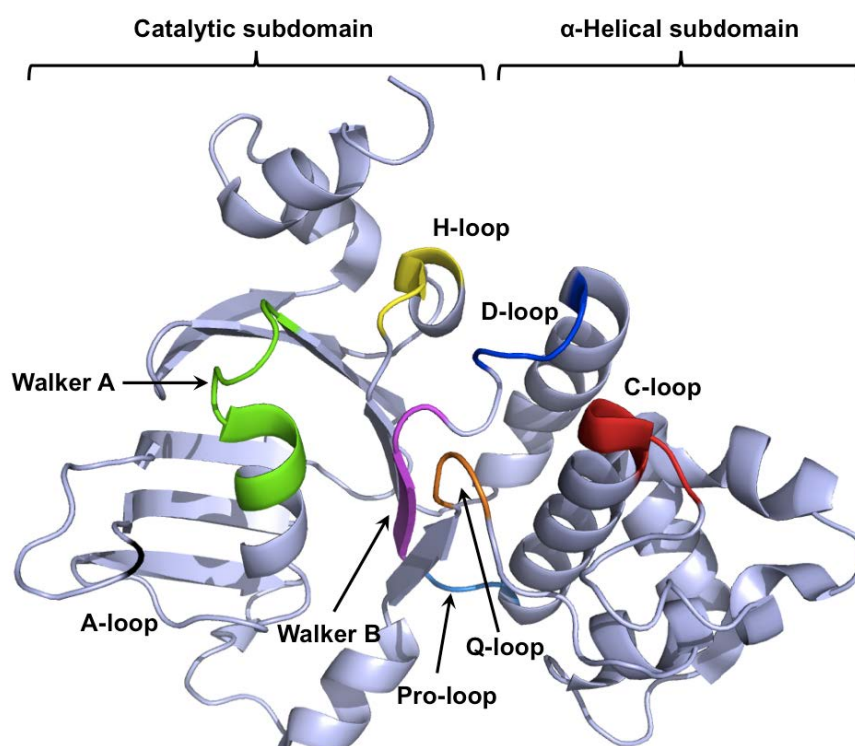


**Figure 4** NBD of the ABC transporter haemolysin B. Structure of the NBD monomer of the haemolysin B (HlyB) ABC transporter is shown in cartoon representation (PDB accession number 1XEF) (78,80). The Walker A motif is highlighted in green, the Walker B motif in magenta, the H-loop in yellow, the D-loop in blue, the Q-loop in orange, the pro-loop in marine and the A-loop in black. The hallmark of ABC transporters, the C-loop or ABC signature motif, is shown in red.

Structures in the presence of ATP or ATP analogs demonstrate that the NBDs dimerize in a head-to-tail arrangement, in which each monomer contributes to the binding pocket of ATP (Figure 5) (72,80-84). One ATP is bound from the Walker A and the Walker B motif of one monomer and the ABC signature motif of the opposing monomer and vice versa. In detail, the Walker A motif interacts with all three phosphate moieties of ATP, either directly or via a magnesium ion, whereas the A-loop coordinates the adenine ring via  $\pi$ - $\pi$ -stacking. The Walker B motif contacts the bound ATP via the magnesium ion and a water molecule. C-terminal to the Walker B aspartate is a glutamate, which activates the water molecule for nucleophilic attack on the  $\gamma$ -phosphate (64,85,86) stabilized by the H-loop (80). The ABC signature motif of the opposing NBD hydrogen bonds mainly with the  $\gamma$ -phosphate group and with the ribose moiety of the bound ATP. The D-loop contacts with the  $\gamma$ -phosphate indirectly via the water and the magnesium ion and hydrogen bonds with the Walker A motif and the H-loop of the opposing NBD. Thus, the D-loop is involved in interaction between the two monomers. The Q-loop connects the catalytical core subdomain to the  $\alpha$ -helical subdomain of the NBD and is located at a base of a groove on the surface of the NBD (82). Furthermore, the Q-loop is involved in NBD:TMD communication (see section 1.3.4).

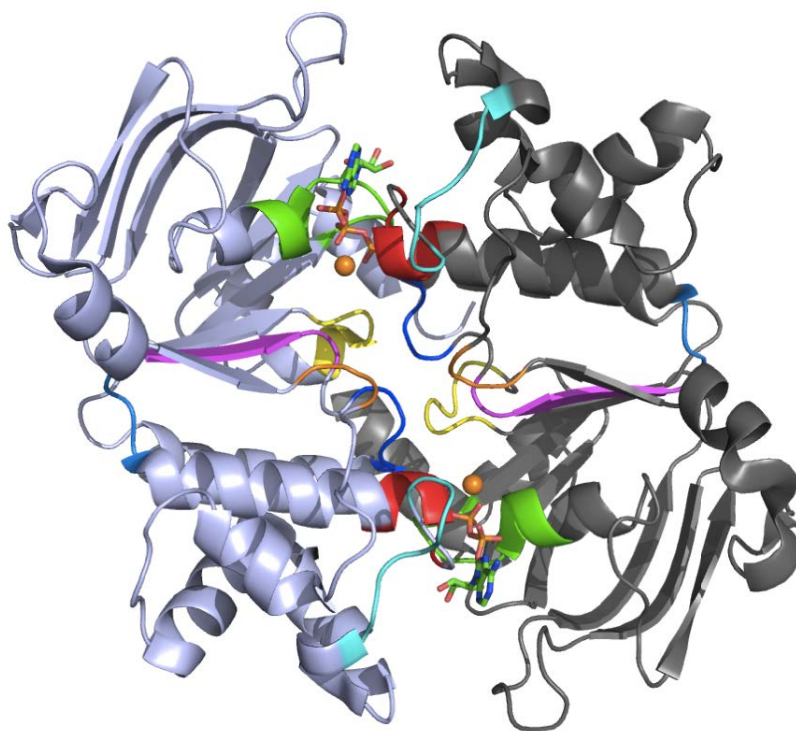


**Figure 5** Dimer of the NBD. The NBD of HlyB are arranged in a head-to tail orientation with two bound ATP coordinated by the Walker A and Walker B motifs of NBD1 (light blue) and the C-loop of NBD2 (grey) (PDB accession number 1XEF) (80). The structure of the dimer is colored as described in legend of figure 4. In addition, the structural diverse region (SDR) containing the X-loop is colored in cyan. ATP is shown in stick representation and the magnesium ion is colored in orange.

In summary, in the presence of ATP, ATP binds to its binding pocket and induces the dimerization of the NBDs. This leads to an inward rotation of the  $\alpha$ -helical subdomain. After hydrolysis of ATP,  $P_i$  and subsequently ADP are released and the dimer falls apart (81,82). Currently, two models are proposed to explain the mechanism of ATP binding and hydrolysis by the NBD sites, the processive clamp model (87,88) and the alternating catalytic site model (89,90). However, these models cannot clarify the phenomenon that in certain systems only one composite site contains the canonical sequences and enables ATP binding and hydrolysis (91-93). To date, only the ATP/substrate stoichiometry of the osmoregulated importer OpuA from *L. lactis* was demonstrated with the hydrolysis of two molecules of ATP per molecule of glycine betaine translocated (94). No conclusion can be drawn whether one or two ATP molecules are hydrolyzed per catalytical cycle by ABC exporters.

### 1.3.3 The transmembrane domains

The transmembrane domains (TMDs) form the translocation pathway and provide the substrate specificity of the ABC transporter (95). For example, the maltose importer from *E. coli* binds maltose only at one TMD (MalF) (65), whereas the structure of multidrug resistance protein 1 (MDR1, P-glycoprotein) possesses two different inhibitors within a cavity formed by both TMDs (96). In contrast to the NBD, the TMD is highly diverse and varies in primary sequence, length, architecture and the number of transmembrane helices (TMHs) (97). To date, four distinct folds are discovered, based on the structures of type I and type II importer, ECF importer and exporter (Figure 3). This section exclusively focuses on the exporter fold.

In 2006, the first medium-resolution structure of the multidrug resistance protein Sav1866 from *Staphylococcus aureus* was reported by Dawson *et al.* (Figure 6) (71,72). Subsequently, the structures of P-glycoprotein from *Mus musculus*, *Cyanidioschyzon merolae* and *Caenorhabditis elegans* (Figure 8), ABCB10 from *Homo sapiens* and Atm1 from *Saccharomyces cerevisiae* were published (96,98-101). These exporters share a common core architecture that consists of six transmembrane helices (TMHs) per TMD, or a total of 12 TMHs for a functional ABC transporter. Unexpectedly, the TMDs cross the membrane in two bundles of TMHs in a so-called domain swapped arrangement (Figure 6). This means that TMH1 and TMH2 from one TMD and TMHs 3-6 of the other TMD form one bundle. Because of this arrangement, TMHs 1-3 are related to TMHs 4-6 by an approximate two-fold rotation around a symmetry axis perpendicular to the membrane plane (71,72,102).



Furthermore, the TMHs are connected by long intracellular loops (ICLs), which extend the TMHs beyond the membrane approximately 25 Å into the cytoplasm (72). The ICLs 2 and 3 and ICLs 4 and 5 are connected each by a short helix, the so-called coupling helices. The coupling helices of one TMD interact with both NBDs, in which coupling helix 1 contacts both NBDs and coupling helix 2 exclusively contacts the opposite NBD (71,103). This results in extensive interactions between the TMD and both NBDs and enables the communication between the TMDs and the NBDs.

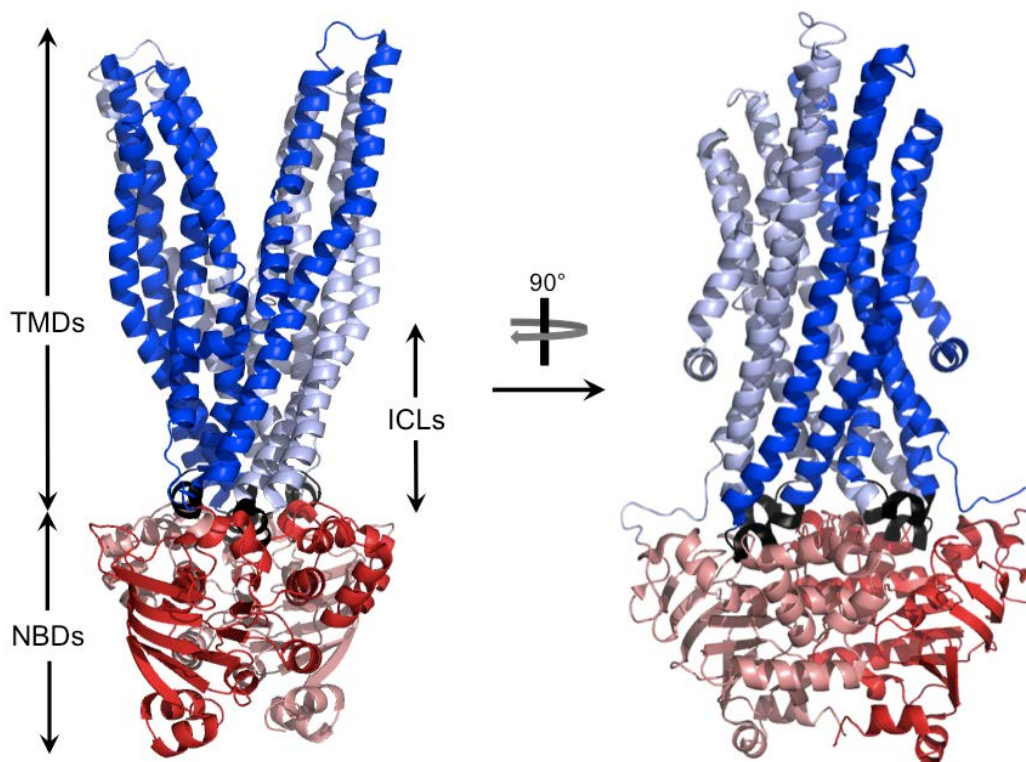


**Figure 6** Crystal structure of Sav1866 from *S. aureus*. The homodimeric MDR transporter Sav1866 was solved in an outward facing conformation with bound ADP (PDB accession number 2HYD) and AMP-PNP (PDB accession 2ONJ) analog, respectively (71,72). Each TMD is colored in blue or light blue and each NBD in red or light red. The intracellular loops (ICLs) extend the TM helices beyond the membrane into the cytoplasm and are connected by the coupling helices (black).

#### 1.3.4 The transmission interface

The ATP-dependent closure of the NBDs generates molecular motion, which is transmitted to the TMDs via non-covalent interactions to facilitate substrate transport. In contrast to importers, ABC exporters lack the conserved EAA motif located within the coupling helices of the TMDs. The EAA motif was shown to make extensive contacts with the opposite NBD (67,104). The TMD of ABC importers contain only one coupling helix, while in ABC exporters two coupling helices of one TMD contact each NBD, because of the domain swapped arrangement. Despite the high diversity of the TMD folds, the coupling helices of



ABC transporters interact with grooves formed at the boundaries of the two subdomains of the NBDs (Figure 7) (71,72,97). More precisely, the coupling helices interact with the Q-loop of the NBD allowing the transmission of the conformational changes induced by ATP binding and hydrolysis to the TMD (105). This is in good agreement with mutational studies of the cystic fibrosis transmembrane conductance regulator (CFTR/ABCC7). ICL4 of CFTR was implicated to interact with the NBDs (106). Recently, mutational and cross-linking studies of P-glycoprotein demonstrated that ICL2 and ICL3 form a hydrophobic transmission interface together with the second NBD (107) and molecular dynamic simulations of MalEFGK showed that the EAA loops and the Q-loop mediate the coupling between TMDs and NBDs (108).

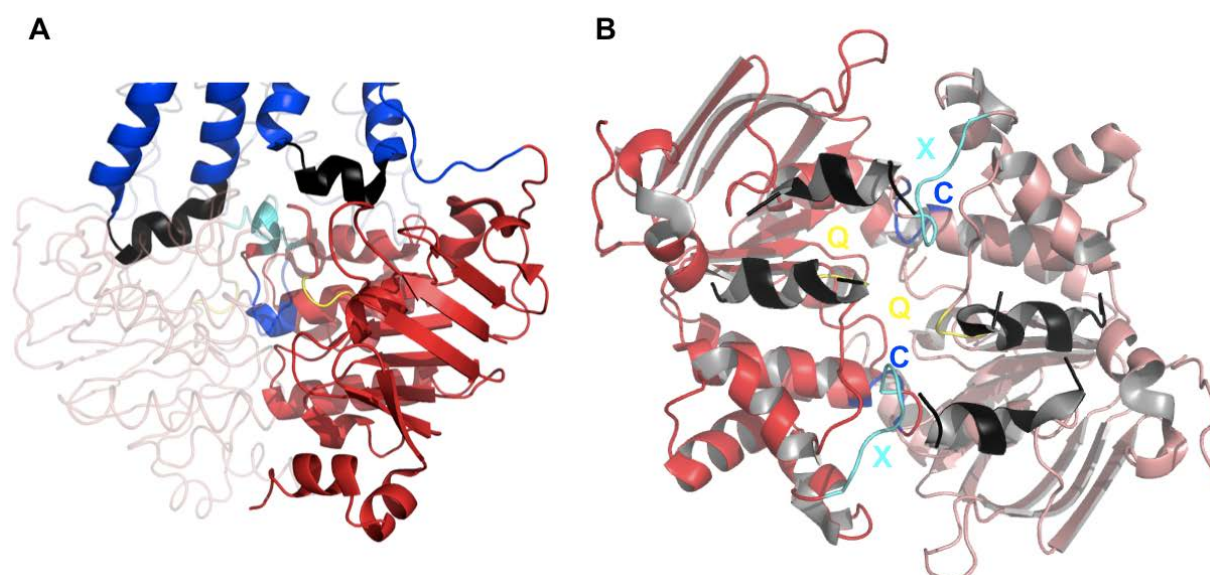


**Figure 7** Transmission interface between NBDs and TMDs. (A) The close up view of Sav1866 shows that the coupling helices (black) of one TMD interact with both NBDs (red) via the Q-loop (yellow) and the X-loop (cyan), which is located in direct proximity of the C-loop (blue). (B) Cartoon representation of the transmission interface from the periplasmic surface rotated 90° from (A) view.

Furthermore, in ABC exporters the  $\alpha$ -helical subdomain of the NBD contains a structurally diverse region (SDR) with a highly conserved motif, the X-loop (TEVGERG) (72,78). The X-loop was demonstrated to be crucial for the communication between NBD and TMD of the transporter associated with antigen processing (ABCB2/B3) (109) and of the chloride channel CFTR (110). For the first time, the X-loop of the human MDR3 was investigated and reported in chapter 4.

## 1.4 ABC transporters mediated lipid transport – The human ABCB family

In the human genome 48 ABC transporters are encoded and classified into seven subfamilies (A-G) based on the amino acid sequence similarity, domain organization and phylogenetic analysis (55,111). Nearly half of the 48 human ABC transporters are thought to translocate lipids (Table 1) (23,38) and mutations of these ABC transporters are related to lipid-linked diseases such as adrenoleukodystrophy (ABCD1) (112), tangier disease (ABCA1) (113), and Stargardt disease (ABCA4) (114). The ABCB subfamily (MDR/TAP) comprises four full-size and seven half-size transporters, which show high diversity in substrate specificity. The half-size transporter ABCB2/B3 (transporter associated with antigen processing; TAP1/2) is involved in peptide transport, whereas ABCB1 (multidrug resistance protein 1; MDR1; P-glycoprotein) maintains multidrug resistance and ABCB11 (bile salt export pump; BSEP) and ABCB4 (multidrug resistance protein 3; MDR3) fulfill bile formation. Two examples of the subfamily MDR1 and MDR3 are focused in-depth on in the section below.

Table 1. Evidence for human ABC transporter involved in phospholipid transport. Taken from (23,38).

Name	Trivial name	Involvement	Lipids
ABCA1	ABC1	Macrophage lipid homeostasis HDL deficiencies Tangier disease Phagocytosis	Cholesterol Phospholipids
ABCA2	ABC2	Macrophage lipid homeostasis? Neural development?	Steroids?
ABCA3	ABC3	Lung surfactant synthesis?	PC
ABCA4	ABCR Rim	Dark adaption Stargardt disease	N-retinylidene-PE
ABCA6		Macrophage lipid homeostasis?	
ABCA7	ABCX	Hematopoiesis? Macrophage lipid homeostasis? Keratinocyte differentiation?	Cholesterol Phospholipids Ceramide
ABCA9		Hematopoiesis?	
ABCA10		Macrophage lipid homeostasis?	
ABCB1	MDR1 P-glycoprotein	Detoxification Multidrug resistance Adrenal secretion Dendritic cell migration	Steroids Cholesterol GlcCer, PS, SM, PAF
ABCB4	MDR2/3 P-glycoprotein	Bile formation Progressive familial intrahepatic cholestasis	PC
ABCC1	MRP1	Detoxification Multidrug resistance?	
ABCC6	MRP6	LTC inflammatory response Pseudoxanthoma elasticum Lipid transport and metabolism	
ABCD1	ALDP	Beta oxidation X-Adrenoleukodystrophy Peroxisome biogenesis	
ABCD2	ALDRP/ALDL1	Beta oxidation	
ABCD3	PMP70 PXMP1	Beta oxidation Peroxisome biogenesis	

(continued)

Table 1: Evidence for human ABC transporter involved in phospholipid transport. (Continued)

Name	Trivial name	Involvement	Lipids
ABCD4	PXMPIL/P70R/PMP69	Beta oxidation	
ABCG1	WHITE	Macrophage lipid homeostasis	
ABCG2	BCRP1	Detoxification	
	MXR1/ABCP	Multidrug resistance	
ABCG5	WHITE3	Bile steroid secretion	
		Sitosterolemia	
ABCG8	WHITE4	Bile steroid secretion	
		Sitosterolemia	

#### 1.4.1 The multidrug resistance protein 1

The multidrug resistance protein 1 (MDR1), also called P-glycoprotein (P-gp) was the first cloned and most intensively studied human ABC transporter. MDR1 was identified in tumor cells showing resistance against a multitude of drugs, a phenomenon called multidrug resistance (MDR) (115-120). In addition, MDR1 is endogenously expressed in kidney, intestine, liver, blood-brain barrier and fetomaternal barrier (121). The knock-down of the orthologous genes *Mdr1a/1b* in mice displays a disrupted blood-brain barrier and leads to neurotoxic effects (122,123). One of the major physiological functions of MDR1 is the protection of the organism against potentially toxic compounds by exporting these into the urine, gut or bile (124). MDR1 is a full-size transporter and translocates a wide range of hydrophobic structural unrelated substances (125).

Interestingly, several studies indicated that MDR1 can translocate phospholipids across the membrane (126-132). The methods to determine lipid translocation are described in detail in chapter 1. Ueda *et al.* demonstrated that MDR1 translocates the steroids cortisol and dexamethasone, while progesterone was not translocated in *MDR1*-transfected cells (126). The first evidence that MDR1 flops short-chain analogs of PC, PE, SM and glucosylceramide (GlcCer) was obtained by van Helvoort and co-workers (127). Furthermore, *in vitro* studies with MDR1 reconstituted in proteoliposomes using a fluorescence quenching assay showed low vanadate-sensitive flipping of a variety of lipid analogs such as short chain analogs of PC, PS, PE, and SM in the presence of ATP (129,130,133). Rothnie *et al.* observed low ATP-dependent translocation of fluorescent-labeled short-chain analogs of PC, PE, ceramide (Cer) and of short-chain spin-labeled analogs of PC, PE, glucosylceramide (GlcCer) and SM. The activity of MDR1 was only obtained in the presence of cholesterol (132). However, after numerous studies on the transport activity of MDR1 it is arguable, whether MDR1 flops endogenous lipids with two long acyl chains or is still a multidrug transporter. For example, *Mdr1a/1b* cannot replace the PC floppase function of its close homolog multidrug resistance

protein 2 (Mdr2; human MDR3, ABCB4) in *Mdr2* knock-out mice (134). In addition, MDR1 did not translocate lipids in HEK293 cells also in the presence of sodium taurocholate, while MDR3-mediated PC translocation was demonstrated in this system (135). This suggested that natural long-chain PC is not a MDR1 substrate. The function of MDR3 will be discussed in section 1.4.2.

In 2009, the crystal structure of mouse *Mdr1a* was solved in the absence of ATP at 3.8 Å (96,136) followed by the structure of P-glycoprotein from *C. elegans* at 3.4 Å (98) and the homologous structure of the half-size transporter from *C. merolae* at 2.8 Å (98,99) (Figure 8). The structures showed a similar inward facing conformation with an internal cavity, which enable the binding of the multiplicity of substrates (137). Sequence homology alignments between members of the ABCB family identified the presence of highly conserved residues in TMH1-3 that have been proposed to form a part of the substrate-binding region and coordinate the hydrophilic part of an amphipathic substrate (100). Based on the structure of P-glycoprotein from *C. merolae*, Kodan *et al.* suggested that TMH4 is a “gatekeeper”, which allows the substrate to entry from the inner leaflet of the membrane (99). In contrast to the outward facing conformation of Sav1866 (Figure 6), in the inward facing conformation the NBDs are separated with a large distance. This indicates that during substrate transport the NBDs fulfill a rigid-body movement.

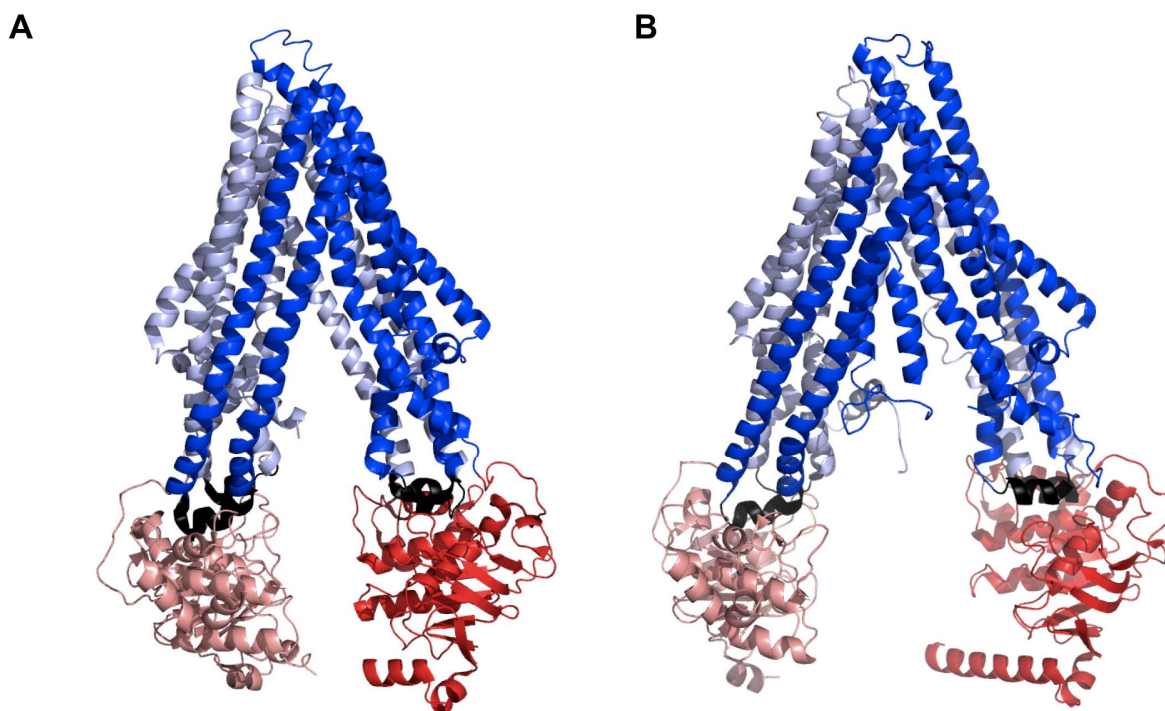


**Figure 8** Crystal structures of P-glycoprotein. Both P-glycoprotein structures A) from *Mus musculus* (PDB accession 4M1M (96,136)) and B) from *Caenorhabditis elegans* (PDB accession 4F4C (98)) were crystallized in an inward facing conformation in the absence of ATP. Each TMD is shown in blue or light blue and each NBD in red or light red. The coupling helices are colored in black.

### 1.4.2 The multidrug resistance protein 3

The multidrug resistance protein 3 (MDR3, mouse *Mdr2*), also called ATP-binding cassette subfamily B member 4 (ABCB4), shares up to 75% identity and 86% homology with MDR1 in the amino acid sequences (138). While MDR1 is a multidrug transporter, MDR3 is highly substrate specific and transports PC from the inner to the outer leaflet of the canalicular membrane of hepatocytes into the bile (Figure 9) (134). MDR3 is a 1279-amino acid large full-size glycoprotein and is localized in canalicular membranes. Low concentrations of MDR3 mRNA were also found in muscle, placenta, testis and ileum, but the protein was not detected (139).

Chapter 1 of this doctoral thesis gives an in-depth introduction about the history and characteristics of MDR3. The first evidence that MDR3 is a PC floppase was observed in *Mdr2* disrupted mice (*Mdr2*<sup>-/-</sup> mice) leading to a complete absence of PC in the bile (134). The function of *Mdr2* could be rescued in these mice by expressing the human *MDR3* gene, indicating that MDR3 acts as a phospholipid translocase (140). Further studies revealed that human MDR3 exclusively translocates PC in a bile salt-dependent manner (127,135,141,142). It is still discussed whether MDR3 transports drugs *in vivo*. There are indications that MDR3 transports drugs such as digoxin, paclitaxel, vinblastine and ivermectine (143), which was inhibited by the MDR1 specific inhibitors verapamil, cyclosporin A and PSC833 (143). The chimera protein containing the TMDs of MDR1 and the NBDs of MDR3 exhibited a 10-fold lower drug-stimulated ATPase activity compared to wild type MDR1 (144). Thus, the NBDs of MDR3 are capable to provide the energy for drug transport. Chapter 5 of this thesis focused on the drug-modulated ATPase activity of MDR3.

Mutations of the *MDR3* gene, located at chromosome 7q21.1, caused different types of liver diseases like progressive familial intrahepatic cholestasis type 3 (PFIC-3) (145,146), intrahepatic cholestasis of pregnancy (ICP) and low-phospholipid associated cholelithiasis (LPAC) (147,148). PFIC-3 is characterized by a complete absence of PC from the bile resulting in damage and apoptosis of the hepatocytes. Therapies of PFIC-3 included the application of the bile salt ursodeoxycholate (UDCA) that down-regulates the *de novo* synthesis of bile salts (149). In many cases liver transplantation is the last option (150,151). In contrast, LPAC is a mild form of chronic cholestasis, which provokes cholesterol gallstones and ICP is a reversible form during the third semester of pregnancy (147,152). For the first time, the influence of a single mutation within the X-loop found in a patient with PFIC-3 on the *in vitro* ATPase function of MDR3 is investigated in chapter 4.

### 1.4.2.1 MDR3 and its role in bile formation

Twelve ABC transporters are localized in the liver and are important for diverse physiological functions such as detoxification and bile formation. Bile formation takes place in the canaliculi of hepatocytes, which compose 80% of the liver volume. Hepatocytes are polarized cells with a basolateral (sinusoidal) membrane and a apical (canalicular) membrane (Figure 9) (153). The basolateral membrane borders the blood stream facilitating the uptake of nutrients and xenobiotics from the blood, whereas the canalicular membranes form small bile ducts, the canaliculi. Bile is a complex mixture that includes bile salts, phosphatidylcholine, cholesterol, bilirubin and electrolytes and is crucial for the digestion of fat and for the absorption of lipids and lipophilic vitamins in the small intestine (154,155).

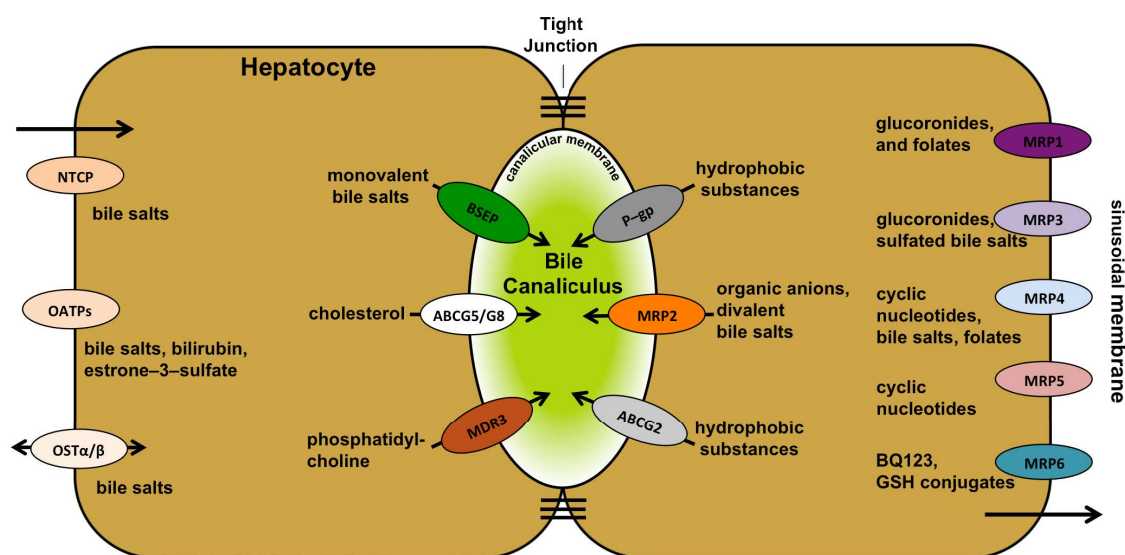


**Figure 9** Localization of transporters in the hepatocytes. Bile salts are taken up at the sinusoidal membrane through the sodium–taurocholate cotransporting peptide (NTCP) in a sodium–dependent manner and to a lesser extent through a sodium–independent transport by organic anion transporting proteins (OATPs). They are then further shuttled to the canalicular membrane and transported via the bile salt export pump (BSEP) into the canaliculus. Multidrug resistance protein 3 (MDR3) and Sterolin 1 (ABCG5/G8) complete the bile formation by flopping phosphatidylcholine (PC) from the inner to the outer leaflet as well as transporting cholesterol. Bile salts, PC and cholesterol form mixed micelles which constitute the basis of bile. P–glycoprotein and the breast cancer resistance protein (ABCG2) transport a variety of hydrophobic substances into the bile and confer multidrug resistance (MDR). Furthermore, a substantial number of multidrug–related proteins (MRPs) are localized in the sinusoidal membrane except MRP2. They transport a broad range of organic anions and conjugated substances. They also participate in MDR and some of them, e.g. MRP4 as well as the organic solute transporter (OST) act as salvage system for too high bile salt concentrations within the cell. Figure taken from chapter 1.

Bile salts are synthesized from cholesterol in the hepatocytes and transported into the lumen of the canaliculi by the ABC transporter bile salt export pump (BSEP, ABCB11) (156,157). There, bile salts extract PC from the outer leaflet of the canalicular membrane to form mixed micelles that reduce the detergent activity of bile salts and to protect the biliary ducts (Figure 10) (158,159), because high concentrations of free bile salts in the lumen have



destructive effects on hepatocytes (160,161). A second function of the bile salt-PC micelles is the absorption of cholesterol that prevents the crystallization of cholesterol in the biliary ducts and the formation of cholesterol gallstones (148). Cholesterol is transported by the heterodimeric ABC transporter ABCG5/G8 (162). A further protein that is essential for bile formation is the P4-type flippase ATP8B1. ATP8B1 compensates the detrimental effects of MDR3 on barrier function of the canalicular membrane by flipping PS from the outer to the inner leaflet of the canalicular membrane (142). Subsequently, bile is stored in the gall bladder and expelled into the duodenum after food intake. Finally, up to 95% of bile salts and PC are reabsorbed in the intestine and return to the hepatocytes via the portal vein to complete the enterohepatic cycle.

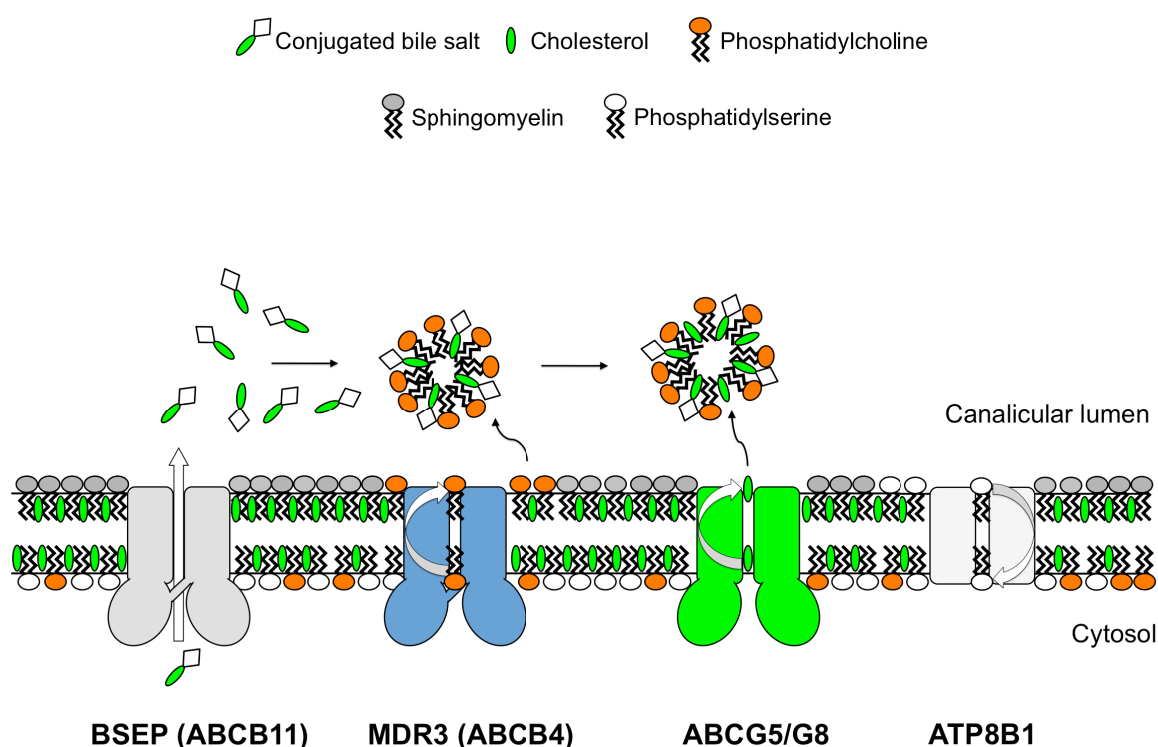


**Figure 10** Bile formation at the canalicular membrane of hepatocytes. Bile salts are translocated by the bile salt export pump (BSEP) and extracted PC either from the outer leaflet of the membrane or PC is directly accessible from the ABC transporter MDR3. AbcG5/G8 facilitates the translocation of cholesterol, which is extracted by the bile salt-PC mixed micelles. The figure was taken from Stindt (163) with permission.

#### 1.4.2.2 Regulation of MDR3 function

The regulation of MDR3 function plays a key role in bile formation. More than 250 *MDR3* gene mutations and single nucleotide polymorphism (SNPs) have been identified and cause different severities of cholestasis (147,148,151,164). However, the consequences of the most abundant MDR3 variants on the transport function and defects of the regulation pathway with

respect to the targeting and retention of MDR3 at the canalicular membrane remain to be elucidated. The functions of ABC transporters are regulated by various mechanisms including transcriptional regulation, post-translational modifications and protein-protein interactions. The level of gene expression controls the amount of transporter synthesized by the cell. Bile salts have been shown to interact with the nuclear bile salt receptor farnesoid-X receptor (FXR), whose induction leads to increased export of bile salts and PC from the hepatocytes (165-167). Recently, Gautherot *et al.* found that the mutations T34M and R47G, which are located in N-terminal cytoplasmic loop, impaired MDR3 phosphorylation and reduce the PC translocation without affecting the localization at the plasma membrane (168). Thus, phosphorylation appears to be one regulatory mechanism of MDR3 function. Furthermore, the function of MDR3 is regulated by the amount of inserted MDR3 in the canalicular membrane. Currently, it is not known how MDR3 is targeted from the ER and inserted into the membrane and subsequently recycled. Chapter 6 of this doctoral thesis focuses on the identification of new adapter proteins of human MDR3 *in vitro*.

## **1.5 Mechanisms of lipid transbilayer transport by ABC transporters**

Based on biochemical, biophysical and structural data various distinct transport mechanisms for ABC exporters have been proposed. The most elementary model of substrate transport across membranes is the alternating access model (169). This model bases on two distinct conformations of the ABC transporter, an outward facing conformation with low affinity site for the substrate and an inward facing conformation with a high substrate affinity site (169). This is in coincident with the structures of Sav1866 revealing an outward facing conformation in the presence of an ATP analogue (Figure 6) and P-glycoprotein in an ATP free inward facing conformation (Figure 8) (71,96). However, how ABC transporters mediate the transport of amphipathic compounds such as lipids are still not entirely understood. This section addresses the mechanisms of lipid transbilayer transport by ABC transporters.

The ATP-switch model summarizes the recent advances in the field of ABC transporter (95,170). This general model is widely accepted and comprises four distinct steps (Figure 11). First, the ABC transporter is in the high-affinity inward facing conformation with an open NBD dimer allowing the lipid substrate to bind from the inner leaflet of the membrane to the TMDs regulated by the intramembrane gatekeeper TMH 4 (98,133,171,172). Therefore the substrate-binding site has to be accessible from the lipid phase. This results in a conformational change in the NBDs and induces an increased affinity of the NBD sites for



ATP (173,174). Secondly, ATP binding induces dimerization of the NBDs, which induces a large conformational change in the TMDs leading to the substrate release from an outward facing low affinity binding site (81,83). In the third step, ATP is hydrolyzed and destabilizes the NBD dimer and the fourth step comprises phosphate and subsequently ADP release triggering the dissociation of the NBD dimer and restoring the ABC transporter to the initial state.

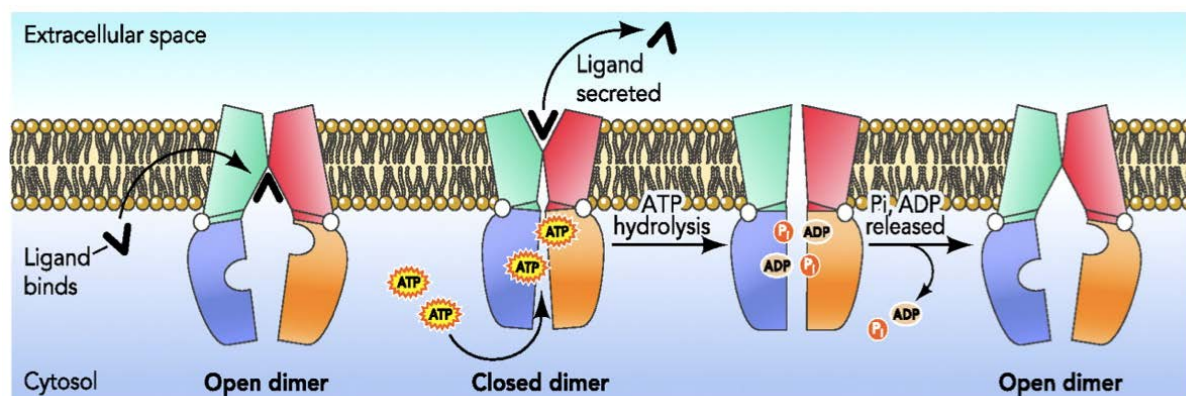


**Figure 11** Scheme of the ATP switch model for ABC transporter. This model comprises four distinct steps including I) substrate (ligand) binding, II) ATP binding, NBD dimerization and substrate release, III) ATP hydrolysis and dimer destabilization and IV) ADP and Pi release restoring the ABC transporter. Picture taken from (170).

To date, two models have been proposed to elucidate how ABC transporters extrude substrates such as lipids from the cell, i) the flippase model and ii) the vacuum cleaner model (Figure 12) (175). In the flippase model the lipid binds to the substrate-binding site of the ABC transporter. Subsequently, ATP binding induces a conformational change and enables the substrate to flip from the cytoplasmic to the exoplasmic leaflet. The lipid accumulates in the outer leaflet generating an asymmetric lipid bilayer and subsequently is extracted by an acceptor.

In contrast, the vacuum cleaner model proposes that the lipid interacts with the substrate-binding site from the inner leaflet of the membrane, enters a hydrophobic cavity of the ABC transporter and is ejected directly into the extracellular space (176-178). This mechanism hypothesizes a complete hydration of the lipid. Assuming that ABC exporters have a stoichiometry of one to two molecules of ATP hydrolyzed per substrate molecule, a complete hydration of the lipid would consume more energy than it can be provided by ATP hydrolysis (178,179).

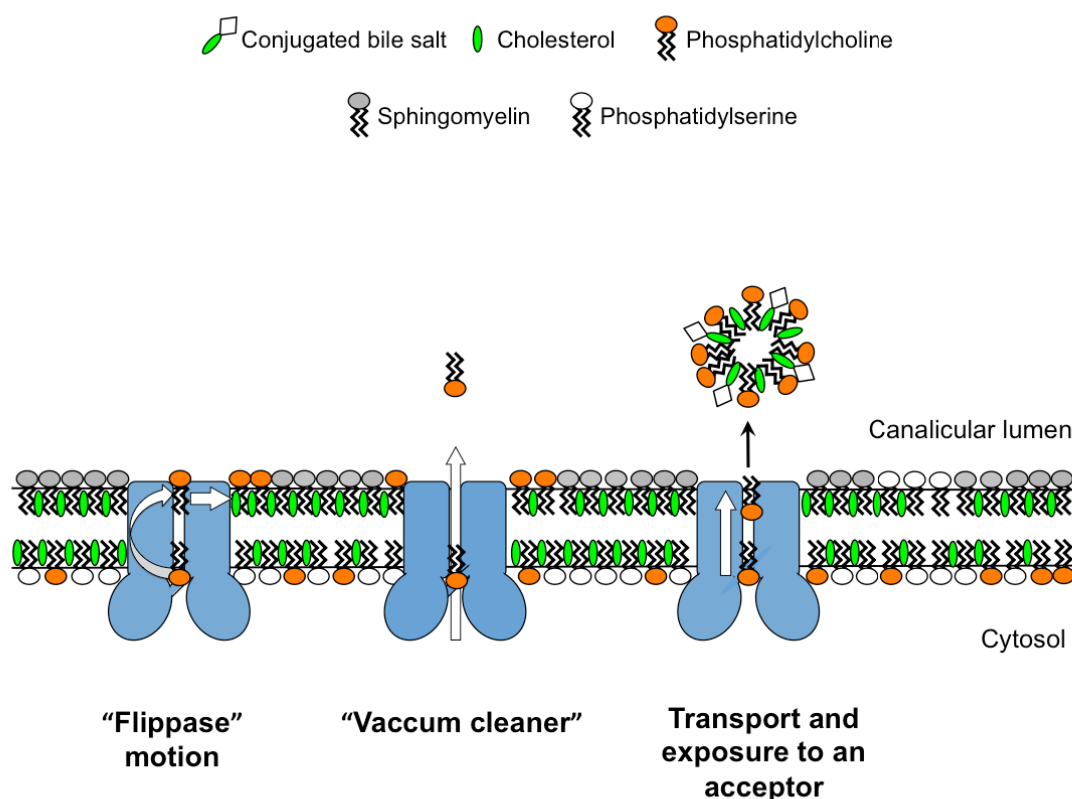


**Figure 12** Models for ABC transporter mediated lipid transport. The flippase model proposed that the ABC transporter (blue) flips the lipid (red) across the membrane with a reorientation of the polar headgroup. Contrary, in the vacuum cleaner model the lipid is ejected directly into the extracellular space. The third activated model based on the vacuum cleaner model, in which the lipid is exposed to an acceptor A.

An expansion of the vacuum cleaner model displays the activated model of ABC transporter-mediated lipid transport (23,162,178). Currently, it is arguable whether ABC transporter primarily play a role in lipid asymmetry or are rather involved in the exposure of specific lipids on the exoplasmatic leaflet allowing their uptake by acceptors, which is proposed in the activated model (Figure 12). In principle, the lipid binds to the substrate-binding site from the cytoplasmic leaflet and is transported to the exoplasmic side of the transporter without reorientation of the polar head group and a hydration of the lipid caused by the exoplasmic medium. The lipid is in an energetically unfavorable activated state, which facilitate the uptake of the lipid by an acceptor. However, substrate release would take place only in the presence of the acceptor. This model was preferred for the cholesterol transporter ABCG5/G8. It is proposed that ABCG5/G8 facilitates an activated state of cholesterol so that it can be easily extracted by acceptors like bile salt-PC micelles (162). Furthermore, for mouse Mdr2 it was demonstrated that bile salt translocation is the main driving force for assisted secretion of PC into the bile (135,180).

## 2 Aims and Objectives

The human multidrug resistance protein 3 (MDR3), also referred as ATP-binding cassette subfamily B member 4 (ABCB4), is crucial in the process of bile formation. Dysfunction of MDR3 caused by mutations is associated with severe hereditary cholestatic diseases. Thus, it is important to understand how lipid transport is mediated by MDR3 using *in vitro* structural-functional analysis, which was the overall aim of this doctoral thesis.

The first aim of this thesis was to establish the heterologous expression of human MDR3 in the yeast *Pichia pastoris* and subsequently the purification with adequate quantities for structural-functional analysis. The major challenge in purification of transmembrane proteins is to find an appropriate detergent, which solubilizes the transmembrane protein in a functional state. Hence, around 100 different detergents were analyzed with respect to their solubilization efficacy and monodispersity of detergent-soluble MDR3. The ATPase activity of MDR3 revealed the functionality of MDR3 and was characterized in terms of substrate specificity, kinetic parameters and inhibition by phosphate analogs. Further analysis should provide insights into the mechanistic coupling between ATP binding and hydrolysis and the translocation of phosphatidylcholine. Therefore, a mutation of the extended X-loop, which was found in a patient with PFIC-3, was introduced in *MDR3* gene and PC-induced ATPase activity was determined.

The questions arise are why MDR3 is a specialized PC floppase, while MDR1 is a multidrug pump and do both proteins translocate their substrates with the same mechanism? There are evidences that MDR3 is capable to transport MDR1 reversal agents in polarized pig kidney cells. However, up to date the physiological importance of MDR3 in cancer was not demonstrated. The second aim of this doctoral thesis comprises the modulation of MDR1 substrates and inhibitors on the ATPase activity of human MDR3.

Furthermore, missense mutations not only lead to defects of ATPase or translocation activity, but also lead to the retention of MDR3 in the endoplasmic reticulum. The third aim of this thesis focused on the mechanism of MDR3 cell membrane surface expression at the canalicular membrane by the identification of new adaptor proteins, which facilitate membrane protein-cytoskeletal interaction.



### 3 Results

#### Chapter I – Structure and function of hepatic ABC transporters

**Title:**

**Structure and function of hepatic ABC transporters**

Published in: *Hepatobiliary Transport in Health and Disease, Editors, D.Häussinger, R. Kubitz and V. Keitel, de Gruyter, Berlin*

Impact factor: not available

Own Proportion to this work: 30 %

Writing of the manuscript

## 2 Structure and function of hepatic ABC transporters

*Philipp Ellinger, Marianne Kluth, Susanne Przybylla,  
Sander H. J. Smits, and Lutz Schmitt*

### 2.1 Introduction to human ABC transporters expressed in the liver

Several membrane transporters that belong to a group of ATP-dependent primary transporters, the so-called ABC (ATP binding cassette) transporters, are found in the human genome. In general, ABC transporters contain two transmembrane-spanning domains (TMDs) and two characteristic nucleotide-binding domains (NBDs) localized in the cytosol. In the membrane the two TMDs form a pore-like structure, which facilitates substrate transport against a chemical gradient. One TMD is predicted to have six  $\alpha$ -helices, whereas the soluble NBDs are essential for the supply of energy by hydrolysis of ATP. Compared with the TMD, the NBD harbors highly conserved sequence motifs: the Walker A (GXXGKGKS/T, where X can be for any amino acid), Walker B ( $\Phi\Phi\Phi\Phi$ D, where  $\Phi$  can be any hydrophobic residue) motifs, and the C-loop (ABC-signature motif, LSGGQ) (1). The C loop, which is located roughly 90 amino acids downstream of the Walker A motif and roughly 30 amino acids upstream of the Walker B motif, is actually the characteristic sequence motif of this family; together with the Walker A and B motifs, it serves as a diagnostic clue to the identification of new family members. Additional sequence motifs present in ABC transporters are the Q loop, the D loop (SALD), and a highly conserved histidine residue essential for ATP hydrolysis, which is positioned 30 amino acid downstream of the D loop (2).

To achieve a thermodynamic uphill transport of the substrate, transport has to be coupled to the cycle of ATP hydrolysis. Several high-resolution structures of full-length ABC transporters and isolated NBDs, in combination with biochemical analysis, have provided important contributions to a molecular understanding of substrate binding, ATP hydrolysis, and substrate transport. For example, the highly conserved NBD has an L-shaped structure consisting of a catalytic domain and a helical domain. The catalytic domain contains the Walker A and B motifs while the helical domain harbors the C loop. These two domains are connected by the Q and Pro loops (3). Further analysis of, for example, the isolated haemolysin B-NBD demonstrated that in the presence of ATP, the two NBDs form a homodimer (2). The Walker A and B motifs of one NBD and the C loop of the opposing NBD bind one ATP, so that the two NBDs are set in a head-to-tail arrangement. This ATP-induced dimerization generates mechanical work, which in principle can be transmitted to the TMDs and might serve as another source of energy (see section 2.2.4). The dimeric NBDs cooperate in hydrolysing ATP and provide the free energy to drive the directional transport of the substrate against a concentration gradient. After ATP hydrolysis, ADP and  $P_i$  dissociate from the NBD, the dimer falls apart, and the ground state of the NBDs is restored.

Furthermore, different models for the transport mechanism have been proposed. The simplest model, the alternating access model, describes two basic conformations. One conformation is open to the cytosolic side (inward-facing), with a substrate-binding

site accessible for the substrate only from the cytosol, and the second conformation is open to the extracellular side, containing a binding site, which has a low affinity to the substrate and is accessible only from the extracellular space (4). A continuous model is the ATP-switch model. In the ground state the transporter is in the inward-facing conformation with a high-affinity substrate-binding site and the NBDs exist as monomers, with low affinity to ATP. The ATP-induced dimerization of the NBDs leads to a conformational change in the TMDs such that the substrate-binding site is exposed to the extracellular space, the substrate affinity is reduced, and the bound substrate is finally released (5). However, the exact molecular coupling of the ATP–hydrolysis cycle and substrate transport is still not entirely clear.

In the human hepatocyte, several ABC transporter are expressed: for example, the bile salt export pump (BSEP, ABCB11), responsible for bile salt transport; ABCG5/ABCG8, involved in sterol transport; multidrug resistance protein 3 (MDR3, ABCB4), flopping phosphatidylcholine from the inner to the outer membrane leaflet; and ABCG2, transporting a variety of hydrophobic substances (→Fig. 2.1). Mutations in one of these transporters are associated with different kinds of liver diseases of varying severity. For example, Dubin-Johnson disease is related to mutations in MRP2 (ABCC2), and progressive familial intrahepatic cholestasis type 2 (PFIC2) is associated with a mutations with the bile salt export pump BSEP.

This chapter summarizes experimental insights and focuses on the canalicular ABC transporters BSEP, MDR3, and ABCG2, highlighting their discovery and evolution and the *in vitro* assays from which a mechanistic understanding may be derived.

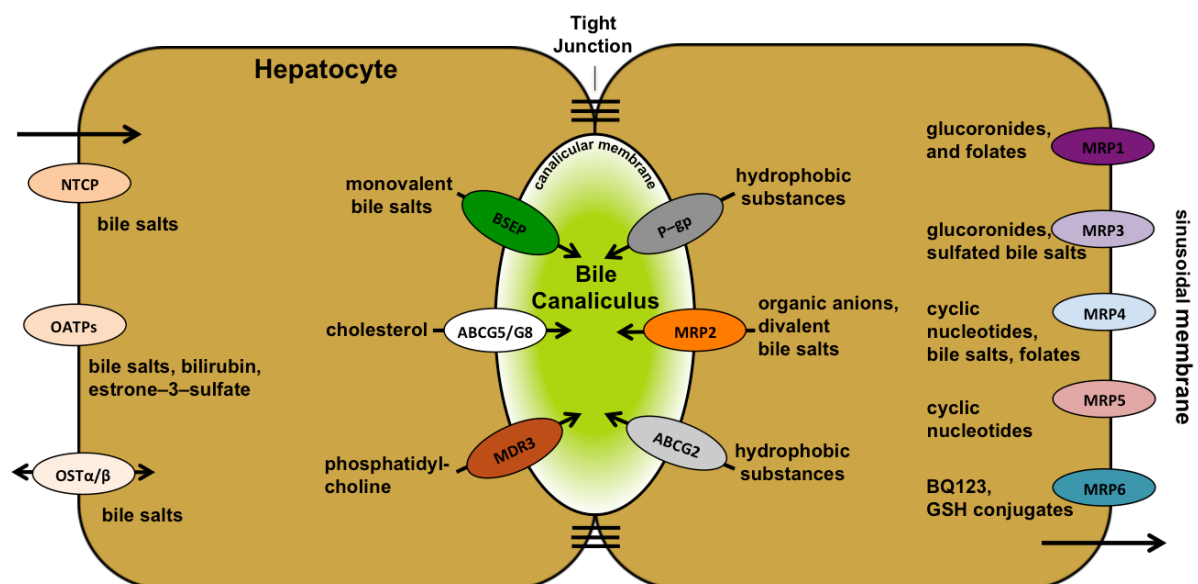


**Fig. 2.1:** Localization of transporters in the hepatocytes. Bile salts are taken up at the sinusoidal (basolateral) membrane through the sodium–taurocholate cotransporting peptide (NTCP) in a sodium–dependent manner and to a lesser extent through a sodium–independent transport by organic anion transporting proteins (OATPs). They are then further shuttled to the canalicular membrane and transported via the bile salt export pump (BSEP) into the canaliculus. Multidrug resistance protein 3 (MDR3) and Sterolin 1

(Continued)



**Fig. 2.1:** (*Continued* )

(ABCG5/G8) complete the bile formation by flopping phosphatidylcholine (PC) from the inner to the outer leaflet as well as transporting cholesterol. Bile salts, PC and cholesterol form mixed micelles which constitute the basis of bile. P-glycoprotein (P-gp) and the breast cancer resistance protein (ABCG2) transport a variety of hydrophobic substances into the bile and confer multidrug resistance (MDR). Furthermore, a substantial number of multidrug-related proteins (MRPs) are localized in the sinusoidal membrane except MRP2. They transport a broad range of organic anions and conjugated substances. They also participate in MDR and some of them, e.g. MRP4 as well as the organic solute transporter (OST) act as salvage system for too high bile salt concentrations within the cell to prevent toxicity.

## 2.2 Structure and function of the bile salt export pump (ABCB11; BSEP)

### 2.2.1 Liver transport of bile salts

Bile salts are essential for the absorption of lipids and fat-soluble vitamins, originated from food intake, by the enterocytes of the small intestine and also for the excretion of endo- and xenobiotics with the bile. They are synthesized by multiple enzymatic reactions in the liver, more precisely in the hepatocytes from cholesterol as educt; this constitutes one of the key function of the liver (6). From there bile salts enter the biliary tree and are stored in the gallbladder upon food intake (7). After they have fulfilled “their mode of action”, bile salts pass through the enterohepatic circulation, meaning that they are reabsorbed to ~90% in the small intestine and then transported back to the liver via the portal blood. There, they are transported again into the hepatocyte and the cycle starts anew with their secretion into the canaliculi (8,9). A single bile salt molecule traverses the cycle approximately up to 10 times a day until it is excreted via the intestine, which makes this circulation an extremely efficient recycling system (10).

Because bile salts are amphipathic molecules, they display a detergent character. Hence a high concentration within the cell is deleterious, leading to damaged mitochondria and apoptosis or necrosis of the hepatocytes owing to the salts’ ability to solubilize or create defects within biological membranes. To prevent this and keep bile salts circulating, a specialized set of bile salt transporters in the hepatocyte is required (9,11,12). In the basolateral membrane (also called the sinusoidal membrane), bile salts are taken up from the portal blood. This is accomplished by the sodium taurocholate co-transporting peptide (NTCP, SLC10A1) in a sodium-dependent transport process (13). In addition, there is the less frequently used sodium-independent transport by the organic anion-transporting polypeptides (OATPs) (14).

After entering the cell, bile salts reach the apical membrane (also called the canalicular membrane); the exact mechanism of this is not yet completely understood. For example, one mechanism involves bile salt-binding proteins (15).

At the canalicular membrane, bile salts are transported into the canalicular lumen by the ATP-binding cassette transporter (ABC transporter) bile salt export pump (ABCB11;



## 26 | 2 Structure and function of hepatic ABC transporters

BSEP) (16,17). BSEP is the main driving force for the bile salt-dependent part of bile flow and a bottleneck in the enterohepatic circulation. It must transport bile salts against a steep concentration gradient to maintain circulation, since the concentration of bile salts in the canaliculus is 1000 fold higher than in the cell, 1 mM and 1  $\mu$ M, respectively (10).

### 2.2.2 Discovery of the bile salt export pump

The electrochemical gradient across the canalicular membrane is  $\sim -35$  mV and its discovery marked the first explanation for bile salt transport across this membrane (18,19). However, this electrochemical gradient alone could not be the entire explanation. Finally, in 1991, an ATP-dependent system for the transport of taurocholate in isolated canalicular membranes of rat liver was described. Other laboratories subsequently confirmed this finding (20,21). Evidence that an ABC transporter was responsible for bile salt secretion into the canaliculus appeared in 1995. It involved an increased level of mRNAs, detected by Northern blotting, in combination with the overexpression of an ABC transporter found via the Western blot technique with a P-glycoprotein antibody (ABCB1, MDR1, P-gp); these were demonstrated in a bile salt-resistant rat hepatoma-derived cell line (22). This suggested that an ABC transporter closely related to P-gp became upregulated in this system. In the same year, Childs et al. screened a pig cDNA library with a probe consisting of a P-gp sequence and identified a gene exclusively expressed in the liver that had a sequence identity of 61% to human P-gp on the amino acid level (23). This gene was named “sister of P-gp” (sP-gp), but its function remained unknown. Gerloff et al. were the first to demonstrate that oocytes exhibited a stimulated taurocholate efflux when liver sP-gp cRNA was injected into *Xenopus laevis* oocytes and the first to express sP-gp in Sf9 (*Spodoptera frugiperda*) cells (24). Furthermore, membrane vesicles derived from these Sf9 cells demonstrated an ATP-dependent taurocholate uptake, much as in previous studies with isolated canalicular membranes. Because of these findings the “sister of P-gp” was renamed “bile salt export pump (BSEP)” and was considered to be the predominant bile salt transporter in the apical membranes of hepatocytes (24). Further strong support for this consideration was obtained by positional cloning of the human *BSEP* gene and mapping it to chromosome 2q24, a locus linked to progressive familial intrahepatic cholestasis type 2 (PFIC2), a severe liver disease (25).

### 2.2.3 Evolution of the bile salt export pump

The production of bile salts and their subsequent transport into the canaliculi is highly conserved among the livers of vertebrates. Over the years, BSEP has been detected and studied in the pig (23), rat (26), mouse (27,28), rabbit (29), dog (30) and human (31,32). Interestingly, full-length BSEP cDNAs have been identified in a variant of the small skate (*Raja erinacea*), a 200-million-year-old marine vertebrate with an amino acid sequence identity of 68.5% to the human orthologue (33). Here, bile salts are transported in large amounts by BSEP. Furthermore, it was demonstrated that mutations leading to PFIC2 in humans had the same effect on substrate transport in skate BSEP (33,34). The bile of this elasmobranch normally consists of bile alcohols (scymnol sulfate) rather than bile salts, which cannot be found in its bile. Probably bile alcohols were the original

substrates for BSEP, and mammalian evolution led to different substrates owing to a selective pressure – for example, more fat in the diet. Interestingly, skate bile does not contain any phospholipids and no MDR3 protein (a phospholipid floppase) is found in the hepatocyte. The function of BSEP and its tight correlation with MDR3 is described in section 2.3. Importantly, however, this finding suggests that BSEP evolved much earlier than the highly identical MDR3 protein (sequence identity between P-gp and MDR3 of ~80%) and probably also by gene duplication (35). The occurrence of lipids in bile was potentially the result of the more deleterious bile acids than of the bile alcohols that arose during evolution. All of these indications demonstrate that BSEP diverged very early from P-gp and that it is highly conserved in vertebrate evolution.

#### 2.2.4 The bile salt export pump – a member of the ABC transporter family

BSEP belongs to the group of ABC transporters. They can be found in all the taxonomic kingdoms (from bacteria to humans), and all possess the same modular architecture and act either as importers or exporters (36). In humans, 48 ABC transporter genes have been identified in addition to a small number of pseudogenes, which are not expressed (37). All known eukaryotic ABC transporters are exporters, whereas ABC importers can be found only in Archaea and Bacteria. In humans, ABC transporters are expressed throughout the body, but some highly tissue-specific and ABC transporters are restricted to the liver (37). Phylogenetic analysis of the entire human ABC transporter sequences has led to the classification of seven subfamilies (A to G) (38). Because of their important roles in human physiology, dysfunction is the cause of very severe diseases, such as cystic fibrosis (39). In terms of mutations of liver ABC transporters BSEP and MDR3, for example, PFIC2 (25) and PFIC3 (40) may develop (see chapter 9). BSEP belongs to the group B (MDR/TAP) subfamily of human ABC transporters because of its high sequence identity to P-gp. The gene is located on chromosomes 2q24 (25) and the 28 exons code for a 1321 amino acid glycosylated ABC transporter with a molecular mass of ~160 kDa (31,32).

ABC transporters have a core architecture consisting of two NBDs and two TMDs. In eukaryotes these modules are encoded on a single gene, but one must distinguish between the full-size transporters (two TMDs and two NBDs) and half-size transporters (only one of each domain). The latter homo- or heterodimerize to form a functional transporter. BSEP is a full-size ABC transporter with a core molecular weight of 146 kDa. Interestingly, the N-terminal NBD (NBD1) of BSEP contains a methionine instead of a glutamate within the Walker B motif. The glutamate normally interacts with ATP through a catalytic water molecule that catalyzes the nucleophilic attack onto the  $\gamma$ -phosphate. ATP binding sites in ABC transporters are composed of the Walker A and B motifs of one NBD and the C-loop of the other NBD. Therefore the ATP-binding site that contains NBD1 (site 1) is a degenerated site. Degeneration of this conserved residue is also seen in other human ABC transporters like TAP1/2 or CFTR (41). Functional studies of other degenerated ABC transporters have demonstrated that this mutation leads to an ATP-deficient site within the NBD dimer. This, of course, implies an asymmetric function of the two NBDs and further suggests that ATP binding site 1 of BSEP is catalytically inactive or active only at drastically reduced levels compared with the other ATP binding site in the composite dimer. This phenomenon has not been investigated for BSEP so far but is of high concern for a molecular understanding of ATP hydrolysis coupled to bile salt transport. The TMDs are located within the membrane and provide the translocation

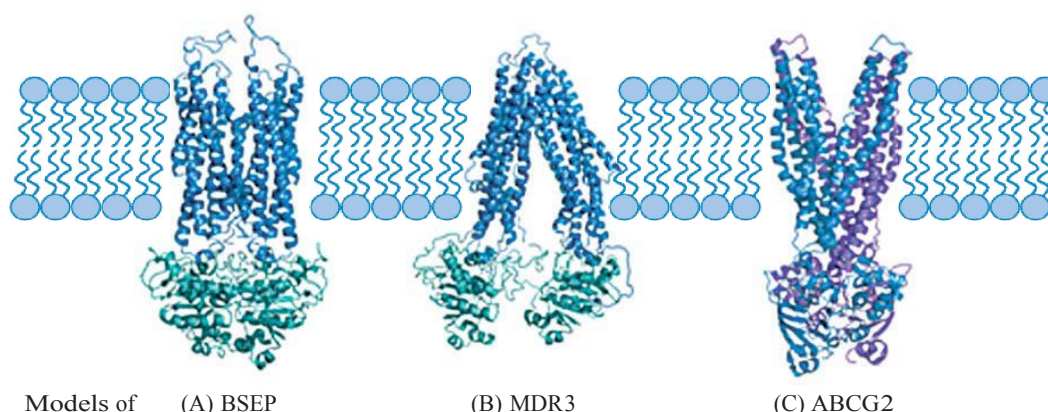


**Fig. 2.2:** Models of BSEP, MDR3 and ABCG2. (A) The model of BSEP based on the known structure of Sav1866 from *Staphylococcus aureus*. The transmembrane domain is highlighted in blue and the nucleotide binding domain in cyan. The used template is deposited under protein data bank (PDB) code 2HYD. (B) The model of MDR3 based on the known structure of P-gp from *Mus musculus*. The transmembrane domain is highlighted in blue and the nucleotide binding domain in cyan. The used template is deposited under PDB code 3G61. (C) The model of ABCG2 based on the known Structure of the multidrug ABC transporter Sav1866 from *Staphylococcus aureus* in complex with AMP-PNP. The used template is deposited under PDB code 2ONJ. Since ABCG2 is a halfsize transporter the two monomers are colour coded differently. Monomer I is highlighted in blue and monomer II in purple. Due to the bound AMP-PNP in the template structure the conformation of ABCG2 represents the potential nucleotide bound state. It is important to clarify that these models are based on the known X-ray structure and the structures obtained from the actual protein might look differently.

pathway for the substrate. In contrast to the NBDs, the TMDs are highly variable in their sequence and thus determine the substrate specificity. It is assumed that many human ABC transporters show the 6 X 6 topology, meaning that they contain six TM helices (TMH) traversing the membrane followed by a cytoplasmically located NBD and again six TMHs and an NBD. This assumption was originally proposed based on cysteine scanning mutagenesis of P-gp and the recently developed x-ray structures of mouse P-gp and bacterial homologues (42); it may be true for BSEP as well. BSEP is also a full-size ABC transporter containing 12 TMHs and two NBDs (→Fig. 2.2). This number of helices is derived from hydrophobicity calculations because structural information on BSEP is lacking. To date only one eukaryotic ABC transporter structure (of mouse P-gp) has been published (42). The second available structure (ABCB10) is deposited only in the Protein Data Bank (PDB database). The P-gp structure shows the typical bundle of six helices crossing the membrane. However, as first observed for Sav1866, a domain swap is present in P-gp, suggesting that such a swapping is a conserved feature of ABC drug pumps. Here, four helices of one bundle and two helices of the other bundle build up one TMD. The TMDs provide a large cavity for substrate binding for mouse P-gp, which may also be true for BSEP. According to the “cholesterol fill-in mechanism,” cholesterol also participates in substrate recognition and fills the volume of the cavity that is not occupied by the substrate, as postulated for P-gp. Besides the amino acids, which constitute the substrate-binding site, this could also be an additional explanation for the fact that those two closely homologous transporters have different substrate spectra and

BSEP is restricted to bile salts. It has been demonstrated that the activity of BSEP critically depends on cholesterol. This might be because BSEP is targeted to detergent-resistant microdomains (DRMs) in the canalicular membrane, which exhibit a high amount of cholesterol and sphingomyelin, or because of the “cholesterol fill-in model.” Whatever the molecular reason(s) for the differences between P-gp and BSEP may be, all the models proposed must be verified experimentally for BSEP in the future. So far most if not all functional information on BSEP results from disease-linked mutations found in patients with, for example, PFIC2 (see chapter 9) and offers insights into the way single amino acids influence the trafficking, stability, and transport capabilities of BSEP.

### 2.2.5 Cloning and expression systems for BSEP

To study a protein biochemically *in vitro*, it is often necessary to obtain sufficient amounts of pure, homogeneous protein. Therefore an expression system must be chosen and recombinant expression constructs must be cloned. All this is true for BSEP, but it has one big drawback. The human cDNA that codes for BSEP has been found to be unstable in *Escherichia coli* (31,32,43). This phenomenon has been observed for several other mammalian membrane proteins as well (44). Because *E. coli* is the most widely used cloning and expression host for standard molecular biology techniques, other strategies must be applied in utilizing the favored expression system. In the case of human BSEP, after several years of struggle, efforts to clone the cDNA into an expression vector were eventually successful. However this led, even after a bacterial promoter in the cDNA was silenced, to a construct with several point mutations within the coding sequence (six missense mutations) and the loss of specific parts of the coding sequence during expression construct propagation (32). All these findings led to the notion that the cDNA of BSEP is “toxic” or “unstable” for cloning and/or the expression host since colonies would no longer grow. One way of circumventing this laborious work is to use homologous recombination (HR) in the yeast *Saccharomyces cerevisiae* (45,46). We therefore established a workflow for human BSEP that can also be applied to any other target (47). Here the expression vector of interest was modified by the introduction of an origin of replication (ori) and a selection marker for *S. cerevisiae* into the backbone of the plasmid. The linearized expression vector and the PCR-amplified BSEP cDNA, which has overlapping ends to the expression vector, are then transformed into yeast. *S. cerevisiae* is capable of recombining those overlapping ends to a circular vector, and only clones that do this correctly are able to grow under selection. The expression vector can be recovered from yeast and transformed in *E. coli* for amplification. We have found that *E. coli* is capable of handling the BSEP cDNA if it is in a closed, circular plasmid form (no nicks, etc.) and grown strictly at or below 30°C. If required, our expression construct can be designed to remove the origin of replication or selection marker to prevent a potential influence of these additional sequences on balanced expression systems. Furthermore, we developed a mutagenesis strategy relying only on yeast. A changed primer design (primers carrying the mutation are not completely complementary to each other) results in a PCR product with overlapping ends (5' and 3' ends) that can be recombined by yeast, resulting in a plasmid containing the desired mutation. With the directed recombination–assisted mutagenesis (DREAM) method, mutations can be introduced more easily and quickly than with commercially available strategies. Therefore this method is seen as a DREAM (47).



The major bottleneck in studying membrane proteins in vitro (e.g. structural and functional studies), is their homo- or heterologous overexpression, making it difficult to purify the protein in adequate amounts. Therefore one must choose between prokaryotic and eukaryotic expression systems. As a prokaryotic expression system, *E. coli* is the most widely used host (48), although there are others like *Lactococcus lactis*, which is also successfully used for the overexpression of membrane proteins (49). Mammalian transporter can be expressed in *E. coli*, but sometimes in an inactive manner. Therefore we also tried to overexpress human BSEP in *E. coli* using the T7-RNA polymerase/promotor system in combination with a synthetic gene, which sequence was optimized for use in *E. coli*. Unfortunately cells stopped growing upon induction of BSEP expression and we were not able to detect BSEP in cell lysates via Western blotting. BSEP is a plasma membrane protein and *E. coli* does not possess the eukaryotic posttranslational modification system, and no cholesterol is present in the inner membrane. Therefore, eukaryotic expression systems are likely the methods of choice for BSEP. Three different expression systems, which are also commercially available, are used the most: yeast, insect, and mammalian cell lines. Mammalian cell lines have the great advantage that they present the native environment of BSEP; these cells contain the native lipid environment, the native secretory/posttranslational pathways, and a known functional expression. Human BSEP could be expressed in different mammalian cell lines (e.g. HEK293 cells (50), HepG2 cells (51), MDCK cells (52) and LLC PK1 (53) cells) and characterized functionally without purification. The most widely used system for the heterologous expression of BSEP is the insect cell system. Human BSEP was expressed in *Sf9* (32,54) as well as HighFive cells (31). Insect cells exhibit a nonnative lipid environment with low levels of cholesterol as well as nonnative glycosylation (generally of the high-mannose type), but they resemble the native conditions more than yeast does. Expression in this system is used to investigate the transport properties of BSEP in vesicular-based transport assays. Cell culture-based systems may generally be suitable for addressing questions of a cellular phenotype, protein trafficking, and the modification of protein interactions. But mammalian and insect cell systems are also costly and maybe not be producible in large the amounts required for purification and structural studies of BSEP. From this point of view, a better choice might be yeast. Two yeast-based systems are used to overexpress mammalian membrane proteins: the previously mentioned *S. cerevisiae* and *Pichia pastoris*. The advantages are obvious: yeast is inexpensive, requires simple culture media, and exhibits well-studied genetics. Furthermore, yeasts have the eukaryotic modification machinery. Of course there are disadvantages, since, for example, the lipid composition of the membrane is different from that of mammalian cells (they contain ergosterol instead of cholesterol) and *S. cerevisiae* often hyperglycosylates proteins (highly branched and extended high-mannose structures), which is not observed in *P. pastoris*. It has been shown that BSEP requires glycosylation for transport activity in MDCK cells (55), although the type of glycosylation seems not to be important, as shown by functional expression in insect cells. *S. cerevisiae* was also used to express human P-gp (56) and MRP1 (57), and we were also able to express BSEP in this host (unpublished data), yielding only low amounts of fully translated protein. Therefore we switched to *P. pastoris*. This yeast was shown to overexpress 25 human ABC transporters (BSEP was not among them) and was also the expression host for mouse P-gp, which in the end and after a long endeavor resulted in the three dimensional x-ray structure (42,58). Recently we demonstrated the heterologous overexpression of human BSEP in

this yeast (47). Another advantage of *P. pastoris* is that this methylotrophic yeast strain can be fermented to high cell densities generating large amounts of biomass, which can be used for subsequent purification.

### 2.2.6 *In vitro* assays to study BSEP

Although BSEP has not been purified to homogeneity yet, assays have been described to study the function of BSEP *in vivo*. A vesicular transport assay is the most important one. It consists of three steps: (a) preparation of membrane vesicles, (b) addition of substrate and an energy source, and (c) readout of substrate uptake into the vesicles. In general there are two ways to prepare membrane vesicles from cells, right-side-out (RSO) and inside-out (IO) vesicles. In RSO vesicles, the cytosolic side of the transporter is localized in the lumen of the vesicles, whereas in IO vesicles it is vice versa. The latter ones are commonly used for primary transporters such as BSEP. With the addition of ATP and substrate, transport is initiated and the substrate begins to accumulate in the lumen of the vesicles. After a defined amount of time, the reaction is stopped by, for example, a rapid-filtration method; then the transported amount of substrate, which is retained in the vesicle on the filter, is quantified (via radioactivity, fluorescence, or LC/MS). With this assay, the substrate spectrum of BSEP was elucidated (see fTab. 2.1 for human BSEP). These assays were mainly performed with BSEP derived from insect cell vesicles (31,32) but also with vesicles originated from HEK293 cells or isolated canalicular membranes (52). Human BSEP transports monovalent conjugated bile salts in the order of taurochenodeoxycholate > taurocholate > tauroursodeoxycholate > glycocholate (it has to be

**Tab. 2.1:** Substrate spectra and Michaelis-Menten constant for human BSEP from different expression systems. For an excellent overview, see reference 60.

Substrate	$K_M$ / $\mu\text{M}$	Source
Taurocholate	8 (32), 20 (30, 61), 15(54)	Sf9
	4 (31)	HighFive
	6 (50)	
Taurochenodeoxycholate	4 (54), 5 (32), 13 (61)	Sf9
	7 (50)	HEK293
Tauroursodeoxycholate	12 (32)	Sf9
Taurodeoxycholate	34 (61)	Sf9
Taurolithocholate	4 (61)	Sf9
Taurolithocholate 3 sulfate	10 (50)	HEK293
Glycocholate	11 (32), 36 (54)	Sf9
	22 (50)	HEK293
Glycochenodeoxycholate	2 (54)	Sf9
	8 (50)	HEK293
Pravastatin	124 (62)	HEK293

mentioned, that the  $K_M$  values vary slightly between different expression systems but not unconjugated ones) (see Tab. 2.1). In most of these studies bile acids are tritium-labeled for readout, but fluorescent bile acid derivatives, such as cholyglycylamidofluorescein and chenodeoxycholyglycylamidofluorescein, have also been investigated (59). In addition, inhibitors were analyzed for their potential impact on BSEP. Inhibition of BSEP by different drugs causes drug-induced cholestasis, leading to severe liver injury (63). Examples of inhibitors that were determined for human BSEP by a vesicular uptake assay in competition experiments with bile salts include cyclosporine, rifampicin, and bosentan. These assays and the recommendation of the European Medicines Agency (64) emphasize the importance of BSEP for drug development. With a vesicular uptake assay for BSEP commercially available, the screening of drug libraries is in principle straightforward. One disadvantage of this kind of assay, however, is that besides the target transporter, the vesicles contain many irrelevant membrane proteins that probably affect the uptake assay. This can be excluded if proper controls are performed, but it complicates the assay.

Mutations in the *BSEP* gene can lead to an impairment of bile salt transport due to the protein's dysfunction. This can lead to PFIC2 or BRIC2, a severe liver disease, which at present can be cured only by liver transplantation (65). Currently, according to the Human Gene Mutation Database (<http://www.hgmd.org/>), 179 disease-related BSEP mutations are known. Thus an understanding of the effect of such mutations could, in the future, lead to therapeutic innovations that might cure this disease without transplantation. If, for example, mutated BSEP is still able to transport and the disease is caused by a trafficking defect, it could also be investigated by the vesicular transport assay, with mutation and localization studies in cell culture systems involving immunostaining or with a fluorescent tag like eGFP or YFP.

Trafficking and the regulation of BSEP in the apical membrane of hepatocytes also requires adaptor proteins. HCLS1-associated protein X-1 (Hax1), for example, was identified using yeast two-hybrid screens as well as pull-down assays with glutathione-S-transferase (GST) tag fusion proteins (soluble parts of BSEP with GST tag) and co-immunoprecipitation (66). Other adaptor proteins are still not known and would be of high interest, especially for the short-term regulation of BSEP or for their potential involvement in trafficking mutants.

## 2.3 Structure and function of the multidrug resistance protein 3 (ABCB4; MDR3)

As described in section 2.2.1, BSEP is essential for the circulation of bile salts. However, bile salts are harsh detergents and possess the power to solubilize any biological membrane. The outer leaflet of the canalicular membrane is destabilized by bile salts, which are translocated in the canaliculus by BSEP (ABCB11). To dampen this effect, bile salts and phosphatidylcholine (PC) form mixed micelles with cholesterol translocated by ABCG5/G8. These mixed micelles have a lower capacity to extract lipids from the membrane. A second function of PC is the solubilization of cholesterol, which prevents the crystallization of cholesterol in the biliary duct and the formation of cholesterol gallstones. The bulk of PC is reabsorbed in the intestine and returns to the hepatocyte within the enterohepatic cycle. However, the half-time of PC to flip spontaneously from

the inner to the outer leaflet of a lipid bilayer is very low; therefore PC must be translocated across the membrane of the hepatocyte by an active transporter. The multidrug resistance protein 3 (MDR3), also called ABCB4, is localized only in the canalicular membrane of the hepatocyte (Fig. 2.1) and is indispensable for the primary active transport of PC from the inner to the outer leaflet of the canalicular membrane against a concentration gradient. The mouse homologue is called *Mdr2* and fulfills the same function as MDR3 to flop PC across the apical membrane of hepatocytes. Mutations in the MDR3 gene caused different types of liver diseases, such as progressive familial intrahepatic cholestasis type 3 (PFIC3), intrahepatic cholestasis of pregnancy (ICP), and low phospholipid-associated cholestasis (LPAC).

### 2.3.1 A brief history of MDR3

During an analysis of cDNAs from human liver in 1987, van der Bliek et al. identified a gene that is highly homologous to the human P-gp and designated it *MDR3*. One year later the complete cDNA sequence was published (67). This sequence is composed of two similar halves. One half consists like BSEP of six putative TMHs and one NBD. The NBDs are identical to those of the human MDR1. Furthermore, the TMDs showed up to 80% identity. Divergence between MDR1 and MDR3 is greatest at the N-terminus and in the 60-amino acid linker connecting the two halves (67).

While MDR1 transports a wide variety of structural unrelated substances and is involved in multidrug resistance (MDR), no drug-pumping activity has been demonstrated for MDR3 (68). Smit and coworkers characterized mice with a disruption of *mdr2* in 1993. They ascertained that the homozygous disruption of the murine homologous *mdr2* gene leads to a complete absence of PC and cholesterol from bile (69). Furthermore, mice heterozygous for *Mdr2* (*Mdr2*<sup>+/+</sup>) have normal amounts of cholesterol and only 40% of PC in bile. Human MDR3 can functionally replace *mdr2* in knockout mice (70). This demonstrates that the closely related *Mdr2* and MDR3 carry out the same function. Direct evidence that MDR3 can translocate endogenous PC has been obtained in enhanced transport of newly synthesized [<sup>3</sup>H]choline-labeled PC to the surface of transgenic fibroblast (71). This suggested that MDR3 translocates specifically PC from the inner to the outer leaflet of the canicular membrane.

Van Helvoort and coworkers (72) were the first to demonstrate specific transport of a short-chain PC in polarized pig kidney epithelial cells transfected with MDR3. In this study they measured lipid translocation across the plasma membrane by extracting fluorescently labeled short-chain lipids from the cell surface into the basolateral and apical media. MDR3 translocated fluorescently labeled PC but not the other lipid analogues (72). However van Helvoort et al. showed that radiolabeled short-chain PC lacking the fluorescence moiety was not translocated into the apical medium by MDR3.

### 2.3.2 MDR3 – an ATP-binding cassette (ABC) transporter

The 141-kDa lipid translocase is postrationally modified by glycosylation at two predicted asparagine residues (N91 and N97) and is allocated to the group of P glycoproteins based on amino acid sequence homology. Like BSEP, MDR3 is a so called full-size transporter and is encoded on one structural gene (NBD-TMD)<sub>2</sub> (see Fig. 2.2).



### 2.3.2.1 Transport machinery – the flippase model

Two models, the “vacuum cleaner model” and the “flippase model”, are postulated for the transport of hydrophobic substrates by ABC transporters. The vacuum cleaner model proposes that the molecule in the cytosol interacts with the transporter, enters a hydrophobic cavity of the ABC-transporter, and is pumped into the extracellular space.

In contrast, Higgins and Gottesman proposed a flippase model for mammalian P-glycoproteins (73). P-gp binds an amphipathic molecule located in the inner leaflet of the plasma membrane and flips the molecule to the exoplasmic leaflet. Therefore a substrate-binding site must be accessible from the lipid phase. The substrate accumulates in the outer leaflet, forming a concentration gradient between the cytosolic and exoplasmic leaflet of the plasma membrane. From the leaflet the substrate can freely diffuse into the extracellular medium. On the basis of the flippase model, it is feasible to explain the observation that PC secretion depends on the expression of Mdr2, the mouse homolog of MDR3, and the bile salt concentration (74). Elferink and coworkers showed if either PC or bile salts were lacking, PC would not be detectable in bile, concluding that bile salts translocation is the main driving force for the secretion of phospholipids (75).

It is assumed that P-gp, which is over 76% identical to MDR3, can bind substrates within the inner leaflet of the membrane as well as from the cytosol. How ABC transporters recognize and translocate substrates is still unclear and the subject of intensive investigation.

### 2.3.2.2 MDR3 – a drug ABC transporter?

MDR3 shares 78% amino acid sequence identity with the well-characterized drug-pumping ABC transporter P-gp. Because of the high amino acid sequence homology between MDR3 and MDR1 (over 85%) it was assumed that MDR3 also translocates drugs. However, initial experiments with MDR3 cDNA or its mouse homolog Mdr2 transfected cells showed no drug resistance (67,76–78) and MDR3 was not detected in MDR cell lines (67,79). The first indication that MDR3 translocates drugs was obtained by Kino et al. (80). They observed that MDR3 transfected yeast cells showed low-level resistance against the antifungal agent aureobasidin A. Another study of MDR3 was performed by Smith et al. (81), who investigated vectorial substrate transport by polarized pig kidney monolayers transfected with MDR3 cDNA of several MDR1 substrates. They observed that the transport of digoxin, paclitaxel, vinblastine, and ivermectine into the apical medium was significantly increased in the MDR3-transfected cells compared with the control cells. Digoxin transport by MDR3 was efficiently inhibited by the MDR1-specific inhibitor verapamil, cyclosporine, and PSC833, which also inhibited the transport of short-chain PC. Verapamil had also previously been shown to inhibit the translocation of short-chain C<sub>6</sub>-NBD-PC (72,82). No significant transport of some other MDR1 substrates, such as cyclosporine or dexamethasone, was determined.

These results suggest that MDR3 is not specific for PC and is able to translocate various typical MDR1 substrates as well. But why is drug transport observed only in polarized monolayers transfected with MDR3 cDNA? Currently there is no satisfactory explanation. Further studies on the translocation of long-chain PC and drugs by MDR3 are required.

### 2.3.3 Analysis of the substrate specificity of the PC translocator

The analysis of lipid transporters is very complex by reason of the difficulty of developing a reliable assay for the molecular mechanism of lipid transporters. Following are described two different ways of analyzing the function of P-glycoproteins and especially lipid translocases. On the one hand, MDR3 translocates PC across the membrane; three different approaches to this have been reported. On the other hand, MDR3 hydrolyzes ATP. The resultant ATPase activity correlates indirectly with the substrate transport.

#### 2.3.3.1 Transport of lipids and lipid analogues by the ABC transporter

Currently no sensitive assay for measuring naturally occurring long-chain protein-mediated lipid translocation from one leaflet to the other leaflet of the membrane exists. Nevertheless Sleight and Pagano used the lower hydrophobicity of short-chain lipids ( $C_5$ - $C_6$  acyl chain) to determine lipid transport of lipid translocases, which allows their free exchange as monomers via the aqueous phase (83). At first short-chain lipids are easily integrated into the surface of the membrane of interest and can be detected by a spin-, fluorescent-, or radiolabel on the short-chain. The transport can be measured by chemically quenching of the spin-labeled or fluorescent analogue in the outer leaflet (84) or by “back-exchange.” To date two different systems to determine short-chain PC transport by MDR3 or the mouse-homologous Mdr2 have been described.

Ruetz and Gros expressed Mdr2 in the membrane of secretory vesicles obtained from a yeast secretion mutant (82). These vesicles can be easily isolated and consist of a pure population of inside-out vesicles, meaning that the cytoplasmic NBDs of the ABC transporter are located on the outside of the vesicle. To determine Mdr2-driven transport of PC from the outer leaflet into the inner leaflet of the vesicular membrane they used fluorescent-labeled short-chain PC –  $C_6$ -NBD-PC: (N-6[7-nitro-2,1,3-benzoxadiazol-4-yl]-amino-hexanoyl-phosphatidylcholine) – which is chemically reduced to the non-fluorescent compound by a membrane-impermeable reducing agent such as sodium dithionite. Dithionite reduces only the  $C_6$ -NBD-PC located in the outer leaflet, whereas the translocated  $C_6$ -NBD-PC in the inner leaflet remains unaffected. Detergent disruption of the vesicles lead to a decrease of fluorescence emission because of the release of translocated  $C_6$ -NBD-PC. With this system Ruetz and Gros proved indeed a very small but specific transport of short-chain PC analogue by Mdr2. Second, they showed that transport was ATP-dependent and inhibited by verapamil, a specific inhibitor for MDR1.

In the “back-exchange” method, short-chain lipids are extracted from the outer leaflet by bovine serum albumin (BSA). BSA has the ability to selectively bind short-chain lipids from the outer leaflet. The lipids are analyzed by two-dimensional thin layer chromatography (TLC) and the transport activity is calculated by the ratio between translocated and total amount of short-chain PC (85).

The floppase activity of MDR3 was confirmed by van Helvoort et al. using LLC-PK1 pig cells transfected with an MDR3 cDNA construct (72). LLC-PK1 cells are able to grow as monolayers on filters and MDR3 is found only in the apical membrane. Cells are cultured in the presence of a short-chain lipid precursor, which is taken up and converted into the corresponding short-chain lipid analogue. The intracellularly synthesized  $C_6$ -NBD-PC was specifically transported by MDR3 but not  $C_6$ -NBD-phosphatidylethanolamine,  $C_6$ -NBD-sphingomyelin, or  $C_6$ -NBD-glucosylceramide. Remarkably, radiolabeled short-chain PC with two  $C_8$  fatty acids lacking the fluorescence moiety

(C<sub>8</sub>C<sub>8</sub>-[<sup>3</sup>H]PC) were slightly translocated into the apical medium. Van Helvoort and colleagues confirmed that the high specificity of MDR3 is determined by the choline head group.

To date, only Smith and coworkers have been able to generate a system for the translocation of long-chain PC through the membrane of fibroblasts from transgenic mice by MDR3 (71). Intracellular synthesized radioactively labeled PC is inserted into the inner leaflet and translocated to the outer leaflet in the presence of MDR3. PC-TP, a PC-specific transfer protein, carries out the exchange of labeled PC from the outer leaflet to acceptor liposomes in the medium. In this study Smith et al. determined an increased translocation of long-chain PC in the presence of MDR3. One main drawback of this system is the high background in the absence of MDR3 by vesicular transport. This makes usage of this assay extremely complicated.

Thus far no in vitro system for the translocation of PC by MDR3 is established because of the challenge of cloning, expressing, and purifying functional MDR3 in sufficient amounts and the technical difficulty of measuring the translocation of natural PC.

### 2.3.3.2 Substrate-stimulated ATPase activity

ABC transporters hydrolyze ATP to energize the transport across the membrane. Since ATP hydrolysis is linked by substrate translocation, the transport activity can be visualized indirectly. Most ABC transporters offer a basal ATPase activity. This ATPase activity is stimulated or inhibited by adding the substrate or inhibitor. There are two assays for measuring the ATPase activity by the determination of released inorganic phosphate: the malachite green assay (86) and the NADH-coupled assay (87,88). Both assays measure the release of free orthophosphate.

The highly sensitive malachite green assay is based on the complex formation of free phosphate with molybdate. The reaction of phosphomolybdate and the dye malachite green results in a green complex, whose absorbance can be easily determined at a wavelength of 620 to 650 nm. Nevertheless, a disadvantage of this method is its inability to observe the hydrolytic reaction continuously. The NADH-coupled assay enables one to follow the rate of ATP hydrolysis in real time by coupling the release of P<sub>i</sub> and the oxidation of NADH to NAD<sup>+</sup>. The ATPase hydrolyzes ATP to ADP and P<sub>i</sub>. ADP is converted to ATP and phosphoenolpyruvate (PEP) to pyruvate by pyruvate kinase. The lactate dehydrogenase reduces pyruvate to lactate, while NADH is oxidized to NAD<sup>+</sup>. The decrease of NADH is then determined at a wavelength of 340 nm.

The precondition to measuring ATPase activity is simple: sufficient expression of MDR3. To date it has not been possible to clone and express functional MDR3 in bacterial systems such as *E. coli* or *L. lactis* because of the “toxic” or “unstable” DNA sequence (as described in section 2.2.5). The expression of MDR3 in mammalian cell lines such as LLC PK1 and insect cells has been demonstrated by different groups (72,82). However, the obtained protein amounts are not sufficient to purify MDR3. Thus, up to now, it has not been possible to measure the PC-stimulated ATPase activity of membrane vesicles containing MDR3 and/or of isolated MDR3 in detergent solution or reconstituted into liposomes. To overcome this major obstacle it is crucial to study MDR3 in vitro and obtain a more detailed knowledge of this interesting ABC transporter as expressed inside the liver.

## 2.4 Structure and function of the breast cancer resistance protein (ABCG2; BCRP)

### 2.4.1 History of ABCG2

ABCG2 was first identified in human (BCRP, ABCG2) carcinoma cells. Despite the absence of overexpression of known multidrug transporters, like P-gp or MRP1, these cells displayed a remarkable resistance to multiple chemotherapeutic drugs such as doxorubicin and mitoxantrone. The gene conferring this resistance was isolated and subsequently used to transfect carcinoma cells, which then displayed a diminished accumulation of daunorubicin in flow cytometry assays. Additionally, this transport function appeared to depend on the presence of ATP, and this transport protein was termed breast cancer resistance protein (BCRP; ABCG2) (89). Independently, ABCG2 was discovered as the determinant responsible for the resistance of human colon carcinoma cells selected in mitoxantrone. Isolated cDNA clones displayed high levels of resistance to mitoxantrone. The gene showed relation to the *Drosophila melanogaster* white gene and homology to ABC transporters; it was named MXR for “mitoxantrone resistance” (90). Furthermore, ABCG2 was identified among a group of new human ABC transporters that were found to be highly expressed in the placenta. The isolated cDNA contained an open reading frame of 655 amino acids consisting an ABC half-size transporter with an N-terminal NBD and a C-terminal TMD (91). Although it was discovered three times in different contexts, the gene involved always encoded ABCG2.

### 2.4.2 Structure and function of ABCG2

ABCG2 is a 72-kDa 655-amino acid glycoprotein. Among the members of the ABC transporter family, ABCG2 has, like other members of the ABCG subfamily, a reverse topology, meaning that the NBD is located N-terminal to the TMD. With only one NBD and one TMD encoded on a single gene, ABCG2 is considered to be a half-size transporter and thought to dimerize to become a functional ABC transporter (see →Fig. 2.2). Several studies have focused on this oligomerization behavior. Interestingly, intermolecular disulfide bonds are required to obtain a dimeric protein. Cysteine scanning mutagenesis revealed that residue C603 of ABCG2 is involved in intermolecular cross-linking via disulfide bonds (92). Additionally, no mutation of any other cysteine residue had an effect on the dimerization of ABCG2 or its activity. In agreement with these results, Henriksen et al. showed that the oligomeric species of ABCG2 was observed with the use of a nonreducing SDS-PAGE can be gradually disrupted by the addition of a reducing agent (93). Here, mutational analysis of the three cysteine residues located in the third extracellular loop showed that only the C603A mutant impaired dimerization. However, a cell survival assay with mitoxantrone showed that this mutation was still as resistant as the wild type, indicating that the disulfide bond is not essential for the transport function. A biotinylation assay supported the idea that the other two cysteine residues in this loop, C592 and C608, form an intramolecular disulfide bond. However, this disulfide bond is important for protein degradation (94).

An important feature of ABCG2 is the GXXXG motif, which has been identified as a recurring transmembrane sequence and is proposed to be an interaction site between the transmembrane  $\alpha$ -helices of different monomers. Polgar et al. investigated the only putative GXXXG motif in transmembrane helix 1 of ABCG2. Mutation of one or both of



the glycine residues resulted in lower ATP hydrolysis and a reduced substrate transport rate, although the protein was still expressed at similar levels on the cell surface. These findings support the hypothesis that the GXXXG motif plays a role for the correct orientation of the transmembrane segments toward each other in the functional transporter. Mutational studies of G553 indicate an involvement of this residue in the dimerization of ABCG2 (95).

Another important characteristic of ABCG2 is its hyperglycosylation, deduced from the apparent molecular weight of the protein in SDS PAGE gels and susceptibility to PNGaseF treatment. The glycosylation, however, appears to have no influence on the trafficking of ABCG2 to the plasma membrane. Surface expression was investigated by immunostaining of human ovarian carcinoma cells and hamster ovary cells. Although three glycosylation sites are predicted to be potentially located in the third extracellular loop, only the N569Q mutant showed impaired glycosylation. As mentioned in section 2.2.5, this impaired glycosylation does not result in mistrafficking, in contrast to, for example, the N557 alanine mutation, which results in a ER localization of ABCG2 (96).

Nonglycosylated ABCG2 still showed reduced accumulation of the substrate rhodamine 123 in flow-cytometric assays and normal ATPase activity, which can be stimulated by prazosin. The results were comparable to levels found for glycosylated ABCG2 in crude membrane preparations, indicating that glycosylation is not essential for the function of ABCG2. Many studies investigating the function of ABCG2 have employed mutagenesis to clarify the role of different residues in the protein. Residues C592, C603, and C608 are involved in intra- or intermolecular disulfide bonds and N596 is glycosylated. Furthermore, residue R482 has been extensively characterized. Early isolates of ABCG2 from carcinoma cell lines showed a mutation at this position. By testing the accumulation of rhodamine 123 in cells expressing the variants R482G and R482T, broader substrate specificity was observed (97). Whereas the wild-type protein conferred no resistance to compounds like rhodamine 123, doxorubicin, or daunorubicin, expression of ABCG2 and the mutants R482G and R482T reduced the accumulation of the drugs and prolonged cell survival in cytotoxicity assays. Other compounds – like mitoxantrone, prazosin, and Hoechst 33342 – are substrates for both mutant and wild-type transporters (98,99). A later study confirmed previous results and additionally observed binding of substrates, which are not transported to the wild-type transporter (100).

A common single-nucleotide polymorphism encoding the mutation Q141K is linked with the occurrence of gout. ABCG2 was shown to be located in the brush-border membrane of kidney proximal tubule cells. Functional assays with *X. laevis* oocytes expressing wild-type ABCG2 or Q141K mutant showed that the latter exhibited urate efflux, thereby linking ABCG2 to this genetic disease (101). A recent study revealed that this mutant is exhibiting increased susceptibility for lysosomal and proteasomal degradation (102).

### 2.4.3 Analysis of the substrate specificity of ABCG2

Owing to the discovery of ABCG2 in drug-resistant cells, the first reported substrates for it were predominantly chemotherapeutic drugs. These included mitoxantrone, flavopiridol, metothrexate, irinotecan and its active metabolite SN-38, porphyrines, and tyrosine kinase inhibitors such as imatinib and gefitinib (103). Other substrates are antibiotics (104,105), flavonoids, antivirals (106,107), folic acid (108), and fluorescent dyes such

as Hoechst 33342. Mutation of the arginine residue at position 482 conveys a broader substrate spectrum including rhodamine 123 and anthracyclines such as doxorubicin. Because of its broad substrate spectrum and its expression in several tissues apart from the liver – such as the small intestine, colon, central nervous system, testis, ovary, and placental syncytiotrophoblasts – the transporter is thought to have a protective role (103,109,110). The number of ABCG2 inhibitors identified is equally large. Fumitremorgin C was the first inhibitor described (111). Its analog, Ko143, was found to be one of the most effective ABCG2 inhibitors (112). Some inhibitors were also inhibitors of P-gp or MRP – among them cyclosporine (113) and elacridar (GF120918)(114). Many compounds are both inhibitors and transported substrates, such as dihydropyridines (115). Despite the great number of substrates and inhibitors described to date, no clear structural requirements for a binding compound could be identified.

#### 2.4.4 Expression, purification, and biochemical studies of ABCG2

To date, ABCG2 has been successfully expressed in a number of different vector systems and host organisms. Early studies have been done with drug-selected mammalian cell lines. Finally, the isolation of the cDNA offered the opportunity to move the expression to some heterologous hosts, such as *Xenopus* oocytes, insect cells, yeast, or bacteria.

Baculovirus-infected insect ovary cells (*Sf9*) and High Five cells offer an alternative to mammalian cell lines and have been successfully used to overexpress ABCG2, although in both cases hypoglycosylation, transport, and ATPase activity were observed (116,117). Other expression systems include yeasts like *P. pastoris* and *S. cerevisiae*. Mao et al. expressed ABCG2 in *P. pastoris*, obtaining active protein comprising about 3% of the total protein in microsome preparations (118). Similar expression levels could be observed in baker's yeast, yielding protein with ATPase activity, which could be stimulated by substrate (119). Additionally, a prokaryotic expression system has been reported employing the gram-positive bacterium *L. lactis* (120). Expression in another bacterial system, *E. coli*, did not yield functional protein (121).

Especially for the purification of ABCG2 from the membrane fraction of the expression host, a high yield is needed. Protein expression of the systems mentioned previously in this section was tested on the ability to obtain high yields of ABCG2 after purification. Solubilization of ABCG2 using different detergents showed the best results with the use of lysophosphatidylcholine (LPC) and n-dodecyl- $\beta$ -D-maltoside ( $\beta$ -DDM) for *P. pastoris* membranes and FosCholine-14 and -16 for ABCG2 expressed in insect cells (122,123). Also used for solubilization of protein from insect cell membranes was CHAPS (117). Purification steps of the amino-terminal-histidine-tagged protein in all cases yielded sufficiently pure protein after immobilized metal-ion affinity chromatography (IMAC). Because of weak binding to the affinity resin, further purification steps were necessary when the insect cell expression system was used. These included ion exchange and size exclusion chromatography (117). ABCG2 retained ATPase activity and substrate binding after its purification.

Because of its ability to efflux a broad variety of substrates, multiple drug binding sites have been proposed for ABCG2. Clark et al. investigated this with heterologous displacement assays. [ $^3$ H]daunomycin binding constants were measured in the presence of other known substrates of the ABCG2 gain-of-function mutant R482G. Three distinct binding sites were proposed, which are interlinked by allosteric communication (124). Several

studies of the substrate specificity and drug binding could be obtained by employing fluorescent substrates of ABCG2. For example 1,4-dihydropyridines could be identified as ABCG2 substrates by photoaffinity labeling with [ $^{125}$ I]Iodoarylazidoprazosin (IAAP) and [ $^3$ H]azidopine (125).

Since the translocation process is ATP-dependent, the ATPase activity of ABCG2 has been measured to confirm its physiologic activity. The majority of kinetic parameters were obtained on membrane preparations containing other ATPases. The wild type and the R482G isoform are capable of hydrolyzing ATP in the absence of any substrate (98). Since the influence of substrates and inhibitors on hydrolytic activity is an indicator of interaction with the protein, the measurement of ATPase activity is the focus of several studies. ATPase activity has been used as a readout in order to identify cholesterol content of the membrane as a major factor in ABCG2 activity (126). Cholesterol loading and depletion experiments showed stimulation of ATPase activity by substrates and improved drug transport in cholesterol-loaded membranes. In contrast, ATPase activity could not be stimulated in cholesterol-depleted membranes, indicating an essential role of membrane cholesterol.

Another tool to gain further knowledge about the topology of ABCG2 is epitope insertion mutagenesis. One study employed hemagglutinin (HA) tags to probe the predicted hydrophilic regions of ABCG2 via immunofluorescence (127). The results supported a model of six transmembrane helices with the amino and carboxy termini located intracellularly. A later study investigated a current homology model of ABCG2 by epitope insertion and found significant differences in the location of the predicted transmembrane segments (122).

To date there are no high-resolution structural data on ABCG2, although some attempts to obtain such data have been undertaken. These include negative-stain electron cryomicroscopy of purified protein. ABCG2 overexpressed in insect cells was solubilized and retained its stimulated ATPase activity. Analysis of the electron microscopy data revealed large particles (~170 Å in diameter) with a noticeable fourfold symmetry, in agreement with a higher oligomer as postulated by biochemical analysis. The final three-dimensional structure with an estimated resolution of ~18 Å could be accurately fitted with homology models of ABCG2, forming a tetramer. Data from size-exclusion chromatography and blue native PAGE supported the idea that ABCG2 forms a higher-order oligomeric species under the tested conditions (122).

Rosenberg et al. used purified ABCG2 expressed in *P.pastoris* to obtain two-dimensional crystals. The substrate mitoxantrone had a noticeable effect on the crystal shape. Analysis showed a significant change in unit cell dimensions, indicating a conformational change upon drug binding. A new homology model verified by epitope insertion mutagenesis supported the structural data by showing rigid body motion of two transmembrane helices, leading to a more compact conformation of the transporter in the drug-bound state. However, a three-dimensional structure is still a long way off. Eventually that will provide a detailed look at the function of ABCG2 at the molecular level.

## 2.5 Concluding remarks

Several interesting transporters are expressed within the hepatocytes, contributing to the function of these cells. This chapter focused on three of them, BSEP, MDR3, and

ABCG2. A wealth of information is to be derived from studies of their expression and mutation in different mammalian cell lines – studies focusing on their localization, trafficking, and activity. Although such studies have revealed extremely valuable and often essential information, the next step must be to achieve a molecular understanding of these transport mechanisms. Here, the first prerequisite is to elucidate the overexpression of these transporters, which will lead to their characterization directly in isolated membranes and/or after subsequent solubilization and purification in detergent solution. As described and summarized, the expression of membrane proteins is by no means trivial and often hampered by a too low expression in homo- or heterologous expression systems. However, if overexpression can be achieved for BSEP, MDR3, or ABCG2, the gain in knowledge derived from localization studies as well as mutational analysis will shed much light on the molecular mechanism of transport of a large variety of substrates with ATP only as an energizing molecule. Truly it will be a long way to go, but the information obtained will be worth the effort.

## 2.6 References

1. Schmitt L, R Tampe. Structure and mechanism of ABC transporters. *Current opinion in structural biology* 2002;12(6):754–60.
2. Zaitseva J, et al. A molecular understanding of the catalytic cycle of the nucleotide-binding domain of the ABC transporter HlyB. *Biochemical Society transactions* 2005;33 (Pt 5):990–5.
3. Schmitt L, et al. Crystal structure of the nucleotide-binding domain of the ABC-transporter haemolysin B: identification of a variable region within ABC helical domains. *Journal of molecular biology* 2003;330(2):333–42.
4. Jardetzky O. Simple allosteric model for membrane pumps. *Nature* 1966;211(5052):969–70.
5. Higgins CF, KJ Linton. The ATP switch model for ABC transporters. *Nature structural & molecular biology* 2004;11(10): 918–26.
6. Russell DW. Fifty years of advances in bile acid synthesis and metabolism. *Journal of lipid research* 2009;S120–5.
7. Hofmann AF. Bile acids: trying to understand their chemistry and biology with the hope of helping patients. *Hepatology* 2009;49(5):1403–18.
8. Hofmann AF, LR Hagey. Bile acids: chemistry, pathochemistry, biology, pathobiology, and therapeutics. *Cellular and molecular life sciences: CMLS* 2008;65(16):2461–83.
9. Kullak-Ublick GA, B Stieger, PJ Meier. Enterohepatic bile salt transporters in normal physiology and liver disease. *Gastroenterology* 2004;126(1):322–42.
10. Hofmann AF. Bile acids: the good, the bad, and the ugly. *News in physiological sciences : an international journal of physiology produced jointly by the International Union of Physiological Sciences and the American Physiological Society* 1999;14:24–9.
11. Meier PJ, B Stieger. Bile salt transporters. *Annual review of physiology* 2002;64:635–61.
12. Kullak-Ublick GA, et al. Hepatic transport of bile salts. *Seminars in liver disease* 2000;20(3):273–92.
13. Hagenbuch B, P Dawson. The sodium bile salt cotransport family SLC10. *Pflügers Archiv: European journal of physiology* 2004;447(5):566–70.
14. Meier PJ, et al. Substrate specificity of sinusoidal bile acid and organic anion uptake systems in rat and human liver. *Hepatology* 1997;26(6):1667–77.
15. Agellon LB, EC Torchia. Intracellular transport of bile acids. *Biochimica et biophysica acta* 2000;1486(1):198–209.



## 42 | 2 Structure and function of hepatic ABC transporters

16. Arrese M, M Ananthanarayanan. The bile salt export pump: molecular properties, function and regulation. *Pflugers Archiv: European journal of physiology* 2004;449(2):123–31.
17. Stieger B, Y Meier, PJ Meier. The bile salt export pump. *Pflugers Archiv: European journal of physiology* 2007;453(5):611–20.
18. Meier PJ, AS Meier-Abt, JL Boyer. Properties of the canalicular bile acid transport system in rat liver. *The Biochemical journal* 1987;242(2):465–9.
19. Weinman SA, J Graf, JL Boyer. Voltage-driven, taurocholate-dependent secretion in isolated hepatocyte couplets. *The American journal of physiology* 1989;256(5 Pt 1):G826–32.
20. Adachi Y, et al. ATP-dependent taurocholate transport by rat liver canalicular membrane vesicles. *Hepatology* 1991;14(4 Pt 1):655–9.
21. Muller M, et al. ATP-dependent transport of taurocholate across the hepatocyte canalicular membrane mediated by a 110-kDa glycoprotein binding ATP and bile salt. *The Journal of biological chemistry* 1991;266(28):18920–6.
22. Brown RS, Jr., et al. Enhanced secretion of glycocholic acid in a specially adapted cell line is associated with overexpression of apparently novel ATP-binding cassette proteins. *Proceedings of the National Academy of Sciences of the United States of America* 1995;92(12):5421–5.
23. Childs S, et al. Identification of a sister gene to P-glycoprotein. *Cancer research* 1995;55(10):2029–34.
24. Gerloff T, et al. The sister of P-glycoprotein represents the canalicular bile salt export pump of mammalian liver. *The Journal of biological chemistry* 1998;273(16):10046–50.
25. Strautnieks SS, et al. A gene encoding a liver-specific ABC transporter is mutated in progressive familial intrahepatic cholestasis. *Nature genetics* 1998;20(3):233–8.
26. Green RM, F Hoda, KL Ward. Molecular cloning and characterization of the murine bile salt export pump. *Gene* 2000;241(1):117–23.
27. Lecureur V, et al. Cloning and expression of murine sister of P-glycoprotein reveals a more discriminating transporter than MDR1/P-glycoprotein. *Molecular pharmacology* 2000;57(1):24–35.
28. Noe J, et al. Characterization of the mouse bile salt export pump overexpressed in the baculovirus system. *Hepatology* 2001;33(5):1223–31.
29. Xu G, et al. Removal of the bile acid pool upregulates cholesterol 7 $\alpha$ -hydroxylase by deactivating FXR in rabbits. *Journal of lipid research* 2002;43(1):45–50.
30. Yabuuchi H, et al. Cloning of the dog bile salt export pump (BSEP; ABCB11) and functional comparison with the human and rat proteins. *Biopharmaceutics & drug disposition* 2008;29(8):441–8.
31. Byrne JA, et al. The human bile salt export pump: characterization of substrate specificity and identification of inhibitors. *Gastroenterology* 2002;123(5):1649–58.
32. Noe J, B Stieger, PJ Meier. Functional expression of the canalicular bile salt export pump of human liver. *Gastroenterology* 2002;123(5):1659–66.
33. Ballatori N, et al. Bile salt excretion in skate liver is mediated by a functional analog of Bsep/Spgp, the bile salt export pump. *American journal of physiology. Gastrointestinal and liver physiology* 2000;278(1):G57–63.
34. Cai SY, et al. Bile salt export pump is highly conserved during vertebrate evolution and its expression is inhibited by PFIC type II mutations. *American journal of physiology. Gastrointestinal and liver physiology* 2001;281(2):G316–22.
35. Moitra K, M Dean. Evolution of ABC transporters by gene duplication and their role in human disease. *Biological chemistry* 2011;392(1–2):29–37.
36. Higgins CF. ABC transporters: from microorganisms to man. *Annual review of cell biology* 1992;8:67–113.
37. Dean M, A Rzhetsky, R Allikmets. The human ATP-binding cassette (ABC) transporter superfamily. *Genome research* 2001;11(7):1156–66.

38. Allikmets R, et al. Characterization of the human ABC superfamily: isolation and mapping of 21 new genes using the expressed sequence tags database. *Human molecular genetics* 1996;5(10):1649–55.
39. Gadsby DC, P Vergani, L Csanady. The ABC protein turned chloride channel whose failure causes cystic fibrosis. *Nature* 2006;440(7083):477–83.
40. Davit-Spraul A, et al. The spectrum of liver diseases related to ABCB4 gene mutations: pathophysiology and clinical aspects. *Seminars in liver disease* 2010;30(2):134–46.
41. Ernst R, et al. Engineering ATPase activity in the isolated ABC cassette of human TAP1. *The Journal of biological chemistry* 2006;281(37):27471–80.
42. Aller SG, et al. Structure of P-glycoprotein reveals a molecular basis for poly-specific drug binding. *Science* 2009;323(5922):1718–22.
43. Byrne JA, et al. Missense mutations and single nucleotide polymorphisms in ABCB11 impair bile salt export pump processing and function or disrupt pre-messenger RNA splicing. *Hepatology* 2009;49(2):553–67.
44. Vu K, et al. The functional expression of toxic genes: lessons learned from molecular cloning of CCH1, a high-affinity Ca<sup>2+</sup> channel. *Analytical biochemistry* 2009;393(2):234–41.
45. Ma H, et al. Plasmid construction by homologous recombination in yeast. *Gene* 1987;58(2–3):201–16.
46. Oldenburg KR, et al. Recombination-mediated PCR-directed plasmid construction in vivo in yeast. *Nucleic acids research* 1997;25(2):451–2.
47. Stindt J, et al. Heterologous overexpression and mutagenesis of the human bile salt export pump (ABCB11) using DREAM (Directed REcombination-Assisted Mutagenesis). *PloS one* 2011;6(5): e20562.
48. Schlegel S, et al. Revolutionizing membrane protein overexpression in bacteria. *Microbial biotechnology* 2010;3(4):403–11.
49. Kunji ER, et al. Eukaryotic membrane protein overproduction in *Lactococcus lactis*. *Current opinion in biotechnology* 2005;16(5):546–51.
50. Hayashi H, et al. Transport by vesicles of glycine- and taurine-conjugated bile salts and tauroolithocholate 3-sulfate: a comparison of human BSEP with rat Bsep. *Biochimica et biophysica acta* 2005;1738(1–3):54–62.
51. Kubitz R, et al. Trafficking of the bile salt export pump from the Golgi to the canalicular membrane is regulated by the p38 MAP kinase. *Gastroenterology* 2004;126(2):541–53.
52. Hayashi H, et al. Two common PFIC2 mutations are associated with the impaired membrane trafficking of BSEP/ABCB11. *Hepatology* 2005;41(4):916–24.
53. Mita S, et al. Vectorial transport of unconjugated and conjugated bile salts by monolayers of LLC-PK1 cells doubly transfected with human NTCP and BSEP or with rat Ntcp and Bsep. *American journal of physiology. Gastrointestinal and liver physiology* 2006;290(3):G550–6.
54. Kis E, et al. Effect of membrane cholesterol on BSEP/Bsep activity: species specificity studies for substrates and inhibitors. *Drug metabolism and disposition: the biological fate of chemicals* 2009;37(9):1878–86.
55. Mochizuki K, et al. Two N-linked glycans are required to maintain the transport activity of the bile salt export pump (ABCB11) in MDCK II cells. *American journal of physiology. Gastrointestinal and liver physiology* 2007;292(3):G818–28.
56. Mao Q, GA Scarborough. Purification of functional human P-glycoprotein expressed in *Saccharomyces cerevisiae*. *Biochimica et biophysica acta* 1997;1327(1):107–18.
57. Lee SH, GA Altenberg. Expression of functional multidrug-resistance protein 1 in *Saccharomyces cerevisiae*: effects of N- and C-terminal affinity tags. *Biochemical and biophysical research communications* 2003;306(3):644–9.

## 44 | 2 Structure and function of hepatic ABC transporters

58. Chloupkova M, et al. Expression of 25 human ABC transporters in the yeast *Pichia pastoris* and characterization of the purified ABCC3 ATPase activity. *Biochemistry* 2007;46(27):7992–8003.
59. Mita S, et al. Inhibition of bile acid transport across Na<sup>+</sup>/taurocholate cotransporting polypeptide (SLC10A1) and bile salt export pump (ABCB11)-coexpressing LLC-PK1 cells by cholestasis-inducing drugs. *Drug metabolism and disposition: the biological fate of chemicals* 2006;34(9):1575–81.
60. Stieger B. The role of the sodium-taurocholate cotransporting polypeptide (NTCP) and of the bile salt export pump (BSEP) in physiology and pathophysiology of bile formation. *Handbook of experimental pharmacology* 2011;(201):205–59.
61. Yamaguchi K, et al. Measurement of the transport activities of bile salt export pump using LC-MS. *Analytical sciences: the international journal of the Japan Society for Analytical Chemistry* 2009;25(9): 1155–8.
62. Hirano M, et al. Bile salt export pump (BSEP/ABCB11) can transport a nonbile acid substrate, pravastatin. *The Journal of pharmacology and experimental therapeutics* 2005;314(2):876–82.
63. Pauli-Magnus C, PJ Meier, B Stieger. Genetic determinants of drug-induced cholestasis and intrahepatic cholestasis of pregnancy. *Seminars in liver disease* 2010;30(2):147–59.
64. (EMA), T.E.M.A., Guideline on the Investigation of Drug Interactions 2010: 38.
65. Stapelbroek JM, et al. Liver disease associated with canalicular transport defects: current and future therapies. *Journal of hepatology* 2010;52(2):258–71.
66. Ortiz DF, et al. Identification of HAX-1 as a protein that binds bile salt export protein and regulates its abundance in the apical membrane of Madin-Darby canine kidney cells. *The Journal of biological chemistry* 2004;279(31):32761–70.
67. van der Bliek, AM, et al. Sequence of *mdr3* cDNA encoding a human P-glycoprotein. *Gene* 1988;71(2):401–11.
68. Gros P, E Buschman. The mouse multidrug resistance gene family: structural and functional analysis. *International review of cytology* 1993;137C:169–97.
69. Smit JJ, et al. Homozygous disruption of the murine *mdr2* P-glycoprotein gene leads to a complete absence of phospholipid from bile and to liver disease. *Cell* 1993;75(3):451–62.
70. Smith AJ, et al. Hepatocyte-specific expression of the human MDR3 P-glycoprotein gene restores the biliary phosphatidylcholine excretion absent in *Mdr2* (-/-) mice. *Hepatology* 1998;28(2):530–6.
71. Smith AJ, et al. The human MDR3 P-glycoprotein promotes translocation of phosphatidylcholine through the plasma membrane of fibroblasts from transgenic mice. *FEBS letters* 1994;354(3):263–6.
72. van Helvoort A, et al. MDR1 P-glycoprotein is a lipid translocase of broad specificity, while MDR3 P-glycoprotein specifically translocates phosphatidylcholine. *Cell* 1996;87(3):507–17.
73. Higgins CF, MM Gottesman. Is the multidrug transporter a flippase? *Trends in biochemical sciences* 1992;17(1):18–21.
74. Elferink RP, et al. Class III P-glycoproteins mediate the formation of lipoprotein X in the mouse. *The Journal of clinical investigation* 1998;102(9):1749–57.
75. Oude Elferink RP, AK Groen. Mechanisms of biliary lipid secretion and their role in lipid homeostasis. *Seminars in liver disease* 2000;20(3):293–305.
76. Gros P, et al. Cloning and characterization of a second member of the mouse *mdr* gene family. *Molecular and cellular biology* 1988;8(7):2770–8.
77. Buschman E, P Gros. Functional analysis of chimeric genes obtained by exchanging homologous domains of the mouse *mdr1* and *mdr2* genes. *Molecular and cellular biology* 1991;11(2):595–603.

78. Buschman E, P Gros. The inability of the mouse *mdr2* gene to confer multidrug resistance is linked to reduced drug binding to the protein. *Cancer research* 1994;54(18):4892–8.
79. Raymond M, et al. Physical mapping, amplification, and overexpression of the mouse *mdr* gene family in multidrug-resistant cells. *Molecular and cellular biology* 1990;10(4):1642–51.
80. Kino K, et al. Aureobasidin A, an antifungal cyclic depsipeptide antibiotic, is a substrate for both human MDR1 and MDR2/P-glycoproteins. *FEBS letters* 1996;399(1–2):29–32.
81. Smith AJ, et al. MDR3 P-glycoprotein, a phosphatidylcholine translocase, transports several cytotoxic drugs and directly interacts with drugs as judged by interference with nucleotide trapping. *The Journal of biological chemistry* 2000;275(31):23530–9.
82. Ruetz S, P Gros. Phosphatidylcholine translocase: a physiological role for the *mdr2* gene. *Cell* 1994;77(7):1071–81.
83. Sleight RG, RE Pagano. Transbilayer movement of a fluorescent phosphatidylethanolamine analogue across the plasma membranes of cultured mammalian cells. *The Journal of biological chemistry* 1985;260(2):1146–54.
84. Margolles A, et al. The purified and functionally reconstituted multidrug transporter LmrA of *Lactococcus lactis* mediates the transbilayer movement of specific fluorescent phospholipids. *Biochemistry* 1999;38(49):16298–306.
85. van Genderen I, G van Meer. Differential targeting of glucosylceramide and galactosylceramide analogues after synthesis but not during transcytosis in Madin-Darby canine kidney cells. *The Journal of cell biology* 1995;131(3):645–54.
86. Baykov AA, OA Evtushenko, SM Avaeva. A malachite green procedure for orthophosphate determination and its use in alkaline phosphatase-based enzyme immunoassay. *Analytical biochemistry* 1988;171(2):266–70.
87. Kornberg A, WE Pricer, Jr. Enzymatic phosphorylation of adenosine and 2,6-diaminopurine riboside. *The Journal of biological chemistry* 1951;193(2):481–95.
88. Lindsley JE. Use of a real-time, coupled assay to measure the ATPase activity of DNA topoisomerase II. *Methods in molecular biology* 2001;95:57–64.
89. Doyle LA, et al. A multidrug resistance transporter from human MCF-7 breast cancer cells. *Proceedings of the National Academy of Sciences of the United States of America* 1998;95(26):15665–70.
90. Miyake K, et al. Molecular cloning of cDNAs which are highly overexpressed in mitoxantrone-resistant cells: demonstration of homology to ABC transport genes. *Cancer research* 1999;59(1):8–13.
91. Allikmets R, M Dean. Cloning of novel ABC transporter genes. *Methods in enzymology* 1998;292:116–30.
92. Kage K, T Fujita, Y Sugimoto. Role of Cys-603 in dimer/oligomer formation of the breast cancer resistance protein BCRP/ABCG2. *Cancer science* 2005;96(12):866–72.
93. Henriksen U, et al. Identification of intra- and intermolecular disulfide bridges in the multidrug resistance transporter ABCG2. *The Journal of biological chemistry* 2005;280(44):36926–34.
94. Wakabayashi K, et al. Intramolecular disulfide bond is a critical check point determining degradative fates of ATP-binding cassette (ABC) transporter ABCG2 protein. *The Journal of biological chemistry* 2007;282(38):27841–6.
95. Polgar O, et al. Mutational studies of G553 in TM5 of ABCG2: a residue potentially involved in dimerization. *Biochemistry* 2006;45(16):5251–60.
96. Motamedi K, et al. Villonodular synovitis (PVNS) of the spine. *Skeletal radiology* 2005;34(4):185–95.
97. Honjo Y, et al. Acquired mutations in the MXR/BCRP/ABCP gene alter substrate specificity in MXR/BCRP/ABCP-overexpressing cells. *Cancer research* 2001;61(18):6635–9.



## 46 \ 2 Structure and function of hepatic ABC transporters

98. Ozvegy C, A Varadi, B Sarkadi. Characterization of drug transport, ATP hydrolysis, and nucleotide trapping by the human ABCG2 multidrug transporter. Modulation of substrate specificity by a point mutation. *The Journal of biological chemistry* 2002;277(50):47980–90.
99. Robey RW, et al. Mutations at amino-acid 482 in the ABCG2 gene affect substrate and antagonist specificity. *British journal of cancer* 2003;89(10):1971–8.
100. Ejendal KF, et al. The nature of amino acid 482 of human ABCG2 affects substrate transport and ATP hydrolysis but not substrate binding. *Protein science: a publication of the Protein Society* 2006;15(7):1597–607.
101. Woodward OM, et al. Identification of a urate transporter, ABCG2, with a common functional polymorphism causing gout. *Proceedings of the National Academy of Sciences of the United States of America* 2009;106(25):10338–42.
102. Furukawa T, et al. Major SNP (Q141K) variant of human ABC transporter ABCG2 undergoes lysosomal and proteasomal degradations. *Pharmaceutical research* 2009;26(2):469–79.
103. Polgar O, RW Robey, SE Bates. ABCG2: structure, function and role in drug response. *Expert opinion on drug metabolism & toxicology* 2008;4(1):1–15.
104. Merino G, et al. Breast cancer resistance protein (BCRP/ABCG2) transports fluoroquinolone antibiotics and affects their oral availability, pharmacokinetics, and milk secretion. *Drug metabolism and disposition: the biological fate of chemicals* 2006;34(4):690–5.
105. Merino G, et al. Transport of anthelmintic benzimidazole drugs by breast cancer resistance protein (BCRP/ABCG2). *Drug metabolism and disposition: the biological fate of chemicals* 2005;33(5):614–18.
106. Wang X, et al. Breast cancer resistance protein (BCRP/ABCG2) induces cellular resistance to HIV-1 nucleoside reverse transcriptase inhibitors. *Molecular pharmacology* 2003;63(1):65–72.
107. Wang X, et al. Induction of cellular resistance to nucleoside reverse transcriptase inhibitors by the wild-type breast cancer resistance protein. *Biochemical pharmacology* 2004;68(7):1363–70.
108. Chen ZS, et al. Transport of methotrexate, methotrexate polyglutamates, and 17beta-estradiol 17-(beta-D-glucuronide) by ABCG2: effects of acquired mutations at R482 on methotrexate transport. *Cancer research* 2003;63(14):4048–54.
109. Litman T, et al. Use of peptide antibodies to probe for the mitoxantrone resistance-associated protein MXR/BCRP/ABCP/ABCG2. *Biochimica et biophysica acta* 2002;1565(1):6–16.
110. Fetsch JF, WB Laskin, M Miettinen. Nerve sheath myxoma: a clinicopathologic and immunohistochemical analysis of 57 morphologically distinctive, S-100 protein- and GFAP-positive, myxoid peripheral nerve sheath tumors with a predilection for the extremities and a high local recurrence rate. *The American journal of surgical pathology* 2005;29(12):1615–24.
111. Rabindran SK, et al. Fumitremorgin C reverses multidrug resistance in cells transfected with the breast cancer resistance protein. *Cancer research* 2000;60(1):47–50.
112. Allen JD, et al. Potent and specific inhibition of the breast cancer resistance protein multidrug transporter in vitro and in mouse intestine by a novel analogue of fumitremorgin C. *Molecular cancer therapeutics* 2002;1(6):417–25.
113. Qadir M, et al. Cyclosporin A is a broad-spectrum multidrug resistance modulator. *Clinical cancer research: an official journal of the American Association for Cancer Research* 2005;11(6):2320–6.
114. de Bruin M, et al. Reversal of resistance by GF120918 in cell lines expressing the ABC half-transporter, MXR. *Cancer letters* 1999;146(2):117–26.

115. Zhou S, et al. Increased expression of the Abcg2 transporter during erythroid maturation plays a role in decreasing cellular protoporphyrin IX levels. *Blood* 2005;105(6):2571–6.
116. Ozvegy C, et al. Functional characterization of the human multidrug transporter, ABCG2, expressed in insect cells. *Biochemical and biophysical research communications* 2001;285(1):111–17.
117. Pozza A, et al. Purification of breast cancer resistance protein ABCG2 and role of arginine-482. *Cellular and molecular life sciences: CMLS* 2006;63(16):1912–22.
118. Mao Q, et al. Functional expression of the human breast cancer resistance protein in *Pichia pastoris*. *Biochemical and biophysical research communications* 2004;320(3):730–7.
119. Jacobs A, et al. Recombinant synthesis of human ABCG2 expressed in the yeast *Saccharomyces cerevisiae*: an experimental methodological study. *The protein journal* 2011;30(3):201–11.
120. Janvilisri T, et al. Sterol transport by the human breast cancer resistance protein (ABCG2) expressed in *Lactococcus lactis*. *The Journal of biological chemistry* 2003;278(23):20645–51.
121. Pozza A, JM Perez-Victoria, A Di Pietro. Insect cell versus bacterial overexpressed membrane proteins: an example, the human ABCG2 transporter. *Methods in molecular biology* 2010;654:47–75.
122. Rosenberg MF, et al. The human breast cancer resistance protein (BCRP/ABCG2) shows conformational changes with mitoxantrone. *Structure* 2010;18(4):482–93.
123. McDevitt CA, et al. Purification and 3D structural analysis of oligomeric human multidrug transporter ABCG2. *Structure* 2006;14(11):1623–32.
124. Clark R, ID Kerr, R Callaghan. Multiple drugbinding sites on the R482G isoform of the ABCG2 transporter. *British journal of pharmacology* 2006;149(5):506–15.
125. Shukla S, et al. The calcium channel blockers, 1,4-dihydropyridines, are substrates of the multidrug resistance-linked ABC drug transporter, ABCG2. *Biochemistry* 2006;45(29):8940–51.
126. Pal A, et al. Cholesterol potentiates ABCG2 activity in a heterologous expression system: improved in vitro model to study function of human ABCG2. *The Journal of pharmacology and experimental therapeutics* 2007;321(3):1085–94.
127. Wang H, et al. Membrane topology of the human breast cancer resistance protein (BCRP/ABCG2) determined by epitope insertion and immunofluorescence. *Biochemistry* 2008;47(52):13778–87.

## Chapter II – Optimization of the Expression and Purification of MDR3

### Title:

**Expression of human *MDR3* in *Saccharomyces cerevisiae* and *Pichia pastoris*  
and optimization of the purification using cyclodextrin**

Own Proportion to this work: 80 %

Expression of human MDR3 in *S. cerevisiae* and *P. pastoris*  
Subcellular localization of MDR3 in *S. cerevisiae* and  
*P. pastoris* using sucrose gradient centrifugation  
Detergent screen  
Purification of MDR3 by tandem-affinity purification  
Size exclusion chromatography

## **Expression of human *MDR3* in *Saccharomyces cerevisiae* and *Pichia pastoris* and optimization of the purification using cyclodextrin**

In humans, 48 ATP-binding cassette (ABC) transporters were identified and classified into seven subfamilies, ABCA-ABCG, based on primary sequence similarity, domain organization and phylogenetic analysis (1). These ABC transporters play important roles in processes such as ion transport, resistance against various cytotoxic compounds and bile formation. A number of hereditary diseases such as cystic fibrosis, Tangier disease, Stargardt disease and liver injury are related to the dysfunction of these transporters (2-5). The most prominent member is the multidrug resistance protein 1 (MDR1), also called ABCB1 or P-glycoprotein. MDR1 was identified in tumor cells showing resistance against a multitude of drugs, a phenomenon called multidrug resistance (MDR) (6-11). So far, the physiological function of MDR1 is the protection of the organism against potentially toxic compounds by exporting these into the urine, gut or bile (12,13). MDR1 shares 76% primary sequence identity and 85% similarity with the multidrug resistance protein 3 (MDR3/ABCB4), but both ABC transporters fulfill completely different physiological functions (14). MDR3 is located in the canalicular membrane of hepatocytes and flops phosphatidylcholine (PC) lipids across the canalicular membrane (15-18). In polarized pig kidney epithelial cells (LLC-PK1), MDR3 was capable to transport MDR1 reversal agents such as digoxin, paclitaxel, vinblastine and ivermectin. This transport was inhibited by either verapamil, cyclosporin A or PSC833 (19). However, the transport rate was low for most drugs and MDR3 is not involved in MDR. The question arises why MDR3 is a specialized PC floppase, while MDR1 is a multidrug pump and do both proteins translocate their substrates by the same mechanism?

The first step to investigate the function of MDR3 *in vitro* was to express and purify MDR3 in quantities suitable for functional analysis. Besides the appropriate choice of detergent for solubilization, monodispersity of the purified protein is a requirement for the structural analysis of membrane proteins. To improve the monodispersity of MDR3, additives such as glycerol, the cholesterol derivate cholesteryl hemi-succinate (CHS) and cyclodextrins were tested during purification. Because cyclodextrins are known to capture a wide variety of detergents and often used for the incorporation of membrane proteins into liposomes (20,21), excess of FC-16 attached to MDR3 should be removed resulting in an increased monodispersity of MDR3.



## EXPERIMENTAL PROCEDURES

*Chemicals and Routine Procedures* – All chemicals were supplied by Sigma-Aldrich except detergents, which were obtained from Affymetrix. The protein concentration was determined by a Bradford assay using the Coomassie Plus Assay (Pierce). The Mini-Protean 3 system (Bio-Rad) was used for SDS-PAGE on 7% gels. Immunoblotting was performed with a Tank blot system (Bio-Rad) employing standard procedures.

*Cloning and expression of human MDR3 in S. cerevisiae* – cDNA of human *MDR3* gene isoform A (NCBI accession NM\_000443.3) was amplified with a C-terminal octahistidin-tag using the forward primer 5'-ATAAGAAGATAGGATCCTTTAATTATCAAACAATATCA-ATATGGATCTTGAGGCGGCAAAGAACGGA-3' and the reverse primer 5'-CGATGTC-GACCTCGAGACGCGTCTAATGGTGATGGTGATGGTGATGGTGACCTAAGTTCTGTGTCCCAGCCTGGACACTGACCATT-3'. The PCR product was integrated into YEpHIS by homologous recombination (22). The sequence was verified by DNA sequencing (BMFZ, HHU Duesseldorf). YEpCHisMDR3 was transformed into chemical competent *S. cerevisiae* ΔPP strain (23) using polyethylene glycol (PEG)/LiAc-based method and 5-10 µg carrier DNA (Clontech). *MDR3* was constitutively expressed. Therefore, one liter drop-out (DO) medium without leucine was inoculated to 0.1 OD<sub>600</sub> with a pre-culture of *S. cerevisiae* transformed with YEpCHisMDR3. After 7 h, 10 h and 24 h 300 mL cell culture was harvested, washed with 50 mL Tris-HCl pH 8.0 (4000 xg, 4°C, 10 min), flash-frozen in liquid nitrogen and stored at -80°C.

*Cloning of human MDR3 and expression screening in P. pastoris* – We cloned human *MDR3* (NCBI accession NM\_000443.3) as previously described (24). *MDR3* expression construct was transformed into electro-competent *P. pastoris* X33 cells (Invitrogen) using standard procedures and the expression level was analyzed as described in Ellinger *et al.* (24). After 7 h, 24 h and 48 h 300 mL cells were harvested, flash-frozen in liquid nitrogen.

*Fermentation of MDR3 transformed P. pastoris cells* – *P. pastoris* cells containing the chromosomal integrated wild type *MDR3* gene were fermented in a 15 liter table-top glass fermenter (Applikon Biotechnology) according to the Invitrogen *Pichia* fermentation guidelines and as reported in (24).

*Crude membrane vesicles preparation* – Cells were resuspended into 15 mL homogenization buffer (50 mM Tris-HCl, pH 8.0, 0.33 M sucrose, 75 mM NaCl, 1 mM EDTA, 1 mM EGTA, 100 mM 6-Aminocaproic acid, 2 mM  $\beta$ -mercaptoethanol) supplemented with protein inhibitor cocktail (Roche) and lysed by three passages through a pre-colded TS Series Cell Disrupter (Constant Systems) at 2.7 kbar. The cell lysate was centrifuged two times for 30 min, 15,000 xg, 4°C. Crude membranes were harvested by centrifugation for 1 h, 125,000 xg, 4°C and the resulting pellet was resuspended in 100  $\mu$ L – 300  $\mu$ L buffer A (50 mM Tris-HCl pH 8.0, 50 mM NaCl, 15% Glycerin). For purification, crude membrane vesicles were prepared as described in (24). Crude membrane samples equivalent to 10  $\mu$ g total protein amount were separated by SDS-PAGE and *MDR3* expression was visualized by immunoblotting with C219 antibody (Merck).

*Subcellular fractionation of crude membrane vesicles from S. cerevisiae or P. pastoris* – The subcellular fractionation of whole cell membranes from *S. cerevisiae* was performed as described in (22). 200  $\mu$ L *MDR3*-containing crude membranes from *P. pastoris* with a concentration of 30 mg/mL were diluted in 2 mL hypo-osmotic buffer (50 mM Tris-HCl pH 7.5, 200 mM sorbitol, 1 mM EDTA) and carefully layered on top of a sucrose gradient. The sucrose gradient was prepared discontinuously from 22% to 60% sucrose (Table 1). After separation of the membranes by ultracentrifugation for 16 h at 130,000 xg (SW40Ti rotor, Beckman Coulter) and 4°C, the gradient was fractionated into 600  $\mu$ L aliquots by carefully pipetting from the top. The fractions were analyzed by SDS-PAGE and immunoblotting using antibodies against *MDR3* (Merck), *Pdr5* (kind gift from Prof. K. Kuchler) and *DpmI* (Molecular Probes) (22).

Table 1: Composition of sucrose gradient

Volume [mL]	Sucrose solution [% (w/w)]
	in 10 mM HEPES/KOH, pH 7.2, 1 mM EDTA, 0.8 M sorbitol
0.5	60
1	40
1	37
1.5	34
2	32
2	29
1.5	27
1.5	22

*Solubilization of MDR3-containing P. pastoris crude membrane vesicles* – For finding the optimal solubilization conditions, crude membrane vesicles were diluted to 10 mg/mL protein concentration and solubilized in 1% (w/v) of Fos-Choline-14 (FC-14), Fos-Choline-16 (FC-

16), lauryldimethylamin-N-oxid (LDAO), dodecyl- $\beta$ -D-maltoside (DDM), Triton X-100, Zwittergent 3-6 or sodium cholate (NaCholate) for 1 h at 18°C. Afterwards, the samples were centrifuged (125,000 xg, 1 h, 4°C) and the non-solubilized membrane vesicles were resuspended in the reaction volume with buffer A. Pellets and supernatants were analyzed by SDS-PAGE and immunoblotting using an antibody against MDR3 (C219, Merck). Large-scale solubilization was performed similarly with crude membranes vesicles equivalent to 100 g wet cells and described in Ellinger *et al.* (24).

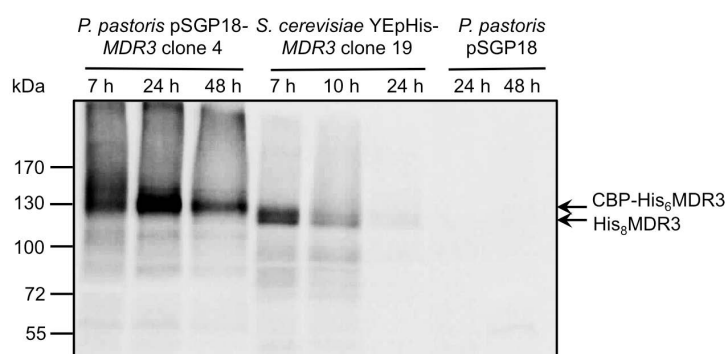
*Purification of MDR3 by tandem-affinity purification (TAP)* – The purification of MDR3 was performed as described in Ellinger *et al.* (24). The collected fractions were analyzed by SDS-PAGE and concentrated with an Amicon Ultra Centrifugal Filter device (100 kDa molecular weight cut-off, Millipore) to a final concentration of 1.5 – 2 mg mL<sup>-1</sup>. The purified protein was stored on ice until further usage or flash-frozen in liquid nitrogen and stored at -80°C.

*Size exclusion chromatography with TAP-purified MDR3* – Size-exclusion chromatography (SEC) with a Superose 6 3.2/30 column (GE Healthcare) was performed with 20 mM Tris-HCl pH 8.0, 20 mM NaCl, 5%-10% (v/v) glycerol, 1.5x critical micelle concentration (cmc) FC-16 and a flow rate of 0.04 mL/min. TAP-purified MDR3 was incubated for 10 min at room temperature with a defined concentration of  $\alpha$ -cyclodextrin or methyl- $\beta$ -cyclodextrin of a 50 mM stock solution and subsequently centrifuged at 100,000 xg, 4°C for 10 min, before 50  $\mu$ L protein was loaded onto the column. The progress of SEC was analyzed by the detection of the UV signal at 280 nm wavelength and coomassie brilliant blue (CBB)-stained SDS-PAGE.

*Precipitation of purified MDR3 with cyclodextrins* –  $\alpha$ -Cyclodextrin or methyl- $\beta$ -cyclodextrin was added to 18  $\mu$ g purified MDR3 with a molar ratio of cyclodextrin to detergent ranging from 1:1 to 48:1 and incubated for 10 min on ice. Aggregated protein was separated by centrifugation at 20,000 xg, 4°C for 30 min and the supernatant was analyzed by CBB-stained SDS-PAGE.

## RESULTS

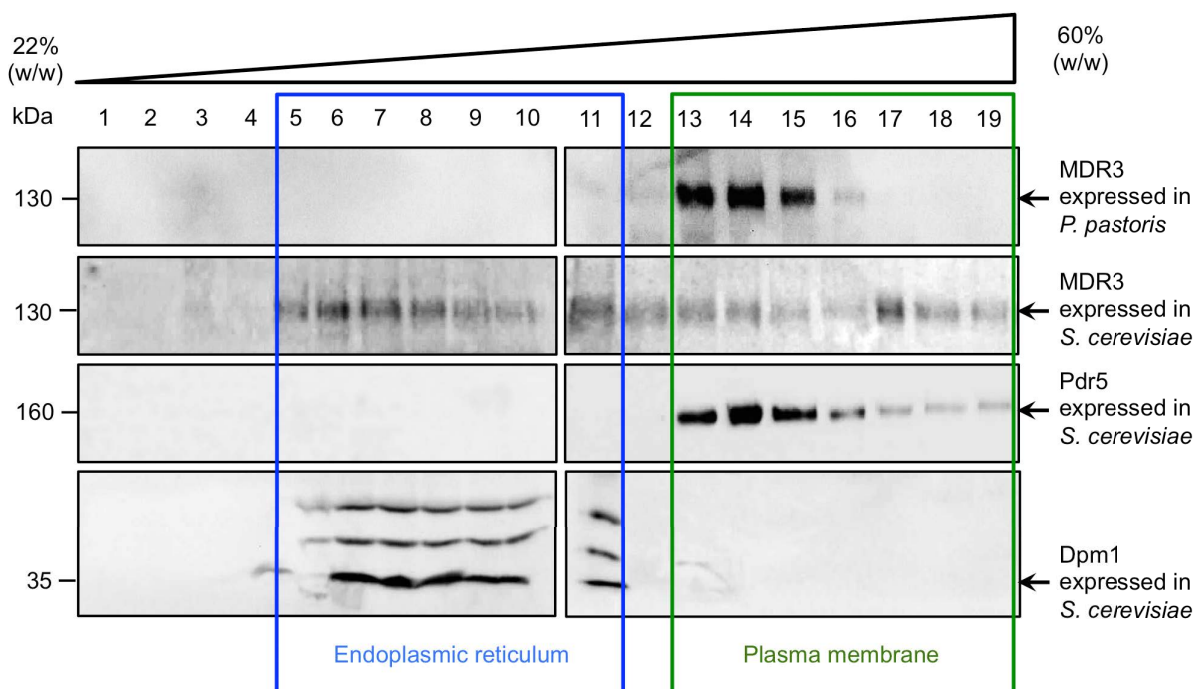
*Expression of MDR3 in S. cerevisiae and P. pastoris* – Yeasts such as *Saccharomyces cerevisiae* and *Pichia pastoris* are suitable hosts to express mammalian ABC transporters (25,26). For example, the overexpression of the pleiotropic drug resistance transporter Pdr5 and a number of membrane proteins using the Pdr5 promoter of *S. cerevisiae* was demonstrated resulting in adequate amounts of functional protein (25). In *P. pastoris* 25 of 48 human ABC transporters were analyzed for expression, but MDR3 was not among them (26). MDR3 was cloned via homologous recombination in *S. cerevisiae*, which is an efficient approach for general cloning of toxic or unstable genes of ABC transporters and was previously reported for cloning the *bile salt export pump* (BSEP) (24,27). The expression of MDR3 was conducted in both expression hosts and the expression levels were compared at distinct time points (Figure 1). In *S. cerevisiae*, MDR3 was constitutively expressed and the highest expression level was observed after seven hours, which decreased over time. In contrast, in *P. pastoris* MDR3 expression was induced by the addition of methanol using the AOX1 promoter and the highest yield was observed after 24 hours after induction (Figure 1). The expression level was 10-fold higher in *P. pastoris* compared to that in *S. cerevisiae* without visual degradation. Furthermore, the main advantage of *P. pastoris* is that it can be grown to high cell densities during fermentation yielding 200 g of wet cell weight (wcw) per liter starting medium, whereas 2.5 g wcw per liter medium was obtained of *S. cerevisiae*.



**Figure 1.** Comparison of MDR3 expression in *P. pastoris* and *S. cerevisiae*. The expression levels were determined after 7 h, 10 h, 24 h and 48 h and 10 µg crude membrane vesicles were analyzed by SDS-PAGE and immunoblotting using the C219 antibody. The empty plasmid pSGP18 was used as negative control.

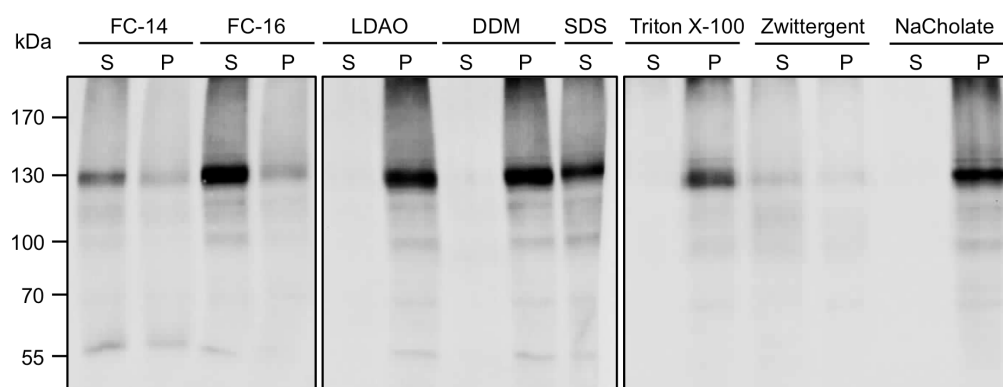
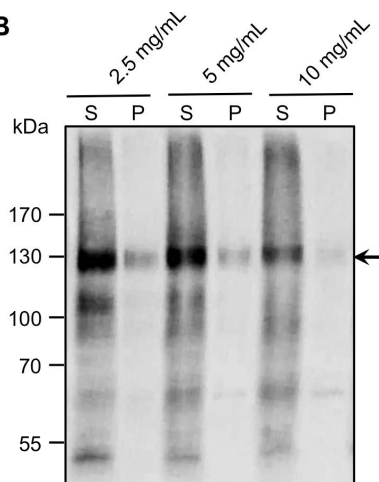
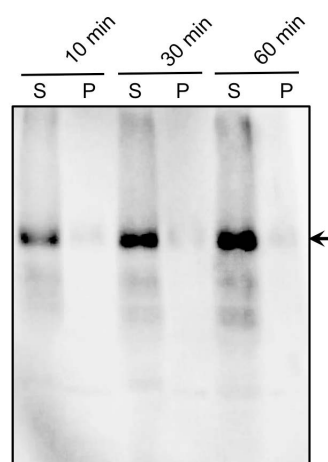
*Localization of MDR3 in S. cerevisiae and P. pastoris* – To examine whether MDR3 was properly folded and trafficked to the plasma membrane (PM) of the expression host, the localization of MDR3 in whole cell membranes was determined by sucrose density centrifugation. MDR3 expressed in *S. cerevisiae* was co-localized with the ER marker Dpm1

and the PM marker Pdr5 (Figure 2) indicating that MDR3 was partially localized at the PM, which was observed before (22). In clear contrast, MDR3 was exclusively located at the PM of *P. pastoris* (Figure 2). These data indicate that MDR3 expressed in *P. pastoris* is properly folded in *P. pastoris*. Thus, all further experiments were conducted with MDR3-containing crude membranes obtained from *P. pastoris*.



**Figure 2.** Subcellular localization of MDR3 in *P. pastoris* and *S. cerevisiae*. MDR3-containing whole cell membrane vesicles from *P. pastoris* or *S. cerevisiae* were separated by centrifugation through a discontinuous sucrose gradient. The Pdr5 transporter is a yeast plasma membrane (PM) marker, while Dpm1 is a membrane-resident yeast enzyme marker for the endoplasmic reticulum (ER).

*Solubilization screen of MDR3 from P. pastoris membrane vesicles* – The first step to investigate membrane proteins *in vitro* is the extraction of the particular membrane protein from vesicles by detergents. Because membrane proteins tend to unfold or lose their activity during this process, the preservation of the native membrane protein fold is challenging and there are no general rules for selection of an appropriate detergent. Thus, MDR3-containing membranes were solubilized with 1% (w/v) detergent at 18°C for 1 h, subsequently centrifuged and the supernatant (S) and pellet (P), which contained the insoluble membranes, were analyzed by SDS-PAGE and immunoblotting with C219 antibody (Figure 3). MDR3 was effectively extracted with the zwitter-ionic detergent Fos-Choline-16 (FC-16), while the non-ionic detergents DDM and Triton X-100 as well as the zwitter-ionic detergent LDAO and the ionic detergent sodium cholate did not solubilize MDR3 from membrane vesicles (Figure 3 A). The detergents FC-14 and Zwittergent 3-6 solubilize MDR3 with less efficacy compared to FC-16.

**A****B****C**

**Figure 3.** Solubilization screen of MDR3. **(A)** MDR3-containing crude membrane vesicles with 10 mg/mL total protein concentration were solubilized using the indicated detergents at 1% (w/v) for 1 h at 18°C. After centrifugation the supernatant (S) and insolubilized membranes (P) were analyzed by SDS-PAGE and immunoblotting using C219 antibody. Sodium dodecylsulfate (SDS) was used as positive control and represents 100% solubilization of MDR3. **(B)** Solubilization of MDR3-containing membrane vesicles with 2.5 mg/mL, 5 mg/mL and 10 mg/mL total protein concentrations and 1% (w/v) FC-16 for 1 h at 18°C. **(C)** Solubilization of 10 mg/mL MDR3-containing membrane vesicles with 1% (w/v) FC-16 for 10 min, 30 min and 60 min.

The next step was to determine the optimal protein concentration and period of time for solubilization of MDR3. For this purpose, on the one hand membrane vesicles containing 2.5 mg/mL, 5 mg/mL and 10 mg/mL total protein concentration were solubilized with 1% (w/v) FC-16 for 1 hour and on the other hand the solubilization of MDR3-containing membrane vesicles (10 mg/mL) with 1% (w/v) FC-16 was analyzed after 10 minutes, 30 minutes and 60 minutes. MDR3 was solubilized with similar efficacy with 2.5 mg/mL, 5 mg/mL and 10 mg/mL total protein concentration (Figure 3 B) and was detectable in the supernatant with high quantity. Furthermore, the quantity of solubilized MDR3 increased over time (Figure 3 C). After 60 minutes MDR3 was almost exclusively detected in the supernatant. Because a high ratio of FC-16 to protein might result in delipidation and

denaturation of MDR3, 10 mg/mL protein concentration and 60 minutes were chosen for solubilization of MDR3.

*Purification of MDR3 by tandem-affinity purification* – MDR3 was purified by tandem-affinity (TAP, see Experimental Procedures) purification, which is composed of an immobilized metal ion affinity chromatography (IMAC) and a calmodulin binding peptide affinity purification (CBP). For IMAC commonly used transition metal ions are  $\text{Ni}^{2+} > \text{Zn}^{2+} = \text{Co}^{2+} > \text{Cu}^{2+}$  with decreasing affinity to the histidine-tag. First the metal ions  $\text{Co}^{2+}$  and  $\text{Zn}^{2+}$  were tested for purification of MDR3. However, MDR3 did not bind to the matrix and was mainly detected in the flow through (data not shown). Thus,  $\text{Ni}^{2+}$  was used for purification and MDR3 was visualized on a CBB-stained SDS-PA gel and verified by immunoblot analysis (Figure 4). MDR3 was successfully eluted by a one-step elution with 200 mM imidazole, but a high number of impurities were co-purified. To increase the purity of MDR3 an additional CBP step was applied resulting in reproducible amounts of highly pure protein with a yield of 6.3 mg per 100 g wcw in eight independent purifications (Figure 4 A). Immunoblot analysis revealed a number of degradation products of MDR3 indicating that MDR3 is not stable under the chosen conditions. The exchange of the detergent or the addition of the cholesterol derivate cholesteryl hemi-succinate (CHS) during purification has been shown to improve protein stability of ABCA4, ABCB1 and BSEP (24,28). FC-16 was substituted by DDM and CHS. However, no improvement in the monodispersity of purified MDR3 was observed (data not shown).

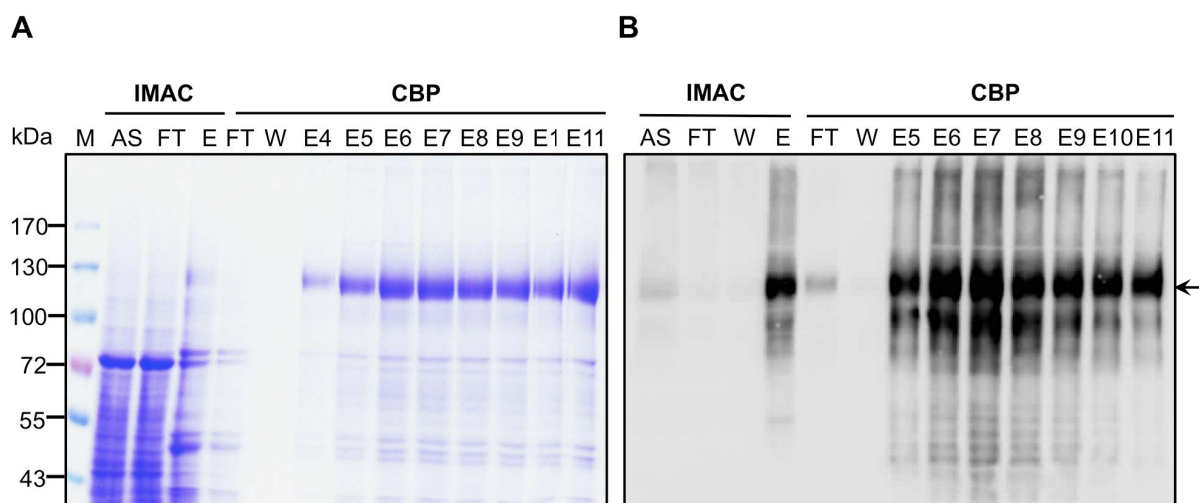


**Figure 4.** Tandem-affinity purification of MDR3. First an immobilized metal ion affinity chromatography (IMAC) and subsequently a calmodulin binding peptide (CBP) purification was performed. MDR3 was solubilized and purified using FC-16. The collected fractions were analyzed by (A) CBB-stained SDS-PAGE and (B) immunoblotting employing C219 antibody (right panel). M = Marker, AS = after solubilization, FT = flow through, W = wash, E = elution.



*Optimization of the monodispersity of purified MDR3 by glycerol* – Size exclusion chromatography (SEC) was performed to determine the stability and monodispersity of purified MDR3. First the effect of glycerol was analyzed. Therefore, the running buffer was supplemented with either 5% (v/v) or 10 % (v/v) glycerol and the progress of SEC was determined by the detection of UV absorbance and the collected fractions were analyzed by CBB-stained SDS-PAGE (Figure 5).

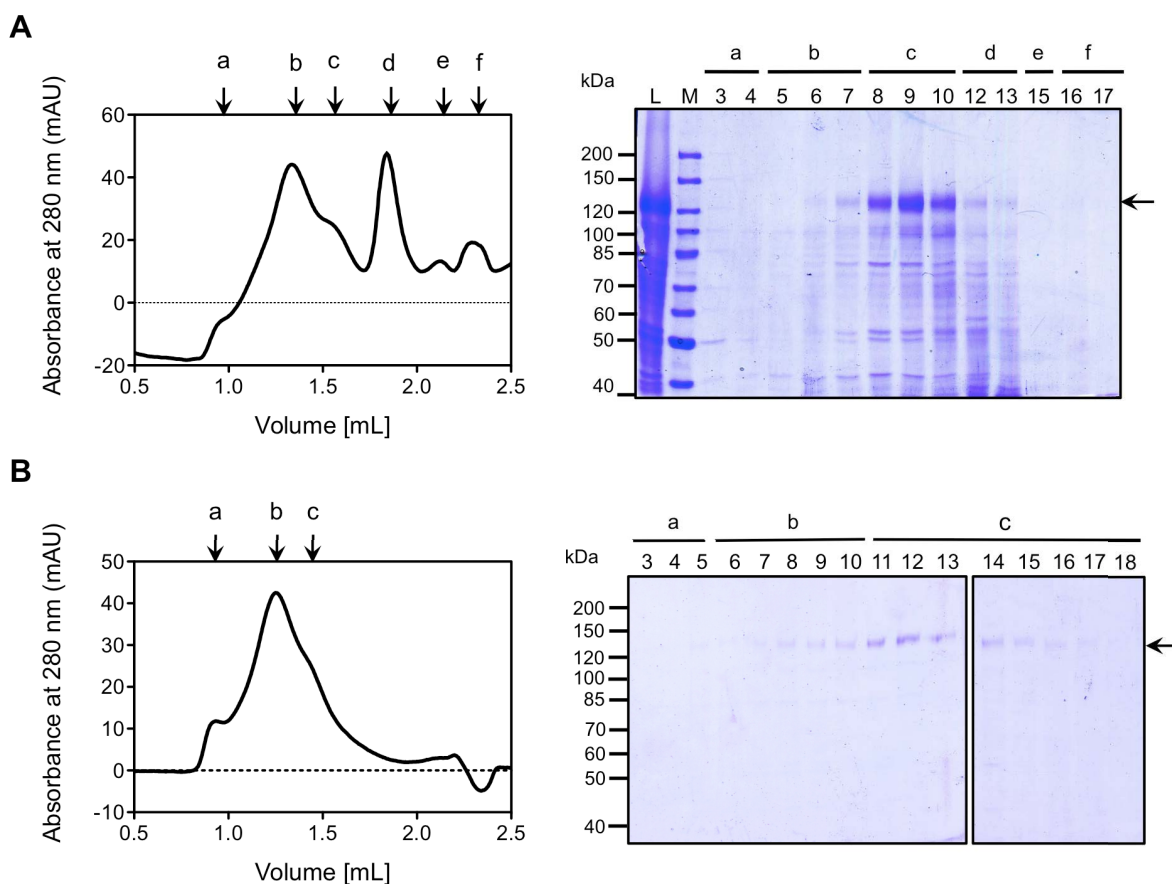


**Figure 5.** Size exclusion chromatography (SEC) of detergent-soluble MDR3 using (A) 5 % (v/v) glycerol and (B) 10 % (v/v) glycerol at 8°C. For the SEC chromatogram the absorbance at a wavelength of 280 nm in arbitrary units was plotted against the retention volume in milliliter (left panel) and the collected fractions were analyzed by CBB-stained SDS-PAGE (right panel).

A small shoulder at 0.8 mL retention volume was observed for SEC, which is likely due to aggregation of MDR3 and correspond to the void volume (Figure 5 A and B). With 5% (v/v) glycerol MDR3 was distributed over the complete column volume with the highest amount eluting at 1.5 mL retention volume (Figure 5 A). Furthermore, impurities could not be separated from MDR3 indicating that the impurities and MDR3 are incorporated into the same lipid/detergent micelles. To reduce the degradation of MDR3 during concentration process, the glycerol content was increased to 20 % (v/v) and subsequently a SEC with

10% (v/v) glycerol was conducted (Figure 5 B). Besides the aggregation signal at 0.8 mL retention volume, a broad signal was observed ranging from 1.0 mL to 1.6 mL with a shoulder at 1.5 mL retention volume. MDR3 was mainly determined in that shoulder signal without visible impurities (Figure 5 B). On the basis of this result, it is likely that MDR3 is incorporated into different species of lipid/detergent micelles with variable molecular weights resulting in two overlapping signals.

*Optimization of the monodispersity of MDR3 by cyclodextrins* – Mass spectrometry analysis of a FC-16 solubilized and purified sample of MDR3 revealed that high amounts of detergent were attached to MDR3 (data not shown). Cyclodextrins are widely used to capture a wide variety of detergents and often used for reconstitution of membrane proteins into liposomes (20,21). We assumed that excess of FC-16 bound to MDR3 might be removed by the addition of cyclodextrin resulting in an increased monodispersity of MDR3. First, the molar ratio of  $\alpha$ - or methyl- $\beta$ -cyclodextrin to detergent was determined at which MDR3 precipitated. It is assumed that one molecule cyclodextrin binds one molecule detergent (20). Molar ratios ranging from 1:1 to 48:1 cyclodextrin to FC-16 were selected and  $\alpha$ -cyclodextrin or methyl- $\beta$ -cyclodextrin was added to the purified MDR3 sample. The mixture was incubated for 10 minutes and soluble MDR3 was separated from precipitate by centrifugation. A 48-molar excess of  $\alpha$ - or methyl- $\beta$ -cyclodextrin was not sufficient to precipitate MDR3 as shown by CBB-stained SDS-PAGE (Figure 6). This results indicate that neither  $\alpha$ -cyclodextrin (Figure 6 A) nor methyl- $\beta$ -cyclodextrin (Figure 6 B) bound FC-16 or a higher content of FC-16 is bound to MDR3 than the used cyclodextrins could absorb.

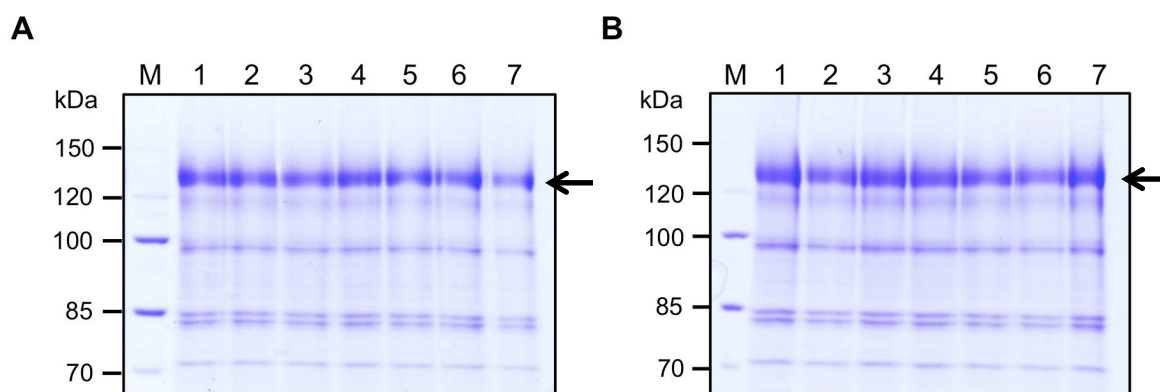


**Figure 6.** Precipitation of purified MDR3 by (A)  $\alpha$ -cyclodextrin and (B) Methyl- $\beta$ -cyclodextrin. CBB-stained SDS-PAGE of the purified MDR3 after incubation without (1) and with cyclodextrins using molar ratio of cyclodextrin to detergent of (2) 1.0 (0.0325 mM CD), (3) 1.2 (0.039 mM CD), (4) 2.4 (0.078 mM CD), (5) 4.8 (0.156 mM CD), (6) 24 (0.78 mM CD) and (7) 48 (1.56 mM CD).

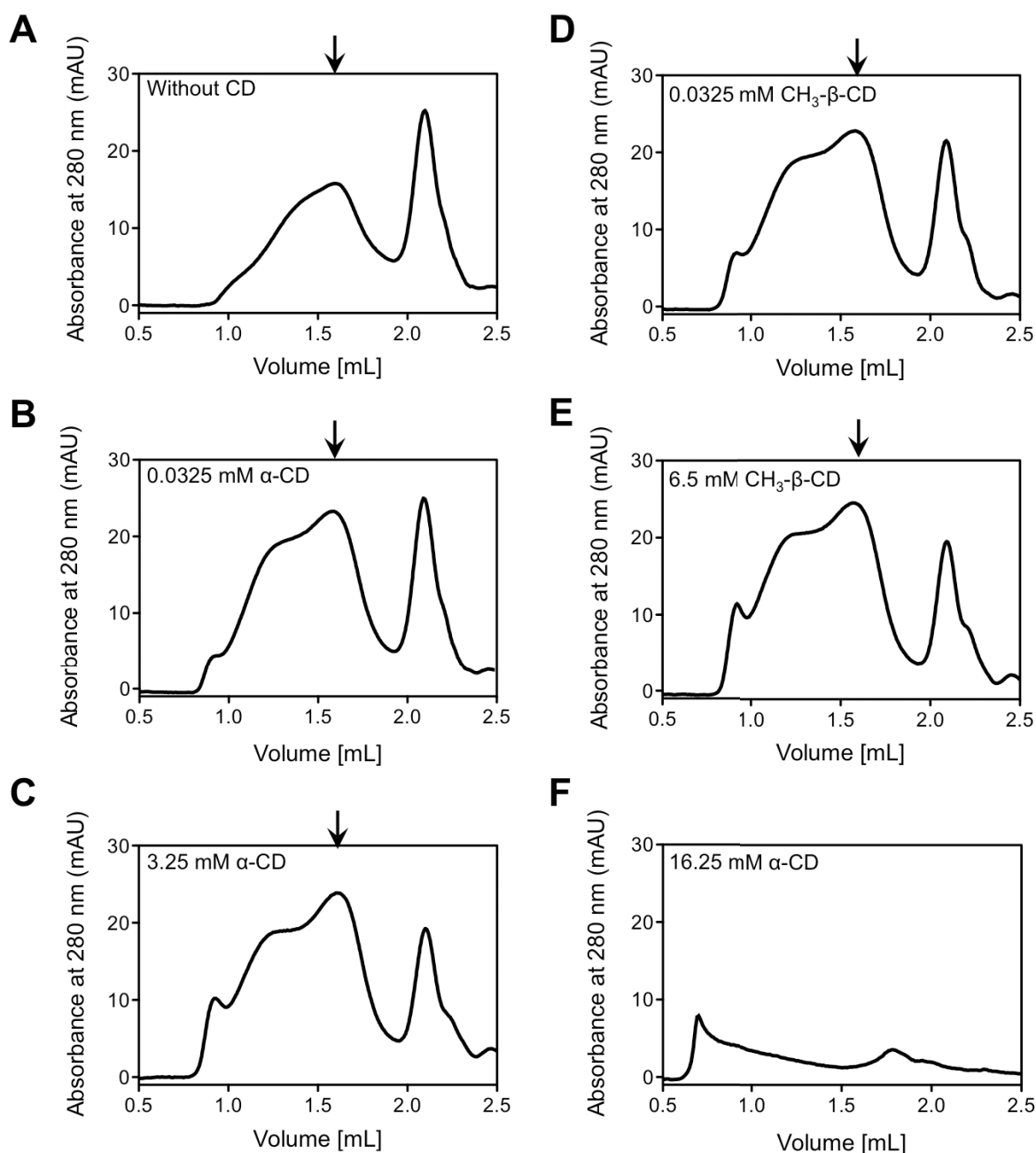


**Figure 7.** Size exclusion chromatography (SEC) of detergent-soluble MDR3 with  $\alpha$ -cyclodextrin ( $\alpha$ -CD) (**B** and **C**) and methyl- $\beta$ -cyclodextrin ( $\text{CH}_3$ - $\beta$ -CD) (**D** and **E**) and 5% (v/v) glycerol. SEC was performed at 8°C (**A**) without and with cyclodextrin and using molar ratio of cyclodextrin to FC-16 of (**B**) 1 (0.0325 mM  $\alpha$ -CD), (**C**) 100 (3.25 mM  $\alpha$ -CD), (**D**) 1 (0.0325 mM Methyl- $\beta$ -CD), (**E**) 200 (6.5 mM Methyl- $\beta$ -CD) and (**F**) 500 (16.25 mM  $\alpha$ -CD). For the SEC chromatogram the absorbance at a wavelength of 280 nm in arbitrary units was plotted against the retention volume in milliliter. The arrow indicates the position of MDR3 elution.

To determine whether the addition of cyclodextrin improves the monodispersity of MDR3, molar ratios of 1:1, 100:1 and 500:1 of  $\alpha$ -cyclodextrin to FC-16 (Figure 7 B, C and F) and 1:1 and 200:1 of methyl- $\beta$ -cyclodextrin to FC-16 (Figure 7 D and E) were selected and the reactions were incubated for 10 min at room temperature. After centrifugation, a SEC was performed with 5 % (v/v) glycerol. The SEC without cyclodextrin (Figure 7 A) was

comparable to the one shown in Figure 5 A. Besides the signal for aggregated protein at 0.8 mL retention volume and the broad signal ranging from 1.0 mL to 1.8 mL retention volume, an additional UV signal appeared at 2.1 mL retention volume, which are presumably impurities or degradation products of MDR3 (Figure 7 A). The shoulder of MDR3 was slightly shifted to 1.55 mL retention volume, which could be due to the system used. The addition of a molar ratio of 1:1  $\alpha$ -cyclodextrin or methyl- $\beta$ -cyclodextrin to detergent already increased the signal at 1.55 mL of MDR3. However, an optimal monodispersity of MDR3 could not be obtained and higher contents of  $\alpha$ -cyclodextrin caused MDR3 aggregation and precipitation indicated by the decrease of the UV signal (Figure 7 F). These data indicate that the heterogeneity of MDR3 is caused by heterogeneous lipid/detergent micelles.

Taken together, MDR3 was stably expressed in *P. pastoris* and located at the plasma membrane. Tandem-affinity purification yielded amounts of highly pure (>90%) protein suitable for biochemical analysis of MDR3. For structural analysis such as X-ray crystallography monodisperse protein is a prerequisite. The addition of glycerol and cyclodextrin increased monodispersity of MDR3. However, further investigations such as detergent-free solubilization by using a polymer such as polystyrene-co-maleic acid (SMA) (29) might result in an improved monodispersity of MDR3.

## DISCUSSION

Mammalian expression systems such as insect cells or tumor cell lines are the first choice for the expression of human membrane proteins. MDR3 was stably expressed in insect (*Sf9*) cells, polarized pig kidney epithelial cells (LLC PK1) and human embryonic kidney 293 cells (HEK293) (15,16,19). However, these cell culture systems are very costly and yielded low quantities of purified protein insufficient to study the molecular mode of action of MDR3-mediated lipid transport and ATPase activity, respectively. Posttranslational modifications such as phosphorylation were demonstrated to be important for the function of MDR3 (30). In this study, MDR3 was successfully expressed at the plasma membrane in the eukaryotic expression systems *S. cerevisiae* and *P. pastoris*, which harbors the posttranslational modification machinery required for modification of MDR3. Previously, it was demonstrated that purification of MDR3 expressed in *S. cerevisiae* yielded 200  $\mu$ g partial purified protein per liter cell culture (22). Because of the low expression level and yield of purified MDR3, the expression system was changed to the methylotrophic yeast *P. pastoris*. Chloupková *et al.* analyzed 25 of 48 human ABC transporters for expression in *P. pastoris* (26). Especially ABC transporters of the liver such as MDR1 (ABCB1), ABCG2, ABCG5/G8 and ABCC1, 3

and 6 (multidrug resistance related protein (MRP) 1, 3 and 6) could be expressed and partially purified with yields of about 1-6 mg per 100 g wcw, while for example ABCC2 (MRP2) could not be expressed (26,31-35).

The choice of an appropriate detergent is important to maintain a native and functional protein. Unanticipatedly, exclusively small-micelle forming detergents Fos-Choline-16, Fos-Choline-14 and Zwittergent 3-6 solubilized MDR3 with decreased efficacy. The tandem-affinity purification of MDR3 with Fos-Cholin-16 yielded in 6 g/mL highly pure protein from 100 g wcw. However, SEC indicated a heterogeneous distribution of MDR3. While Pollock *et al.* reported an increased stability and monodispersity of the lipid floppase ABCA4 (ABCR) and MDR1 using CHS (28), no improvement in monodispersity of MDR3 was observed. It is known that glycerol generates a more native environment for membrane proteins by reducing the concentration of water and increasing the hydrophobicity (36). Furthermore, cyclodextrins bind detergent such as DDM and digitonin and were used for reconstitution of supermolecular complexes and membrane proteins (20,21). The addition of glycerol during SEC increased monodispersity of MDR3 (Figure 5 B), while MDR3 monodispersity was only slight improved in the presence of cyclodextrins (Figure 7). These data indicate that heterogeneity of MDR3 is caused by different sizes of detergent/lipid micelles. However, optimal monodispersity could not be achieved. This study provides the foundation to study the function of MDR3 *in vitro*.

## REFERENCES

1. Dean, M., Rzhetsky, A., and Allikmets, R. (2001) The human ATP-binding cassette (ABC) transporter superfamily. *Genome Res.* **11**, 1156-1166
2. Riordan, J. R., Rommens, J. M., Kerem, B., Alon, N., Rozmahel, R., Grzelczak, Z., Zielenski, J., Lok, S., Plavsic, N., Chou, J. L., and et al. (1989) Identification of the cystic fibrosis gene: cloning and characterization of complementary DNA. *Science* **245**, 1066-1073
3. Bodzioch, M., Orso, E., Klucken, J., Langmann, T., Bottcher, A., Diederich, W., Drobnik, W., Barlage, S., Buchler, C., Porsch-Ozcurumez, M., Kaminski, W. E., Hahmann, H. W., Oette, K., Rothe, G., Aslanidis, C., Lackner, K. J., and Schmitz, G. (1999) The gene encoding ATP-binding cassette transporter 1 is mutated in Tangier disease. *Nat. Genet.* **22**, 347-351
4. Martinez-Mir, A., Paloma, E., Allikmets, R., Ayuso, C., del Rio, T., Dean, M., Vilageliu, L., Gonzalez-Duarte, R., and Balcells, S. (1998) Retinitis pigmentosa caused by a homozygous mutation in the Stargardt disease gene ABCR. *Nat. Genet.* **18**, 11-12
5. Nicolaou, M., Andress, E. J., Zolnerciks, J. K., Dixon, P. H., Williamson, C., and Linton, K. J. (2012) Canalicular ABC transporters and liver disease. *J. Pathol.* **226**, 300-315

6. Kartner, N., Riordan, J. R., and Ling, V. (1983) Cell surface P-glycoprotein associated with multidrug resistance in mammalian cell lines. *Science* **221**, 1285-1288
7. Didier, A. D., and Loor, F. (1995) Decreased biotolerability for ivermectin and cyclosporin A in mice exposed to potent P-glycoprotein inhibitors. *Int. J. Cancer* **63**, 263-267
8. Ambudkar, S. V., Kimchi-Sarfaty, C., Sauna, Z. E., and Gottesman, M. M. (2003) P-glycoprotein: from genomics to mechanism. *Oncogene* **22**, 7468-7485
9. Cordon-Cardo, C., O'Brien, J. P., Boccia, J., Casals, D., Bertino, J. R., and Melamed, M. R. (1990) Expression of the multidrug resistance gene product (P-glycoprotein) in human normal and tumor tissues. *J. Histochem. Cytochem.* **38**, 1277-1287
10. Tanigawara, Y., Okamura, N., Hirai, M., Yasuhara, M., Ueda, K., Kioka, N., Komano, T., and Hori, R. (1992) Transport of digoxin by human P-glycoprotein expressed in a porcine kidney epithelial cell line (LLC-PK1). *J. Pharm. Exp. Ther.* **263**, 840-845
11. Gottesman, M. M., Fojo, T., and Bates, S. E. (2002) Multidrug resistance in cancer: role of ATP-dependent transporters. *Nat Rev Cancer* **2**, 48-58
12. Fromm, M. F. (2004) Importance of P-glycoprotein at blood-tissue barriers. *Trends Pharmacol. Sci.* **25**, 423-429
13. Ford, J. M., and Hait, W. N. (1990) Pharmacology of drugs that alter multidrug resistance in cancer. *Pharmacol. Rev.* **42**, 155-199
14. van der Bliek, A. M., Kooiman, P. M., Schneider, C., and Borst, P. (1988) Sequence of *mdr3* cDNA encoding a human P-glycoprotein. *Gene* **71**, 401-411
15. van Helvoort, A., Smith, A. J., Sprong, H., Fritzsche, I., Schinkel, A. H., Borst, P., and van Meer, G. (1996) MDR1 P-glycoprotein is a lipid translocase of broad specificity, while MDR3 P-glycoprotein specifically translocates phosphatidylcholine. *Cell* **87**, 507-517
16. Morita, S. Y., Kobayashi, A., Takanezawa, Y., Kioka, N., Handa, T., Arai, H., Matsuo, M., and Ueda, K. (2007) Bile salt-dependent efflux of cellular phospholipids mediated by ATP binding cassette protein B4. *Hepatology* **46**, 188-199
17. Ruetz, S., and Gros, P. (1994) Phosphatidylcholine translocase: a physiological role for the *mdr2* gene. *Cell* **77**, 1071-1081
18. Smit, J. J., Schinkel, A. H., Oude Elferink, R. P., Groen, A. K., Wagenaar, E., van Deemter, L., Mol, C. A., Ottenhoff, R., van der Lugt, N. M., van Roon, M. A., and et al. (1993) Homozygous disruption of the murine *mdr2* P-glycoprotein gene leads to a complete absence of phospholipid from bile and to liver disease. *Cell* **75**, 451-462
19. Smith, A. J., van Helvoort, A., van Meer, G., Szabo, K., Welker, E., Szakacs, G., Varadi, A., Sarkadi, B., and Borst, P. (2000) MDR3 P-glycoprotein, a phosphatidylcholine translocase, transports several cytotoxic drugs and directly interacts with drugs as judged by interference with nucleotide trapping. *J. Biol. Chem.* **275**, 23530-23539
20. Degrip, W. J., Vanoostrum, J., and Bovee-Geurts, P. H. (1998) Selective detergent-extraction from mixed detergent/lipid/protein micelles, using cyclodextrin inclusion compounds: a novel generic approach for the preparation of proteoliposomes. *Biochem. J.* **330 ( Pt 2)**, 667-674
21. Dezi, M., Di Cicco, A., Bassereau, P., and Levy, D. (2013) Detergent-mediated incorporation of transmembrane proteins in giant unilamellar vesicles with controlled physiological contents. *Proc. Natl. Acad. Sci. U. S. A.* **110**, 7276-7281
22. Stindt, J. (2010) Studies on ABC Transporters from Human Liver in Heterologous Systems. *Dissertation, HHU Düsseldorf*
23. Ernst, R., Kueppers, P., Klein, C. M., Schwarzmüller, T., Kuchler, K., and Schmitt, L. (2008) A mutation of the H-loop selectively affects rhodamine transport by the yeast multidrug ABC transporter Pdr5. *Proc. Natl. Acad. Sci. U. S. A.* **105**, 5069-5074

24. Ellinger, P., Kluth, M., Stindt, J., Smits, S. H., and Schmitt, L. (2013) Detergent screening and purification of the human liver ABC transporters BSEP (ABCB11) and MDR3 (ABCB4) expressed in the yeast *Pichia pastoris*. *PLoS One* **8**, e60620
25. Gupta, R. P., Kueppers, P., and Schmitt, L. (2014) New examples of membrane protein expression and purification using the yeast based Pdr1-3 expression strategy. *J. Biotechnol.*
26. Chloupkova, M., Pickert, A., Lee, J. Y., Souza, S., Trinh, Y. T., Connelly, S. M., Dumont, M. E., Dean, M., and Urbatsch, I. L. (2007) Expression of 25 human ABC transporters in the yeast *Pichia pastoris* and characterization of the purified ABCC3 ATPase activity. *Biochemistry* **46**, 7992-8003
27. Stindt, J., Ellinger, P., Stross, C., Keitel, V., Haussinger, D., Smits, S. H., Kubitz, R., and Schmitt, L. (2011) Heterologous overexpression and mutagenesis of the human bile salt export pump (ABCB11) using DREAM (Directed REcombination-Assisted Mutagenesis). *PLoS One* **6**, e20562
28. Pollock, N. L., McDevitt, C. A., Collins, R., Niesten, P. H., Prince, S., Kerr, I. D., Ford, R. C., and Callaghan, R. (2014) Improving the stability and function of purified ABCB1 and ABCA4: the influence of membrane lipids. *Biochim. Biophys. Acta* **1838**, 134-147
29. Gulati, S., Jamshad, M., Knowles, T. J., Morrison, K. A., Downing, R., Cant, N., Collins, R., Koenderink, J. B., Ford, R. C., Overduin, M., Kerr, I. D., Dafforn, T. R., and Rothnie, A. J. (2014) Detergent-free purification of ABC (ATP-binding-cassette) transporters. *Biochem. J.* **461**, 269-278
30. Gautherot, J., Delautier, D., Maubert, M. A., Ait-Slimane, T., Bolbach, G., Delaunay, J. L., Durand-Schneider, A. M., Firrincieli, D., Barbu, V., Chignard, N., Housset, C., Maurice, M., and Falguieres, T. (2014) Phosphorylation of ABCB4 impacts its function: Insights from disease-causing mutations. *Hepatology*
31. Aller, S. G., Yu, J., Ward, A., Weng, Y., Chittaboina, S., Zhuo, R., Harrell, P. M., Trinh, Y. T., Zhang, Q., Urbatsch, I. L., and Chang, G. (2009) Structure of P-glycoprotein reveals a molecular basis for poly-specific drug binding. *Science* **323**, 1718-1722
32. Zehnpfennig, B., Urbatsch, I. L., and Galla, H. J. (2009) Functional reconstitution of human ABCC3 into proteoliposomes reveals a transport mechanism with positive cooperativity. *Biochemistry* **48**, 4423-4430
33. Johnson, B. J., Lee, J. Y., Pickert, A., and Urbatsch, I. L. (2010) Bile acids stimulate ATP hydrolysis in the purified cholesterol transporter ABCG5/G8. *Biochemistry* **49**, 3403-3411
34. Wang, Z., Stalcup, L. D., Harvey, B. J., Weber, J., Chloupkova, M., Dumont, M. E., Dean, M., and Urbatsch, I. L. (2006) Purification and ATP hydrolysis of the putative cholesterol transporters ABCG5 and ABCG8. *Biochemistry* **45**, 9929-9939
35. Lerner-Marmarosh, N., Gimi, K., Urbatsch, I. L., Gros, P., and Senior, A. E. (1999) Large scale purification of detergent-soluble P-glycoprotein from *Pichia pastoris* cells and characterization of nucleotide binding properties of wild-type, Walker A, and Walker B mutant proteins. *J. Biol. Chem.* **274**, 34711-34718
36. Arnold, T., and Linke, D. (2008) The use of detergents to purify membrane proteins. *Current protocols in protein science / editorial board, John E. Coligan ... [et al.]* **Chapter 4**, Unit 4 8 1-4 8 30



## Chapter III – Detergent Screening and Purification of BSEP and MDR3

### Title:

**Detergent Screening and Purification of the Human Liver  
ABC Transporters BSEP (ABCB11) and MDR3 (ABCB4)  
expressed in the yeast *Pichia pastoris***

Published in: *PLOS ONE*

Impact factor: 3.53 (2013/2014)

Own Proportion to this work: 45 % (shared first authorship)

Expression of human MDR3 in *P. pastoris*

Detergent screen with dot blot and Fluorescence-detection  
size-exclusion chromatography (FSEC)

Purification of MDR3 and ATPase activity determination

Writing of the manuscript

# Detergent Screening and Purification of the Human Liver ABC Transporters BSEP (ABCB11) and MDR3 (ABCB4) Expressed in the Yeast *Pichia pastoris*

Philipp Ellinger<sup>✉</sup>, Marianne Kluth<sup>✉</sup>, Jan Stindt<sup>□</sup>, Sander H. J. Smits, Lutz Schmitt\*

Institute of Biochemistry, Heinrich Heine University, Düsseldorf, Germany

## Abstract

The human liver ATP-binding cassette (ABC) transporters bile salt export pump (BSEP/ABCB11) and the multidrug resistance protein 3 (MDR3/ABCB4) fulfill the translocation of bile salts and phosphatidylcholine across the apical membrane of hepatocytes. In concert with ABCG5/G8, these two transporters are responsible for the formation of bile and mutations within these transporters can lead to severe hereditary diseases. In this study, we report the heterologous overexpression and purification of human BSEP and MDR3 as well as the expression of the corresponding C-terminal GFP-fusion proteins in the yeast *Pichia pastoris*. Confocal laser scanning microscopy revealed that BSEP-GFP and MDR3-GFP are localized in the plasma membrane of *P. pastoris*. Furthermore, we demonstrate the first purification of human BSEP and MDR3 yielding 1 mg and 6 mg per 100 g of wet cell weight, respectively. By screening over 100 detergents using a dot blot technique, we found that only zwitterionic, lipid-like detergents such as Fos-cholines or Cyclofos were able to extract both transporters in sufficient amounts for subsequent functional analysis. For MDR3, fluorescence-detection size exclusion chromatography (FSEC) screens revealed that increasing the acyl chain length of Fos-Cholines improved monodispersity. BSEP purified in n-dodecyl- $\beta$ -D-maltoside or Cymal-5 after solubilization with Fos-choline 16 from *P. pastoris* membranes showed binding to ATP-agarose. Furthermore, detergent-solubilized and purified MDR3 showed a substrate-inducible ATPase activity upon addition of phosphatidylcholine lipids. These results form the basis for further biochemical analysis of human BSEP and MDR3 to elucidate the function of these clinically relevant ABC transporters.

Citation: Ellinger P, Kluth M, Stindt J, Smits SHJ, Schmitt L (2013) Detergent Screening and Purification of the Human Liver ABC Transporters BSEP (ABCB11) and MDR3 (ABCB4) Expressed in the Yeast *Pichia pastoris*. PLoS ONE 8(4): e60620. doi:10.1371/journal.pone.0060620

Editor: Anthony George, University of Technology Sydney, Australia

Received January 14, 2013; Accepted February 28, 2013; Published April 4, 2013

Copyright: © 2013 Ellinger et al. This is an open-access article distributed under the terms of the Creative Commons Attribution License, which permits unrestricted use, distribution, and reproduction in any medium, provided the original author and source are credited.

Funding: This work was supported by the Clinic Research Unit 217 (KFO 217) "Hepatobiliary transport and liver diseases" (project TP3 to L.S.). The funders had no role in study design, data collection and analysis, decision to publish, or preparation of the manuscript.

Competing Interests: The authors have declared that no competing interests exist.

\* E-mail: Lutz.Schmitt@hhu.de

□ Current address: Department of Gastroenterology, Hepatology and Infectiology, Heinrich-Heine-University, Düsseldorf, Germany

✉ These authors contributed equally to this work.

## Introduction

ATP-binding cassette (ABC) transporters constitute one of the largest families of membrane transport proteins present in all three kingdoms of life. They transport a wide variety of different substrates ranging from small ions to large proteins across biological membranes using ATP as energy source [1,2]. ABC transporters are composed of two transmembrane domains (TMDs) and two highly conserved nucleotide-binding domains (NBDs). TMDs determine the substrate specificity and the NBDs fuel the transport by binding and hydrolyzing ATP. In eukaryotes, the TMDs and NBDs are encoded on one gene and build up either a full-size transporter (one gene encoding two TMDs and two NBDs) or a half-size transporter (one gene encoding one TMD and one NBD), which hetero- or homodimerize to form the functional unit.

Within the human genome 48 genes encode for ABC proteins, which are involved mainly in transport [3]. Mutations in these ABC protein genes can lead to severe diseases such as cystic fibrosis, X-linked Adrenoleukodystrophy or Tangier disease. Beside this, ABC transporters are also involved in processes like

multidrug resistance of cancer cells [4,5,6,7]. In hepatocytes, eleven ABC transporters are expressed. Except for the transport of different cyclic nucleotides, glucuronide and glutathione conjugates through MRPs (MRP 1–6, note that MRP1 is detected only in fetal hepatocytes) [8] and the transport of endo- and xenobiotics by MDR1 (P-gp) [9] and ABCG2 [10], one of the main function of ABC transporters in the liver is the formation of bile depending on the ABC transporters BSEP (ABCB11), MDR3 (ABCB4) and ABCG5/8 [11]. Bile is essential for the digestion of fat as well as for the absorption of lipids and fat-soluble vitamins originating from food ingestion in the small intestine. In the intestine the main components of bile, bile salts and phosphatidylcholine are recycled via the enterohepatic circulation [12]. Bile salts, phosphatidylcholine and cholesterol form mixed micelles in the canalculus, which dampen the detergent effect of the amphiphatic bile salts as well as prevent the formation of cholesterol crystals. Bile formation is dependent on the three ABC transporters BSEP (ABCB11), MDR3 (ABCB4) and ABCG5/8 [13].

The bile salt export pump (BSEP) is the main bile salt transporter in humans and is localized in the apical membrane of hepatocytes [14]. It is a 1321 amino acid large, glycosylated

full-size ABC transporter and mediates the ATP-dependent bile flow by transporting monovalent bile salts like taurine and glycine conjugates of primary and secondary bile salts (e.g. tauro- and glycocholate or taurodeoxycholate) into the canaliculus [15]. The human multidrug resistance protein 3 (MDR3) is a close homologue of MDR1 (P-glycoprotein, ABCB1) with an amino acid sequence identity of nearly 80%. However, MDR3 exclusively translocates phosphatidylcholine from the inner to the outer leaflet of the apical membrane [16]. MDR3 is like BSEP a glycosylated full-size transporter composed of 1288 amino acid [17]. The heterodimeric ABC transporter ABCG5/G8 completes the bile forming machinery by transporting cholesterol [18,19].

Mutations within the BSEP and MDR3 gene can lead to different cholestatic diseases, e.g. progressive familial intrahepatic cholestasis type 2 and 3 (PFIC2 and PFIC3) [20,21,22], benign recurrent intrahepatic cholestasis type 2 (BRIC2) [23] or intrahepatic cholestasis of pregnancy (ICP) [24] and low-phospholipid associated cholestasis (LPAC) [25]. Therapy for cholestatic disease includes treatment with e.g. ursodeoxycholic acid or surgical biliary diversion [26]. If none of those treatments is successful, the only alternative therapy is liver transplantation. New successful forms of therapy include treatment with chemical chaperones like 4-phenylbutyrate for misfolded BSEP mutants [27].

Because of their high clinical interest, MDR3 and especially BSEP have been characterized extensively in cell culture as well as animal models [22,28,29,30,31,32]. A well-established system for investigating BSEP are for example insect cell-based vesicles, which allow to perform transport studies and to study kinetics, inhibitors or mutants [13,33]. Less is known about MDR3, because of the difficulty to establish a robust activity assay. Together, all these assays are performed in whole cells or membranes and not with the isolated proteins.

To investigate the function of BSEP and MDR3 in its isolated form, a substantial expression of these proteins is required. To date, no reports regarding the purification of both proteins from cell culture systems or other expression systems have been reported. An alternative to cell culture is the use of yeast expression systems such as *Saccharomyces cerevisiae* or *Pichia pastoris*, which also harbor the eukaryotic protein processing machinery and can be grown to high cell densities. Chloupková et al. tested 25 human ABC transporters for expression in *P. pastoris* [34], but BSEP and MDR3 were not included in this study, while for example MRP2, another human liver ABC transporter, could not be expressed.

In general, *S. cerevisiae* has been used frequently to express eukaryotic membrane proteins [35]. After successful establishment of an expression system, the purification of a membrane protein requires first of all its solubilization with detergents from the membrane of the expression host. However, finding an adequate detergent for extraction and purification that preserves the membrane protein in a stable and functional form is an empirical process. High throughput methods have been developed in order to screen the influence of detergents on stability and monodispersity of the purified membrane protein [36,37,38,39,40,41,42]. One of these approaches is fluorescence-detection size exclusion chromatography (FSEC) based on the fluorescence of a green fluorescent protein (GFP) tag fused to the membrane protein. In this approach solubilized crude membranes are loaded on a size exclusion column and the elution is monitored via the fluorescence of GFP. Thereby only the membrane-GFP fusion protein is visible and the result can be evaluated based on the shape of the elution peak [43,44]

In this study, we established the heterologous overexpression in the yeast *P. pastoris* and the subsequent solubilization and purification of human BSEP and MDR3. To achieve this, we applied a dot blot technique and FSEC to identify the most suitable detergent for BSEP and MDR3. The purified protein could be isolated in a functional state as judged by substrate-induced ATPase activity of MDR3 and ATP binding in the case of BSEP.

## Materials and Methods

### Materials

All detergents were obtained from Affymetrix with the exception of Digitonin, which was purchased from Sigma. Lipids were from Sigma or Avanti Polar Lipids.

### Routine Procedures

SDS-PAGE on 7% gels used the Bio-Rad Minigel system. Immunoblotting followed standard procedures using the monoclonal anti-P-gp C219 antibody in case of MDR3 (Abcam), the F-6 anti-BSEP antibody (Santa Cruz Biotechnology) or an anti-GFP antibody (Sigma). Protein concentration was estimated by the Bradford method using a Coomassie Plus Assay (Pierce).

### Cloning of human BSEP and MDR3 and GFP fusion expression constructs for *Pichia pastoris*

The general cloning procedure is described in detail in Stindt et al. [45]. The *P. pastoris* expression vector pSGP18 was made compatible for *Saccharomyces cerevisiae* by introducing a 2m origin of replication into its backbone. The 2m origin of replication was PCR-amplified from the YEpHIS vector with the primer pairs 2m for pPIC S1 and 2m for pPIC S2 (for oligonucleotide sequences see Table 1). The resulting PCR product and the pSGP18 vector were digested with PciI and ligated yielding pSGP18-2m. The coding sequences for human BSEP and MDR3 (NCBI accession code: NM\_003742.2 and NM\_000443.3) were PCR-amplified with the primer pairs BSEP-HR-PP-S1 and BSEP-HR-PP-S2 and MDR3-HR-PP-S1 and MDR3-HR-PP-S2, respectively. For *Pichia* expression of the GFP-tagged transporters, the respective coding sequences were amplified either with the primer pair BSEP-PP-HR-S1 and YEpN14HIS-BSEP-S2 or with MDR3-PP-HR-S1 and YEpN14HIS-MDR3-S2. The S65T-GFP sequence of pFA6a-GFP(S65T)-kanMX6 [27] was either amplified with primer pair GFP-BSEP-HR-S1 and GFP-PP-HR-S2 or primer pair GFP-MDR3-HR-S1 and GFP-PP-HR-S2. This includes the necessary homologous overlaps to the PCR products for in-frame recombination into pSGP18-2m. pSGP18 contains a 3C protease cleavage site, a calmodulin binding peptide (CBP) tag and a RGS-6xhis-tag C-terminal to the proteins in the multiple cloning site [34]. For expression of the GFP-fusion proteins, tags were replaced by GFP in the process of recombination. The BsmBI linearized pSGP18-2m vector and the PCR fragments were gel-purified, mixed in equimolar amounts (either with BSEP or MDR3 or each together with GFP) and transformed into *S. cerevisiae* [45]. The ATP hydrolysis deficient mutant of MDR3 was generated by introduction of two point mutations in the conserved NBD. Therefore, we replaced Glu 558 and Glu 1207 of the Walker B motif by Gln using the QuikChange XL Site-Directed Mutagenesis Kit (Agilent Technologies). The sequence of all constructs were verified by DNA sequencing.

### Transformation of *P. pastoris*

BSEP and MDR3 expression constructs were transformed into competent *P. pastoris* X33 (Invitrogen) cells using standard

Table 1. PCR oligonucleotides used in this study.

Oligonucleotide	Sequence 5'R 3'
pSGP18-2m-ori-S1	TAATACGGTTATCCACAGAATCAGGGGATAACGACGAAAGAACATGTAAATATTGCGAATACCGCTCCACAAACATTG
pSGP18-2m-ori-S2	AACGCGGCCTTTTACGGTTCCTGGCCTTTTGCTGGCCTTTTGCTCACATGTTATTCACACCGCATATATCGGATCGTACT
BSEP-HR-PP-S1	ATCAAAAAACAATAATTATTCGAACGAGGTAAAAGAATGTCTGACTCAGTAATCTTCGAAGT ATA
BSEP-HR-PP-S2	ACGTTTGGACCTTGGAAAAGACTTCTAAGGAGTTGGAGGCACTGATGGGGATCCAGTGGTACTAGTTT
MDR3-HR-PP-S1	ATCAAAAAACAATAATTATTCGAACGAGGTAAAAGAATGGATCTTGAGCGCGCAAGAAGCGGAACA
MDR3-HR-PP-S2	ACGTTTGGACCTTGGAAATAAGACTTCTAAGGAGTTGGAGGCTAAGTTCTGTTCAGCTGGACACTGACATTGAAAAATAG
YEpN14HIS-BSEP-S2	GAATAAGGTAAACATGGTAGCGATGTCGACCTCGAGACGCGTCTAACTGATGGGGGATCCAGTGGTACT
YEpN14HIS-MDR3-S2	GAATAAGGTAAACATGGTAGCGATGTCGACCTCGAGACGCGTCTATAAGTTCTGTGTCCAGCTGGACACTGACCAAT
GFP-BSEP-HR-S1	AGCCTACTACAACTAGTCCACCTGGATCCCCCATCAGTGGTGGTGGTCGACGGATCCCCGGGTGA
GFP-PP-HR-S2	ACGTTTGGACCTTGGAAATAAGACTTCTAAGGAGTTGGAGGCTATTATTGTATATGTCATCCATGCCATGT
GFP-MDR3-HR-S1	TTTCAATGGTCAGTGTCCAGGCTGGAACAAAGAGACAAAGTGGTGGTCGACGGATCCCCGGGTGA MDR3-
E558Q S1	GATCCTTCTGCTGGATCAAGCCACGTCAGCATTGGACAC
MDR3-E558Q S2	GTGTCCAATGCTGACGTGGCTTGATCCAGCAGAAGGATC
MDR3-E1207Q S1	CAAATCCTCTGTTGGATCAAGCTACATCAGCTCTGGATAC
MDR3-E1207Q S2	GTATCCAGAGCTGATGTAGCTTGATCCAACAGGAGGATTGT

doi:10.1371/journal.pone.0060620.t001

procedures (Invitrogen). Briefly, 10–20 mg DNA of the expression construct were linearized using PmeI (New England Biolabs) to facilitate homologous recombination at the AOX1 locus, extracted by phenol/chloroform, re-suspended in 10 ml sterile H<sub>2</sub>O and transformed into 80 ml electro-competent *P. pastoris* cells by electroporation (1.500 V, 5 ms). Cells were incubated in 1 M sorbitol without shaking for 1 h at 30°C, 1 ml YPD was subsequently added and cells were shaken for 2 h at 200 rpm and 30°C. 100 ml of this suspension was plated onto YPDS plates containing 100 mg/ml Zeocin or higher and incubated for 30°C until colonies appeared. 10 to 20 colonies were re-streaked on YPD plates containing Zeocin and used for expression studies.

#### Expression screening of BSEP and MDR3 transformed *P. pastoris* cells

Small-scale expression screens of BSEP or MDR3 *P. pastoris* clones were performed similarly as described by Wang et al. [46]. 50 ml cultures were grown overnight in MGY medium (1.34% (w/v) yeast nitrogen base, 1% (v/v) glycerol and  $4 \times 10^{-5}$ % (w/v) biotin) at 30°C and 220 rpm, harvested by centrifugation, re-suspended in 50 ml MMY (1.34% (w/v) yeast nitrogen base, 0.5% (v/v) methanol and  $4 \times 10^{-5}$ % (w/v) biotin) and incubated for another 24 h to induce protein expression. 2 ml of these cells were harvested, washed in 2 ml of homogenization buffer (50 mM Tris-HCl, pH 8.0, 0.33 M sucrose, 75 mM NaCl, 1 mM EDTA, 1 mM EGTA, 100 mM 6-Aminocaproic acid, 2 mM  $\beta$ -Mercaptoethanol) supplemented with protein inhibitor cocktail (Roche) and re-suspended in 500 ml of homogenization buffer. Cells were lysed with 1 ml of acid-washed zirconia beads (Roth) by vortexing 6 times for 1 min with 1 min breaks on ice. Disrupted cells were centrifuged for 5 min, 12,000 xg, 4°C and the supernatant was adjusted to 10 mM MgCl<sub>2</sub> and incubated on ice for 15 min. Precipitated membranes were harvested by centrifugation for 30 min, 20,000 xg, 4°C and the resulting pellet was re-suspended in SDS sample buffer and loaded onto a 7% SDS-PAGE. Expression was visualized by immuno blotting.

#### Fermentation of BSEP and MDR3

For large-scale expression, BSEP, BSEP-GFP and MDR3 expressing clones were fermented in a 15 liter table-top glass fermentor (Applikon Biotechnology) according to the Invitrogen Pichia fermentation guidelines [26] using the basal salt media. Typically a volume of 6 l media was inoculated with 1 l of an overnight culture grown in MGY (1.34% yeast nitrogen base, 1% glycerol and  $4 \times 10^{-5}$ % biotin) media. Aeration was kept above 20% O<sub>2</sub> saturation and the glycerol fed-batch was performed for 5 h feeding 500 ml of 50% (v/v) glycerol. Protein expression was induced by addition of 3.6 ml/h 1 (1000 ml) methanol for 48 h. Cells were harvested by centrifugation (5,000 xg, 10 min, 4°C), flash-frozen in liquid nitrogen and stored at –80°C until further use. Under these conditions approximately 1–1.4 kg of wet cell mass could be obtained.

#### Expression of GFP fusion proteins in shaking flask cultures

Clones either expressing BSEP-GFP or MDR3-GFP were inoculated in 2 l shaking flasks containing 0.5 l of MGY media and shaken overnight at 30°C and 220 rpm. Protein expression was induced with methanol by harvesting the cells in sterile centrifuge buckets (5,000 xg, 10 min, 4°C) and re-suspended in 0.5 l methanol-containing media (MMY). 24 h after induction, methanol was added to a final concentration of 0.5% and after 48 h the cells were harvested (5,000 xg, 10 min, 4°C), flash-frozen in liquid nitrogen and stored at –80°C until further usage.

#### Confocal fluorescence microscopy of GFP fusion proteins

*P. pastoris* cells expressing either BSEP-GFP or MDR3-GFP were directly spotted onto microscope slides coated with poly-L-lysine (Thermo Scientific) from shaking flasks and mounted with a coverslip. Images were acquired using an Olympus FV1000 confocal laser scanning microscope equipped with a 60 $\times$  UPLSAPO objective (N.A. 1.35). GFP was excited at 488 nm and emission was recorded at 500 nm–600 nm.

#### Preparation of crude membrane vesicles for protein purification

100 g batches of *P. pastoris* cells expressing BSEP or MDR3 were thawed on ice, washed with ddH<sub>2</sub>O and re-suspended at a concentration of 0.5 g cells/ml in homogenization buffer containing protease inhibitor cocktail (Roche). Cells were disrupted by two passages through a pre-cooled TS Series Cell Disrupter (Constant Systems) at 2.5 kbar. After cell debris was spun down by two centrifugation steps (15 min at 5,000 xg, 4°C and 30 min at 15,000 xg, 4°C), crude membrane vesicles were prepared by ultracentrifugation for 1 h at 125,000 xg, 4°C. Membrane vesicles were re-suspended in buffer A (50 mM Tris-HCl pH 8.0, 75 mM NaCl, 30% (v/v) glycerol) and flash frozen in liquid N<sub>2</sub>.

#### Solubilization screen via the Dot Blot technique

Membranes were thawed on ice and solubilized in 200 µl buffer A. Membrane concentration was kept at 5 mg/ml during solubilization and detergents were used at a concentration of 1% (w/v) or higher according to their critical micellar concentration (cmc). A complete list of the used detergents is provided in Table S1 in File Supplementary Information. Samples were solubilized for 1 h at 4°C on a rotator, centrifuged (100,000 xg, 30 min, 4°C) and the supernatant was supplemented with SDS sample buffer. The samples were heated to 65°C for 10 min and 3 µl were spotted onto a dry nitrocellulose membrane. After extensive drying of the sample, the membrane was blocked for 1 h in TBS-T with 5% (w/v) milk powder and then probed with a 1:2000 dilution of the respective primary antibody. Dot blots were quantified using the GeneTools software (Syngene).

#### Fluorescence-detection size-exclusion chromatography (FSEC)

BSEP-GFP or MDR3-GFP containing membranes were solubilized in detergents based on the results of the dot blot analysis. 100 µl of the solubilized sample was applied to a Biosep SEC-S4000 size-exclusion chromatography column (Phenomenex) connected to a HPLC system (Hitachi) equipped with a fluorescence detector (L-2485, Hitachi), which was equilibrated in running buffer (50 mM Tris-HCl, pH 8.0, 150 mM NaCl, 15% (v/v) glycerol and 0.02% (w/v) b-DDM). The UV absorption of the proteins was followed at 280 nm and for online fluorescence detection, the GFP tag was excited at  $\lambda_{ex}$  = 470 nm to improve the signal to noise ratio and fluorescence emission was detected at  $\lambda_{em}$  = 512 nm.

#### Solubilization and Purification of MDR3 and BSEP

The purification of MDR3 and BSEP was performed by tandem-affinity purification (TAP) consisting of an immobilized metal ion affinity chromatography (IMAC) step followed by a calmodulin binding peptide affinity purification (CBP). All procedures were carried out at 4°C. Crude membrane vesicles equivalent to 100 g wet cells were thawed at 4°C, diluted to a final concentration of 5 mg/ml total protein with buffer A as determined by the Coomassie Plus Assay (Pierce) and solubilized in 1% (w/v) of Fos-choline-16 or other detergents for 1 h at 4°C (for cmc values see Table S1 in File Supplementary Information). Non-solubilized membrane vesicles were removed by centrifugation at 100,000 xg, 4°C for 1 h. The supernatant supplemented with 20 mM imidazole was loaded onto a Ni<sup>2+</sup>-loaded HiTrap Chelating column (5 ml, GE Healthcare) and washed with 10 column volumes of buffer A supplemented with 20 mM imidazole and typically 2.5× cmc of detergent. Proteins were eluted in one step with buffer B (50 mM Tris-HCl pH 8.0, 75 mM NaCl,

200 mM imidazole, 20% (v/v) glycerol) supplemented with 2.5× cmc detergent. The IMAC eluate was diluted 5-times with CaCl<sub>2</sub> binding buffer (50 mM Tris-HCl pH 8.0, 150 mM NaCl, 1 mM MgCl<sub>2</sub>, 2 mM CaCl<sub>2</sub> and 20% (v/v) glycerol) containing 2.5× cmc detergent, applied to 4 ml calmodulin affinity resin equilibrated in CaCl<sub>2</sub> binding buffer and incubated with the calmodulin resin over night at 4°C on a rotator. The resin was transferred into a gravity flow column and washed with 10 column volumes of CaCl<sub>2</sub> binding buffer containing 2.5× cmc detergent. The proteins were eluted with 3 bed volumes of EGTA elution buffer (2 mM EGTA, 50 mM Tris-HCl pH 7.4, 150 mM NaCl, and 20% (v/v) glycerol) supplemented with 2.5× cmc detergent. The purified protein was directly used for ATPase activity or further concentrated using an Amicon Ultra-15 filter (Millipore) with a cut-off of 100 kDa, aliquoted, snap frozen in liquid nitrogen and stored at -80°C. Aliquots of the sample were analyzed by Coomassie blue stained SDS-PAGE and immunoblotting.

#### ATP Agarose binding assay of BSEP

To test the ability of detergent solubilized BSEP to bind ATP, 25 µl of a 1:1 slurry of C8-linked ATP-agarose resin (Sigma) equilibrated in buffer A was added to 20 mg of purified BSEP in the detergent to be examined and incubated at 4°C on a rotator. After 1 h, the resin was pelleted by centrifugation (8200 xg, 2 min, 4°C) and the resin was washed three more times with 250 µl of buffer A supplemented with 2.5× cmc of the detergent. Bound proteins were eluted in SDS sample buffer by heating the resin to 65°C for 20 min. The pellet samples were subjected to SDS-PAGE and analyzed by immunoblotting.

#### ATPase activity measurements of MDR3

The ATPase activity of MDR3 was examined with the malachite green assay by determination of released free inorganic orthophosphate as described previously [47]. Reactions were performed in a total volume of 100 µl in buffer C (50 mM Tris-HCl pH 7.4, 50 mM NaCl, 15% (v/v) glycerol) containing 2.5× cmc detergent and 10 mM MgCl<sub>2</sub>. 5 – 20 mg purified, detergent-soluble MDR3 was used. The reaction was started by typically adding 2 mM ATP at 37°C and stopped at appropriate time points by the addition of 25 µl of the reaction into 175 µl of 20 mM ice-cold H<sub>2</sub>SO<sub>4</sub>. Subsequently, 50 µl dye solution (0.096% (w/v) malachite green, 1.48% (w/v) ammonium molybdate, and 0.173% (w/v) Tween-20 in 2.36 M H<sub>2</sub>SO<sub>4</sub>) was added. After 15 min the amount of free phosphate was quantified spectroscopically by measuring the absorption at 595 nm. For subsequent data evaluation, all appropriate controls were performed and subtracted. For calibration of free phosphate concentrations a Na<sub>2</sub>HPO<sub>4</sub> standard curve was used. For substrate stimulated ATPase activity, purified MDR3 was incubated with the equal volume of 2–5 mM lipid stock solution at room temperature for 20 min and sonified for 30 s to facilitate the incorporation of lipids into the detergent-protein micelles. The lipid-protein sample was stored on ice until further usage.

## Results

### Cloning and Expression of human BSEP and MDR3 in *P. pastoris*

For the expression of human BSEP and MDR3 in the methylotrophic yeast *P. pastoris* we used the expression plasmid pSGP18, which was used before to express 25 human ABC transporters in *P. pastoris* [34]. BSEP and MDR3 were not included in this study likely due to the inherent toxicity of the cDNAs, which hampers the cloning procedure and often results in

the failure of obtaining suitable expression plasmids [13]. We custom modified the plasmid by introducing a 24 origin of replication for *S. cerevisiae* in its backbone and cloned the human BSEP and MDR3 cDNA via homologous recombination into pSGP18-2 $\mu$ . After transformation in *P. pastoris*, ten clones were tested for expression. A clone for each transporter was chosen for fermentation, which yielded about 1.0–1.4 kg of wet cell weight (wcw) in a typical fermentation. As can be seen by immunoblotting both wild-type proteins were expressed in *P. pastoris* (Fig. 1A and C, middle lanes). The wild-type proteins exhibited a distinct protein band at  $\approx$ 130 kDa that cross-reacted with monoclonal antibodies against BSEP or MDR3. No signal was obtained using the empty plasmid as a control (see Fig. 1, neg ctrl).

#### Localization and judging the quality of BSEP and MDR3 in *P. pastoris*

For the determination of the trafficking and localization of human BSEP and MDR3 in *P. pastoris* cells, we generated and expressed the corresponding GFP-fusion proteins, BSEP-GFP and MDR3-GFP. The C-terminal GFP-tag was confirmed by immunoblot analysis against GFP (Fig. 1B and D) as well as by a shift to a higher molecular weight visualized by antibodies against BSEP and MDR3, respectively (Fig. 1A and C, right lane). Both the fusion proteins migrated at  $\approx$ 160 kDa. The correct trafficking of the GFP-fusion proteins to the plasma membrane of *P. pastoris* was checked by confocal laser scanning microscopy (Fig. 2, upper row). Induced cells expressing BSEP-GFP or MDR3-GFP showed clear ring-shaped fluorescence at the plasma membrane, which co-localized with the cell surrounding of the differential interference contrast (DIC) scan (Fig. 2, bottom row, merged pictures). As control only GFP was expressed in *P. pastoris* and the fluorescence

was distributed homogenously within the cell, which leads to the conclusion that BSEP and MDR3 are processed and trafficked correctly in *P. pastoris*. Non-induced cells did not show any fluorescence (data not shown). We also employed sucrose density centrifugation of whole cell membranes containing BSEP or MDR3, which demonstrated co-localization of a plasma membrane marker with BSEP or MDR3, respectively (data not shown).

#### Solubilization Screen via the Dot Blot technique

To find an appropriate detergent for membrane protein extraction, we tested over 100 different detergents for their ability to solubilize BSEP and MDR3 via dot blot analysis. These detergents covered all four classes: non-ionic (N), anionic (A), cationic (C) as well as zwitterionic (Z) (Table S1 in File Supplementary Information). Most of the detergents were used at a concentration of 1% (w/v). However, depending on the critical micellar concentration (cmc) other concentrations were also chosen when necessary (see Table S1 in File Supplementary Information).

Membranes were solubilized for 1 h at 4°C, subsequently centrifuged and the supernatant was spotted on the dot blot membrane. For BSEP, we tested solubilization of the wild-type protein as well as the GFP-fusion protein, to investigate if the GFP-tag had any influence on the solubilization. Therefore, the BSEP-GFP fusion protein was fermented the same way as the wild-type BSEP protein for comparison. As seen in Fig. 3A and 3B, BSEP-GFP could be extracted more efficiently than BSEP by maltosides and glucosides (D-I 1-5). Furthermore, some differences can be seen in a more efficient extraction of BSEP-GFP in Fos-choline-unisat-11-10 and Fos-choline-8 (G8 and G9). Despite this, there are large similarities between BSEP and BSEP-GFP, in fact only

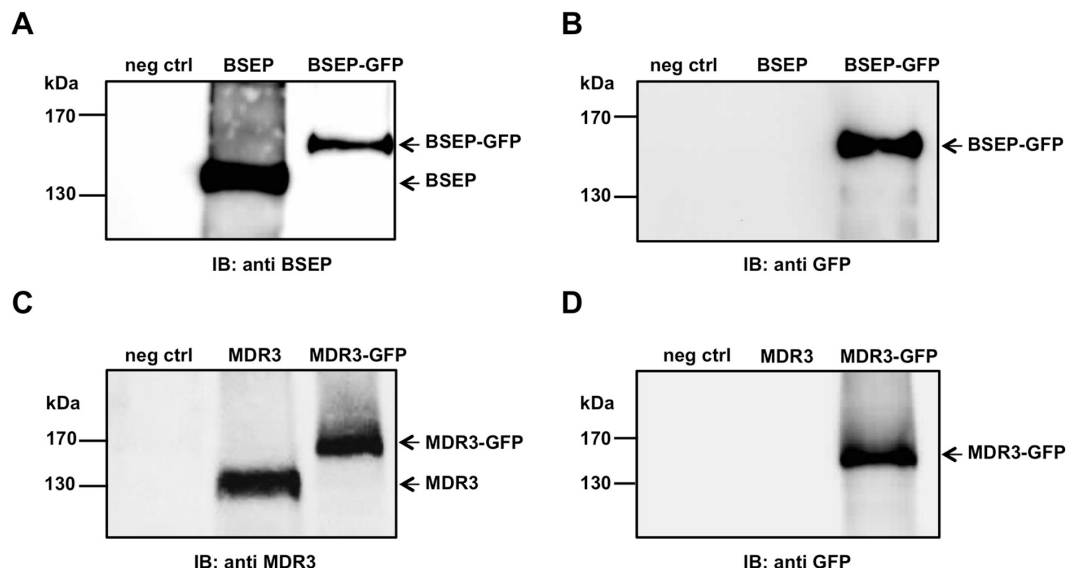


**Figure 1.** Human BSEP and MDR3 expression in *Pichia pastoris*. A 5 mg of membranes derived from *P. pastoris* cells carrying the empty expression plasmid pSGP18 (neg ctrl), BSEP or BSEP-GFP were subjected to SDS-PAGE and immunoblotting (lanes from left to right). The negative control (left lane) did not react with the monoclonal antibody (F-6), while BSEP (middle lane) and BSEP-GFP (right lane) could be detected by the same antibody. B Identical samples were probed with a monoclonal GFP antibody. The negative control (left lane) as well as BSEP (middle lane) showed no signal with anti-GFP antibody, while BSEP-GFP could be detected (right lane). C In case of MDR3 the negative control (left lane) showed no signal with the monoclonal antibody C219; MDR3 (middle lane) as well as MDR3-GFP (right lane) could be detected with the monoclonal antibody C219. D Identical MDR3 samples were probed with a monoclonal GFP antibody. The negative control (left lane) as well as MDR3 (middle lane) showed no signal with anti-GFP antibody, while MDR3-GFP could be detected (right lane). The position of the molecular weight markers are shown on the left. doi:10.1371/journal.pone.0060620.g006



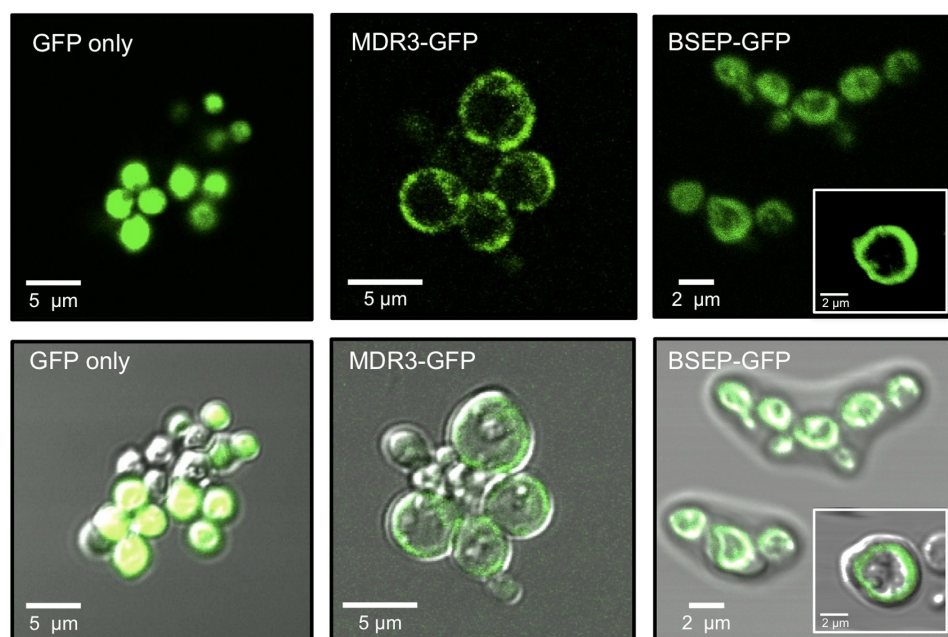


Figure 2. Fluorescence microscopy of BSEP-GFP and MDR3-GFP expressing *Pichia pastoris* cells. *P. pastoris* cells expressing GFP, BSEP-GFP or MDR3-GFP were harvested 48 h after induction and examined for GFP fluorescence (upper row) by confocal LSM. BSEP-GFP as well as MDR3-GFP was located in the plasma membrane of *P. pastoris* cells in contrast to soluble GFP, which was homogeneously distributed within the cell. Bottom row: merge of the GFP fluorescence and the Differential Interference Contrast (DIC) scans. doi:10.1371/journal.pone.0060620.g006

the Fos-choline and Cyclofos detergents were able to solubilize both proteins in large quantities (Fig. 3A and B, D7-10, E7-10, F7-9). Also the Anapoe detergents (A-C 1-5) solubilized BSEP, but to a lesser extent. Furthermore, the anionic detergent dodecanoyl sarcosine (A9) as well as the zwitterionic detergents AnzergentH 3-14 (C8) and 2-carboxy- $\nu$ -heptadecenamido-propyldimethylamine (J8) resulted in strong signals in the dot blot.

In contrast to BSEP, we observed that only lipid-like detergents like the Fos-choline series (Fig. 3C, E9-E10, F6-F9, G8) and Cyclofos series (Fig. 3C, D8-D10) were able to solubilize MDR3 in high amounts. In addition, the anionic detergents sodium dodecanoyl sarcosine (A9) and *n*-dodecyl- $\beta$ -iminodipropionic acid (A10) were also able to solubilize MDR3. Furthermore, very low amounts of MDR3 were solubilized by AnzergentH 3-14 (C8) and 2-carboxy- $\nu$ -heptadecenamido-propyldimethylamine (J8). None of the Anapoes except Anapoe-58 (A4), none of the glucosides, none of the thio-maltosides, none of the maltosides or any other series of detergents showed a signal indicating that MDR3 was completely resistant to solubilization. In the case of MDR3, we did not analyze the GFP-fusion protein, because wild-type MDR3 displayed a substrate-induced ATPase activity (see below). Thus, the dot blot based solubilization screen revealed that only the lipid-like and more “harsh” detergents of the Fos-choline and Cyclofos series were able to solubilize both, BSEP and MDR3, in a near quantitative manner. For a quantification of the dot blots see Figure S1 in File S1.

#### Fluorescence-detection Size Exclusion Chromatography of selected detergents

Based on this analysis, the result of selected detergents used for the solubilization of BSEP and MDR3 were examined by

fluorescence-detection size exclusion chromatography (FSEC). SEC is a common tool for monitoring the monodispersity and stability of proteins. In combination with a fluorescence detector, we were able to ascertain a high number of detergents using the GFP fusion proteins as reporter. This strategy requires only nanogram quantities of non-purified GFP-fusion protein by directly using solubilized membrane proteins in the detergent to be investigated. Our criteria for FSEC profiles in terms of monodispersity and stability were a sharp and symmetrical peak, no or only a small peak in the void volume or no signal corresponding to free GFP, which would indicate degradations of the fusion protein (for a FSEC profile of free GFP see Figure S2 in File S1).

The Fos-choline series as well as some maltosides and other detergents (see Figure S3 in File S1) solubilized BSEP-GFP, although the latter only resulted a weak signal in the dot blot. Fos-choline 8 and 9 did not give a significant signal in FSEC. A reliable signal was only obtained in the case of Fos-cholines containing long acyl chains. The signal increased with increasing acyl chain length from 10 to 16 carbon atoms (Fig. 4A). BSEP-GFP eluted to a certain portion in the void volume in Fos-choline detergents (10–11 min retention time), especially in Fos-choline-12 (Fig. 4A) indicating aggregated protein. The main BSEP-GFP peak (between 16 and 17 minutes) became more non-symmetrical and more BSEP-GFP degradation product (20–21 min retention time, free GFP) was detected for detergents with longer acyl chains (Fig. 4A and Fig S3 in File S1). On the other hand, the maltosides gave sharp and symmetrical FSEC chromatograms and only very little aggregation was detected. This was very pronounced for  $\beta$ -DM,  $\beta$ -DDM and Cymal5. This implies that the protein was monodisperse and stable. Other detergents tested such as the



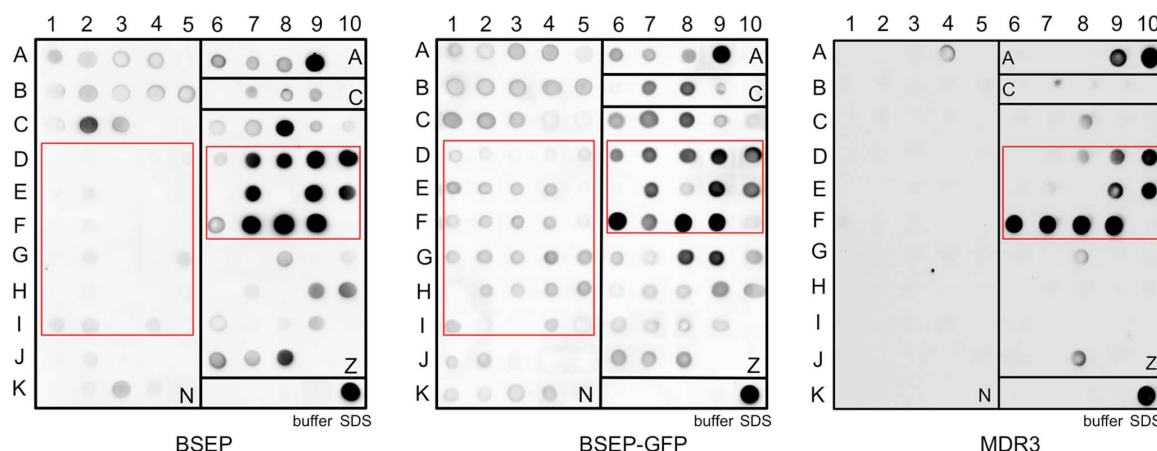


Figure 3. Solubilization screen of human BSEP and MDR3 using Dot Blot. Solubilization screen of *P. pastoris* membranes containing BSEP (A), BSEP-GFP (B) or MDR3 (C) with over 100 different detergents were analysed regarding the solubilization efficiency. The solubilized protein was spotted onto a nitrocellulose membrane and examined via dot blotting with BSEP or MDR3 specific monoclonal antibodies (F-6 and C219). Compared areas are marked with a red box. All dot blots were performed in duplicate.

doi:10.1371/journal.pone.0060620.g006

anionic detergent sodium dodecanoyl sarcosine resulted in a non-symmetrical peak (Figure S3 in File S1). These observations, suggested that the length of the acyl chain of either group of detergents had a profound influence on the monodispersity and that an acyl chain length between 10 to 13 carbon atoms preserved the monodispersity of the transporters.

The FSEC profiles obtained for MDR3-GFP using the aforementioned detergents are summarized in Figure 4B and Figure S2 in File S1. None of the detergents showed perfect monodisperse peaks. The anionic detergent n-dodecyl-biminodipropionic acid was able to solubilize MDR3 (Figure S2 in File S1), however, the FSEC peak resulted in a major signal in the void volume of the SEC (molecular weight  $\approx$  1 MDa). This suggested aggregation. Sodium dodecanoyl sarcosine and the group of Cyclofos detergents showed a very inhomogeneous SEC profile (Figure S2 in File S1). The lipid-like Fos-cholines solubilized MDR3 with high efficiency nearly to the same extent as the SDS sample, which was used as control for solubilization efficiency (Fig. 4B). Importantly, the length of the acyl chain had again an impact on the monodispersity and stability of MDR3-GFP. The longer the acyl chain became, the more symmetrically the MDR3-GFP peak was observed (FC-16  $\approx$  FC-15  $\approx$  FC-14  $\approx$  FC-13  $\approx$  FC-12). The most promising result of solubilization efficiency and monodispersity was obtained for FC-16, so that all further experiments such as purification and ATPase activity were performed in this particular detergent.

#### Purification of the human ABC transporter MDR3 and BSEP

For functional analysis, we purified both transporter in the detergents, which showed the most promising results in the dot blot and FSEC analysis. The procedure we applied for the purification of human BSEP and MDR3 was established by Wang et al. based on the purification of the human ABC-transporters ABCG5/G8 and ABCC3 expressed in *P. pastoris* [34,46] and is described in detail in “Materials and Methods”. MDR3 and BSEP both contain a tandem affinity tag consisting of a calmodulin binding-peptide tag (CBP-tag) and a 6xhis-tag at their C-termini. Briefly, BSEP and MDR3 were purified by immobilized metal-ion

affinity chromatography (IMAC) and calmodulin affinity resin (CBP) after solubilization of crude membranes in the appropriate detergent isolated from fermenter cultures.

We chose Fos-choline-16 as detergent of choice for solubilization of BSEP, because of its high efficacy. During the purification process, we exchanged the detergent on the CBP affinity column to maltoside detergents (e.g. b-DDM and Cymal-5), which according to the FSEC profiles corresponded to monodisperse protein (Fig. 4A). BSEP could be purified and yielded 1 mg of protein from solubilized membranes of 100 g (wcw) of *Pichia* cells with a purity of roughly 75% (Fig. 5A).

MDR3 was solubilized with Fos-choline-16 and purified via an identical tandem affinity approach. The MDR3 transporter was visualized on a Coomassie blue-stained SDS-gel and further identified by immunoblot analysis (Fig. 6A). We obtained  $\approx$  6 mg of highly purified protein from 100 g yeast cells with a purity of more than 90% as judged by SDS-PAGE analysis.

#### Binding of solubilized human BSEP to ATP-Agarose

BSEP was tested for ATPase activity in detergent solubilized state, but no reliable activity could be detected. Therefore, we investigated the capability of BSEP to bind to ATP coupled to agarose beads (ATP-beads) in the detergent-solubilized state, which would indicate that the protein is in a state where the nucleotide can bind, but the conformation is likely locked in a non-productive state, which inhibits hydrolysis. As shown in Figure 5B BSEP purified in Fos-choline-16 was not eluted from the ATP-beads after incubation suggesting that BSEP cannot bind to ATP in Fos-choline. Maltosides are known as mild detergents and often find usage to preserve the functionality of the membrane protein such as LmrA [47]. Accordingly, we solubilized BSEP with Fos-choline-16 and exchanged the detergent to  $\beta$ -DDM or Cymal-5 during purification. In these two detergents, BSEP bound to the ATP-beads. This result is in agreement with the FSEC results in those detergents (Fig. 4A).

#### ATPase Activity of purified human MDR3

We further examined whether purified MDR3 exhibits ATPase activity that could be stimulated by its natural substrate

## Purification of Human BSEP and MDR3

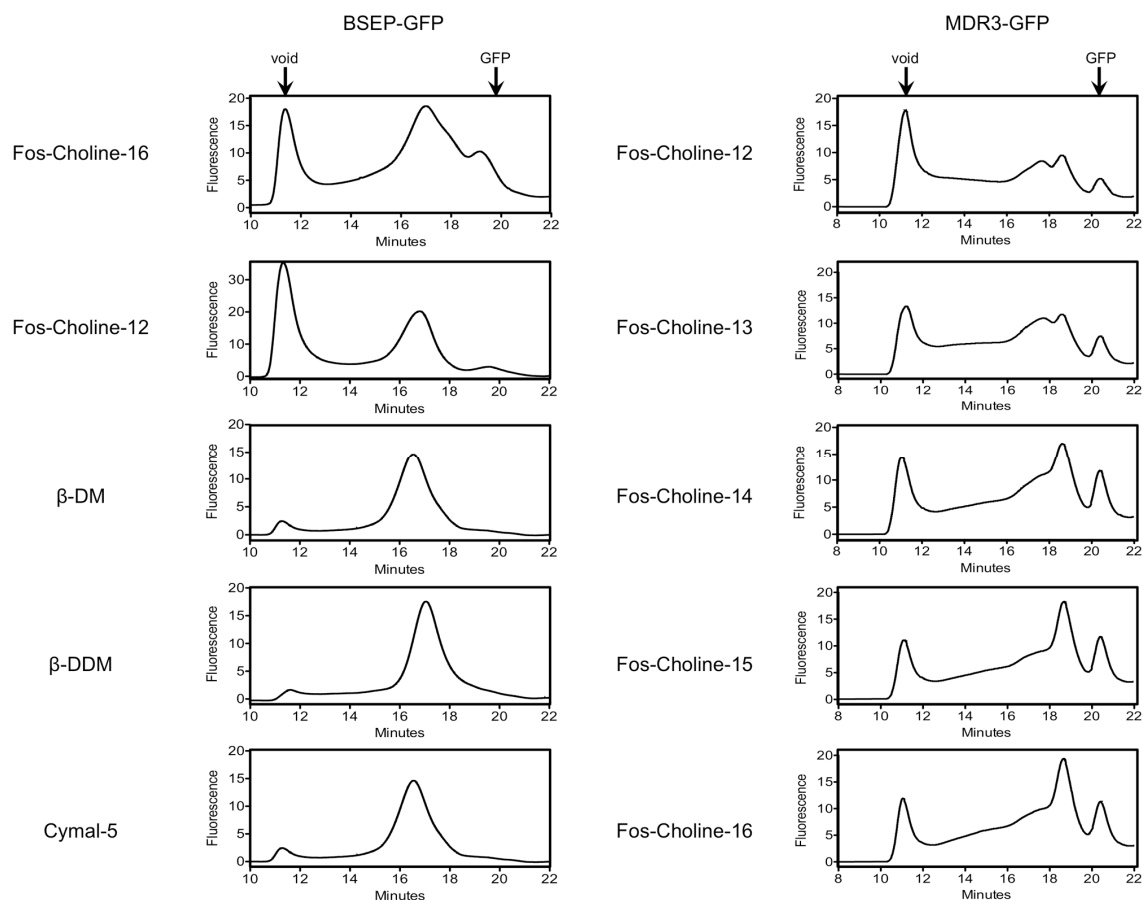


Figure 4. Detergent screening utilizing FSEC. FSEC analysis of BSEP-GFP (A) in five representative detergents and MDR3-GFP in five detergents (B). The arrows indicate the estimated elution position of the void volume and free GFP. Additional FSEC profiles are summarized in the supplementary material.

doi:10.1371/journal.pone.0060620.g006

phosphatidylcholine (PC) lipids. For this purpose we added two synthetic PC lipids (DPPC and DOPC) to the purified protein and measured the ATPase activity at 37°C up to 60 min (Fig. 6B). Under these conditions, we observed an approximately 2.5 fold stimulation of ATPase activity. Because co-purification of contaminating ATPases cannot be excluded, we cloned an ATP hydrolysis deficient mutant by introducing two point mutations and purified the mutant as described for the wild-type protein. The exchange of Glu to Gln in the highly conserved Walker B motif ( $\Phi\Phi\Phi\Phi\Phi\Phi$ , where  $\Phi$  can be every hydrophobic amino acid) of MDR3 prevents hydrolysis of ATP. The ATPase inactive mutant (E558Q, E1207Q, further called EQ/EQ mutant) exhibited basal ATPase activity comparable to the wild-type protein. This suggested that the observed activity was derived from co-purified ATPases. However and most important, no stimulation of activity was observed in the presence of PC lipids. ATPase activity of ABC transporters is often stimulated after addition of lipids. To demonstrate that the increased ATPase activity of MDR3 is caused by a substrate-specific and not by a conformational stabilization effect of PC lipids, we added DPPE and DOPE lipids to MDR3 wild-type as well as to the ATPase-deficient EQ/EQ mutant. The MDR3 wild-type ATPase activity is slightly

increased by a factor of 1.4 for DPPE and 1.6 for DOPE, whereas the ATPase activity of the EQ/EQ mutant are not increased compared to PC added ATPase activity. The data demonstrates a substrate-specific ATPase activity of 15 nmol/min per mg MDR3 wild-type in comparison to the DOPE-stimulated ATPase activity. We ascertained that the stimulation of ATPase activity is MDR3 specific by PC and indicated that MDR3 is functional in the detergent-solubilized state with respect to its capability to bind and hydrolyze ATP.

## Discussion

In this study, we presented a high-throughput detergent screening and purification approach for the human liver-localized ABC transporters BSEP and MDR3 expressed in the methylotrophic yeast *Pichia pastoris*. This expression host has all the advantages of other eukaryotic expression systems, such as post-translational modifications or trafficking machinery. However, the overexpression per cell is only moderate and therefore requires fermentation to compensate this by high biomass. This system was used before for expression trials of human ABC transporters, which showed its general applicability for this class of transporter.

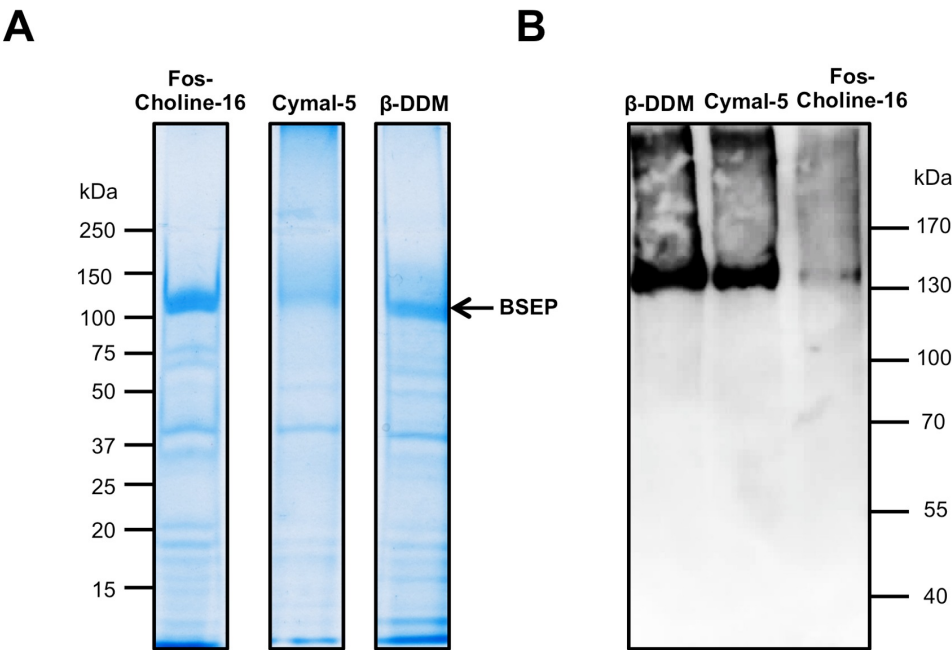


Figure 5. Purification and nucleotide binding of human BSEP. A Coomassie Brilliant Blue-stained SDS-PAGE of purified BSEP solubilized in Fos-choline-16 or in β-DDM and Cymal5, which were exchanged after solubilization. Molecular weight markers are indicated on the left. B Purified BSEP in all three detergents was incubated with ATP-agarose and bound protein was eluted in SDS sample buffer and examined with immunoblotting with a monoclonal antibody (F-6). BSEP signals could be detected in β-DDM and Cymal5, but not in Fos-Choline-16, indicating only binding to ATP in maltosides.  
doi:10.1371/journal.pone.0060620.g006

Especially ABC transporters of the liver like MDR1 (P-gp, ABCB1), ABCG2, ABCG5/G8 or ABCC1, ABCC3 and ABCC6 (MRP 1, 3 and 6) could be expressed and partially purified [34,46,48,49,50,51]. Since BSEP and MDR3 were not included in this expression screen, we cloned these genes into the expression vector pSGP18. The cDNA of BSEP and MDR3 is unstable and cannot be cloned by conventional cloning in *E. coli* [45]. Therefore, we modified the pSGP18 vector. Both transporters as

well as the GFP-fusion proteins were expressed without detectable degradation products (Fig. 1). To analyze whether processing and especially targeting of BSEP and MDR3 to the plasma membrane in *P. pastoris* occurs, we employed fluorescence microscopy. Fluorescence microscopy of heterologous expressed proteins, particularly with distinct destinations in the cell is a valuable tool to directly judge the quality of the overexpressed protein. These experiments revealed that both transporters were targeted

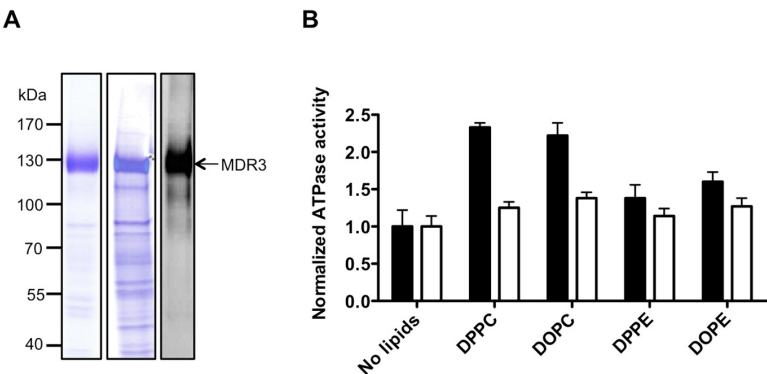


Figure 6. Characterization of purified human MDR3 in Fos-choline-16. A Coomassie Brilliant Blue-stained SDS-PAGE and immunoblot using an anti-MDR3 antibody of purified MDR3 wild-type and the MDR3 EQ/EQ-mutant via TAP. Molecular weight markers are shown on the left. B Normalized ATPase activity of MDR3 wild-type (black) and of an ATPase deficient mutant (E558Q E1207Q, white) in FC-16 without and with different phospholipids. The ATPase activity of three independent MDR3 purifications was determined  $\pm$  SD (n=3).  
doi:10.1371/journal.pone.0060620.g006

correctly and no intracellular retention occurred. This adverts correct folding of BSEP and MDR3.

To date high-throughput methods are available to systematically screen a huge number of detergents in an appropriate time frame for their capability to solubilize the membrane protein of interest. We used a dot blot based solubilization screen on an analytical scale similar to approaches used for GPCRs heterologously expressed in *P. pastoris* or *E. coli* [36,52]. We analyzed more than 100 different detergents covering all four classes of detergents. Only detergents of the Fos-choline as well as Cyclofos series were able to solubilize BSEP and MDR3 in a nearly quantitative manner. None of the maltosides, thio-maltosides or glycosides were able to solubilize BSEP and MDR3. Surprisingly, BSEP-GFP could be solubilized to some degree by those detergents suggesting that the GFP tag enhances solubilization. The zwitterionic Fos-choline and Cyclofos series are lipid-like detergents and possess a head group consisting of phosphocholine, but differ in the hydrophobic part as Fos-cholines have a plain acyl chain with varying number of carbon atoms and Cyclofos detergents additionally contain a cyclohexane ring at the omega position of the acyl chain. This result is in contrast to other used detergents for liver ABC transporters expressed heterologously in *P. pastoris*. ABCG3 was solubilized in b-DDM like ABCG5/G8 [34,53]. MDR1 was solubilized in various detergents from *P. pastoris* membranes including b-DM, b-DDM, Lyso-PC, deoxycholic acid or Triton-X100 [48,54,55,56,57]. Despite the high degree of sequence identity between MDR1 and MDR3 (85% homology to human MDR1, 80% to mouse MDR1), MDR3 behaves different, since it could not be solubilized with Triton-X100 (data not shown), which was used to crystallize mouse MDR1 [54]. Also ABCG2 was solubilized in b-DDM, but could only be solubilized in Fos-Choline-16 when expressed in High Five cells [46,49].

GFP fusion proteins cannot only be used as quality marker for heterologous expression, but also as a tool to screen the influence of a detergent to the membrane protein using FSEC. We employed this technique to investigate those detergents more in detail that were successfully identified in the dot blot screen. The Fos-Choline series displayed a clear dependence on the acyl chain length, i. e. increasing the acyl chain length increased the monodispersity of the protein sample. For BSEP-GFP, we also tested some maltoside detergents, although the solubilization efficacy was moderate for BSEP-GFP as judged from the dot blot. All tested maltosides showed very monodisperse FSEC profiles with less aggregation and a symmetrical peak, e.g. with Cymal-5 or b-DDM. b-DDM in general is believed to be a mild detergent and is often used for solubilization, purification and crystallization trails. On the other hand, the Fos-cholines showed a large aggregation peak and with increasing acyl chain length, a BSEP-GFP degradation product was more visible indicating instability of the membrane protein, and the peak became more unsymmetrically. Nonetheless, we decided to use Fos-choline-16 for BSEP and MDR3 for solubilization because of its efficacy and its use for other ABC transporter like LmrA [47], BmrC/D [58] and the aforementioned ABCG2 [46].

We were able to purify MDR3 and BSEP for the first time yielding 3.6 mg and 3.1 mg of protein per 100 g of cells, respectively. This is in good agreement with ABCB1 (3.6 mg) or ABCG3 (3.9 mg) [34,48]. BSEP is expressed at lower levels than MDR3 in *P. pastoris* and thus the yield is lower underlining the variance of expression of different proteins. Both transporters were purified by TAP from crude membranes, which resulted in a homogeneous preparation for MDR3 as judged by SDS-PAGE. In case of BSEP, the purity was not as high.

BSEP and MDR3 belong to the ABC transporter family and ATP hydrolysis drives translocation of bile salts or phosphatidylcholine. However, we could not detect any ATPase activity for BSEP in the detergent-solubilized state, neither basal nor substrate induced. To see whether BSEP was purified in a state, which at least allows binding of ATP, we employed ATP beads. Here, we could confirm that purified BSEP is able to bind ATP in the presence of  $\beta$ -DDM and Cymal-5. This indicates that at least the NBDs of BSEP are properly folded, which is a prerequisite for proper functioning and that Fos-choline-16 likely locks the protein in a binding-incompatible state, whereas b-DDM and Cymal-5 invert this state. For BSEP it is known, that its transport activity is depending on cholesterol [59]. Enrichment of *S. cerevisiae* cell membranes expressing BSEP with cholesterol drastically increases its transport activity [60]. If cholesterol is bound to the transporter itself or is just required as a membrane component has not been clarified yet. In the yeast expression host however, ergosterol is the predominant sterol instead of cholesterol like in other mammalian cells. Both sterols differ by two additional double bonds (in the ring and in the tail) in the case of ergosterol. The striking dependence of transport activity of BSEP on cholesterol and the absence of this sterol in yeast might explain the lack of ATPase activity. However, even in the absence of cholesterol, BSEP is able to bind to ATP in the detergent-solubilized state.

MDR3 displayed a substantial ATPase activity. This observation was sustained by analysis of an ATP hydrolysis deficient EQ double mutant (E558Q, E1207Q). Generally, a mutation of the glutamine of the Walker B motif renders ABC transporters ATPase inactive. Here, we generated the double mutant to ensure that the observed stimulation of ATPases was not due to contaminating ATPases. The substrate specificity for MDR3 was already investigated using *S. cerevisiae* secretory vesicles or cell-culture based methods [16,32,61]. All experiments showed, that MDR3 translocates short chain PC lipids ( $C_8$ ) or long chain derivatives ( $C_{16}$ ), but not PE, sphingomyelin or ceramides.

Here, we demonstrate for the first time that the ATPase activity of detergent-solubilized MDR3 in the presence of phosphatidylcholine lipids could be stimulated by a factor of almost 2.5, while the EQ/EQ mutant did not display any stimulation. Furthermore, it was shown that the specificity resulted from the phosphatidylcholine headgroup. We proved that MDR3 ATPase activity is specifically stimulated by PC lipids and not by PE lipids, which differ only in the headgroup.

In summary, we demonstrate for the first time the expression of two human ABC transporters, MDR3 and BSEP, in the yeast *P. pastoris* and their correct targeting to the plasma membrane. BSEP could bind to ATP in detergent, but no hydrolytic activity could be detected. Furthermore, we established a purification procedure for human MDR3, which resulted in purified and functional protein. This study provides the foundation for further investigations of the human liver ABC transporters BSEP and MDR3.

## Supporting Information

File S1 Combined file of supporting figures and tables. Figure S1: Dot Blot quantification of BSEP (A), BSEP-GFP (B) and MDR3 (C). Average values from two independent dot blots are shown ( $n = 2$ )  $\pm$  SD. Large errors for e.g. the Fos-Choline series resulted from saturation of the detector. The intensity of SDS was set to 100% and all other values were normalized to SDS. Black bars represent zwitter-ionic detergents, grey bars ionic detergents and white bars non-ionic detergents. Figure S2: FSEC profiles of free GFP and MDR3-GFP in selected detergents. The x-axis shows time in minutes, the y-axis fluorescence in arbitrary units.

Figure S3: FSEC profiles of BSEP-GFP in selected detergents. The x-axis shows time in minutes, the y-axis fluorescence in arbitrary units. Table S1: Used detergents for solubilization of BSEP and MDR3 and Dot Blot analysis; N: Non-ionic detergents; Z: Zwitterionic detergents; A: Anionic detergents; C: Cationic detergents. (DOCX)

## Acknowledgments

We are indebted to Dr. Mark E. Dumont (University of Rochester Medical Center, NY, USA) for the pSGP18 plasmid. We thank Martinique

Frentrup and Maria Bous for technical assistance, André Abts for help with the HPLC usage and Peter Zentis and Prof. Dr. Claus Seidel, Institute of Molecular Physical Chemistry, Heinrich Heine University Düsseldorf for assistance with the confocal microscopy measurements.

## Author Contributions

Conceived and designed the experiments: PE MK SS LS. Performed the experiments: PE MK JS. Analyzed the data: PE MK SS LS. Contributed reagents/materials/analysis tools: JS. Wrote the paper: PE MK SS LS.

## References

- Schmitt L, Tampe R (2002) Structure and mechanism of ABC transporters. *Current opinion in structural biology* 12: 754–760.
- Davidson AL, Dassa E, Orelle C, Chen J (2008) Structure, function, and evolution of bacterial ATP-binding cassette systems. *Microbiology and molecular biology reviews* 72: 317–364, table of contents.
- Dean M, Rzhetsky A, Allikmets R (2001) The human ATP-binding cassette (ABC) transporter superfamily. *Genome research* 11: 1156–1166.
- Riordan JR, Rommens JM, Kerem B, Alon N, Rozmahel R, et al. (1989) Identification of the cystic fibrosis gene: cloning and characterization of complementary DNA. *Science* 245: 1066–1073.
- Mosser J, Douar AM, Sarde CO, Kioschis P, Feil R, et al. (1993) Putative X-linked adrenoleukodystrophy gene shares unexpected homology with ABC transporters. *Nature* 361: 726–730.
- Bodzioch M, Orso E, Klucken J, Langmann T, Bottcher A, et al. (1999) The gene encoding ATP-binding cassette transporter 1 is mutated in Tangier disease. *Nature genetics* 22: 347–351.
- Brooks-Wilson A, Marcil M, Clee SM, Zhang LH, Roomp K, et al. (1999) Mutations in ABC1 in Tangier disease and familial high-density lipoprotein deficiency. *Nature genetics* 22: 336–345.
- Keppeler D (2011) Multidrug resistance proteins (MRPs, ABCs): importance for pathophysiology and drug therapy. *Handbook of experimental pharmacology*: 299–323.
- Ambudkar SV, Kimchi-Sarfaty C, Sauna ZE, Gottesman MM (2003) P-glycoprotein: from genomics to mechanism. *Oncogene* 22: 7468–7485.
- Ni Z, Bikadi Z, Rosenberg MF, Mao Q (2010) Structure and function of the human breast cancer resistance protein (BCRP/ABCG2). *Current drug metabolism* 11: 603–617.
- Meier PJ, Stieger B (2002) Bile salt transporters. *Annual review of physiology* 64: 635–661.
- Hofmann AF, Hagey LR (2008) Bile acids: chemistry, pathochemistry, biology, pathobiology, and therapeutics. *Cellular and molecular life sciences: CMLS* 65: 2461–2483.
- Noe J, Stieger B, Meier PJ (2002) Functional expression of the canalicular bile salt export pump of human liver. *Gastroenterology* 123: 1659–1666.
- Kubitz R, Droge C, Stindt J, Weissenberger K, Haussinger D (2012) The bile salt export pump (BSEP) in health and disease. *Clinics and research in hepatology and gastroenterology*.
- Stieger B (2011) The role of the sodium-taurocholate cotransporting polypeptide (NTCP) and of the bile salt export pump (BSEP) in physiology and pathophysiology of bile formation. *Handbook of experimental pharmacology*: 205–259.
- van Helvoort A, Smith AJ, Sprong H, Fritzsche I, Schinkel AH, et al. (1996) MDR1 P-glycoprotein is a lipid translocase of broad specificity, while MDR3 P-glycoprotein specifically translocates phosphatidylcholine. *Cell* 87: 507–517.
- Oude Elferink RP, Paulusma CC (2007) Function and pathophysiological importance of ABCB4 (MDR3 P-glycoprotein). *Pflügers Archiv: European journal of physiology* 453: 601–610.
- Graf GA, Yu L, Li WP, Gerard R, Tuma PL, et al. (2003) ABCG5 and ABCG8 are obligate heterodimers for protein trafficking and biliary cholesterol excretion. *The Journal of biological chemistry* 278: 48275–48282.
- Small DM (2003) Role of ABC transporters in secretion of cholesterol from liver into bile. *Proceedings of the National Academy of Sciences of the United States of America* 100: 4–6.
- Strautnieks SS, Kagalwalla AF, Tanner MS, Knisely AS, Bull L, et al. (1997) Identification of a locus for progressive familial intrahepatic cholestasis PFIC2 on chromosome 2q24. *American journal of human genetics* 61: 630–633.
- Deleuze JF, Jacquemin E, Dubuisson C, Cresteil D, Dumont M, et al. (1996) Defect of multidrug-resistance 3 gene expression in a subtype of progressive familial intrahepatic cholestasis. *Hepatology* 23: 904–908.
- Dzagania T, Engelmann G, Haussinger D, Schmitt L, Flechtenmacher C, et al. (2012) The histidine-loop is essential for transport activity of human MDR3. A novel mutation of MDR3 in a patient with progressive familial intrahepatic cholestasis type 3. *Gene* 506: 141–145.
- van Mil SW, van der Woerd WL, van der Brugge G, Sturm E, Jansen PL, et al. (2004) Benign recurrent intrahepatic cholestasis type 2 is caused by mutations in ABCB11. *Gastroenterology* 127: 379–384.
- Glantz A, Marschall HU, Mattsson LA (2004) Intrahepatic cholestasis of pregnancy: Relationships between bile acid levels and fetal complication rates. *Hepatology* 40: 467–474.
- Rosmorduc O, Hermelin B, Poupon R (2001) MDR3 gene defect in adults with symptomatic intrahepatic and gallbladder cholesterol cholelithiasis. *Gastroenterology* 120: 1459–1467.
- Jacquemin E (2012) Progressive familial intrahepatic cholestasis. *Clinics and research in hepatology and gastroenterology* 36 Suppl 1: S26–35.
- Gonzales E, Grosse B, Cassio D, Davit-Spraul A, Fabre M, et al. (2012) Successful mutation-specific chaperone therapy with 4-phenylbutyrate in a child with progressive familial intrahepatic cholestasis type 2. *Journal of hepatology* 57: 695–698.
- Kubitz R, Sutfels G, Kuhlkamp T, Kolling R, Haussinger D (2004) Trafficking of the bile salt export pump from the Golgi to the canalicular membrane is regulated by the p38 MAP kinase. *Gastroenterology* 126: 541–553.
- Mita S, Suzuki H, Akita H, Hayashi H, Onuki R, et al. (2006) Vectorial transport of unconjugated and conjugated bile salts by monolayers of LLC-PK1 cells doubly transfected with human NTCP and BSEP or with rat Ntcp and Bsep. *American journal of physiology Gastrointestinal and liver physiology* 290: G550–556.
- Wang R, Chen HL, Liu L, Sheps JA, Phillips MJ, et al. (2009) Compensatory role of P-glycoproteins in knockout mice lacking the bile salt export pump. *Hepatology* 50: 948–956.
- Hayashi H, Takada T, Suzuki H, Akita H, Sugiyama Y (2005) Two common PFIC2 mutations are associated with the impaired membrane trafficking of BSEP/ABCB11. *Hepatology* 41: 916–924.
- Green A, Romero MR, Kunne C, Hoosdally SJ, Dixon PH, et al. (2011) Complementary functions of the flippase ATP8B1 and the floppase ABCB4 in maintaining canalicular membrane integrity. *Gastroenterology* 141: 1927–1937.e1921–1924.
- Byrne JA, Strautnieks SS, Mieli-Vergani G, Higgins CF, Linton KJ, et al. (2002) The human bile salt export pump: characterization of substrate specificity and identification of inhibitors. *Gastroenterology* 123: 1649–1658.
- Chloupkova M, Pickert A, Lee JY, Souza S, Trinh YT, et al. (2007) Expression of 25 human ABC transporters in the yeast *Pichia pastoris* and characterization of the purified ABCB3 ATPase activity. *Biochemistry* 46: 7992–8003.
- Junge F, Schneider B, Reckel S, Schwarz D, Dotsch V, et al. (2008) Large-scale production of functional membrane proteins. *Cellular and molecular life sciences: CMLS* 65: 1729–1755.
- Zeder-Lutz G, Cherouati N, Reinhart C, Pattus F, Wagner R (2006) Dot-blot immunodetection as a versatile and high-throughput assay to evaluate recombinant GPCRs produced in the yeast *Pichia pastoris*. *Protein expression and purification* 50: 118–127.
- Newstead S, Kim H, von Heijne G, Iwata S, Drew D (2007) High-throughput fluorescent-based optimization of eukaryotic membrane protein overexpression and purification in *Saccharomyces cerevisiae*. *Proceedings of the National Academy of Sciences of the United States of America* 104: 13936–13941.
- Mizutani K, Yoshioka S, Mizutani Y, Iwata S, Mikami B (2011) High-throughput construction of expression system using yeast *Pichia pastoris*, and its application to membrane proteins. *Protein expression and purification* 77: 1–8.
- Drew D, Newstead S, Sonoda Y, Kim H, von Heijne G, et al. (2008) GFP-based optimization scheme for the overexpression and purification of eukaryotic membrane proteins in *Saccharomyces cerevisiae*. *Nature protocols* 3: 784–798.
- Eshaghi S (2009) High-throughput expression and detergent screening of integral membrane proteins. *Methods in molecular biology* 498: 265–271.
- Gutmann DA, Mizohata E, Newstead S, Ferrandon S, Postis V, et al. (2007) A high-throughput method for membrane protein solubility screening: the ultracentrifugation dispersity sedimentation assay. *Protein science: a publication of the Protein Society* 16: 1422–1428.
- Vergis JM, Purdy MD, Wiener MC (2010) A high-throughput differential filtration assay to screen and select detergents for membrane proteins. *Analytical biochemistry* 407: 1–11.

## Purification of Human BSEP and MDR3

43. Hattori M, Hibbs RE, Gouaux E (2012) A fluorescence-detection size-exclusion chromatography-based thermostability assay for membrane protein precrystallization screening. *Structure* 20: 1293–1299.
44. Kawate T, Gouaux E (2006) Fluorescence-detection size-exclusion chromatography for precrystallization screening of integral membrane proteins. *Structure* 14: 673–681.
45. Stindt J, Ellinger P, Stross C, Keitel V, Haussinger D, et al. (2011) Heterologous overexpression and mutagenesis of the human bile salt export pump (ABCB11) using DREAM (Directed REcombination-Assisted Mutagenesis). *PLoS one* 6: e20562.
46. McDevitt CA, Collins R, Kerr ID, Callaghan R (2009) Purification and structural analyses of ABCG2. *Advanced drug delivery reviews* 61: 57–65.
47. Infed N, Hanekop N, Driessen AJ, Smits SH, Schmitt L (2011) Influence of detergents on the activity of the ABC transporter LmrA. *Biochimica et biophysica acta* 1808: 2313–2321.
48. Lerner-Marmarosh N, Gimi K, Urbatsch IL, Gros P, Senior AE (1999) Large scale purification of detergent-soluble P-glycoprotein from *Pichia pastoris* cells and characterization of nucleotide binding properties of wild-type, Walker A, and Walker B mutant proteins. *The Journal of biological chemistry* 274: 34711–34718.
49. Rosenberg MF, Bikadi Z, Chan J, Liu X, Ni Z, et al. (2010) The human breast cancer resistance protein (BCRP/ABCG2) shows conformational changes with mitoxantrone. *Structure* 18: 482–493.
50. Cai J, Daoud R, Alqawi O, Georges E, Pelletier J, et al. (2002) Nucleotide binding and nucleotide hydrolysis properties of the ABC transporter MRP6 (ABCC6). *Biochemistry* 41: 8058–8067.
51. Cai J, Daoud R, Georges E, Gros P (2001) Functional expression of multidrug resistance protein 1 in *Pichia pastoris*. *Biochemistry* 40: 8307–8316.
52. Ren H, Yu D, Ge B, Cook B, Xu Z, et al. (2009) High-level production, solubilization and purification of synthetic human GPCR chemokine receptors CCR5, CCR3, CXCR4 and CX3CR1. *PLoS one* 4: e4509.
53. Johnson BJ, Lee JY, Pickert A, Urbatsch IL (2010) Bile acids stimulate ATP hydrolysis in the purified cholesterol transporter ABCG5/G8. *Biochemistry* 49: 3403–3411.
54. Aller SG, Yu J, Ward A, Weng Y, Chittaboina S, et al. (2009) Structure of P-glycoprotein reveals a molecular basis for poly-specific drug binding. *Science* 323: 1718–1722.
55. Beaudet L, Urbatsch IL, Gros P (1998) Mutations in the nucleotide-binding sites of P-glycoprotein that affect substrate specificity modulate substrate-induced adenosine triphosphatase activity. *Biochemistry* 37: 9073–9082.
56. Bai J, Swartz DJ, Protasevich II, Brouillette CG, Harrell PM, et al. (2011) A gene optimization strategy that enhances production of fully functional P-glycoprotein in *Pichia pastoris*. *PLoS one* 6: e22577.
57. Urbatsch IL, Beaudet L, Carrier I, Gros P (1998) Mutations in either nucleotide-binding site of P-glycoprotein (MDR3) prevent vanadate trapping of nucleotide at both sites. *Biochemistry* 37: 4592–4602.
58. Galian C, Manon F, Dezi M, Torres C, Ebel C, et al. (2011) Optimized purification of a heterodimeric ABC transporter in a highly stable form amenable to 2-D crystallization. *PLoS one* 6: e19677.
59. Paulusma CC, de Waart DR, Kunne C, Mok KS, Elferink RP (2009) Activity of the bile salt export pump (ABCB11) is critically dependent on canalicular membrane cholesterol content. *The Journal of biological chemistry* 284: 9947–9954.
60. Kis E, Ioja E, Nagy T, Szente L, Heredi-Szabo K, et al. (2009) Effect of membrane cholesterol on BSEP/Bsep activity: species specificity studies for substrates and inhibitors. *Drug metabolism and disposition: the biological fate of chemicals* 37: 1878–1886.
61. Ruetz S, Gros P (1994) Phosphatidylcholine translocase: a physiological role for the *mdr2* gene. *Cell* 77: 1071–1081.

## **Supplementary Information**

### **Detergent Screening and Purification of the Human Liver ABC Transporters BSEP (ABCB11) and MDR3 (ABCB4) expressed in the yeast *Pichia pastoris***

Philipp Ellinger, Marianne Kluth, Jan Stindt, Sander H. Smits and Lutz Schmitt

Institute of Biochemistry, Heinrich Heine University, Düsseldorf. Germany

#### **Supplementary Information comprises:**

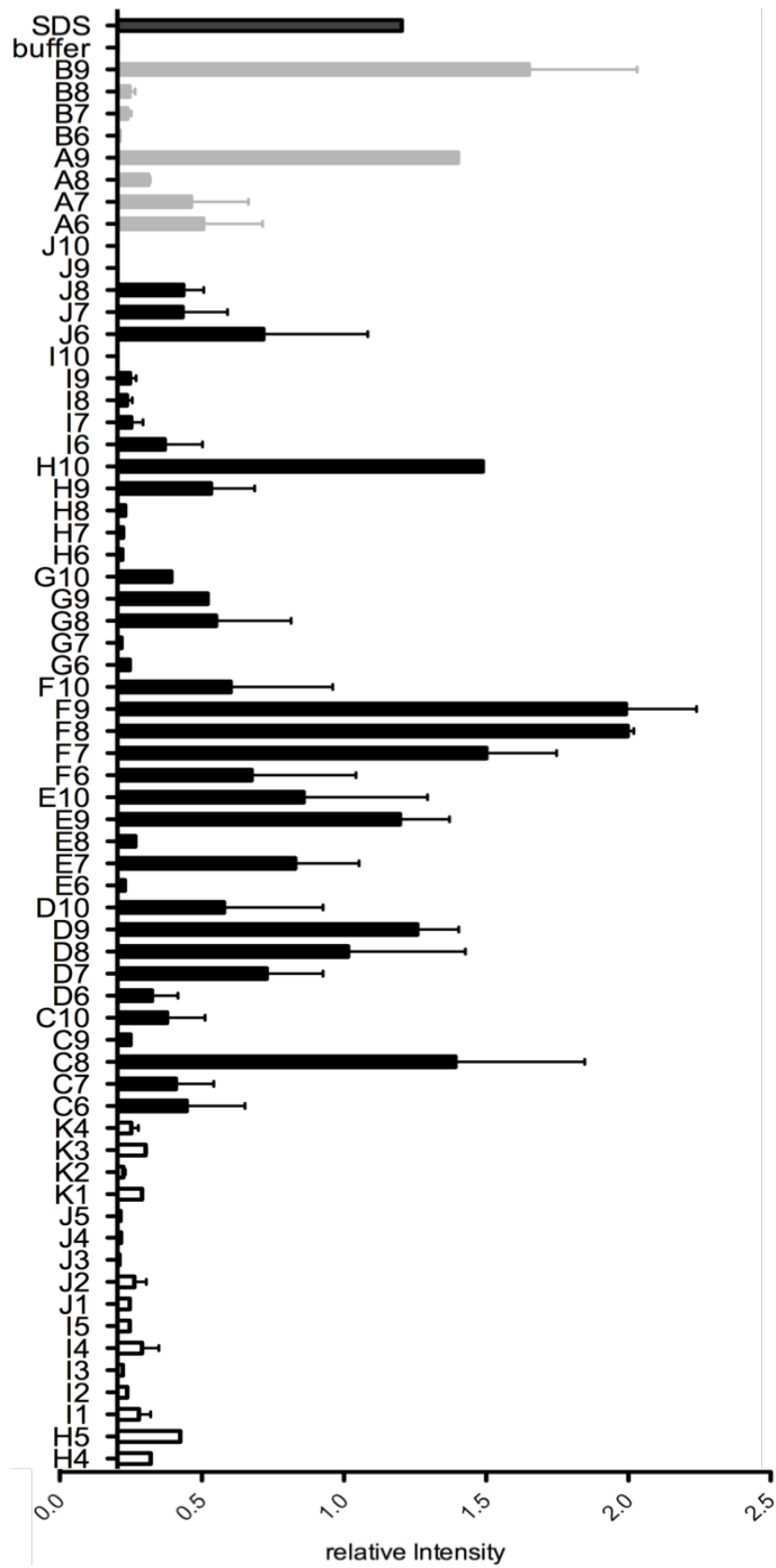
Supplementary Figures 1-3

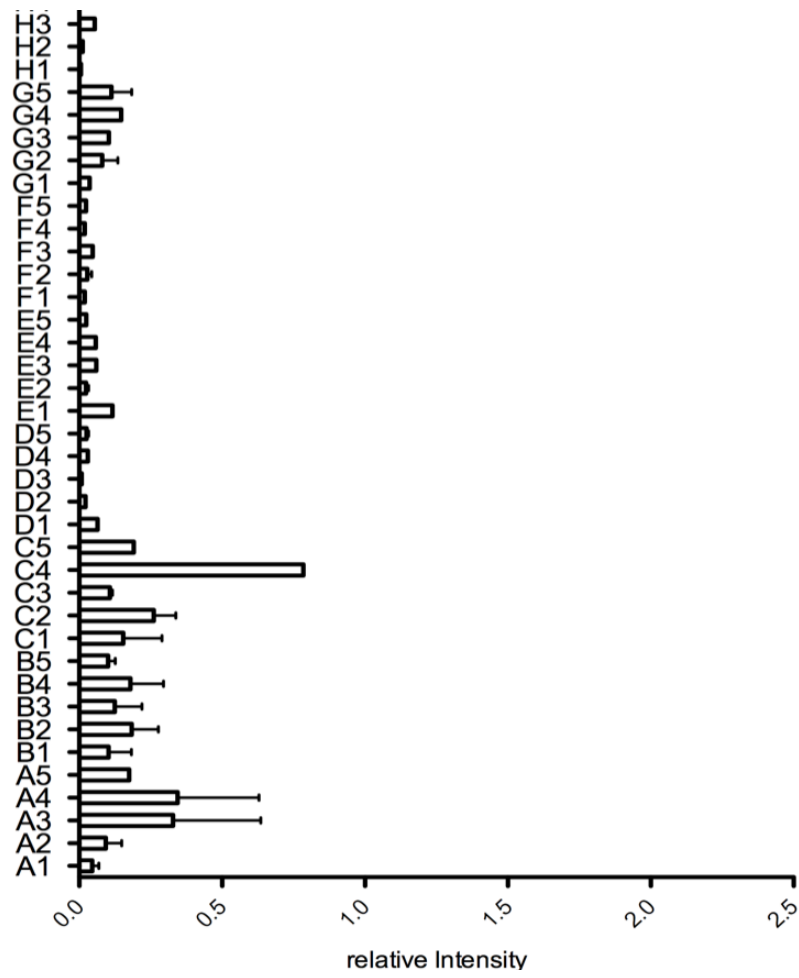
Supplementary Table 1

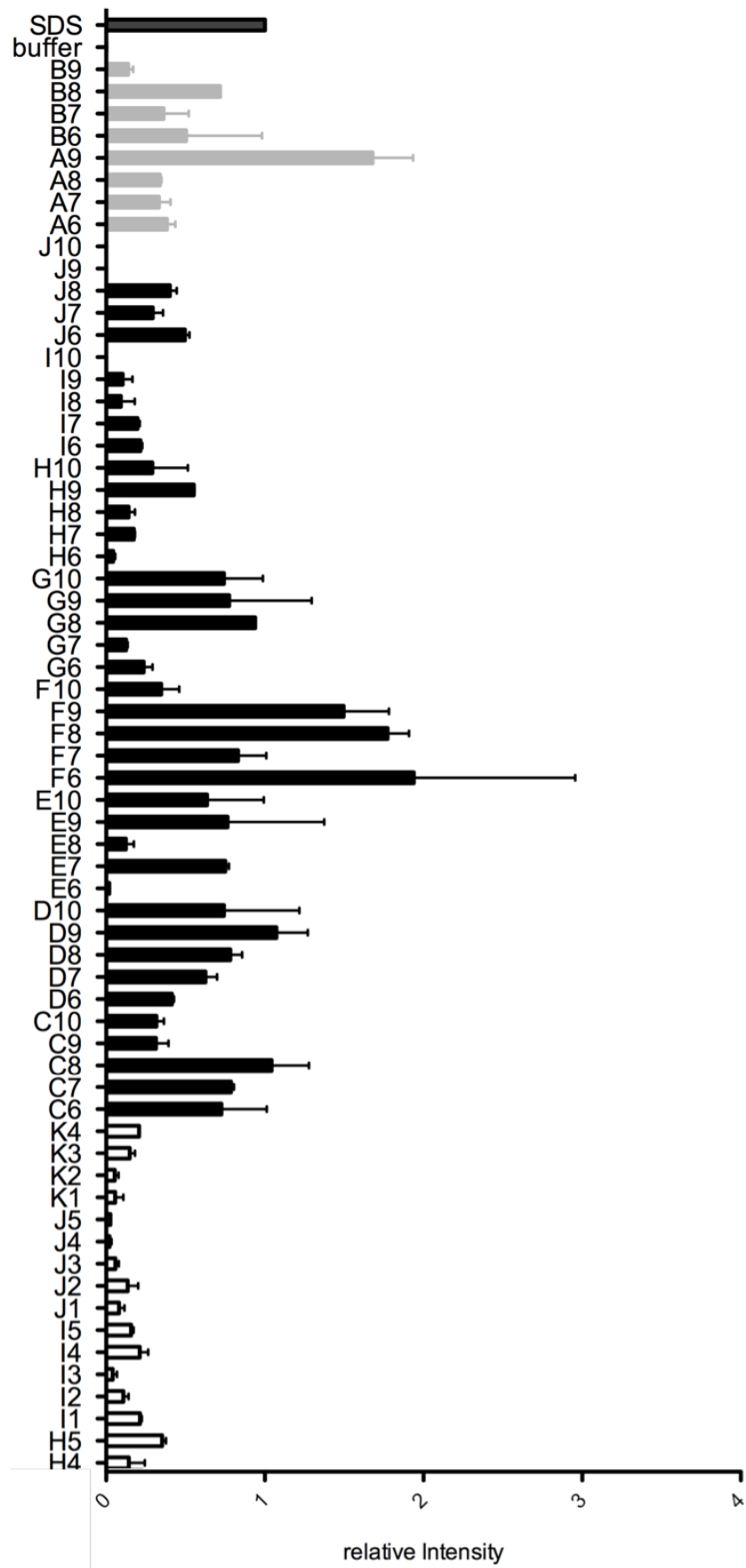


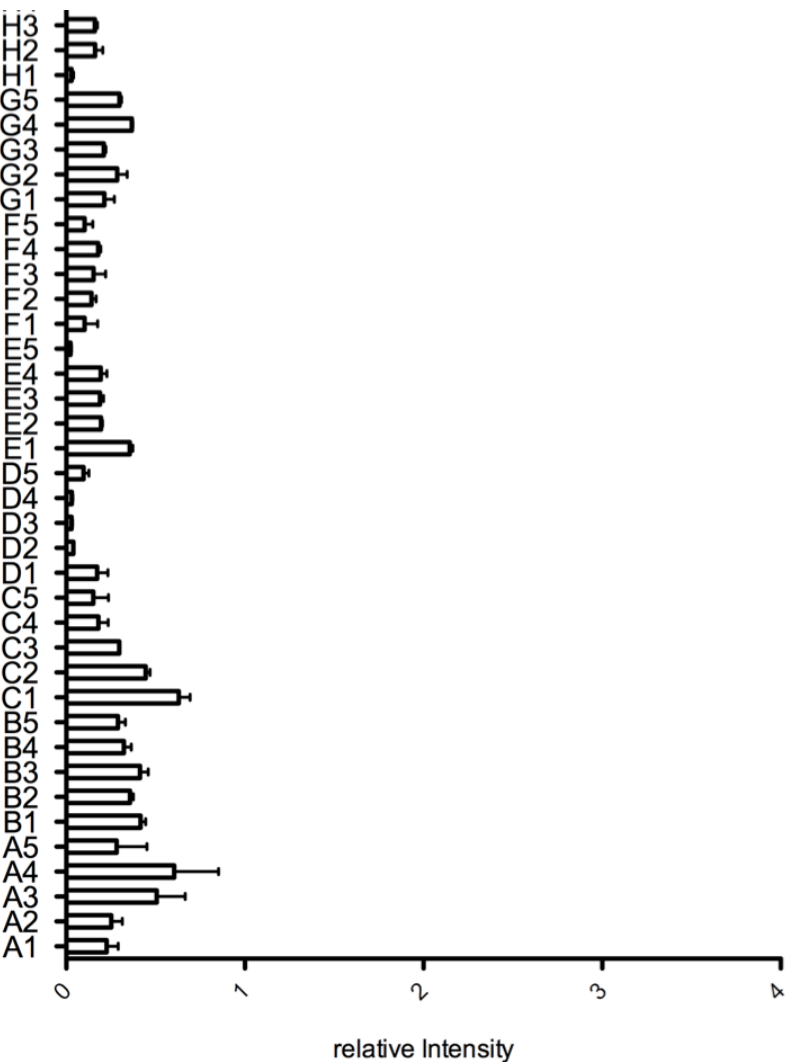
## Supplementary Figure S1

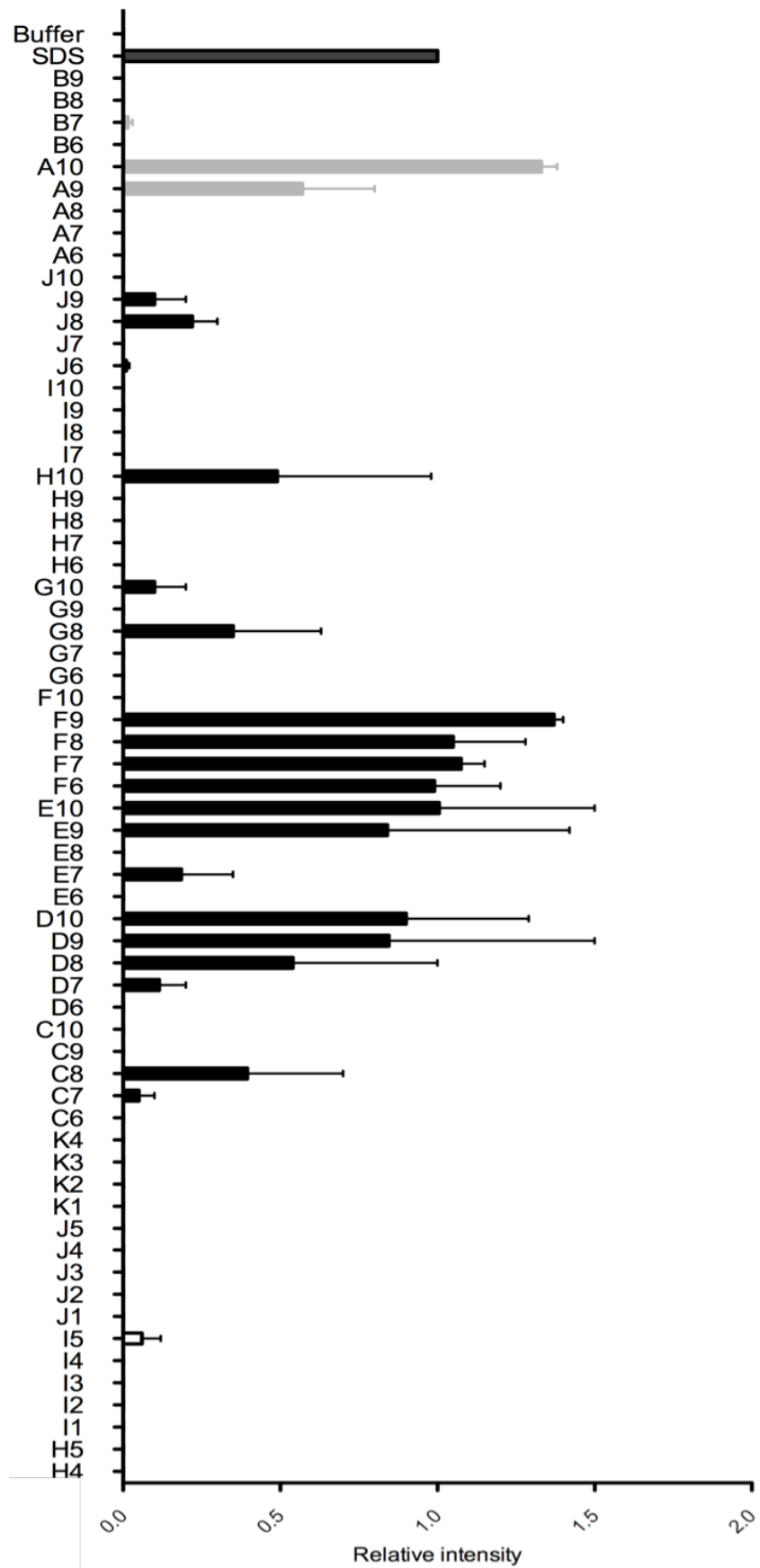
A

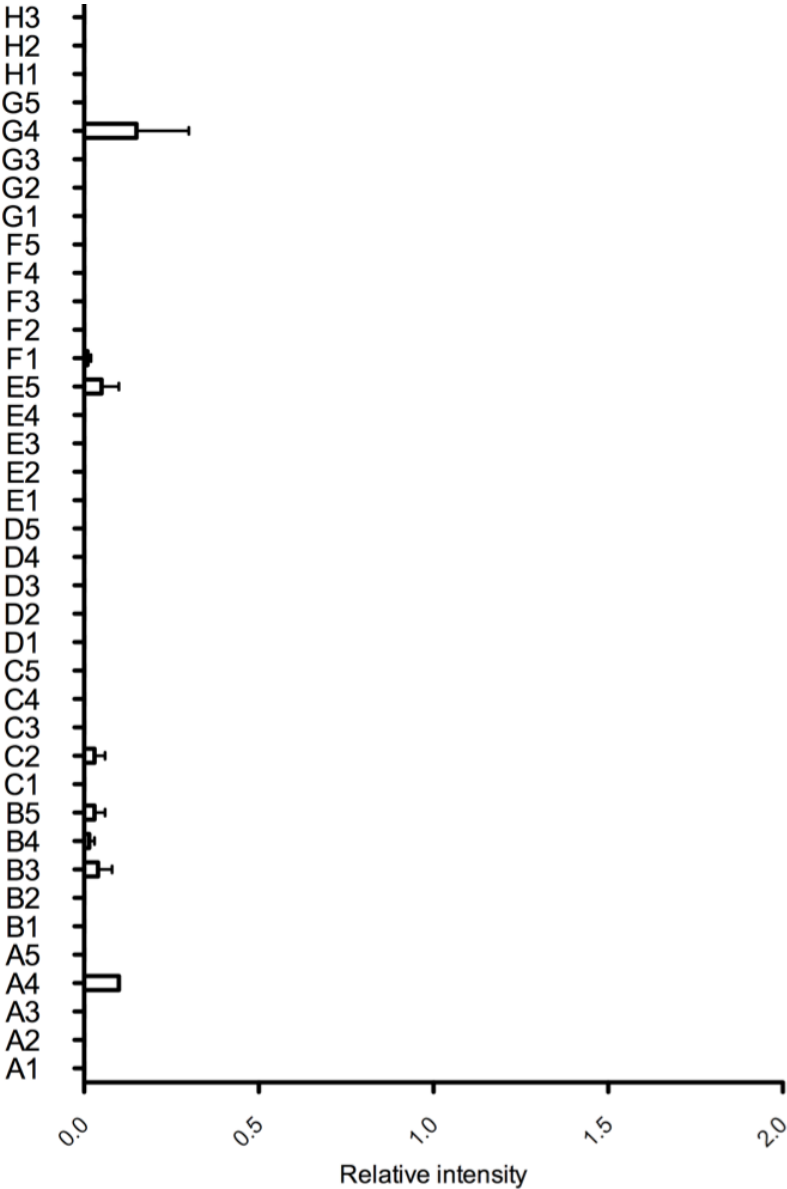




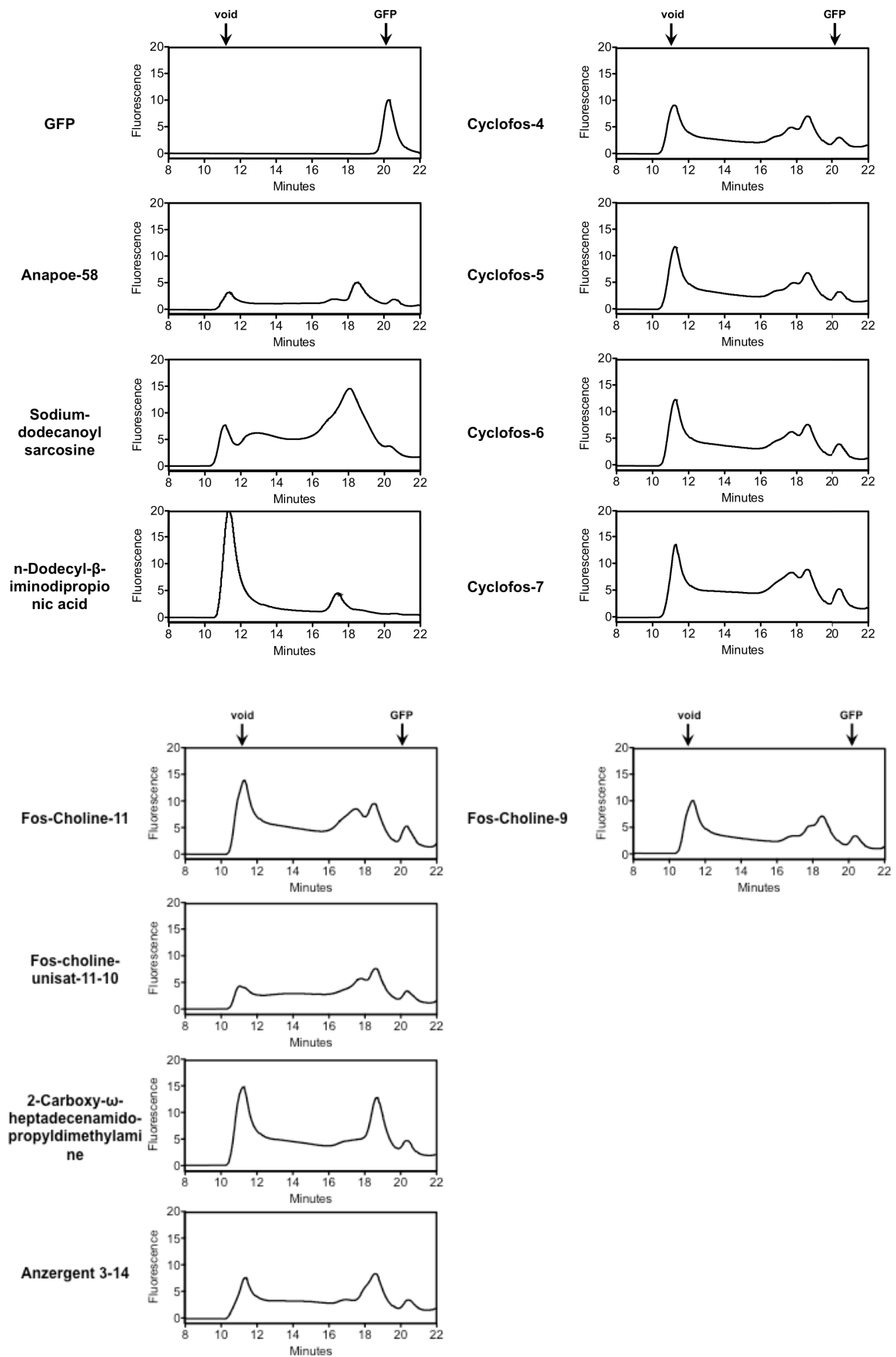
**B**



**C**

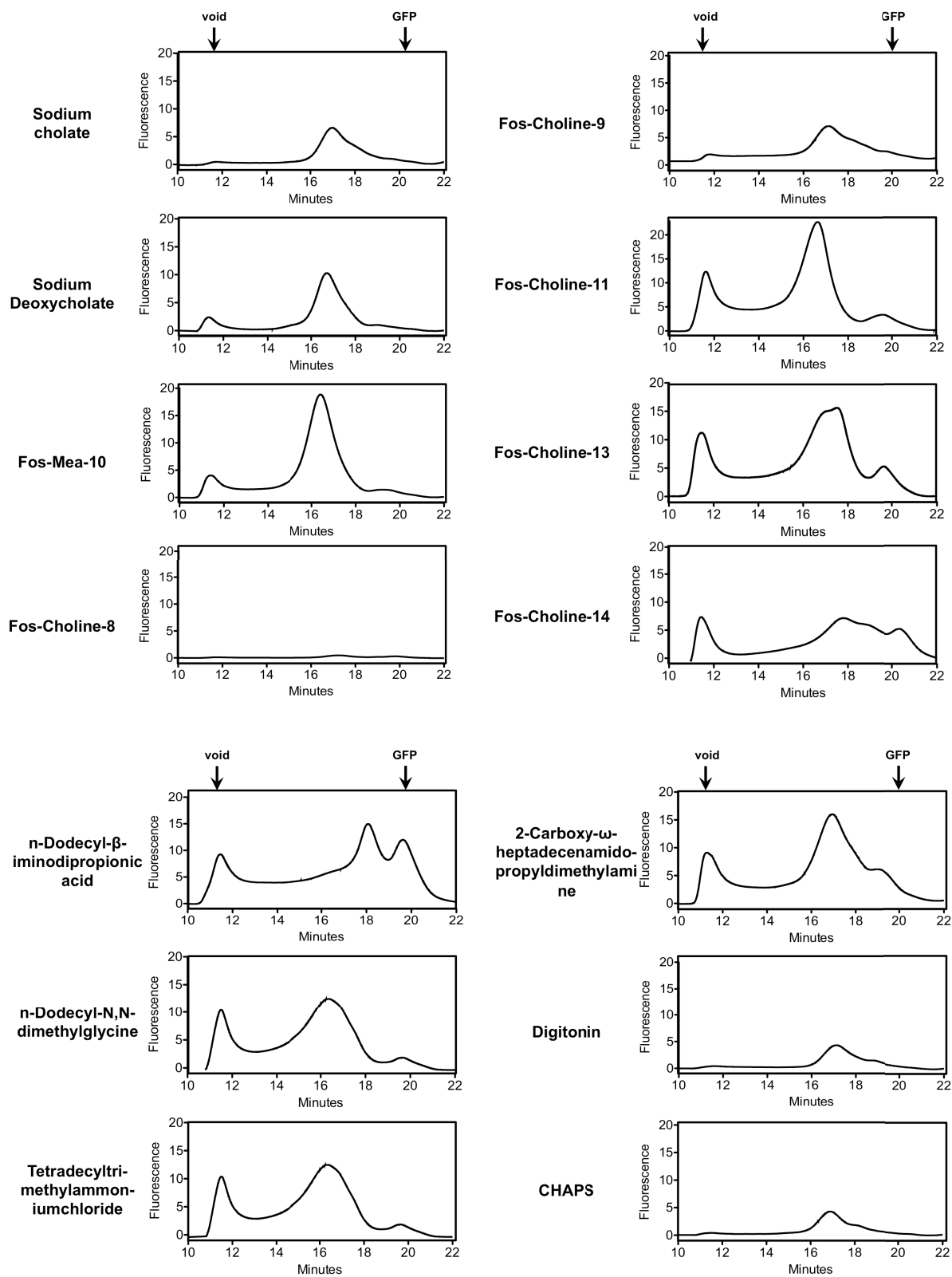


## Supplementary Figure S2





Supplementary Figure S3



**Supplementary Table S1**

Position	Detergent	cmc %	used %	nature
A1	Anameg®-7	0.65	1%	N
A2	Anapoe®-20	0.0072	1%	N
A3	Anapoe®-35	0.001	1%	N
A4	Anapoe®-58	0.00045	1%	N
A5	Anapoe®-80	0.0016	1%	N
B1	Anapoe®-C10E6	0.025	1%	N
B2	Anapoe®-C10E9	0.053	1%	N
B3	Anapoe®-C12E8	0.0048	1%	N
B4	Anapoe®-C12E9	0.003	1%	N
B5	Anapoe®-C12E10	0.2	1%	N
C1	Anapoe®-C13E8	0.0055	1%	N
C2	Anapoe®-X-100	0.015	1%	N
C3	Anapoe®-X-114	0.011	1%	N
C4	Anapoe®-X-305	–	1%	N
C5	Anapoe®-X-405	0.16	1%	N
D1	Big CHAP	0.25	1%	N
D2	Big CHAP deoxy	0.12	1%	N
D3	CYGLU®-3	0.86	2%	N
D4	CYMAL®-1	15	2%	N
D5	CYMAL®-2	5.4	2%	N
E1	CYMAL®-3	0.37	1%	N
E2	2,6-Dimethyl-4-heptyl- $\beta$ -D-maltose	1.2	2%	N
E3	2-propyl-1-pentyl maltose	1.9	2%	N
E4	MEGA-8	2.5	2%	N
E5	n-Octyl- $\beta$ -D-glucoside	0.53	2%	N
F1	n-Nonyl- $\beta$ -D-glucoside	0.2	1%	N
F2	n-Octyl- $\beta$ -D-maltoside	0.89	2%	N
F3	n-Nonyl- $\beta$ -D-maltoside	0.28	2%	N
F4	n-Decyl- $\alpha$ -D-maltoside	–	1%	N
F5	n-Tetradecyl- $\beta$ -D-maltoside	0.00054	1%	N
G1	n-Undecyl- $\alpha$ -D-maltoside	0.029	1%	N
G2	n-Undecyl- $\beta$ -D-maltoside	0.029	1%	N
G3	n-Dodecyl- $\alpha$ -D-maltoside	0.0076	1%	N
G4	n-Dodecyl- $\beta$ -D-maltoside	0.0087	1%	N
G5	n-Tridecyl- $\beta$ -D-maltoside	0.0017	1%	N
H1	n-Heptyl- $\beta$ -D-thioglucoside	0.85	2%	N
H2	n-Octyl- $\beta$ -D-thiomaltoside	0.4	2%	N
H3	n-Nonyl- $\beta$ -D-thiomaltoside	0.15	1%	N
H4	n-Decyl- $\beta$ -D-thiomaltoside	0.045	1%	N
H5	n-Undecyl- $\beta$ -D-thiomaltoside	0.011	1%	N
I1	n-Dodecyl- $\beta$ -D-thiomaltoside	0.0026	1%	N
I2	Pentaethylene glycol monododecylether(C10E5)	0.031	1%	N
I3	Tetraethylene glycol monoethylether(C8E4)	0.25	1%	N
I4	Sucrose monododecanoate	0.016	1%	N
I5	Dimethyldecylphosphine oxide	0.1	1%	N
J1	Tripglu	3.6	2%	N
J2				

J3	Decyl-β-D-glucoside	0.07	1%	N
J4				
J5	CYGLU®-4	0.058	2%	N
K1	CYMAL®-5	0.12	2%	N
K2	MEGA-10	0.21	2%	N
K3	NP40	0.05-0.3	1%	N
K4	Cyclohexyl-n-hexyl-β-D-maltoside	–	1%	N
C6	Anzergent® 3-10	1.2	2%	Z
C7	Anzergent®3-12	0.094	1%	Z
C8	Anzergent® 3-14	0.007	1%	Z
C9	CHAPS	0.49	2%	Z
C10	CHAPSO	0.5	2%	Z
D6	C-DODECAFOS™	0.77	2%	Z
D7	Cyclofos™-4	0.45	2%	Z
D8	Cyclofos™-5	0.15	1%	Z
D9	Cyclofos™-6	0.094	1%	Z
D10	Cyclofos™-7	0.022	1%	Z
E6	Cyclofos™-2	7.5	1%	Z
E7	Fos-Choline®-9	1.2	2%	Z
E8	Cyclofos™-3	1.3	2%	Z
E9	Fos-Choline®-11	0.062	1%	Z
E10	Fos-Choline®-12	0.047	1%	Z
F6	Fos-Choline®-13	0.027	1%	Z
F7	Fos-Choline®-14	0.0046	1%	Z
F8	Fos-Choline®-15	0.0027	1%	Z
F9	Fos-Choline®-16	0.00053	1%	Z
F10	Fos-Choline®-Iso-9	0.99	2%	Z
G6	Fos-Choline®-Iso-11	0.9	2%	Z
G7	Fos-Choline®-Iso-11-6U	0.87	2%	Z
G8	Fos-Choline®-Unisat-11-10	0.21	1%	Z
G9	Fos-Choline®-8	3.4	2%	Z
G10	Fosfen™-9	0.014	1%	Z
H6	Nopol-Fos™	1.4	2%	Z
H7	PMAL™-8	–	1%	Z
H8	PMAL™-C10	–	1%	Z
H9	n-Decyl-N,N-dimethylglycine	0.46	2%	Z
H10	n-Dodecyl-N,N-dimethylglycine	0.041	1%	Z
I7	n-Tetradecyl-N,N-dimethylamine-N-oxide	0.0075	1%	Z
I8	n-Dodecyl-N,N-dimethylamine-N-oxide	0.023	1%	Z
I9	Tripao	4.5	2%	Z
I10	n-Tetradecyl-N,N-dimethylamine-N-oxide	0.0075	1%	Z
J6	LAPAO	0.052	2%	Z
J7	PMAL™-C-12	–	2%	Z
J8	2-Carboxy-w-heptadecenamidopropyldimethylamine	–	1%	Z
J9	2-Carboxy-5-pentadecenamidopropyldimethylamine	–	1%	Z
J10	N,N dimethyl(3-carboxy-4-dodec-5-	0.0178	1%	Z

	ene)aminopropylamine			
<b>A6</b>	Deoxycholic acid. sodium salt	0.24	1%	A
<b>A7</b>	Sodium cholate	0.41	2%	A
<b>A8</b>	Fosmea®-10	0.15	1%	A
<b>A9</b>	Sodium dodecanoyl sarcosine	0.42	2%	A
<b>A10</b>	n-Dodecyl- $\beta$ -iminodipropionic acid (only used for MDR3)	N/A	1%	A
<b>B6</b>	Decyltrimethylammonium chloride	0.07	1%	C
<b>B7</b>	Dodecyltrimethylammonium chloride	0.0012	1%	C
<b>B8</b>	Hexadecyltrimethylammonium chloride	0.000102	1%	C
<b>B9</b>	Tetradecyltrimethylammonium chloride	0.0009	1%	C



**Chapter IV – *In vitro* ATPase activity of wild type MDR3 and mutants****Title:**

**A mutation within the extended X loop abolished substrate-induced  
ATPase activity of the human liver ABC Transporter MDR3**

In revision: *Journal of Biological Chemistry*

Impact factor: 4.65 (2013)

Own Proportion to this work: 85 %

Cloning and Expression of human wild type *MDR3* and  
mutants in *P. pastoris*

Purification of MDR3

ATPase activity determination

Writing of the manuscript

## A mutation within the extended X loop abolished substrate-induced ATPase activity of the human liver ABC Transporter MDR3

Marianne Kluth<sup>†</sup>, Jan Stindt<sup>‡</sup>, Carola Droege<sup>‡</sup>, Doris Linnemann<sup>‡</sup>, Ralf Kubitz<sup>‡</sup> and Lutz Schmitt<sup>†,\*</sup>

From the <sup>†</sup>Institute of Biochemistry, Heinrich Heine University, Düsseldorf, Germany and the <sup>‡</sup>Department of Gastroenterology, Hepatology and Infectiology, University Hospital, Düsseldorf, Germany

Running title: ATPase activity of human MDR3

To whom correspondence should be addressed: Lutz Schmitt, Institute of Biochemistry, Heinrich-Heine-University Düsseldorf, Universitätsstr. 1, 40225 Düsseldorf, Germany, Tel.: +49-211-81-10773; Fax: +49-211-81-15310; E-Mail: Lutz.Schmitt@hhu.de

**Keywords:** ABC Transporter; ATPase; Lipid transport; Liver injury; PFIC-3; MDR3; MDR1; Multidrug transporters; Transmission interface; X loop

**Background:** A mutation of the extended X loop of MDR3 caused hereditary liver cholestasis.

**Results:** Wild type MDR3 exhibited PC-induced ATPase activity, while the Q1174E mutant displayed no stimulation.

**Conclusion:** The glutamine preceding the ABC signature motif communicates substrate binding within the TMD to the extended X loop of the NBD.

**Significance:** This study provides evidence for a transmission interface coupling ATP hydrolysis to substrate transport.

### ABSTRACT

The human multidrug resistance protein 3 (MDR3/ABCB4) belongs to the ubiquitous family of ATP binding cassette (ABC) transporters and is located in the canalicular membrane of hepatocytes. There it flops phospholipids of the phosphatidylcholine family from the inner to the outer leaflet. Here, we report the characterization of wild type MDR3 and the Q1174E mutant, which was identified previously in a patient with progressive familial intrahepatic cholestasis type 3 (PFIC-3). We expressed different variants of MDR3 in the yeast *Pichia pastoris*, purified the proteins via tandem-affinity chromatography and determined MDR3 specific ATPase activity in the presence or absence of phospholipids. The ATPase activity of wild type MDR3 was stimulated twofold by liver PC or DOPC lipids. Furthermore, the crosslinking of MDR3 with

a thiol-reactive fluorophore blocked ATP hydrolysis and exhibited no PC stimulation. Similar, phosphatidylethanolamine (PE), phosphatidylserin (PS) and sphingomyelin (SM) lipids did not induce an increase of wild type MDR3 ATPase activity. The phosphate analogues BeF<sub>x</sub> and AlF<sub>x</sub> led to complete inhibition of ATPase activity, while orthovanadate inhibited exclusively the PC-stimulated ATPase activity of MDR3. The Q1174E mutation is located in the nucleotide-binding domain (NBD) in direct proximity of the leucine of the ABC signature motif and extended the X loop, which is found in ABC exporters. Our data on the Q1174E mutant demonstrated basal ATPase activity, but PC lipids were incapable of stimulating ATPase activity highlighting the role of the extended X loop in the crosstalk of the NBD and the transmembrane domain.

The human multidrug resistance protein 3 (MDR3/ABCB4) belongs to the family of ATP binding cassette (ABC) transporters and is highly expressed in the canalicular membrane of hepatocytes. In the canalculus, phosphatidylcholine (PC) lipids form mixed micelles with bile salts and cholesterol to reduce the destructive detergent activity of bile salts and to protect the biliary ducts (1). Because the flop of PC lipids from the inner leaflet of the lipid bilayer to the outer leaflet is a very slow process, PC lipids are translocated by the PC floppase MDR3 energized by ATP binding and hydrolysis (2-7).



*ATPase activity of human MDR3*

The first evidence that MDR3 flops phospholipids (PLs) was obtained by the generation of homozygous knock-out mice for the murine *Mdr2* gene (*Mdr2*<sup>-/-</sup> mice), which is homologous to human MDR3 (2). These mice showed a complete absence of PLs from bile. The function of *Mdr2* could be substituted in these mice by expressing the human *MDR3* gene, indicating that MDR3 acts as a PL floppase (3). Further studies used the lower hydrophobicity of short chain lipids (C<sub>5</sub>-C<sub>6</sub> chain) to determine *Mdr2*/MDR3 mediated lipid translocation in yeast and cultured mammalian cells, respectively. Direct evidence that MDR3 translocates exclusively PLs of the phosphatidylcholine family was obtained by van Helvoort and co-workers (5). They reported the translocation of fluorescently labeled, short chain PC lipids in polarized pig kidney epithelial cells transfected with MDR3. Subsequently, it was demonstrated in HEK293 cells stably expressing MDR3 that PC lipids are excreted in a bile salt-dependent manner (6-8).

MDR3 is a 1279-amino acid glycoprotein and is composed of two nucleotide-binding domains (NBDs) and two transmembrane domains (TMDs), which are encoded on a single gene forming a so-called full-size ABC transporter (9). MDR3 shares up to 76% identity and 86% similarity in the amino acid sequence with the human multidrug resistance protein 1 (MDR1/ABCB1), but fulfills a different physiological function (9-15). As of yet, no specific ATPase activity of MDR3 could be determined when the protein was expressed at high levels in insect (*Sf9*) cells or HEK293 cells, while MDR1 exhibited high ATPase activity in these systems (16,17). Smith *et al.* demonstrated vanadate-dependent nucleotide trapping of MDR3 in *Sf9* plasma membranes, which could be inhibited by the MDR1 reversal agents verapamil and cyclosporin A (16). In addition, Ishigami *et al.* ascertained the drug-stimulated ATPase activity of a chimera protein containing the TMDs of MDR1 and the NBDs of MDR3. They demonstrated that the purified chimera protein exhibited 10-fold lower drug stimulated ATPase activity compared to MDR1 (17). These findings confirmed that the NBDs of MDR3 bind ATP, but that ATP hydrolysis takes place with an apparent low turnover number.

Previously, we demonstrated that human wild type MDR3 exhibited PC-induced ATPase activity, while the ATPase deficient mutant of both Walker B motifs did not show

stimulation (18). In the present study, we characterized the ATPase activity of wild type MDR3 in terms of kinetic parameters, substrate spectrum and effect of phosphate analogues.

Furthermore, we analyzed the ATPase activity of the MDR3 Q1174E mutant *in vitro*, which was identified in a patient with progressive familial intrahepatic cholestasis type 3 (PFIC-3) and described previously in Kubitz *et al.* (19). This mutation is located in the extended X loop of NBD2 (TRVGDKD/TQ). Based on structural and biochemical data, the NBDs dimerize in a head-to-tail orientation in the presence of ATP (20-22). Each ATP binding site harbors highly conserved motifs, the Walker A (GXXGXGKS/T, where X can be any amino acid residue) and Walker B motif (ΦΦΦΦD, where Φ can be any hydrophobic residue) of one NBD and the ABC signature motif (C loop, LSGGQ) of the opposing NBD (23). A highly conserved motif, the X loop (TEVGERG), which is located in close proximity of the ABC signature motif was identified by Dawson *et al.* in ABC exporters (22). The X loop contacts the first intracellular loop (ICL1) of the TMD and likely transmits conformational changes generated by ATP binding and hydrolysis to the TMD (22,24,25). To date, the molecular function of this transmission interface with respect to coupling of the ATP hydrolysis cycle with substrate translocation is still not entirely clear. We expressed the Q1174E mutant in *P. pastoris* and purified the mutant via tandem affinity purification (TAP). The detergent-solubilized Q1174E mutant exhibited basal ATPase activity, which was demonstrated by modifying this mutant with a thiol-reactive fluorophore, but no substrate-stimulated ATPase activity in contrast to the wild type floppase. Thus, we suggest that glutamine 1174 is involved in the crosstalk of NBD and TMD.

## EXPERIMENTAL PROCEDURES

*Chemicals and Routine Procedures* – Foscholine 16 (FC-16) was obtained from Affymetrix and lipids were purchased from Avanti Polar Lipids. All other chemicals were from Sigma-Aldrich. The protein concentration was determined by a Bradford assay using the Coomassie Plus Assay (Pierce). The Mini-Protein 3 system (Bio-Rad) was used for SDS-PAGE on 7% gels. Immunoblotting was performed with a Tank blot system (Bio-Rad) using the monoclonal anti-P-gp C219 antibody (Merck) employing standard procedures.

*Cloning of human MDR3 and Site-directed Mutagenesis* – We cloned human wild type MDR3 (NM\_000443.3) as previously described (18). Site-directed mutagenesis was carried out with the QuikChange® XL (Agilent Technologies) and the Phusion Site-Directed Mutagenesis Kit (Thermo Scientific), respectively. To generate the ATPase deficient mutant, we exchanged Glu 558 and Glu 1207 of the conserved Walker B motif against Gln with the primer pair as described before (18). The Q1174E mutant was introduced into MDR3 with the Phusion Site-Directed Mutagenesis Kit (Thermo Scientific) using forward primer 5'-GATAAGGGGACTGAGCTCTCAGGAGGTC AAAAAC-3' and the reverse primer 5'-CCCACTCTTGTTCATATTTGTGGGGTAA CG-3'. The sequences of all constructs were verified by DNA sequencing (GATC Biotech).

*Transformation of P. pastoris and expression screening* – MDR3 expression constructs were transformed into electro-competent *P. pastoris* X33 cells (Invitrogen) using standard procedures and the expression level was analyzed as described in Ellinger *et al.* (18).

*Fermentation of MDR3 transformed P. pastoris cells* – For large-scale expression, *P. pastoris* cells containing the chromosomal integrated wild type MDR3, the E558Q/E1702Q double mutant or the Q1174E mutant gene were fermented in a 15 liter table-top glass fermenter (Applikon Biotechnology) according to the Invitrogen *P. pastoris* fermentation guidelines. Usually, a volume of 7 L basal salt media was inoculated with 1 L of an overnight culture grown in MGY (1.34% yeast nitrogen base, 1% glycerol and  $4 \times 10^{-5}$  % biotin) media. The glycerol fed-batch was performed for 4 h feeding ~500 mL of 50 % (v/v) glycerol added with 12 mL/L PTM1 salts. Protein expression was induced by addition of 3.6 mL/h/L methanol for 48 h. During the complete fermentation the temperature was set at 30°C, oxygenation was kept above 20% O<sub>2</sub> saturation and the mixer was set at 1000 rpm. Cells were harvested by centrifugation (5.000 xg, 10 min, 4°C), flash-frozen in liquid nitrogen and stored at -80°C until further use. Under these conditions, 1.4 kg of wet cell mass were routinely obtained.

*Preparation of crude membrane vesicles for protein purification* – Generally, 100 g of frozen *P. pastoris* cells expressing the respective MDR3 protein (wild type or mutant) were thawed on ice, washed with 500 mL ice cold 50 mM Tris-HCl, pH 8.0 and re-suspended at a

concentration of 0.5 g cells/mL in homogenization buffer (50 mM Tris-HCl, pH 8.0, 0.33 M sucrose, 75 mM NaCl, 1 mM EDTA, 1 mM EGTA, 100 mM 6-aminocaproic acid, 1 mM DTT) containing a protease inhibitor cocktail (Roche). Cells were disrupted by two passages through a pre-cooled TS Series Cell Disrupter (Constant Systems) at 2.7 kbar. After cell debris was removed by three centrifugation steps (10 min at 5000 xg, 4°C and 2x 30 min at 15,000 xg, 4°C), crude membrane vesicles were prepared by ultracentrifugation for 1 h at 125,000 xg at 4°C. Membrane vesicles were re-suspended in buffer A (50 mM Tris-HCl pH 8.0, 50 mM NaCl, 30% (v/v) glycerol) and flash frozen in liquid N<sub>2</sub>.

*Solubilization and purification of MDR3* – The purification of wild type MDR3 or mutant was performed as described previously with a few modifications (18). All procedures were carried out at 4°C. Crude membrane vesicles equivalent to 100 g wet cells were diluted to a final concentration of 15 mg/mL total protein with buffer A and solubilized with 1% (w/v) of FC-16 for 1 h at 4°C. Non-solubilized membrane vesicles were removed by centrifugation at 125.000 xg at 4°C for 1 h. All buffers typically contained 2x cmc FC-16 (0.0011 % (w/v) FC-16) and cooled to 4°C. The supernatant supplemented with 20 mM imidazole was loaded onto a Ni<sup>2+</sup>-loaded HiTrap Chelating column (5 ml, GE Healthcare) and washed with 10 column volumes of buffer A supplemented with 20 mM imidazole. Proteins were eluted in one step with buffer B (50 mM Tris-HCl pH 8.0, 50 mM NaCl, 200 mM imidazole, 20% (v/v) glycerol). The IMAC eluate was diluted 5-times with CaCl<sub>2</sub> binding buffer (50 mM Tris-HCl pH 8.0, 150 mM NaCl, 1 mM MgCl<sub>2</sub>, 2 mM CaCl<sub>2</sub> and 20% (v/v) glycerol), applied to 4 mL calmodulin affinity resin equilibrated in CaCl<sub>2</sub> binding buffer and incubated with the calmodulin resin overnight at 4°C on a rotator. The resin was transferred into a gravity flow column and washed with 10 column volumes of CaCl<sub>2</sub> binding buffer. Protein was eluted with 5 column volumes of EGTA elution buffer (2 mM EGTA, 50 mM Tris-HCl pH 7.4, 150 mM NaCl, and 20% (v/v) glycerol). The purified protein was directly used for ATPase activity measurements or aliquoted, snap frozen in liquid nitrogen and stored at -80°C. Aliquots of the samples were analyzed by Coomassie blue stained SDS-PAGE and immunoblotting.

*ATPase activity of human MDR3*

**Labeling of MDR3 with Bodipy® FL maleimide** – Purified wild type MDR3 and mutants were incubated with 10-fold molar excess of bodipy®FL maleimide (BodipyFL N-(2-aminoethyl)maleimide, Molecular Probes Inc.) at room temperature for 20 min. Bodipy®FL maleimide was added from a stock solution prepared in DMSO. The concentration of DMSO in the mixture did not exceed 0.2% (v/v). The reaction was terminated by the addition of 20-fold molar excess of dithiothreitol and samples were stored on ice until ATPase activity measurements. The labeling was analyzed by SDS-PAGE and fluorescence imaging at 488 nm excitation and emission wavelength.

**ATPase activity measurements of MDR3** – The ATPase activity of MDR3 was examined with the malachite green assay by determination of released free inorganic orthophosphate as described previously with a few changes in the experimental procedures (18,26,27). Reactions were performed in a total volume of 100 µl in 50 mM Tris-HCl pH 7.5 (at 37°C) containing 2 x cmc FC-16 and 10 mM MgCl<sub>2</sub>. 5 – 10 µg of purified, detergent-solubilized MDR3 were used and the reaction was started by adding 2 mM ATP at 37°C and stopped after zero and 40 min by the addition of 25 µL of the reaction mixture into 175 µL of 20 mM ice-cold H<sub>2</sub>SO<sub>4</sub>. Subsequently, 50 µL dye solution (0.096% (w/v) malachite green, 1.48% (w/v) ammonium molybdate, and 0.173% (w/v) Tween-20 in 2.36 M H<sub>2</sub>SO<sub>4</sub>) was added. After 15 min, the amount of free phosphate was quantified by measuring the absorption at 595 nm. For substrate stimulated ATPase activity, purified MDR3 was incubated at room temperature for 20 min with a defined volume taken from a 5 mM lipid stock solution and sonicated for 30 s to facilitate the incorporation of lipids into the detergent-protein micelles. The lipid-protein sample was directly used for ATPase activity measurement. For determination of kinetic parameters, ATP concentration was varied. The kinetic data were analyzed according to Michaelis-Menten kinetics:

$$v = \frac{v_{\max} [S]}{K_M + [S]} \quad (1)$$

Here,  $v$  describes the reaction velocity,  $v_{\max}$  the maximal reaction velocity,  $S$  the substrate

concentration and  $K_M$  the Michaelis-Menten constant.

Inhibition by phosphate analogues was assayed with stock solutions containing 100 mM BeCl<sub>2</sub> complemented with 500 mM NaF (100 mM BeF<sub>x</sub>) and 100 mM AlCl<sub>3</sub> complemented with 500 mM NaF (100 mM AlF<sub>x</sub>), respectively. Ortho-vanadate solutions (100 mM and 10 mM) were prepared from Na<sub>3</sub>VO<sub>4</sub> at pH 10 and boiled for 2 min prior to use (28). To determine the IC<sub>50</sub> values, the ATPase activity was plotted against the log of inhibitor concentration. The data were analyzed according to:

$$y = y_{\min} + \frac{y_{\max} - y_{\min}}{1 + 10^{((\log IC_{50} - x) \cdot \text{slope})}} \quad (2)$$

Here,  $y_{\max}$  denotes the ATPase activity in the starting plateau and  $y_{\min}$  the ATPase activity of the final, inhibited plateau.  $Y$  describes the ATPase activity value and  $x$  represents the logarithmic concentration of the inhibitor. The IC<sub>50</sub> value is calculated as the value of the inhibitor concentration used at an ATPase activity inhibition of 50%. This corresponds to the inflection point of the resulting curves.

For subsequent data evaluation, a reaction with EDTA (fc. 20 mM) was performed and the autohydrolysis of ATP was subtracted. For calibration of free phosphate concentrations a Na<sub>2</sub>HPO<sub>4</sub> standard curve was used. All experiments were generally performed three times if not otherwise stated. Fitting was carried out using the GraphPad Prism Software (V.5.0a).

**Immunofluorescence of liver tissue and MDR3-EYFP transfected HEK293 cells** – Immunofluorescence staining and confocal microscopy were performed as described recently (29,30). Briefly, snap-frozen sample liver tissue was cryo-sectioned and incubated with the transporter-specific antibodies K24 for BSEP and P3I126 for MDR3 (Thermo Scientific) (31). Staining was then performed with secondary antibodies conjugated to Alexa Fluor 488 (green) and Alexa Fluor 546 (red). HEK293 cells were transiently transfected with either wild type MDR3-EYFP or MDR3<sup>Q1174E</sup>-EYFP for 48 h using the pEYFP-N1 vector and polyethylene imine (PEI, average M.W. 25kDa; Sigma Aldrich) as a transfection agent. After fixation for 30 seconds with ice-cold methanol, plasma membranes were immunostained with a monoclonal Na<sup>+</sup>/K<sup>+</sup>-ATPase antibody (clone

M7-PB-E9, Sigma Aldrich). Goat anti-mouse-Cy3 (Dianova) was used as the secondary antibody. Tissue and cells were visualized with a LSM 510 Meta confocal laser scanning microscope (Zeiss) using excitation wavelengths of 488 nm for EYFP and Alexa Fluor 488 or 543 nm for Cy3 and Alexa Fluor 546, respectively. 505-530 nm (green) and 560-615 nm band pass filters (red) were used for signal detection.

## RESULTS

*Expression and Purification of the human ABC transporter MDR3 in Pichia pastoris* – Previously, we described the expression of wild type MDR3 and the ATP hydrolysis deficient mutant (E558Q / E1207Q, further on called the EQ/EQ mutant) in the methylotrophic yeast *P. pastoris*. To determine the influence of the Q1174E mutation located in the extended X loop on the ATPase activity, we mutated the Gln to Glu at position 1174 of MDR3 and expressed the mutant in *P. pastoris*. The fermentation of each *P. pastoris* strain, containing MDR3 chromosomally integrated, yielded about 1.4 kg of wet cell weight. We found that the detergent Fos-choline 16 (FC-16) solubilized MDR3 in large quantities and fluorescence-detection size exclusion chromatography (FSEC) analysis demonstrated an appropriate quality in terms of monodispersity of MDR3 solubilized in FC-16 (18). Therefore, we solubilized and purified all three MDR3 variants in FC-16 by means of tandem-affinity chromatography (TAP), which was established by Rigaut *et al.* (32). The purity of wild type MDR3, EQ/EQ and Q1174E mutant was analyzed by Coomassie Brilliant Blue (CBB) stained SDS gels and MDR3 was identified by immunoblot analysis using the C219 antibody, which is specific for the human ABC transporters MDR1 and MDR3 (Figure 1 A, left and middle panel). For wild type MDR3, we obtained 6.3 mg of highly purified (>90%) protein from 100 g wet cell weight in eight independent purifications compared to MDR3 EQ/EQ mutant with 3.4 mg protein and the MDR3 Q1174E mutant with 2.1 mg protein per 100 g wet cell weight (Table 1). The lower yield and purity of the mutants compared to the wild type was likely due to the reduced expression levels of the mutants in *P. pastoris* (data not shown).

*ATPase activity of isolated wild type MDR3, EQ/EQ mutant and maleimide-bodipy labeled MDR3* – In a previous study, we demonstrated that MDR3 exhibits a PC-induced ATPase

activity of  $15 \text{ nmol min}^{-1}$  per mg purified MDR3 in comparison to the ATPase activity of the ATP hydrolysis deficient Walker B (EQ/EQ) mutant in the presence of 2 mM ATP and 10 mM  $\text{Mg}^{2+}$  (18). We used mass spectrometry to analyze a FC-16 solubilized and purified sample of wild type MDR3. Here, we observed that high amounts of detergent molecules were attached to MDR3 (data not shown). We increased the ratio of MDR3 containing crude membranes to FC-16 during solubilization and reduced the amount of FC-16 during the purification protocol as described in experimental procedures. Thereby, we obtained a sixfold higher stimulation of  $105 \pm 30 \text{ nmol min}^{-1} \text{ mg}^{-1}$  in the presence of DOPC lipids and 2 mM ATP (Figure 1 B). A similar effect was reported for the multidrug resistance protein LmrA from *Lactococcus lactis* (27).

In a first step of analyzing MDR3 related ATPase activity in detergent solution in the presence or absence of lipids, we determined the maximal reaction velocity  $v_{\text{max}}$  and the Michaelis Menten constant  $K_M$  of ATP hydrolysis of wild type MDR3 and EQ/EQ mutant in the absence and presence of DOPC lipids, respectively. Purified protein was first activated with 300  $\mu\text{M}$  DOPC lipids and the amount of released inorganic phosphate was measured at various ATP concentrations at 37°C for 40 min.

The ATP hydrolysis deficient EQ/EQ mutant exhibited an ATPase activity with a  $v_{\text{max}}$  of  $240 \pm 5 \text{ nmol min}^{-1} \text{ mg}^{-1}$ , but could not be stimulated by adding DOPC lipids ( $v_{\text{max}} = 245 \pm 5 \text{ nmol min}^{-1} \text{ mg}^{-1}$ ) (Table 1). The  $K_M$  value and turnover number  $k_{\text{cat}}$  of the EQ/EQ mutant did not differ in the absence ( $K_M = 1.03 \pm 0.20 \text{ mM}$ ;  $k_{\text{cat}} = 0.57 \pm 0.01 \text{ s}^{-1}$ ) or presence ( $K_M = 1.24 \pm 0.10 \text{ mM}$ ;  $k_{\text{cat}} = 0.58 \pm 0.01 \text{ s}^{-1}$ ) of DOPC lipids, respectively, within experimental error (Table 1). The exchange of the highly conserved Glu to Gln in the Walker B motif of ABC transporter prevents in general the hydrolysis of ATP in both nucleotide-binding sites (NBS) (21). Additionally, Groen *et al.* reported an important cytotoxicity caused by expression of wild type MDR3 in HEK293T cells, which was counteracted by the single mutation E558Q of the Walker B motif of the first NBD resulting in an inactive floppase (7). This suggests that the observed ATPase activity EQ/EQ mutant is likely derived from co-purified contaminating ATPases. For wild type MDR3 we obtained an increased  $v_{\text{max}}$  value of  $354 \pm 13 \text{ nmol min}^{-1} \text{ mg}^{-1}$  and a  $k_{\text{cat}}$  value of  $0.83 \pm 0.03 \text{ s}^{-1}$  in the absence of DOPC lipids (Figure 1 B, left panel; Table 1).

*ATPase activity of human MDR3*

In clear contrast to the EQ/EQ mutant, ATPase activity of wild type MDR3 as well as the corresponding  $k_{\text{cat}}$  value was increased in the presence of DOPC lipids. We observed a  $v_{\text{max}}$  value of  $536 \pm 11 \text{ nmol min}^{-1} \text{ mg}^{-1}$  corresponding to a  $k_{\text{cat}}$  value of  $1.26 \pm 0.03 \text{ s}^{-1}$  (Figure 1 B, right panel; Table 1). Furthermore, the activity of wild type MDR3 displayed a relatively high  $K_{\text{M}}$  value of  $2.17 \pm 0.20 \text{ mM}$  in the absence and  $1.78 \pm 0.10 \text{ mM}$  in the presence of DOPC lipids. Within experimental error, these values are more or less identical. The subtraction of the maximal ATPase activity of ATP-deficient EQ/EQ mutant from the measured  $v_{\text{max}}$  value of wild type MDR3 resulted in the maximal basal ATPase activity of  $114 \text{ nmol min}^{-1} \text{ mg}^{-1}$  for wild type MDR3. However, a higher ATPase activity of wild type MDR3 cannot be ruled out, because of the differences in quality of the purified proteins. To get rid of contaminating ATPases we performed additional purification steps such as ion exchange chromatography or size exclusion chromatography, but both purification steps resulted in no improvement (data not shown).

Crosslinking of Cys in the Walker A motif of MDR1 with maleimide derivatives was demonstrated to block ATP hydrolysis and the covalent modification was used to investigate the function of MDR1 (33-35). Because the Cys residues 433 and 1073 in the Walker A motifs are conserved in MDR3 and MDR1 and both proteins share high amino acid sequence identity, we reasoned that crosslinking of Cys of MDR3 using a maleimide-fluorophore might block ATP hydrolysis of MDR3. Thus, the difference in activity of wild type and modified MDR3 should reflect the basal ATPase activity. We labeled wild type MDR3 and mutants with the thiol reactive fluorophore maleimide-bodipy (further called MDR3-Bodipy). Full-length MDR3 was predominantly labeled beside degradation products of MDR3 determined by comparison of the fluorescence image and the immunoblot (Figure 1 A, middle and right panel). To exclude that labeling also inhibited the ATP hydrolysis of co-purified ATPases we compared the ATPase activity of EQ/EQ mutant with the corresponding labeled protein in the presence of 2 mM ATP and observed a slight decrease of the ATPase activity of  $17 \text{ nmol min}^{-1} \text{ mg}^{-1}$  (Figure 1 C), while the ATPase activity of wild type MDR3-Bodipy was decreased by  $67 \text{ nmol min}^{-1} \text{ mg}^{-1}$  in the presence of 2 mM ATP. This difference therefore reflects the basal

activity of MDR3. To examine whether co-purified ATPases exhibited PC-induced stimulation we determined the ATPase activity of MDR3-Bodipy in the presence of DOPC lipids and observed no stimulation (Figure 1 B and 1 C). In the absence of DOPC lipids we determined a  $v_{\text{max}}$  value of  $186 \pm 6 \text{ nmol min}^{-1} \text{ mg}^{-1}$  and corresponding  $K_{\text{M}}$  value of  $1.26 \pm 0.10 \text{ mM}$ , which was identical in the presence of DOPC lipids within the experimental error ( $v_{\text{max}} = 175 \pm 10 \text{ nmol min}^{-1} \text{ mg}^{-1}$ ,  $K_{\text{M}} = 1.43 \pm 0.19 \text{ mM}$ ) (Figure 1 B, Table 1). This data demonstrated that MDR3 exhibited a basal ATPase activity between 114 and  $168 \text{ nmol min}^{-1} \text{ mg}^{-1}$  and that the PC-induced ATPase activity exclusively reflected MDR3 specific ATP hydrolysis.

*The head group of the lipids moiety determines MDR3 substrate specificity* – The physiological function of MDR3 is the flop of PC lipids into the canalculus of hepatocytes. Transport experiments with MDR3 transfected polarized pig kidney epithelial cells demonstrated that MDR3 flops fluorescently labeled short chain PC lipids, but not the corresponding PE variants. Furthermore, van Helvoort *et al.* ascertain that MDR3 distinguished between PC and sphingomyelin (SM) lipids. These findings led to the conclusion that MDR3 binds predominantly phospholipids with a choline head group and a diacyl backbone (5).

To exclude that the increased ATPase activity in the presence of PC lipids is caused by an unspecific effect of these lipids on MDR3, we determined the ATPase activity of wild type MDR3 in the presence of brain PE, DOPE, PS and SM lipids. Data derived for other human ABC transporters demonstrated that lipids might display a stabilizing effect on the conformation of the protein, which would result in an increased ATPase activity (36-39). We found that neither the presence of brain PE nor DOPE lipids increased MDR3 ATPase activity (Figure 2 A and 2 B). Furthermore, the addition of PS or SM lipids resulted in no significant stimulation (Figure 2 C and 2 D). To further investigate the influence of liver PC and DOPC lipids on the ATPase activity of wild type MDR3 in the solubilized state,  $K_{\text{M}}$  and  $v_{\text{max}}$  values were determined by Michaelis-Menten kinetic analysis (Figure 2 E and 2 F). Liver PC and DOPC lipids stimulated the ATPase activity in a concentration dependent manner. The maximal velocity  $v_{\text{max}}$  was slightly increased for liver PC

( $109.8 \pm 5.9 \text{ nmol min}^{-1} \text{ mg}^{-1}$ ) as compared to DOPC lipids ( $84.0 \pm 3.4 \text{ nmol min}^{-1} \text{ mg}^{-1}$ ) (Table 2). Assuming that hundred percent homogeneous and active MDR3 is present in the ATPase assay, approximately four seconds are required to catalyze the flop of one lipid molecule by one molecule of MDR3 in the case of DOPC and liver PC lipids. The  $K_M$  values were  $16.6 \pm 2.6 \text{ }\mu\text{M}$  for liver PC lipids and  $12.0 \pm 1.6 \text{ }\mu\text{M}$  for DOPC lipids.

*Inhibition of MDR3 ATPase by transition and ground state analogues* – Next we examined whether MDR3 specific ATP hydrolysis could be inhibited by transition and ground state analogues of phosphate. Phosphate analogues have been extensively used to analyze for example the catalytic mechanism of MDR1 and other human ABC transporters (36,40-42). We determined the ATPase activity of MDR3 after adding  $\text{BeF}_x$ ,  $\text{AlF}_x$  and ortho-vanadate in the presence and absence of DOPC lipids, respectively (Figure 3).  $\text{BeF}_x$  and  $\text{AlF}_x$  led to complete inhibition of ATP hydrolysis at a concentration of 1 mM and abolished the ATPase activity of MDR3 as well as the hydrolysis activity of the co-purified ATPases. No inhibition of the ATPase activity by ortho-vanadate was observed in the absence of DOPC lipids even at concentrations up to 3 mM. However, ATP hydrolysis in the presence of DOPC lipids is inhibited stronger than in the absence of DOPC lipids (approximately 20%) at a concentration of 3 mM ortho-vanadate. Hence, ortho-vanadate inhibited exclusively the PC stimulated ATPase activity of wild type MDR3. Furthermore, we investigated the half maximal inhibitory concentration ( $\text{IC}_{50}$ ) of  $\text{BeF}_x$ ,  $\text{AlF}_x$  and ortho-vanadate in the absence and presence of DOPC lipids. The calculated  $\text{IC}_{50}$  values are summarized in Table 3. The  $\text{IC}_{50}$  value for  $\text{BeF}_x$  is slightly decreased in the presence of DOPC lipids ( $28.6 \pm 1.0 \text{ }\mu\text{M}$ ) compared to the  $\text{IC}_{50}$  value of  $38.0 \pm 1.1 \text{ }\mu\text{M}$  in the absence of DOPC lipids. In good agreement with this, the half-maximal ATPase inhibition of the close homologue MDR1 was achieved at a concentration of 23  $\mu\text{M}$   $\text{BeF}_x$  (43).  $\text{AlF}_x$  exhibited similar  $\text{IC}_{50}$  values of MDR3 ATPase activity of  $199.8 \pm 1.0 \text{ }\mu\text{M}$  in the absence and  $183.8 \pm 1.0 \text{ }\mu\text{M}$  in the presence of DOPC lipids, respectively. Interestingly, ortho-vanadate inhibited the MDR3 specific DOPC stimulated ATPase activity and we determined an  $\text{IC}_{50}$  value of  $397.5 \pm 2.0 \text{ }\mu\text{M}$ . In contrast, purified human MDR1, which shares above 86% amino

acid similarity to MDR3, exhibited an  $\text{IC}_{50}$  of 2.3  $\mu\text{M}$  (41,44).

*MDR3 expression in a PFIC-3 patient's liver biopsy and in transfected HEK293 cells* – A 3-year-old girl with a PFIC-3 phenotype was compound heterozygous for a nucleotide exchange (c.3520C>G) in coding exon 26, resulting in the missense mutation Q1174E, as well as for the intronic donor splice-site mutation c.286+1G>A of ABCB4 (Gene ID: 5244; mRNA reference NM\_000443.3), which likely disrupts MDR3-mRNA expression from the related allele (19). Immunofluorescence staining of the patient's liver revealed an apparently normal immunoreactivity for MDR3 and the bile salt export pump (BSEP, used here as a canalicular marker protein) at the canalicular membrane as compared to a normal liver (Figure 4 A). HEK293 cells were transiently transfected with wild type MDR3-EYFP or MDR3 Q1174E-EYFP (Figure 4 B). Both MDR3 variants were equally targeted to the plasma membrane. This indicates that the amino acid exchange allows normal protein folding and trafficking and that the mutation more likely results in a functional defect of MDR3.

*The extended X loop mutation Q1174E abolished PC induced ATPase activity* – In ABC exporters the highly conserved X loop (TEVGERG) is localized in the helical subdomain of the NBD in direct proximity of the ABC signature motif. X-ray structures of two bacterial ABC exporters, Sav1866 from *Staphylococcus aureus* and MsbA from *Salmonella typhimurium* and five eukaryotic ABC transporters, MDR1 from *mus musculus*, *Cyanidioschyzon merolae* and *Caenorhabditis elegans*, ABCB10 from *homo sapiens* and Atm1 from *Saccharomyces cerevisiae* revealed an enlarged transmission interface of the NBD and the TMD (22,45-50). This transmission interface comprises the X loop, which contacts the intracellular loop 1 (ICL1) of the opposing TMD and transmits signals of ATP binding and hydrolysis by the nearby ABC signature motif to the TMD (22). Oancea *et al.* substituted the conserved glutamate (E602) of the X loop of the transporter associated with antigen processing (TAP1/2) and demonstrated that peptide binding was not effected, however transport activity was reduced from 20% for the E602D mutant to complete disruption for the E602R mutant, suggesting a pivotal role in transmitting conformational changes generated by ATP

*ATPase activity of human MDR3*

hydrolysis and substrate translocation (24). However, the molecular function of this transmission interface in terms of the coupling of the ATP hydrolysis cycle and substrate translocation is still not entirely clear.

We focused on the interaction between the glutamine at position 1174 of the NBD2, which is located in the extended X loop (TRVGDKD/TQ) next to the leucine of the ABC signature motif and conserved in human ABC transporters such as MDR1, TAP1/2 and the cystic fibrosis transmembrane conductance regulator (CFTR) (Figure 5 A) (24,25,46). We hypothesized that the glutamine (Gln 1174) is indispensable for the transmission of the conformational change of the NBD2 to the ICL1 of the TMD.

Previously, we generated the homology model of human wild type MDR3 based on the crystal structure of the homologue of multidrug resistance ABC transporters Sav1866 (pdb entry 2HYD) as a structural template and the amino acid sequence of the isoform B of MDR3 (Figure 5 B) (51). The isoform B of MDR3 contains seven additional amino acids within the NBD2 compared to the major isoform A, which was used in our experiments. Nevertheless, more considerable the Gln of isoform A at position 1174 and of isoform B at position 1181 did not differ in the homology model of NBD2, because the orientation of the side chain of Gln1174 represents a rotamer of Gln1181 (Figure 5 C). The NBD structures of both isoforms are well aligned and had an RMSD value of 1.6 Å over 229 Cα atoms. Thus, we used this structural model of MDR3 to generate the structure of the MDR3 Q1181E mutant (Q1174E isoform A). The close up view of the transmission interface clearly indicates that Gln 1181 of human MDR3 can be replaced by a Glu without large conformational rearrangement, but prohibited hydrogen bonding between Gln 1181 (Q1174 of isoform A) and Asp 166 of the coupling helix of ICL1 (Figure 5 D).

To ascertain whether the mutation of Gln 1174 to Glu abrogates ATP hydrolysis *in vitro*, we purified MDR3 Q1174E via TAP and assayed ATPase stimulation with DOPC, DPPC and liver PC lipids (Figure 6). These data clearly demonstrated that all tested PC lipids were incapable of stimulating ATPase activity of MDR3, a situation comparable with the ATPase deficient EQ/EQ mutant and the labeled wild type MDR3-Bodipy sample. To clarify whether the Q1174E mutant exhibits basal ATPase

activity or abrogates the ATPase activity completely we determined ATPase activity of Q1174E mutant and the corresponding Cys-labeled Q1174E-Bodipy sample in the presence of 2 mM ATP (Figure 1 C). The ATPase activity of Q1174E was higher as compared to wild type MDR3 likely due to higher degree of protein impurities in the purified sample. Considerably, the inhibition of ATPase activity of Q1174E-Bodipy (86 nmol min<sup>-1</sup> mg<sup>-1</sup>) was comparable with wild type MDR3-Bodipy (67 nmol min<sup>-1</sup> mg<sup>-1</sup>) indicating that the Q1174E mutant exhibited basal ATPase activity. On the basis of this data we suggest that the signals of substrate binding and substrate transport are not transmitted properly in this mutant.

**DISCUSSION**

Recently, we established the expression of human *MDR3* in the yeast *P. pastoris* and purified the protein in amounts suitable for a detailed functional analysis with a purity of more than 90% in the case of wild type MDR3 (Figure 1). In ABC transporters, binding of the substrate to the TMD typically stimulates ATP hydrolysis at the NBDs and the energy from the hydrolysis is used to translocate the substrate across the membrane (52). The modulation of ATP hydrolysis upon substrate binding and translocation has been reported for several ABC transporters and is frequently used as a readout of transporter function and activity (36,40,44,53,54). However, no specific ATPase activity of MDR3 has been reported so far (16,17). We demonstrated previously that wild type MDR3 exhibited a PC-stimulated ATPase activity (18). In this study, we characterized the ATPase activity of wild type MDR3 in terms of kinetic parameters, substrate spectrum and effect of phosphate analogues. We demonstrated that lower amounts of FC-16 increased the ATPase activity of MDR3. Former studies have shown that especially these zwitterionic detergents tend to deactivate proteins (55). The influence of the concentration of detergent on the ATPase activity was also demonstrated for MDR1 (37,56). We observed a basal ATPase activity of wild type MDR3, but due to co-purified contaminating impurities that might act as ATPases, the observed basal ATPase activity is derived from MDR3 and impurities. Crosslinking of wild type MDR3 with maleimide-bodipy blocks basal and PC-induced ATPase activity as demonstrated for MDR1 (33-



35), while the ATP hydrolysis deficient EQ double mutant (E558Q/E1207Q) showed no PC stimulation and ATPase activity of labeled EQ/EQ mutant was only marginally reduced (Table 1 and Figure 1). The PC-induced ATPase activity of wild type MDR3 was about 9-fold lower than the described ATPase activity of detergent-soluble mouse ( $1.5 \mu\text{mol min}^{-1} \text{mg}^{-1}$ ) and human MDR1 ( $1.8 \mu\text{mol min}^{-1} \text{mg}^{-1}$ ) in the presence of verapamil and lipids, but comparable to the substrate induced ATPase activity of other members of human liver ABC transporter family such as ABCC3 ( $v_{\text{max}} = 170 \text{ nmol min}^{-1} \text{mg}^{-1}$  in the presence of 1 mM taurocholate) and ABCG5/G8 ( $v_{\text{max}} = 256 \text{ nmol min}^{-1} \text{mg}^{-1}$  in the presence of taurocholate or taurodeoxycholate) (36,37,40,44). Furthermore, purified chimera protein composed of MDR1 TMDs and MDR3 NBDs expressed in HEK293 cells exhibited drug-stimulated ATPase in the presence of vinblastine ( $v_{\text{max}} = 170 \text{ nmol min}^{-1} \text{mg}^{-1}$ ) and verapamil ( $v_{\text{max}} = 450 \text{ nmol min}^{-1} \text{mg}^{-1}$ ), respectively, but did not mediate bile salt-dependent PC efflux (17). These findings confirm that MDR3 NBDs are capable to accomplish substrate stimulated ATP hydrolysis in the detergent solubilized state. Despite the high degree of amino acid sequence identity between MDR1 and MDR3 (>85% homology to human MDR1, 80% to mouse Mdr1a (previously called mouse MDR3)), they exhibited different maximal ATPase activities in the presence of the transport substrate, but similar and relatively high  $K_M$  values for ATP (MDR3,  $K_M = 1.90 \pm 0.27 \text{ mM}$ ; MDR1,  $K_M = 1.5 \text{ mM}$  (44)), which were in a range typical for ABC transporters (36,40,44,57). Because PC lipids are present in high concentration in the plasma membrane, Ishigami *et al.* suggested that MDR3 is a low affinity transporter optimized for PC translocation (17). Our data confirm such a suggestion. Nevertheless, bile salts were shown to be the driving force for PC secretion and currently we cannot rule out whether bile salts influence the ATPase activity of MDR3 (6,7,58).

Furthermore, we demonstrated that PC lipids specifically stimulated MDR3 ATPase activity, whereas brain PE, DOPE and PS and SM lipids did not induce any stimulation (Figure 2). This is consistent with previously reported data (3-6,16). All experiments showed that MDR3 translocates fluorescently labeled short chain PC lipids or long chain derivatives, but not PE, SM or ceramides. In conclusion, MDR3 binds exclusively phospholipids with a choline head

group. However, we cannot exclude that MDR3 translocates MDR1 substrates as well. There is evidence that MDR3 is capable to transport digoxin, paclitaxel and vinblastine and that this transport is inhibited by either verapamil, cyclosporin A or PSC833 (16). Furthermore, MDR3 gene products were found in paclitaxel-, doxorubicin- and vincristine-resistant cell lines, indicating that MDR3 might be involved in multidrug resistance (59). Further investigations are required to address this issue.

The ATPase activity of many ABC proteins, such as MDR1, is efficiently inhibited by phosphate analogues such as ortho-vanadate, aluminum and beryllium fluoride (41,44). For MDR3 it was shown that nucleotide trapping by ortho-vanadate is indeed possible (16). Here, we have demonstrated that aluminum fluoride and beryllium fluoride inhibited ATPase activity of MDR3 and co-purified contaminating NTPases. Importantly, ortho-vanadate inhibited exclusively PC induced MDR3 specific ATPase activity at high concentration. In contrast, mouse Mdr1a was completely inhibited at a concentration of 200  $\mu\text{M}$  ortho-vanadate and human MDR1 showed an  $\text{IC}_{50}$  of 2.3  $\mu\text{M}$ , approximately 165-fold lower than the  $\text{IC}_{50}$  found for MDR3 (Table 3) (41,44). Nevertheless, our data is in agreement with other studies on human ABC transporters. Ortho-vanadate did not inhibit ABCA1 and bile acid stimulated ATPase hydrolysis of ABCG5/G8 was also only inhibited at high ortho-vanadate concentrations (40,54).

Structural studies on full-length ABC transporter Sav1866 have revealed that the NBDs of ABC exporters contain a conserved X loop motif, which transmits the conformational changes of ATP binding and hydrolysis to the ICLs of the TMD (22). The molecular function of this transmission interface relating coupling of the ATP hydrolysis cycle and substrate transport has not been extensively studied yet. To date, only a few studies concerned the X loop of ABC transporters (22,24,25). Previously, the X loop Q1174E mutant of MDR3 in a young patient showing symptoms of PFIC-3 was described in Kubitz *et al.* (19). Thus, we substituted the conserved Gln in the extended X loop of MDR3 to Glu, expressed the Q1174E mutant in *P. pastoris* and purified the protein employing the same procedure as described for wild type MDR3. We observed that the Q1174E mutant was purified with smaller yields and homogeneity, which is likely caused by the

*ATPase activity of human MDR3*

lower expression levels in *P. pastoris*. However, lower integration numbers of the gene expression cassette into the target chromosome cannot be ruled out. Here, we demonstrated that the Q1174E mutant was properly located in the plasma membrane of hepatocytes and MDR3 transfected HEK293 cells indicating a functional defect of MDR3 (Figure 4). Crosslinking of the Q1174E mutant demonstrated that the Q1174E exhibited basal ATPase activity comparable to wild type (Figure 1), but all tested PC lipids were not capable of stimulating ATPase activity (Figure 6). Based on this data and the structural model of MDR3 the exchange of the Gln at position 1174 of NBD2 prohibited the interaction with Asp residue 166 of the ICL1 and the conformational change of the ICL as a result of PC lipid binding were not transmitted to the extended X loop of the NBD (Figure 5).

This is in agreement with mutational and biochemical analysis of the ABC transporter TAP1/2 and CFTR and molecular dynamics (MD) simulation of human MDR1 (24,25,60). The mutational analysis of the conserved Glu within the X loop of TAP1/2 (TEVDEAG/TDVGEKG) demonstrated that substrate binding was not affected, however substrate transport was drastically reduced (24). Moreover, Cys pair crosslinking experiments of the chloride channel CFTR showed that the X loops are in close proximity to ICLs connecting TMDs and also to the ATP-binding sites (25). He *et al.* demonstrated that the interface between NBDs and ICLs of CFTR was involved in the stabilizing of interdomain contacts and regulation of the channel gating (25). Furthermore, Chang *et al.* modeled the structure of human MDR1 based on mouse Mdr1a and investigated the transmission interface between NBDs and TMDs (60). They demonstrated that the amino acid residue Q1175 of NBD2, which is identical to Q1174 in MDR3, hydrogen bond with D164 (D166 in MDR3) of the ICL1 and identified this residue pair D164-Q1175 as key residue pair in the transmission interface. Further, they suggested that the X loop play an important role in formation of the outward-facing conformation of human MDR1 (60). Based on the biochemical data, we suggest that the conserved Gln next to the Leu of the ABC signature motif is crucial for the crosstalk between the extended X loop of the NBD and the coupling helices of the TMDs similar to the role of this region in MDR1. Further investigations are required to clarify the role of

the individual amino acids, which are involved in signal transmission between the extended X loop and ICL1 of the TMDs and should aid our understanding of how mutations relating to cholestatic diseases disrupt interdomain interactions of ATP binding and hydrolysis on a molecular level.

Taken together, we demonstrated that exclusively PC lipids stimulate the ATPase activity of detergent solubilized human MDR3, which was exclusively inhibited by orthovanadate. For the first time this study provides evidence that the glutamine next to the leucine of the ABC signature motif participates in the transmission of the substrate binding at the ICLs of the TMD to the extended X loop of the NBD.

## REFERENCES

1. Oude Elferink, R. P., and Paulusma, C. C. (2007) Function and pathophysiological importance of ABCB4 (MDR3 P-glycoprotein). *Pflugers Arch.* **453**, 601-610
2. Smit, J. J., Schinkel, A. H., Oude Elferink, R. P., Groen, A. K., Wagenaar, E., van Deemter, L., Mol, C. A., Ottenhoff, R., van der Lugt, N. M., van Roon, M. A., and et al. (1993) Homozygous disruption of the murine *mdr2* P-glycoprotein gene leads to a complete absence of phospholipid from bile and to liver disease. *Cell* **75**, 451-462
3. Smith, A. J., de Vree, J. M., Ottenhoff, R., Oude Elferink, R. P., Schinkel, A. H., and Borst, P. (1998) Hepatocyte-specific expression of the human MDR3 P-glycoprotein gene restores the biliary phosphatidylcholine excretion absent in *Mdr2* (-/-) mice. *Hepatology* **28**, 530-536
4. Smith, A. J., Timmermans-Hereijgers, J. L., Roelofsen, B., Wirtz, K. W., van Blitterswijk, W. J., Smit, J. J., Schinkel, A. H., and Borst, P. (1994) The human MDR3 P-glycoprotein promotes translocation of phosphatidylcholine through the plasma membrane of fibroblasts from transgenic mice. *FEBS Lett.* **354**, 263-266
5. van Helvoort, A., Smith, A. J., Sprong, H., Fritzsche, I., Schinkel, A. H., Borst, P., and van Meer, G. (1996) MDR1 P-glycoprotein is a lipid translocase of broad specificity, while MDR3 P-glycoprotein specifically translocates phosphatidylcholine. *Cell* **87**, 507-517
6. Morita, S. Y., Kobayashi, A., Takanezawa, Y., Kioka, N., Handa, T., Arai, H., Matsuo, M., and Ueda, K. (2007) Bile salt-dependent efflux of cellular phospholipids mediated by ATP binding cassette protein B4. *Hepatology* **46**, 188-199
7. Groen, A., Romero, M. R., Kunne, C., Hoosdally, S. J., Dixon, P. H., Wooding, C., Williamson, C., Seppen, J., Van den Oever, K., Mok, K. S., Paulusma, C. C., Linton, K. J., and Oude Elferink, R. P. (2011) Complementary functions of the flippase ATP8B1 and the floppase ABCB4 in maintaining canalicular membrane integrity. *Gastroenterology* **141**, 1927-1937 e1921-1924
8. Oude Elferink, R. P., and Groen, A. K. (2000) Mechanisms of biliary lipid secretion and their role in lipid homeostasis. *Semin. Liver Dis.* **20**, 293-305
9. van der Blik, A. M., Kooiman, P. M., Schneider, C., and Borst, P. (1988) Sequence of *mdr3* cDNA encoding a human P-glycoprotein. *Gene* **71**, 401-411
10. Gottesman, M. M., Fojo, T., and Bates, S. E. (2002) Multidrug resistance in cancer: role of ATP-dependent transporters. *Nat Rev Cancer* **2**, 48-58
11. Ueda, K., Cardarelli, C., Gottesman, M. M., and Pastan, I. (1987) Expression of a full-length cDNA for the human "MDR1" gene confers resistance to colchicine, doxorubicin, and vinblastine. *Proc. Natl. Acad. Sci. U. S. A.* **84**, 3004-3008
12. Gottesman, M. M., and Pastan, I. (1993) Biochemistry of multidrug resistance mediated by the multidrug transporter. *Annu. Rev. Biochem.* **62**, 385-427
13. Buschman, E., and Gros, P. (1991) Functional analysis of chimeric genes obtained by exchanging homologous domains of the mouse *mdr1* and *mdr2* genes. *Mol. Cell. Biol.* **11**, 595-603
14. Buschman, E., and Gros, P. (1994) The inability of the mouse *mdr2* gene to confer multidrug resistance is linked to reduced drug binding to the protein. *Cancer Res.* **54**, 4892-4898
15. Gros, P., and Buschman, E. (1993) The mouse multidrug resistance gene family: structural and functional analysis. *Int. Rev. Cytol.* **137C**, 169-197
16. Smith, A. J., van Helvoort, A., van Meer, G., Szabo, K., Welker, E., Szakacs, G., Varadi, A., Sarkadi, B., and Borst, P. (2000) MDR3 P-glycoprotein, a phosphatidylcholine translocase, transports several cytotoxic drugs and directly interacts with drugs as judged by interference with nucleotide trapping. *J. Biol. Chem.* **275**, 23530-23539
17. Ishigami, M., Tominaga, Y., Nagao, K., Kimura, Y., Matsuo, M., Kioka, N., and Ueda, K. (2013) ATPase activity of nucleotide binding domains of human MDR3 in the context of MDR1. *Biochim. Biophys. Acta* **1831**, 683-690
18. Ellinger, P., Kluth, M., Stindt, J., Smits, S. H., and Schmitt, L. (2013) Detergent screening and purification of the human liver ABC transporters BSEP (ABCB11) and MDR3 (ABCB4) expressed in the yeast *Pichia pastoris*. *PLoS One* **8**, e60620

## ATPase activity of human MDR3

19. Kubitz, R., Bode, J., Erhardt, A., Graf, D., Kircheis, G., Muller-Stover, I., Reinehr, R., Reuter, S., Richter, J., Sagir, A., Schmitt, M., and Donner, M. (2011) Cholestatic liver diseases from child to adult: the diversity of MDR3 disease. *Z. Gastroenterol.* **49**, 728-736
20. Zaitseva, J., Jenewein, S., Wiedenmann, A., Benabdelhak, H., Holland, I. B., and Schmitt, L. (2005) Functional characterization and ATP-induced dimerization of the isolated ABC-domain of the haemolysin B transporter. *Biochemistry* **44**, 9680-9690
21. Zaitseva, J., Jenewein, S., Oswald, C., Jumpertz, T., Holland, I. B., and Schmitt, L. (2005) A molecular understanding of the catalytic cycle of the nucleotide-binding domain of the ABC transporter HlyB. *Biochem. Soc. Trans.* **33**, 990-995
22. Dawson, R. J., and Locher, K. P. (2006) Structure of a bacterial multidrug ABC transporter. *Nature* **443**, 180-185
23. Schmitt, L., and Tampe, R. (2002) Structure and mechanism of ABC transporters. *Curr. Opin. Struct. Biol.* **12**, 754-760
24. Oancea, G., O'Mara, M. L., Bennett, W. F., Tieleman, D. P., Abele, R., and Tampe, R. (2009) Structural arrangement of the transmission interface in the antigen ABC transport complex TAP. *Proc. Natl. Acad. Sci. U. S. A.* **106**, 5551-5556
25. He, L., Aleksandrov, A. A., Serohijos, A. W., Hegedus, T., Aleksandrov, L. A., Cui, L., Dokholyan, N. V., and Riordan, J. R. (2008) Multiple membrane-cytoplasmic domain contacts in the cystic fibrosis transmembrane conductance regulator (CFTR) mediate regulation of channel gating. *J. Biol. Chem.* **283**, 26383-26390
26. Baykov, A. A., Evtushenko, O. A., and Avaeva, S. M. (1988) A malachite green procedure for orthophosphate determination and its use in alkaline phosphatase-based enzyme immunoassay. *Anal. Biochem.* **171**, 266-270
27. Infed, N., Hanekop, N., Driessen, A. J., Smits, S. H., and Schmitt, L. (2011) Influence of detergents on the activity of the ABC transporter LmrA. *Biochim. Biophys. Acta* **1808**, 2313-2321
28. Gordon, J. A. (1991) Use of vanadate as protein-phosphotyrosine phosphatase inhibitor. *Methods Enzymol.* **201**, 477-482
29. Kubitz, R., Sütfels, G., Kuhlkamp, T., Kölling, R., and Häussinger, D. (2004) Trafficking of the bile salt export pump from the Golgi to the canalicular membrane is regulated by the p38 MAP kinase. *Gastroenterology* **126**, 541-553
30. Keitel, V., Burdelski, M., Warskulat, U., Kuhlkamp, T., Keppler, D., Häussinger, D., and Kubitz, R. (2005) Expression and localization of hepatobiliary transport proteins in progressive familial intrahepatic cholestasis. *Hepatology* **41**, 1160-1172
31. Noé, J., Stieger, B., and Meier, P. J. (2002) Functional expression of the canalicular bile salt export pump of human liver. *Gastroenterology* **123**, 1659-1666
32. Rigaut, G., Shevchenko, A., Rutz, B., Wilm, M., Mann, M., and Seraphin, B. (1999) A generic protein purification method for protein complex characterization and proteome exploration. *Nat. Biotechnol.* **17**, 1030-1032
33. Loo, T. W., and Clarke, D. M. (1995) Covalent modification of human P-glycoprotein mutants containing a single cysteine in either nucleotide-binding fold abolishes drug-stimulated ATPase activity. *J. Biol. Chem.* **270**, 22957-22961
34. Loo, T. W., and Clarke, D. M. (1999) Determining the structure and mechanism of the human multidrug resistance P-glycoprotein using cysteine-scanning mutagenesis and thiol-modification techniques. *Biochim. Biophys. Acta* **1461**, 315-325
35. Gabriel, M. P., Storm, J., Rothnie, A., Taylor, A. M., Linton, K. J., Kerr, I. D., and Callaghan, R. (2003) Communication between the nucleotide binding domains of P-glycoprotein occurs via conformational changes that involve residue 508. *Biochemistry* **42**, 7780-7789
36. Chloupkova, M., Pickert, A., Lee, J. Y., Souza, S., Trinh, Y. T., Connelly, S. M., Dumont, M. E., Dean, M., and Urbatsch, I. L. (2007) Expression of 25 human ABC transporters in the yeast *Pichia pastoris* and characterization of the purified ABCC3 ATPase activity. *Biochemistry* **46**, 7992-8003
37. Lerner-Marmarosh, N., Gimi, K., Urbatsch, I. L., Gros, P., and Senior, A. E. (1999) Large scale purification of detergent-soluble P-glycoprotein from *Pichia pastoris* cells and

- characterization of nucleotide binding properties of wild-type, Walker A, and Walker B mutant proteins. *J. Biol. Chem.* **274**, 34711-34718
38. Urbatsch, I. L., Gimi, K., Wilke-Mounts, S., Lerner-Marmarosh, N., Rousseau, M. E., Gros, P., and Senior, A. E. (2001) Cysteines 431 and 1074 are responsible for inhibitory disulfide cross-linking between the two nucleotide-binding sites in human P-glycoprotein. *J. Biol. Chem.* **276**, 26980-26987
  39. Scholz, C., Parcej, D., Ejsing, C. S., Robenek, H., Urbatsch, I. L., and Tampe, R. (2011) Specific lipids modulate the transporter associated with antigen processing (TAP). *J. Biol. Chem.* **286**, 13346-13356
  40. Johnson, B. J., Lee, J. Y., Pickert, A., and Urbatsch, I. L. (2010) Bile acids stimulate ATP hydrolysis in the purified cholesterol transporter ABCG5/G8. *Biochemistry* **49**, 3403-3411
  41. Urbatsch, I. L., Tyndall, G. A., Tomblin, G., and Senior, A. E. (2003) P-glycoprotein catalytic mechanism: studies of the ADP-vanadate inhibited state. *J. Biol. Chem.* **278**, 23171-23179
  42. Russell, P. L., and Sharom, F. J. (2006) Conformational and functional characterization of trapped complexes of the P-glycoprotein multidrug transporter. *Biochem. J* **399**, 315-323
  43. Sankaran, B., Bhagat, S., and Senior, A. E. (1997) Inhibition of P-glycoprotein ATPase activity by beryllium fluoride. *Biochemistry* **36**, 6847-6853
  44. Urbatsch, I. L., Wilke-Mounts, S., Gimi, K., and Senior, A. E. (2001) Purification and characterization of N-glycosylation mutant mouse and human P-glycoproteins expressed in *Pichia pastoris* cells. *Arch. Biochem. Biophys.* **388**, 171-177
  45. Ward, A., Reyes, C. L., Yu, J., Roth, C. B., and Chang, G. (2007) Flexibility in the ABC transporter MsbA: Alternating access with a twist. *Proc. Natl. Acad. Sci. U. S. A.* **104**, 19005-19010
  46. Aller, S. G., Yu, J., Ward, A., Weng, Y., Chittaboina, S., Zhuo, R., Harrell, P. M., Trinh, Y. T., Zhang, Q., Urbatsch, I. L., and Chang, G. (2009) Structure of P-glycoprotein reveals a molecular basis for poly-specific drug binding. *Science* **323**, 1718-1722
  47. Kodan, A., Yamaguchi, T., Nakatsu, T., Sakiyama, K., Hipolito, C. J., Fujioka, A., Hirokane, R., Ikeguchi, K., Watanabe, B., Hiratake, J., Kimura, Y., Suga, H., Ueda, K., and Kato, H. (2014) Structural basis for gating mechanisms of a eukaryotic P-glycoprotein homolog. *Proc. Natl. Acad. Sci. U. S. A.*
  48. Jin, M. S., Oldham, M. L., Zhang, Q., and Chen, J. (2012) Crystal structure of the multidrug transporter P-glycoprotein from *Caenorhabditis elegans*. *Nature* **490**, 566-569
  49. Shintre, C. A., Pike, A. C., Li, Q., Kim, J. I., Barr, A. J., Goubin, S., Shrestha, L., Yang, J., Berridge, G., Ross, J., Stansfeld, P. J., Sansom, M. S., Edwards, A. M., Bountra, C., Marsden, B. D., von Delft, F., Bullock, A. N., Gileadi, O., Burgess-Brown, N. A., and Carpenter, E. P. (2013) Structures of ABCB10, a human ATP-binding cassette transporter in apo- and nucleotide-bound states. *Proc. Natl. Acad. Sci. U. S. A.* **110**, 9710-9715
  50. Srinivasan, V., Pierik, A. J., and Lill, R. (2014) Crystal structures of nucleotide-free and glutathione-bound mitochondrial ABC transporter Atm1. *Science* **343**, 1137-1140
  51. Dzagania, T., Engelmann, G., Haussinger, D., Schmitt, L., Flechtenmacher, C., Rtskhiladze, I., and Kubitz, R. (2012) The histidine-loop is essential for transport activity of human MDR3. A novel mutation of MDR3 in a patient with progressive familial intrahepatic cholestasis type 3. *Gene* **506**, 141-145
  52. Higgins, C. F., and Linton, K. J. (2004) The ATP switch model for ABC transporters. *Nat. Struct. Mol. Biol.* **11**, 918-926
  53. McDevitt, C. A., Collins, R., Kerr, I. D., and Callaghan, R. (2009) Purification and structural analyses of ABCG2. *Adv. Drug Del. Rev.* **61**, 57-65
  54. Takahashi, K., Kimura, Y., Kioka, N., Matsuo, M., and Ueda, K. (2006) Purification and ATPase activity of human ABCA1. *J. Biol. Chem.* **281**, 10760-10768
  55. Seddon, A. M., Curnow, P., and Booth, P. J. (2004) Membrane proteins, lipids and detergents: not just a soap opera. *Biochim. Biophys. Acta* **1666**, 105-117
  56. Doige, C. A., Yu, X., and Sharom, F. J. (1993) The effects of lipids and detergents on ATPase-active P-glycoprotein. *Biochim. Biophys. Acta* **1146**, 65-72

## ATPase activity of human MDR3

57. Pozza, A., Perez-Victoria, J. M., Sardo, A., Ahmed-Belkacem, A., and Di Pietro, A. (2006) Purification of breast cancer resistance protein ABCG2 and role of arginine-482. *Cell. Mol. Life Sci.* **63**, 1912-1922
58. Pohl, A., Devaux, P. F., and Herrmann, A. (2005) Function of prokaryotic and eukaryotic ABC proteins in lipid transport. *Biochim. Biophys. Acta - Molecular and Cell Biology of Lipids* **1733**, 29-52
59. Januchowski, R., Wojtowicz, K., Andrzejewska, M., and Zabel, M. (2014) Expression of MDR1 and MDR3 gene products in paclitaxel-, doxorubicin- and vincristine-resistant cell lines. *Biomedicine & pharmacotherapy* **68**, 111-117
60. Chang, S. Y., Liu, F. F., Dong, X. Y., and Sun, Y. (2013) Molecular insight into conformational transmission of human P-glycoprotein. *J chem phys* **139**, 225102

*Acknowledgments* – We are indebted to Dr. E. Dumont (University of Rochester Medical Center, NY, USA) for the pSGP18 plasmid. We thank Nathalie Walter for technical assistance, Prof. Dr. Patrick Gerner for support. We thank Philipp Ellinger and Nils Hanekop for support and stimulating discussions and Dr. Sander Smits for critical reading the manuscript.

## FOOTNOTES

\*This work was supported by the DFG through the Clinical Research Group 217 (TP 3 to L.S. and TP 1 to R.K.) and the Collaborative Research Center 974 (TP B3 to R.K. and L. S.).

<sup>1</sup>To whom correspondence should be addressed: Lutz Schmitt, Institute of Biochemistry, Heinrich Heine University Düsseldorf, Universitätsstr. 1, 40225 Düsseldorf, Germany, Tel.: +49-211-81-10773; Fax: +49-211-81-15310; E-Mail: Lutz.Schmitt@hhu.de

<sup>2</sup>The abbreviations used are: ABC-ATP binding cassette; BSEP-Bile salt export pump; CBP-Calmodulin binding peptide; CFTR-Cystic fibrosis transmembrane conductance regulator; DOPC-1,2-dioleoyl-sn-glycero-3-phosphocholine; DOPE-1,2-dioleoyl-sn-glycero-3-phosphatidylethanolamine; FSEC-Fluorescence-detection size exclusion chromatography; HEK293 cells-Human embryonic kidney 293 cells; IMAC-Immobilized metal ion affinity chromatography; MDR3/1-Multidrug resistance protein 3/1; NBD-Nucleotide-binding domain; PC-Phosphatidylcholine; PFIC-Progressive Familial Intrahepatic Cholestasis; TAP-Tandem affinity purification; TAP1/2-transporter associated with antigen processing; TMD-Transmembrane domain

## FIGURE LEGENDS

**Figure 1. A** Human wild type MDR3, the E558Q/E1207Q double mutant and the Q1174E mutant purified from *P. pastoris*. The MDR3 variants containing a C-terminal His<sub>6</sub>-tag and a calmodulin binding peptide (CBP) were expressed in the yeast *P. pastoris* and purified as described under Experimental Procedures. 10 µg purified MDR3 was resolved on a 7% SDS-PAGE and either stained with Coomassie brilliant blue (left panel) or detected by immunoblotting (middle panel) using the monoclonal anti-P-gp C219 antibody. MDR3 was cross-linked by the thiol-reactive maleimide-bodipy fluorophore (MDR3-Bodipy) and analyzed by fluorescence imaging using excitation and emission wavelengths at 488 nm (right panel). Molecular weight markers are shown on the left. MDR3 is indicated with an arrow and degradation products of MDR3 are shown with stars. **B** ATPase activity of purified wild type MDR3 (black triangle) and MDR3-Bodipy (blue circles) in the absence (left panel) or presence (right panel) of DOPC lipids. **C** ATPase activity of purified wild type MDR3 (blue), the ATP deficient MDR3 EQ/EQ mutant (green) and the Q1174E mutant (magenta) and the corresponding cross-linked Bodipy derivatives in the presence of 2 mM ATP and 300 µM DOPC (PC).

## ATPase activity of human MDR3

**Figure 2.** Concentration dependence of the ATPase activity of MDR3 in the presence of different kinds of lipids: (A) brain PE lipids, (B) DOPE lipids, (C) PS lipids, (D) SM lipids, (E) liver PC lipids and (F) DOPC lipids, respectively. The ATPase activity was started by addition of 2 mM ATP and assayed for 40 min at 37°C. The ATPase activity in the absence of lipids ( $159 \pm 14 \text{ nmol min}^{-1} \text{ mg}^{-1}$ ) was subtracted from the ATPase activity in the presence of lipids. The data represent the average of at least six independent experiments (mean  $\pm$  SD).

**Figure 3.** Inhibition of MDR3 ATPase activity by phosphate analogues. ATPase activity of purified MDR3 was measured without (w/o, white column) and with 300  $\mu\text{M}$  DOPC lipids (black column) in the presence of ortho-vanadate,  $\text{BeF}_x$  and  $\text{AlF}_x$ . The reaction mixture contained 2 mM ATP and inhibitors at a final concentration of 1 or 3 mM. The data are means  $\pm$  SD of at least four independent experiments.

**Figure 4.** The MDR3 mutation Q1174E does not affect protein localization *in vivo* or *in vitro*. **A** Sample from a liver with normal MDR3 expression (upper panel) and from the patient carrying the heterozygous Q1174E mutation (lower panel). The green fluorescence corresponds to BSEP, which acts as a canalicular marker, while the red fluorescence represents MDR3. **B** Transient expression of human wild type (upper panel) and Q1174E (lower panel) MDR3-eYFP (green) after transfection into HEK293 cells. Cells were fixed after 48 h and stained for the  $\text{Na}^+/\text{K}^+$ -ATPase as a plasma membrane marker (red). Scale bars = 20  $\mu\text{m}$ .

**Figure 5.** **A** Alignment of the amino acid sequence of MDR3 with selected human ABC transporters. The X loop motif is shaded in blue and the ABC signature motif in orange. Gln1174 is colored in red. **B** Homology model of human MDR3 based on the structure of Sav1866 (pdb entry 2HYD) and the amino acid sequence of isoform B of MDR3 (51). One transporter half, consisting of transmembrane domain (TMD) and nucleotide-binding domain (NBD), is shown in blue and the other in yellow. The coupling helices are highlighted in red and the X loop is colored in cyan. **C** Overlay of the MDR3 NBD2 of the isoform A (green) and isoform B (blue). Gln1174 of the isoform A is a rotamer of Gln1181 of the isoform B. **D** Close up view of the interface between TMD and NBD2. Gln1174 of the X loop is shown in stick representation (cyan).

**Figure 6.** ATPase activity of the purified Q1174E mutant was measured without lipids (w/o) and with DOPC, DPPC or liver PC lipids as described in Experimental Procedures. None of these lipids stimulated the ATPase activity of the Q1174E mutant. One hundred percent activity represents  $238 \pm 28 \text{ nmol min}^{-1} \text{ mg}^{-1}$ .

*ATPase activity of human MDR3***TABLES****Table 1.** Purification and ATPase activity of wild type MDR3, the EQ/EQ and the Q1174E mutant.

Purified protein	Yield [mg per 100 g wet cell weight]	No. of purifications	$K_M$ (MgATP) [mM]	$v_{max}$ [nmol min <sup>-1</sup> mg <sup>-1</sup> ]	$k_{cat}$ [s <sup>-1</sup> ]
Wild type	6.3 ± 1.2	8	2.17 ± 0.20	354 ± 13	0.83 ± 0.03
Wild type-Bodipy			1.78 ± 0.10 <sup>a</sup>	536 ± 11 <sup>a</sup>	1.26 ± 0.03 <sup>a</sup>
			1.26 ± 0.10	186 ± 6	0.44 ± 0.01
			1.43 ± 0.19 <sup>a</sup>	175 ± 10 <sup>a</sup>	0.41 ± 0.02 <sup>a</sup>
E558Q/E1207Q	3.4 ± 0.6	5	1.03 ± 0.20	240 ± 5	0.57 ± 0.01
			1.24 ± 0.10 <sup>a</sup>	245 ± 5 <sup>a</sup>	0.58 ± 0.01 <sup>a</sup>
Q1174E	2.0 ± 0.2	3	n.d.	n.d.	n.d.

<sup>a</sup>ATPase activity in the presence of 300  $\mu$ M DOPC lipids; n.d., not determined. The subtraction of the ATPase activity in the absence and presence of DOPC lipids revealed a  $\Delta v_{max}$  of 182 nmol min<sup>-1</sup> mg<sup>-1</sup> and  $\Delta k_{cat}$  of 0.43 s<sup>-1</sup> for wild type, a  $\Delta v_{max}$  of -9 nmol min<sup>-1</sup> mg<sup>-1</sup> and  $\Delta k_{cat}$  of  $\leq 0.03$  s<sup>-1</sup> for labeled wild type MDR3-bodipy and a  $\Delta v_{max}$  of 5 nmol min<sup>-1</sup> mg<sup>-1</sup> and  $\Delta k_{cat}$  of  $\leq 0.01$  s<sup>-1</sup> for the EQ/EQ mutant.



*ATPase activity of human MDR3***Table 2.** Kinetic parameters of MDR3 ATPase activity in the presence of different kinds of lipids.

Lipids	$K_M$ [ $\mu\text{M}$ ]	$v_{\text{max}}$ [ $\text{nmol min}^{-1} \text{mg}^{-1}$ ]	$k_{\text{cat}}$ [ $\text{s}^{-1}$ ]
Liver PC	$16.6 \pm 2.6$	$109.8 \pm 5.9$	$0.26 \pm 0.01$
DOPC	$12.0 \pm 1.6$	$84.0 \pm 3.4$	$0.20 \pm 0.01$

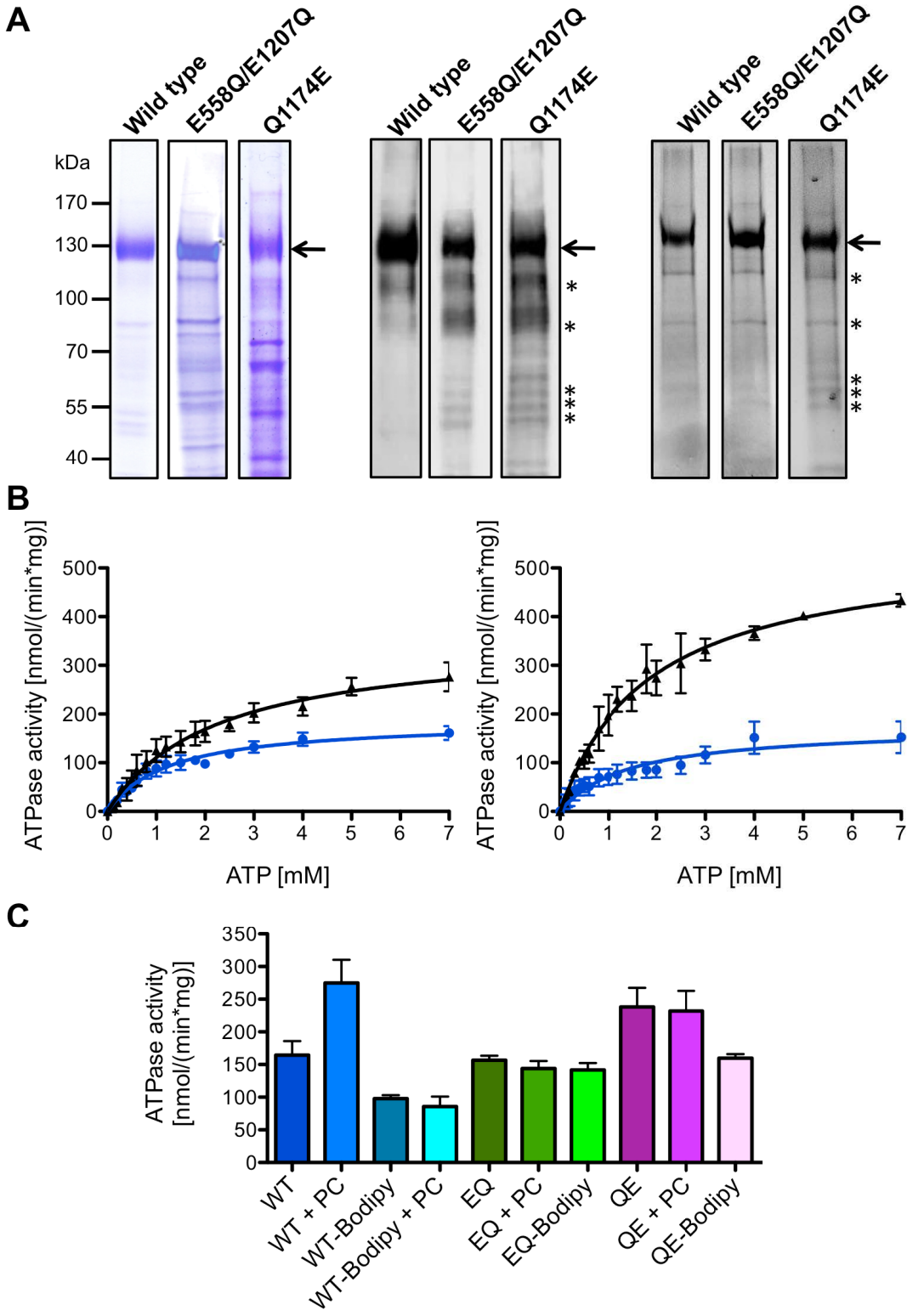
ATPase activity in the absence of lipids were determined and subtracted from the ATPase activity of MDR3 in the presence of liver PC, DOPC, brain PE and DOPE lipids, respectively.

*ATPase activity of human MDR3***Table 3.** IC<sub>50</sub> values of MDR3 ATPase activity inhibited by phosphate analogues in the absence or presence of 300  $\mu$ M DOPC lipids.

Phosphate analogue	IC <sub>50</sub> [ $\mu$ M]	
	– DOPC	+ DOPC
Ortho-vanadate	–	397.5 $\pm$ 2.0
BeF <sub>x</sub>	38.0 $\pm$ 1.1	28.6 $\pm$ 1.0
AlF <sub>x</sub>	199.8 $\pm$ 1.0	183.8 $\pm$ 1.0

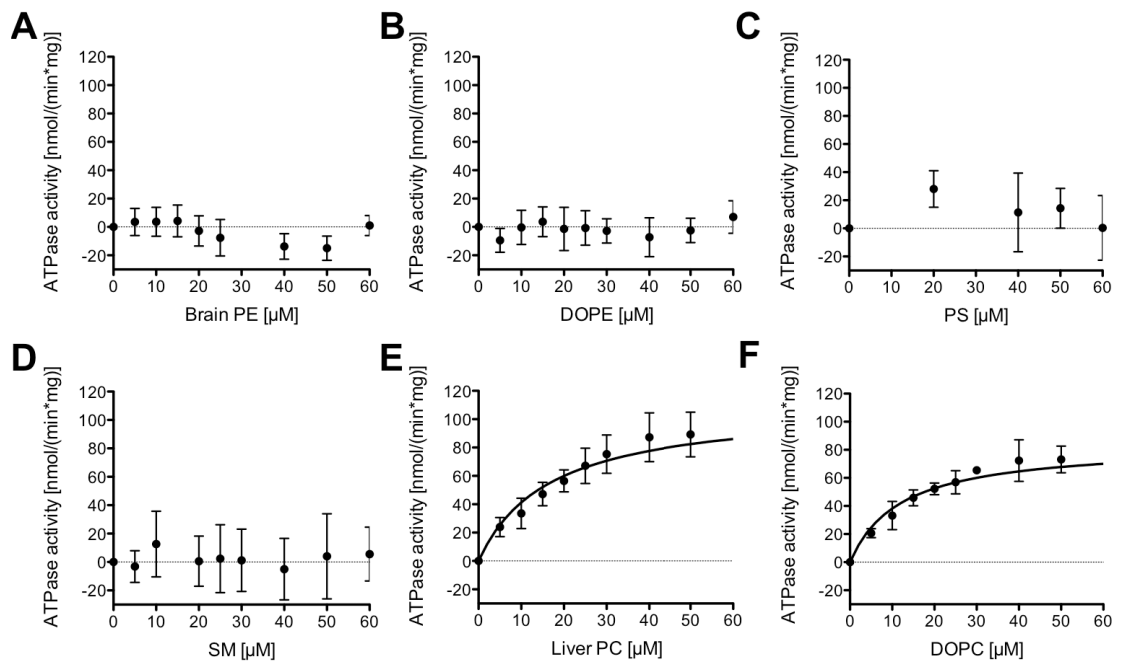
FIGURES

Figure 1



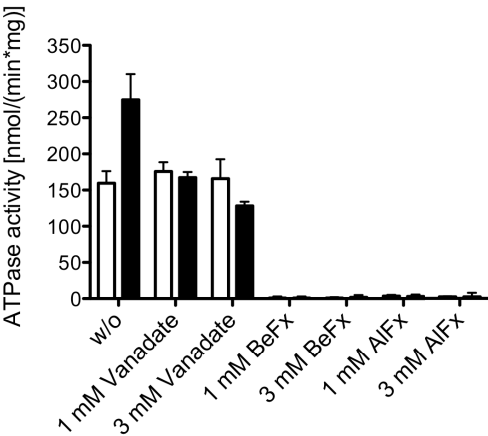
*ATPase activity of human MDR3*

Figure 2



*ATPase activity of human MDR3*

Figure 3



*ATPase activity of human MDR3*

Figure 4

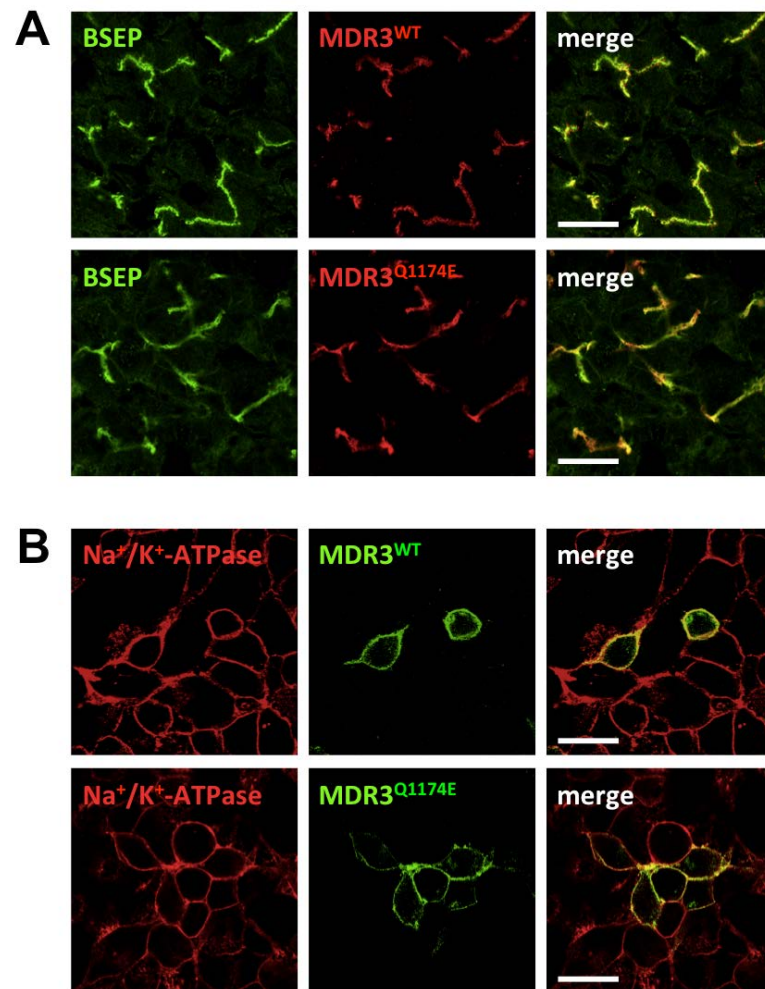
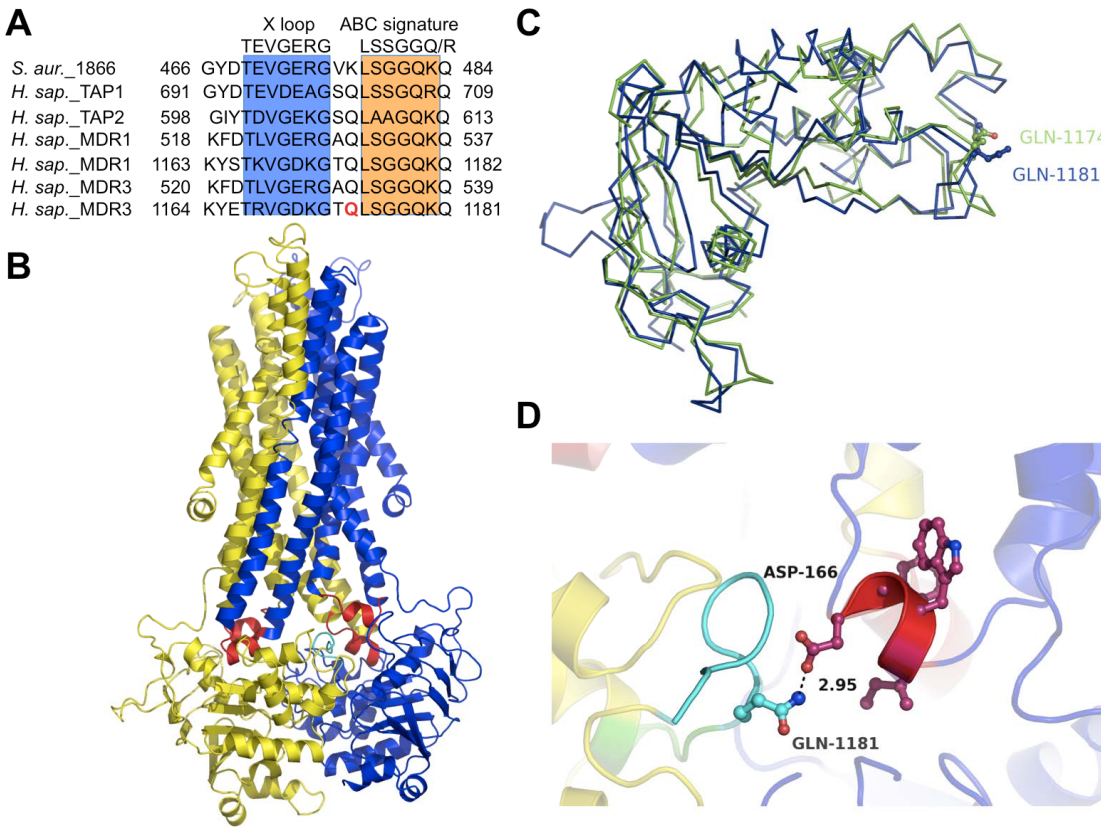
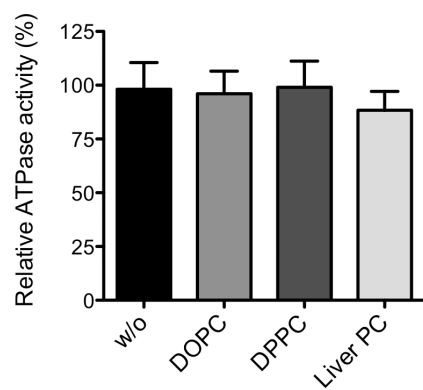


Figure 5



*ATPase activity of human MDR3*

Figure 6







## Chapter V – Drug-modulated ATPase Activity of MDR3

### Title:

**Modulation of the ATPase activity of the human liver  
ABC transporter MDR3 (ABCB4) by taurocholate and  
MDR1 (ABCB1) reversal agents**

Published in: *In preparation*

Impact factor:

Own Proportion to this work: 85 %

Expression of human wild type *MDR3* and mutants in  
*P. pastoris*

Purification of MDR3

ATPase activity determination

*In silico* analysis of MDR3 model

Writing of the manuscript

## Modulation of the ATPase activity of the human liver ABC transporter MDR3 (ABCB4) by taurocholate and MDR1 (ABCB1) reversal agents

Marianne Kluth and Lutz Schmitt \*

From the <sup>1</sup>Institute of Biochemistry, Heinrich Heine University, Düsseldorf, Germany

Running title: Drug-mediated ATPase activity of MDR3

To whom correspondence should be addressed: Lutz Schmitt, Institute of Biochemistry, Heinrich-Heine-University Düsseldorf, Universitätsstr. 1, 40225 Düsseldorf, Germany, Tel.: +49-211-81-10773; Fax: +49-211-81-15310; E-Mail: Lutz.Schmitt@hhu.de

**Keywords:** ABC Transporter; ATPase activity; Lipid transport; drug-induced liver injury; PFIC-3; MDR3; MDR1; Multidrug resistance

### ABSTRACT

The human multidrug resistance (MDR) protein 3 (ABCB4) was classified as MDR transporter based on the amino acid sequence similarity of 86% to the MDR-mediating ATP-binding cassette (ABC) transporter MDR1 (ABCB1). Despite the high degree of sequence identity between human MDR3 (ABCB4) and MDR1 (ABCB1), their physiological substrates are quite different. MDR3 translocates phosphatidylcholine (PC) into bile, while MDR1 extrudes a variety of drugs across the plasma membrane. Nevertheless, low-level directional transport of several MDR1 reversal agents, such as digoxin, paclitaxel and vinblastine, through MDR3-transfected LLC-PK1 cells as well as inhibition by cyclosporin A and verapamil was reported indicating that both MDR proteins share conserved domains for drug recognition. In this study, we investigated whether MDR1 reversal agents modulate the ATPase activity of MDR3. We demonstrated that all tested drugs lead to no stimulation. In contrast, ATPase activity of isolated MDR3 was inhibited by cyclosporin A, verapamil, paclitaxel and zosuquidar. Itraconazole, vinblastine, rifampicin and doxorubicin reduced the ATPase activity only in the presence of high drug concentration. In case of digoxin no modulation of the activity was demonstrated. These results indicate that drug binding to MDR3 blocks the translocase. Furthermore, we demonstrated that the bile salt taurocholate (TC) stimulated the ATPase activity of human MDR3. To our knowledge this is the first study, which provides insights into the modulation of MDR3 ATPase activity by MDR1 reversal agents.

### INTRODUCTION

Multidrug resistance (MDR) is a phenomenon, in which a multitude of cytotoxic agents are extruded out of the cell mediated by ATP-binding cassette (ABC) transporters (1-3). In general, functional ABC transporters are composed of two nucleotide-binding domains (NBDs) and two transmembrane domains (TMDs), which each consists of six transmembrane helices (TMHs) (4). The human multidrug resistance protein 1 (MDR1, ABCB1), also called P-glycoprotein, hydrolyzes ATP by the NBDs and utilizes the free energy to transport a wide variety of structurally unrelated

compounds including anticancer drugs, cardiac glycosides, HIV protease inhibitors, immunosuppressive agents, calcium channel blockers and antibiotics ranging in mass from approximately 300 to 2000 Da (2,5-7). Because of the high amino acid sequence homology (86% homology and 75% identity) between MDR3 (ABCB4) and MDR1 it was assumed that MDR3 also translocates drugs across the canalicular membrane (8). However, initial experiments with MDR3 cDNA or its mouse homolog *Mdr2* transfected cells did not support this hypothesis (8-11).

*Drug-modulated ATPase activity of MDR3*

MDR3 (mouse *Mdr2*) is located in the liver more specifically in the canalicular membrane of hepatocytes and is required for translocation of phosphatidylcholine (PC) into the bile (12-17). In mice, homozygous disruption of *Mdr2* gene demonstrated the complete absence of PC from bile (16). The function of *Mdr2* could be substituted in these mice by expressing the human *MDR3* gene, indicating that MDR3 acts as a phospholipid (PL) floppase (18). Van Helvoort *et al.* demonstrated that MDR3 translocates PC across the apical membrane of MDR3-transfected polarized pig kidney epithelial (LLC-PK1) cells (15).

The first evidence that MDR3 translocates drugs was obtained with MDR3 transfected yeast cells showing low-level resistance against the antifungal agent aureobasidin A (19). Subsequently, Smith *et al.* investigated the vectorial transport by MDR3-transfected LLC-PK1 cells of several MDR1 reversal agents. Although the transport rate was low for most drugs, they demonstrated that the transport of digoxin, paclitaxel, vinblastine and ivermectin into the apical medium was significantly increased in MDR3-transfected cells compared to control cells (20). The transport of digoxin and fluorescent-labeled short-chain PC by MDR3 was efficiently inhibited by the MDR1 reversal agents verapamil, cyclosporin A and PSC833, respectively (20). Verapamil and cyclosporin A were also shown before to inhibit the translocation of endogenous PC and fluorescently labeled short-chain PC (C<sub>6</sub>-NBD-PC) (12,15,21,22). Recently, Januchowski *et al.* identified *MDR3* gene products in paclitaxel-, doxorubicin- and vincristine-resistant cell lines, indicating that MDR3 might be involved in MDR (23). Furthermore, MDR3-mediated translocation of PC was significantly reduced in the presence of itraconazole, whereas the bile salt export pump (BSEP) was not affected (24). Based on these studies, it was suggested that MDR3 and MDR1 exhibited conserved domains for drug recognition. In addition, drug-stimulated ATPase activity of a chimera protein containing the TMDs of MDR1 and the NBDs of MDR3 exhibited 10-fold lower drug-stimulated ATPase activity compared to MDR1, but did not translocate PC (25). This indicates that MDR3 NBDs can energize drug transport.

The question arises why MDR3 is a specialized PC floppase, while MDR1 is a multidrug pump? To pursue the question we investigated the influence of MDR1 reversal agents at the ATPase activity of purified MDR3.

Since ATP hydrolysis is linked by substrate translocation the transport activity can be visualized indirectly.

In this study, we demonstrated that detergent-soluble MDR3 exhibited 7.5-fold stimulation in the presence of taurocholate (TC) suggesting that TC is important for PC translocation. Previously, we demonstrated that the ATPase activity of MDR3 was two-fold stimulated in the presence of PC lipids (26). In contrast, cyclosporin A, verapamil, paclitaxel and zosuquidar lead to complete inhibition of the ATPase activity of MDR3. Itraconazole, vinblastine, rifampicin and doxorubicin reduced the ATPase activity only in the presence of high drug concentration and in case of digoxin no change in ATP hydrolysis was determined.

Furthermore, we modeled a structure of MDR3 in the inward- and outward-facing conformation based on the structures of mouse *Mdr1a* (27,28) and *Sav1866* from *Staphylococcus aureus* (3,29). The substrate-binding pocket and non-conserved amino acid residues were compared between MDR3 and MDR1 to identify important residues, which might gain insights into the translocation pathway. We ascertained that transmembrane helix 1 (TMH1) is the most divergent region, while the verapamil binding pocket (30-36) is conserved in both ABC transporters. Based on these results, we suggest that drugs bind to the substrate-binding pocket of MDR3 and blocks thereby lipid translocation.

**EXPERIMENTAL PROCEDURES**

*Chemicals and Routine Procedures* – All chemicals were obtained from Sigma-Aldrich except Fos-choline 16 (FC-16), which was obtained from Anatrace. The protein concentration was determined by a Bradford assay using the Coomassie Plus Assay (Pierce). The Mini-Protean 3 system (Bio-Rad) was used for SDS-PAGE on 7% gels.

*Fermentation of MDR3 transformed P. pastoris cells* – For large-scale expression, *P. pastoris* cells containing the chromosomal integrated wild type *MDR3* and the E558Q/E1702Q mutant were fermented in a 15 liter table-top glass fermenter (Applikon Biotechnology) according to the Invitrogen *P. pastoris* fermentation guidelines and described in Ellinger *et al* (26).

*Preparation and solubilization of MDR3-containing crude membrane vesicles for protein purification* – Crude membrane vesicles were

prepared according to chapter 4. In brief, 100 g of frozen *P. pastoris* cells were disrupted by two passages through a pre-cooled TS Series Cell Disrupter (Constant Systems) at 2.7 kbar. After cell debris was removed by three centrifugation steps (10 min at 5000 xg and 2x 30 min at 15,000 xg, 4°C), crude membrane vesicles were prepared by ultracentrifugation for 1 h at 125,000 xg at 4°C and subsequently re-suspended in buffer A (50 mM Tris-HCl pH 8.0, 50 mM NaCl, 30% (v/v) glycerol). Crude membrane vesicles equivalent to 100 g wet cells were diluted to a final concentration of 15 mg/mL total protein with buffer A and solubilized with 1% (w/v) of FC-16 for 1 h at 4°C. Non-solubilized membrane vesicles were removed by centrifugation at 125,000 xg at 4°C for 1 h.

**Tandem-affinity purification of MDR3** – The purification of wild type MDR3 or mutant was performed as described in chapter 4.

**Labeling of MDR3 with Bodipy® FL maleimide** – Purified wild type MDR3 was incubated with 10-fold molar excess of bodipy®FL maleimide (BodipyFL N-(2-aminoethyl)maleimide, Molecular Probes Inc.) in dimethyl sulfoxide (DMSO) at room temperature for 20 min. DMSO concentration in the mixture did not exceed 0.2% (v/v). The reaction was terminated by the addition of 20-fold molar excess of dithiothreitol and the samples were stored on ice until ATPase activity measurements.

**ATPase activity measurements of MDR3** – The ATPase activity of MDR3 was examined with the malachite green assay by determination of released free inorganic orthophosphate as described in chapter 4. In brief, ATPase activity measurements were performed in a total volume of 100 µl in 50 mM Tris-HCl pH 7.5 (at 37°C) supplemented with 2 x cmc FC-16 and 10 mM MgCl<sub>2</sub>. 5 – 10 µg of purified, detergent-solubilized MDR3 were used and the reaction was started by adding 2 mM ATP at 37°C and stopped after zero and 40 min by the addition of 25 µl of the reaction mixture into 175 µl of 20 mM ice-cold H<sub>2</sub>SO<sub>4</sub>. Subsequently, 50 µl dye solution (0.096% (w/v) malachite green, 1.48% (w/v) ammonium molybdate, and 0.173% (w/v) Tween-20 in 2.36 M H<sub>2</sub>SO<sub>4</sub>) was added. After 15 min, the amount of free phosphate was quantified by measuring the absorption at 595 nm. Water-insoluble compounds were solved in DMSO and DMSO concentration did not exceed 1% (v/v) in the sample. A sample containing 20 mM EDTA was subtracted as background values

and for calibration of free phosphate concentrations a Na<sub>2</sub>HPO<sub>4</sub> standard curve was used. All experiments were generally performed two times if not otherwise stated.

**Statistical analysis** – Fitting was carried out using the GraphPad Prism Software (V.5.0a). The ATPase activity for inhibitory compounds were analyzed by non-linear regression analysis according to:

$$y = y_{\min} + \frac{y_{\max} - y_{\min}}{1 + 10^{((\log IC_{50} - x) \cdot \text{slope})}} \quad (1)$$

Here,  $y_{\max}$  denotes the ATPase activity in the starting plateau and  $y_{\min}$  the ATPase activity of the maximal inhibited ATPase activity.  $Y$  describes the ATPase activity value and  $x$  represents the logarithmic concentration of the inhibitor. The  $IC_{50}$  value is calculated as the value of the inhibitor concentration required for half-maximal inhibition. This corresponds to the inflection point of the resulting curves.

For taurocholate-stimulated ATPase activity, the data were analyzed according to Michaelis-Menten kinetics:

$$v = \frac{v_{\max} [S]}{K_M + [S]} \quad (2)$$

Here,  $v$  describes the reaction velocity,  $v_{\max}$  the maximal reaction velocity,  $S$  the substrate concentration and  $K_M$  the Michaelis-Menten constant.

## RESULTS

**Taurocholate-stimulated ATPase activity** – In HEK293 cells PC secretion by MDR3 was demonstrated to be dependent on bile acids (12,14). Morita *et al.* reported that taurocholate (TC) remarkably enhanced PC secretion in a concentration-dependent manner (12,14). In a previous study, we expressed the *MDR3* gene in *P. pastoris* and purified MDR3 in a functional state (26). The presence of PC lipids induced a two-fold stimulation of the ATPase activity of detergent-soluble MDR3 (Chapter 4). To determine whether the presence of taurocholate resulted in an increased ATPase activity of MDR3, we measured the ATPase activity of detergent-soluble MDR3 in the presence of TC at 37°C for 40 min (Figure 1). We observed a 7.5-fold stimulation of the ATPase activity of MDR3 with a  $v_{\max}$  value of  $455 \pm 101 \text{ nmol min}^{-1}$

*Drug-modulated ATPase activity of MDR3*

$\text{mg}^{-1}$  and a  $K_M$  value of  $0.30 \pm 0.13 \mu\text{M}$  (Figure 1, blue circle). To exclude that co-purified ATPases exhibited TC-stimulated ATPase activity, we analyzed the influence of TC on the ATP hydrolysis of the ATP hydrolysis deficient mutant (E558Q / E1207Q, further on called the EQ/EQ mutant), which was described previously (26). The EQ/EQ mutant exhibited a TC-induced ATPase activity with a  $v_{\max}$  value of  $151 \pm 43 \text{ nmol min}^{-1} \text{ mg}^{-1}$  and a  $K_M$  value of  $0.30 \pm 0.18 \mu\text{M}$  (Figure 1, black triangle). These data indicate that TC influences the activity of MDR3.

*Modulation of ATPase activity of isolated MDR3 by MDR1 reversal agents* – MDR3 shares up to 86% sequence homology with MDR1, however shows no MDR phenotype in cancer cells (8-11). Several studies suggested that MDR3 binds MDR1 reversal agents (12,15,20-22). To examine whether MDR1 reversal agents modulate the ATPase activity of purified MDR3, we assayed the ATPase activity in the presence of drugs, which are shown in Figure 2. Furthermore, the crosslinking of MDR3 with the thiol-reactive fluorophore bodipy-maleimide abolished the basal ATP hydrolysis activity of MDR3, while co-purified contaminating ATPases were marginal inhibited (Chapter 4). Labeled MDR3, further called MDR3-Bodipy, was used as control to determine the basal ATPase activity of MDR3. Previously, it was shown that MDR3-mediated PC translocation was completely abolished by itraconazole, cyclosporin A and verapamil (12,15,20-22,24). Itraconazole was shown to be a potential inhibitor of MDR1 (37). In the presence of itraconazole complete inhibition of MDR3 activity was not achieved due to the water insolubility of itraconazole. We determined an inhibition of the ATPase activity of MDR3 of 77 % in the presence of  $100 \mu\text{M}$  itraconazole (Figure 3 A). Zosuquidar is a so-called third generation inhibitor of MDR1 (38). Unanticipatedly, zosuquidar inhibited not only the basal ATPase activity of MDR3, but also the contaminating ATPases (Figure 3 A).

Furthermore, cyclosporin A is a widely accepted inhibitor of MDR3. We demonstrated that cyclosporin A as well as verapamil inhibited the ATPase activity of detergent-soluble MDR3 comparable to the MDR3-Bodipy sample (Figure 3). We investigated the half maximal inhibitory concentration ( $\text{IC}_{50}$ ) (Figure 3 B and 3 C) and the  $\text{IC}_{50}$  values are summarized in Table 1. The  $\text{IC}_{50}$  value for verapamil and

cyclosporin A was in the micromolar range of  $53.4 \pm 2.1 \mu\text{M}$  and  $2.3 \pm 0.1 \mu\text{M}$ , respectively.

Because MDR3 mediated the transport of digoxin, paclitaxel and vinblastine in LLC-PK1 cells (20), we assumed that the presence of these drugs stimulates the ATPase activity. However, all three substrates did not lead to any stimulation (Figure 4). In contrast, the presence of  $10 \mu\text{M}$  of paclitaxel and  $100 \mu\text{M}$  vinblastine completely abolished ATP hydrolysis of MDR3. In the case of vinblastine, it cannot be ruled out whether co-purified ATPases are also inhibited due to a higher reduction of ATPase activity compared to the MDR3-Bodipy sample. The presence of high concentrations of digoxin resulted in no change in ATPase activity of detergent-soluble MDR3. Furthermore, we tested the MDR1 substrates doxorubicin and rifampicin, which is an inhibitor for human BSEP (39). Rifampicin as well as doxorubicin resulted in only slight inhibition of  $35\% \pm 3\%$  and  $28\% \pm 10\%$  in the presence of high concentration suggesting that neither rifampicin nor doxorubicin is a modulator of the ATPase activity of MDR3. Based on these data, we suggest that the analyzed MDR1 reversal agents could bind to the substrate-binding pocket of MDR3 and the binding of the most drugs blocked the translocase in the micromolar range.

*Comparison of the substrate-binding pocket of MDR1 with MDR3* – Three X-ray structures of MDR1 homologs from *Mus musculus*, *Caenorhabditis elegans* and *Cyanidioschyzon merolae* were reported in the inward-facing conformation and revealed a large cavity formed by the TMDs (27,28,40,41). Residues in the TMDs were shown by cysteine scanning mutagenesis to form disulphide bonds with different thiol-reactive analogs of MDR1 substrates resulting in MDR1 inhibition (30-36). Residues that were protected by drug substrates from inhibition are suggested to form the drug-binding pocket and are distributed on the surface of the drug-translocation pathway of human MDR1 model based on the X-ray structure of the homolog protein from *C. elegans* (41). To identify whether the drug-binding pocket is preserved in MDR3, first, we aligned the amino acid sequences of mouse and human MDR3 with MDR1A (Figure S1). Secondly, we visualized the identified amino acids (Table 2) in the inward-facing and outward-facing models of MDR3, which was generated based on the structures of mouse Mdr1a (27,28) and the MDR transporter Sav1866 from *S. aureus* (3).

This analysis suggests that residues, which are involved in drug binding, are almost identical in MDR3 compared to MDR1 (Table 2) and located in TMH4, TMH5, TMH6 of the N-terminal TMD and TMH9, TMH10, TMH11 and TMH12 of the C-terminal TMD (Figure 5) indicating that MDR3 is capable to bind MDR1 reversal agents. This is consistent with our biochemical data. Thus, there must be another explanation why the ATPase activity of MDR3 is exclusively stimulated by PC lipids, while the most of the tested drugs showed inhibition. We focused on non-conserved amino acid residues in the TMDs (Table 2) and identified that TMH1, TMH2, TMH3, TMH7, TMH8, TMH9 contain non-conserved residues (Figure 5). Especially, TMH1 and TMH2 of the N-terminal half and TMH7 of the C-terminal half exhibited the polar residues Q52, S58, S69 (TMH1), T139 (TMH2) and T715 (TMH7) instead of hydrophobic residues presented in MDR1. In the modelled structures, these residues are located at the border of the inner membrane leaflet (Figure 5 B) suggesting that they are involved in the interaction of the choline head group of PC lipid.

Further investigations such as mutagenesis analysis would provide insights into the substrate-binding pocket of MDR3. To our knowledge, this is the first study concerning the drug-modulated ATPase activity of full-length MDR3.

## DISCUSSION

In this study, we analysed the ATPase activity of MDR3 in the presence of the bile salt sodium taurocholate (TC). We demonstrated that TC stimulated the ATPase activity of MDR3, while the ATPase deficient mutant was less increased. A better approach would be to determine the ATPase activity of labeled MDR3-Bodipy sample in the presence of TC. This would allow the subtraction of the ATPase activity of co-purified contaminating ATPases. Nevertheless our data are in agreement with existing data (12,22,42). MDR3-mediated PC translocation was remarkably enhanced by in a concentration-dependent manner, while MDR1 activity was not affected (12). In addition, Nagao *et al.* demonstrated that TC and apoA-I promotes the lipid translocation of the ABC transporter ABCA1 (43). Recently, the activated model of ABC transporter-mediated lipid transport was reported (44-46). This model expands the vacuum cleaner model and assumed that an acceptor molecule facilitates substrate release

from the ABC transporter. We speculate that taurocholate acts as acceptor molecule and facilitate MDR3-mediated PC translocation.

While MDR1 transports a wide range of structural unrelated compounds, up to date MDR3 is not involved in MDR (8-11). For example, MDR3-transfected human BRO melanoma cells exhibited no resistance against a range of drugs such as vincristine, colchicine, daunorubicin and doxorubicin (47). Contrary, MDR3 gene products were demonstrated in paclitaxel-, doxorubicin- and vincristine-resistant cells (23).

We investigated the ATPase activity of purified MDR3 in the presence of MDR1 reversal agents (Figure 3 and Figure 4). None of the tested MDR1 reversal agents induce stimulation of ATPase activity. Conversely, verapamil, cyclosporin A and paclitaxel completely abolished the basal activity of MDR3. Itraconazole, vinblastine and doxorubicin inhibited the ATPase activity of MDR3 only at high drug concentration. Exclusively, Digoxin is no inhibitor of MDR3.

This is consistent with previously reported data. Several studies demonstrated that MDR3-mediated translocation was inhibited by cyclosporin A and verapamil (12,15,20-22,24). In contrast, human MDR1 expressed in *P. pastoris* exhibited 30-fold stimulation ( $1.8 \mu\text{mol min}^{-1} \text{mg}^{-1}$ ) in the presence of  $150 \mu\text{M}$  verapamil (48). Cyclosporin A is an established inhibitor of MDR3 and was used to increase MDR3 protein levels at the plasma membrane of HEK293 cells, however PC-translocation of MDR3 was inhibited (14). In addition, cyclosporin A inhibited both the substrate-induced and the basal ATPase activity of MDR1 (49-51). Bile salt translocation in *S. typhimurium* membrane vesicles mediated by BSEP was inhibited by cyclosporin A with an  $\text{IC}_{50}$  value of  $4.6 \pm 1.2 \mu\text{M}$  (52), which is similar to that demonstrated for MDR3. In agreement the presence of itraconazole reduced MDR3-mediated PC translocation in LLP-CK1 cells (24).

However, our data are inconsistent with the transport data of Smith *et al.* (20). They reported that MDR3 mediated the transport of MDR1 substrates such as digoxin and paclitaxel (20). In the MDR3 expressing LLC-PK1 cell system, paclitaxel might not inhibit MDR3 in the micromolar range suggesting that the affinity of MDR3 to paclitaxel is different in a cell system compared to detergent-soluble MDR3. Furthermore, we suggest that transport of digoxin and paclitaxel are energized by the basal

ATPase activity resulting in low-level transport efficacy. In agreement with our data, Smith *et al.* demonstrated that paclitaxel, vinblastine, verapamil, cyclosporin A and valspodar abolished vanadate-dependent ATP trapping, while the nucleotide trapping of MDR1 is greatly stimulated by verapamil (20). In contrast, vanadate trapping of the chimera protein consisting of MDR3 NBDs and MDR1 TMDs was enhanced by verapamil (25). This indicates that substrate binding is coupled to ATP hydrolysis.

We confirmed that the residues forming drug-binding pocket are conserved between MDR1 and MDR3 revealing that both transporter recognize similar substrates. We

further identified non-conserved residues located at the border of the inner membrane leaflet and suggest that they are involved in the interaction of the polar head group of the preferred substrate PC. This is in agreement with mutagenic analysis of TMH1 of MDR1 suggesting that the TMH1 forms part of the substrate-binding pocket and determine substrate specificity (31,36). Taken together, our data implicate that the tested MDR1 reversal agents bind to the substrate-binding pocket and interfere with the ATPase activity of detergent-soluble MDR3. This is consistent with fact that MDR3 is a poor drug transporter and that MDR3 is unable to cause MDR in transfected cells.

## REFERENCES

1. Bolhuis, H., van Veen, H. W., Molenaar, D., Poolman, B., Driessen, A. J., and Konings, W. N. (1996) Multidrug resistance in *Lactococcus lactis*: evidence for ATP-dependent drug extrusion from the inner leaflet of the cytoplasmic membrane. *EMBO J.* **15**, 4239-4245
2. Gottesman, M. M., Fojo, T., and Bates, S. E. (2002) Multidrug resistance in cancer: role of ATP-dependent transporters. *Nat Rev Cancer* **2**, 48-58
3. Dawson, R. J., and Locher, K. P. (2006) Structure of a bacterial multidrug ABC transporter. *Nature* **443**, 180-185
4. Hollenstein, K., Dawson, R. J., and Locher, K. P. (2007) Structure and mechanism of ABC transporter proteins. *Curr. Opin. Struct. Biol.* **17**, 412-418
5. Gottesman, M. M., and Pastan, I. (1993) Biochemistry of multidrug resistance mediated by the multidrug transporter. *Annu. Rev. Biochem.* **62**, 385-427
6. Juranka, P. F., Zastawny, R. L., and Ling, V. (1989) P-glycoprotein: multidrug-resistance and a superfamily of membrane-associated transport proteins. *FASEB J.* **3**, 2583-2592
7. Kartner, N., Riordan, J. R., and Ling, V. (1983) Cell surface P-glycoprotein associated with multidrug resistance in mammalian cell lines. *Science* **221**, 1285-1288
8. van der Blik, A. M., Kooiman, P. M., Schneider, C., and Borst, P. (1988) Sequence of *mdr3* cDNA encoding a human P-glycoprotein. *Gene* **71**, 401-411
9. Gros, P., Raymond, M., Bell, J., and Housman, D. (1988) Cloning and characterization of a second member of the mouse *mdr* gene family. *Mol. Cell. Biol.* **8**, 2770-2778
10. Buschman, E., and Gros, P. (1991) Functional analysis of chimeric genes obtained by exchanging homologous domains of the mouse *mdr1* and *mdr2* genes. *Mol. Cell. Biol.* **11**, 595-603
11. Buschman, E., and Gros, P. (1994) The inability of the mouse *mdr2* gene to confer multidrug resistance is linked to reduced drug binding to the protein. *Cancer research* **54**, 4892-4898
12. Morita, S. Y., Kobayashi, A., Takanezawa, Y., Kioka, N., Handa, T., Arai, H., Matsuo, M., and Ueda, K. (2007) Bile salt-dependent efflux of cellular phospholipids mediated by ATP binding cassette protein B4. *Hepatology* **46**, 188-199
13. Oude Elferink, R. P., and Groen, A. K. (2000) Mechanisms of biliary lipid secretion and their role in lipid homeostasis. *Semin. Liver Dis.* **20**, 293-305
14. Groen, A., Romero, M. R., Kunne, C., Hoosdally, S. J., Dixon, P. H., Wooding, C., Williamson, C., Seppen, J., Van den Oever, K., Mok, K. S., Paulusma, C. C., Linton, K. J., and Oude Elferink, R. P. (2011) Complementary functions of the flippase ATP8B1 and the floppase ABCB4 in maintaining canalicular membrane integrity. *Gastroenterology* **141**, 1927-1937 e1921-1924



15. van Helvoort, A., Smith, A. J., Sprong, H., Fritzsche, I., Schinkel, A. H., Borst, P., and van Meer, G. (1996) MDR1 P-glycoprotein is a lipid translocase of broad specificity, while MDR3 P-glycoprotein specifically translocates phosphatidylcholine. *Cell* **87**, 507-517
16. Smit, J. J., Schinkel, A. H., Oude Elferink, R. P., Groen, A. K., Wagenaar, E., van Deemter, L., Mol, C. A., Ottenhoff, R., van der Lugt, N. M., van Roon, M. A., and et al. (1993) Homozygous disruption of the murine mdr2 P-glycoprotein gene leads to a complete absence of phospholipid from bile and to liver disease. *Cell* **75**, 451-462
17. Smith, A. J., Timmermans-Hereijgers, J. L., Roelofsen, B., Wirtz, K. W., van Blitterswijk, W. J., Smit, J. J., Schinkel, A. H., and Borst, P. (1994) The human MDR3 P-glycoprotein promotes translocation of phosphatidylcholine through the plasma membrane of fibroblasts from transgenic mice. *FEBS Lett.* **354**, 263-266
18. Smith, A. J., de Vree, J. M., Ottenhoff, R., Oude Elferink, R. P., Schinkel, A. H., and Borst, P. (1998) Hepatocyte-specific expression of the human MDR3 P-glycoprotein gene restores the biliary phosphatidylcholine excretion absent in Mdr2 (-/-) mice. *Hepatology* **28**, 530-536
19. Kino, K., Taguchi, Y., Yamada, K., Komano, T., and Ueda, K. (1996) Aureobasidin A, an antifungal cyclic depsipeptide antibiotic, is a substrate for both human MDR1 and MDR2/P-glycoproteins. *FEBS Lett.* **399**, 29-32
20. Smith, A. J., van Helvoort, A., van Meer, G., Szabo, K., Welker, E., Szakacs, G., Varadi, A., Sarkadi, B., and Borst, P. (2000) MDR3 P-glycoprotein, a phosphatidylcholine translocase, transports several cytotoxic drugs and directly interacts with drugs as judged by interference with nucleotide trapping. *J. biol. chem.* **275**, 23530-23539
21. Ruetz, S., and Gros, P. (1994) Phosphatidylcholine translocase: a physiological role for the mdr2 gene. *Cell* **77**, 1071-1081
22. Andress, E. J., Nicolaou, M., Romero, M. R., Naik, S., Dixon, P. H., Williamson, C., and Linton, K. J. (2014) Molecular mechanistic explanation for the spectrum of cholestatic disease caused by the S320F variant of ABCB4. *Hepatology* **59**, 1921-1931
23. Januchowski, R., Wojtowicz, K., Andrzejewska, M., and Zabel, M. (2014) Expression of MDR1 and MDR3 gene products in paclitaxel-, doxorubicin- and vincristine-resistant cell lines. *Biomedicine & pharmacotherapy* **68**, 111-117
24. Yoshikado, T., Takada, T., Yamamoto, T., Yamaji, H., Ito, K., Santa, T., Yokota, H., Yatomi, Y., Yoshida, H., Goto, J., Tsuji, S., and Suzuki, H. (2011) Itraconazole-induced cholestasis: involvement of the inhibition of bile canalicular phospholipid translocator MDR3/ABCB4. *Mol. Pharmacol.* **79**, 241-250
25. Ishigami, M., Tominaga, Y., Nagao, K., Kimura, Y., Matsuo, M., Kioka, N., and Ueda, K. (2013) ATPase activity of nucleotide binding domains of human MDR3 in the context of MDR1. *Biochim. Biophys. Acta* **1831**, 683-690
26. Ellinger, P., Kluth, M., Stindt, J., Smits, S. H., and Schmitt, L. (2013) Detergent screening and purification of the human liver ABC transporters BSEP (ABCB11) and MDR3 (ABCB4) expressed in the yeast *Pichia pastoris*. *PLoS One* **8**, e60620
27. Aller, S. G., Yu, J., Ward, A., Weng, Y., Chittaboina, S., Zhuo, R., Harrell, P. M., Trinh, Y. T., Zhang, Q., Urbatsch, I. L., and Chang, G. (2009) Structure of P-glycoprotein reveals a molecular basis for poly-specific drug binding. *Science* **323**, 1718-1722
28. Li, J., Jaimes, K. F., and Aller, S. G. (2014) Refined structures of mouse P-glycoprotein. *Protein Sci.* **23**, 34-46
29. Dawson, R. J., and Locher, K. P. (2007) Structure of the multidrug ABC transporter Sav1866 from *Staphylococcus aureus* in complex with AMP-PNP. *FEBS Lett.* **581**, 935-938
30. Loo, T. W., Bartlett, M. C., and Clarke, D. M. (2006) Transmembrane segment 7 of human P-glycoprotein forms part of the drug-binding pocket. *Biochem. J.* **399**, 351-359
31. Loo, T. W., Bartlett, M. C., and Clarke, D. M. (2006) Transmembrane segment 1 of human P-glycoprotein contributes to the drug-binding pocket. *Biochem. J.* **396**, 537-545
32. Loo, T. W., Bartlett, M. C., and Clarke, D. M. (2007) Suppressor mutations in the transmembrane segments of P-glycoprotein promote maturation of processing mutants and disrupt a subset of drug-binding sites. *J. Biol. Chem.* **282**, 32043-32052
33. Loo, T. W., Bartlett, M. C., and Clarke, D. M. (2003) Methanethiosulfonate derivatives of rhodamine and verapamil activate human P-glycoprotein at different sites. *J. Biol. Chem.* **278**, 50136-50141

## Drug-modulated ATPase activity of MDR3

34. Loo, T. W., and Clarke, D. M. (2005) Do drug substrates enter the common drug-binding pocket of P-glycoprotein through "gates"? *Biochem. Biophys. Res. Commun.* **329**, 419-422
35. Loo, T. W., and Clarke, D. M. (1997) Identification of residues in the drug-binding site of human P-glycoprotein using a thiol-reactive substrate. *J. Biol. Chem.* **272**, 31945-31948
36. Taguchi, Y., Morishima, M., Komano, T., and Ueda, K. (1997) Amino acid substitutions in the first transmembrane domain (TM1) of P-glycoprotein that alter substrate specificity. *FEBS Lett.* **413**, 142-146
37. Gupta, S., Kim, J., and Gollapudi, S. (1991) Reversal of daunorubicin resistance in P388/ADR cells by itraconazole. *J. Clin. Invest.* **87**, 1467-1469
38. Thomas, H., and Coley, H. M. (2003) Overcoming multidrug resistance in cancer: an update on the clinical strategy of inhibiting p-glycoprotein. *Cancer control* **10**, 159-165
39. Byrne, J. A., Strautnieks, S. S., Mieli-Vergani, G., Higgins, C. F., Linton, K. J., and Thompson, R. J. (2002) The human bile salt export pump: characterization of substrate specificity and identification of inhibitors. *Gastroenterology* **123**, 1649-1658
40. Kodan, A., Yamaguchi, T., Nakatsu, T., Sakiyama, K., Hipolito, C. J., Fujioka, A., Hirokane, R., Ikeguchi, K., Watanabe, B., Hiratake, J., Kimura, Y., Suga, H., Ueda, K., and Kato, H. (2014) Structural basis for gating mechanisms of a eukaryotic P-glycoprotein homolog. *Proc. Natl. Acad. Sci. U. S. A.*
41. Jin, M. S., Oldham, M. L., Zhang, Q., and Chen, J. (2012) Crystal structure of the multidrug transporter P-glycoprotein from *Caenorhabditis elegans*. *Nature* **490**, 566-569
42. Morita, S. Y., and Terada, T. (2014) Molecular mechanisms for biliary phospholipid and drug efflux mediated by ABCB4 and bile salts. *BioMed Res. Int.* **2014**, 954781
43. Nagao, K., Zhao, Y., Takahashi, K., Kimura, Y., and Ueda, K. (2009) Sodium taurocholate-dependent lipid efflux by ABCA1: effects of W590S mutation on lipid translocation and apolipoprotein A-I dissociation. *J. Lipid Res.* **50**, 1165-1172
44. Pohl, A., Devaux, P. F., and Herrmann, A. (2005) Function of prokaryotic and eukaryotic ABC proteins in lipid transport. *Biochim. Biophys.* **1733**, 29-52
45. Small, D. M. (2003) Role of ABC transporters in secretion of cholesterol from liver into bile. *Proc. Natl. Acad. Sci. U. S. A.* **100**, 4-6
46. van Meer, G., Halter, D., Sprong, H., Somerharju, P., and Egmond, M. R. (2006) ABC lipid transporters: extruders, flippases, or floppase activators? *FEBS Lett.* **580**, 1171-1177
47. Schinkel, A. H., Roelofs, E. M., and Borst, P. (1991) Characterization of the human MDR3 P-glycoprotein and its recognition by P-glycoprotein-specific monoclonal antibodies. *Cancer Res.* **51**, 2628-2635
48. Urbatsch, I. L., Wilke-Mounts, S., Gimi, K., and Senior, A. E. (2001) Purification and characterization of N-glycosylation mutant mouse and human P-glycoproteins expressed in *Pichia pastoris* cells. *Arch. Biochem. Biophys.* **388**, 171-177
49. Tamai, I., and Safa, A. R. (1990) Competitive interaction of cyclosporins with the Vinca alkaloid-binding site of P-glycoprotein in multidrug-resistant cells. *J. Biol. Chem.* **265**, 16509-16513
50. Sarkadi, B., Muller, M., Homolya, L., Hollo, Z., Seprondi, J., Germann, U. A., Gottesman, M. M., Price, E. M., and Boucher, R. C. (1994) Interaction of bioactive hydrophobic peptides with the human multidrug transporter. *FASEB J.* **8**, 766-770
51. Sharom, F. J., DiDiodato, G., Yu, X., and Ashbourne, K. J. (1995) Interaction of the P-glycoprotein multidrug transporter with peptides and ionophores. *J. Biol. Chem.* **270**, 10334-10341
52. Stieger, B., Fattinger, K., Madon, J., Kullak-Ublick, G. A., and Meier, P. J. (2000) Drug- and estrogen-induced cholestasis through inhibition of the hepatocellular bile salt export pump (Bsep) of rat liver. *Gastroenterology* **118**, 422-430
53. Dzagania, T., Engelmann, G., Haussinger, D., Schmitt, L., Flechtenmacher, C., Rtskhiladze, I., and Kubitz, R. (2012) The histidine-loop is essential for transport activity of human MDR3. A novel mutation of MDR3 in a patient with progressive familial intrahepatic cholestasis type 3. *Gene* **506**, 141-145

*Acknowledgments* – We are indebted to Dr. Sander Smits for critical reading of the manuscript. We thank Dr. Philipp Ellinger, Dr. Nacera Infed and Dr. Nils Hanekop for support and stimulating discussions. We are indebted to Dr. Jan Stindt, Prof. Dr. Ralf Kubitz and Prof. Dr. Dieter Häussinger for a very productive collaboration.

## FOOTNOTES

\*This work was supported by the DFG through the Clinical Research Group 217 (TP 3 to L.S. and TP 1 to R.K.) and the Collaborative Research Center 974 (TP B3 to R.K. and L. S.).

<sup>1</sup>To whom correspondence should be addressed: Lutz Schmitt, Institute of Biochemistry, Heinrich Heine University Düsseldorf, Universitätsstr. 1, 40225 Düsseldorf, Germany, Tel.: +49-211-81-10773; Fax: +49-211-81-15310; E-Mail: Lutz.Schmitt@hhu.de

<sup>2</sup>The abbreviations used are: ABC-ATP binding cassette; BSEP-Bile salt export pump; CBP-Calmodulin binding peptide; HEK293 cells-Human embryonic kidney 293 cells; IMAC-Immobilized metal ion affinity chromatography; LLC-PK1 cells- Polarized pig kidney epithelial cells; MDR3/1-Multidrug resistance protein 3/1; NBD-Nucleotide-binding domain; PC-Phosphatidylcholine; PFIC-Progressive Familial Intrahepatic Cholestasis; TAP-Tandem affinity purification; TMD-Transmembrane domain

## FIGURE LEGENDS

**Figure 1.** ATPase activity of purified MDR3 (blue circle) and EQ/EQ mutant (black triangle) in the presence of the bile salt sodium taurocholate (TC). The ATPase activity in the absence of TC ( $159 \pm 14 \text{ nmol min}^{-1} \text{ mg}^{-1}$ ) was subtracted from the ATPase activity in the presence of TC and data points were analyzed according Michaelis-Menten kinetic.

**Figure 2.** MDR1 substrates and modulators used in this study.

**Figure 3.** Drug-inhibited ATPase activity of purified MDR3. (A) All inhibitors were added with a final concentration of 100  $\mu\text{M}$  from stock solutions in dimethyl sulfoxide (DMSO concentration  $\leq 1\%$ ) and the ATPase activity was determined at 37°C for 40 min and 2 mM ATP. The same concentration DMSO had no effect on the ATPase activity of MDR3. MDR3 labeled with maleimide-bodipy (MDR3-Bodipy) represents 100% inhibition of MDR3 (Chapter 4). EDTA was added with a final concentration of 20 mM. MDR3 was assayed for ATPase activity in increasing concentrations of (B) cyclosporin A and (C) verapamil and ATPase activity of MDR3-Bodipy sample was subtracted from each data point. Lines represent non-linear regression analysis of the data points.  $\text{IC}_{50}$  values of the data fits are given in Table 1. Data of two independent experiments were plotted (mean  $\pm$  SD).

**Figure 4.** ATPase activity of purified MDR3 in the presence of MDR1 reversal agents (A) paclitaxel, (B) vinblastine, (C) rifampicin, (D) digoxin and (E) doxorubicin. MDR3 labeled with maleimide-bodipy (MDR3-Bodipy) represents 100% inhibition of MDR3. The data are means  $\pm$  SD of at least three independent experiments.

**Figure 5.** Models of human MDR3. (A) Structure of human MDR3 TMDs based on the structure of mouse Mdr1a (Protein Data Bank (PDB) accession number 4M1M (28)) in the inward-facing conformation. TMD is represented in light blue and the other half in light yellow. Non-conserved amino acids between human MDR1 and MDR3 are highlighted in red and verapamil-interacting amino acids are shown in blue (30-36). (B) View of the drug transport pathway in the outward-facing conformation. The model of the outward-facing conformation was previously described in (53) and based on the structure of the multidrug transporter Sav1866 (PDB accession number 2HYD (3)).

*Drug-modulated ATPase activity of MDR3***TABLES****Table 1.** IC<sub>50</sub> values of ATPase activity of purified MDR3.

Compound	IC <sub>50</sub> [μM]
Cyclosporin A	2.3 ± 0.1
Verapamil	53.4 ± 2.1

IC<sub>50</sub> = half-maximal inhibitory concentration

**Table 2.** Summary of sequence alignment of MDR3 and MDR1

Transmembrane helix	Non-conserved aa of MDR3 <sup>a</sup>	Non-conserved aa of MDR1 <sup>a</sup>	Drug protected/MDR3 <sup>b</sup>	Drug protected/MDR1 <sup>c</sup>
1	Q52 S58 M63 A66 S69	L46 V52 A57 I60 A63		
2	T139	C137		
3	A204	T202		
4			S224	S222
5	I303	A301	I308	I306
6	C353	S351	L341 I342 A344 F345 F728	L339 I340 A342 F343 F728
7	T715 A720	V715 I720		
8	F760	A761		
9	A836	T837	A840	A841
10			I867 S870	I868 A872
11			F941	F942
12			S944 I974 I980 V981 A984 V985	T945 L975 V981 V982 A984 M985

<sup>a</sup>conserved between mouse and human MDR3; <sup>b</sup>Drug-interacting residues were identified by sequence comparison of MDR3 with MDR1; <sup>c</sup>Drug-interacting residues identified by Cys-scanning mutagenesis (30-36). Non-conserved residues are highlighted in red, identical residues in grey and similar residues in green.

**FIGURES**

Figure 1

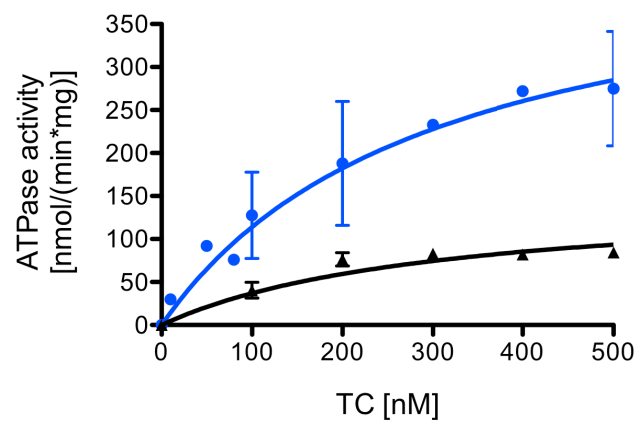
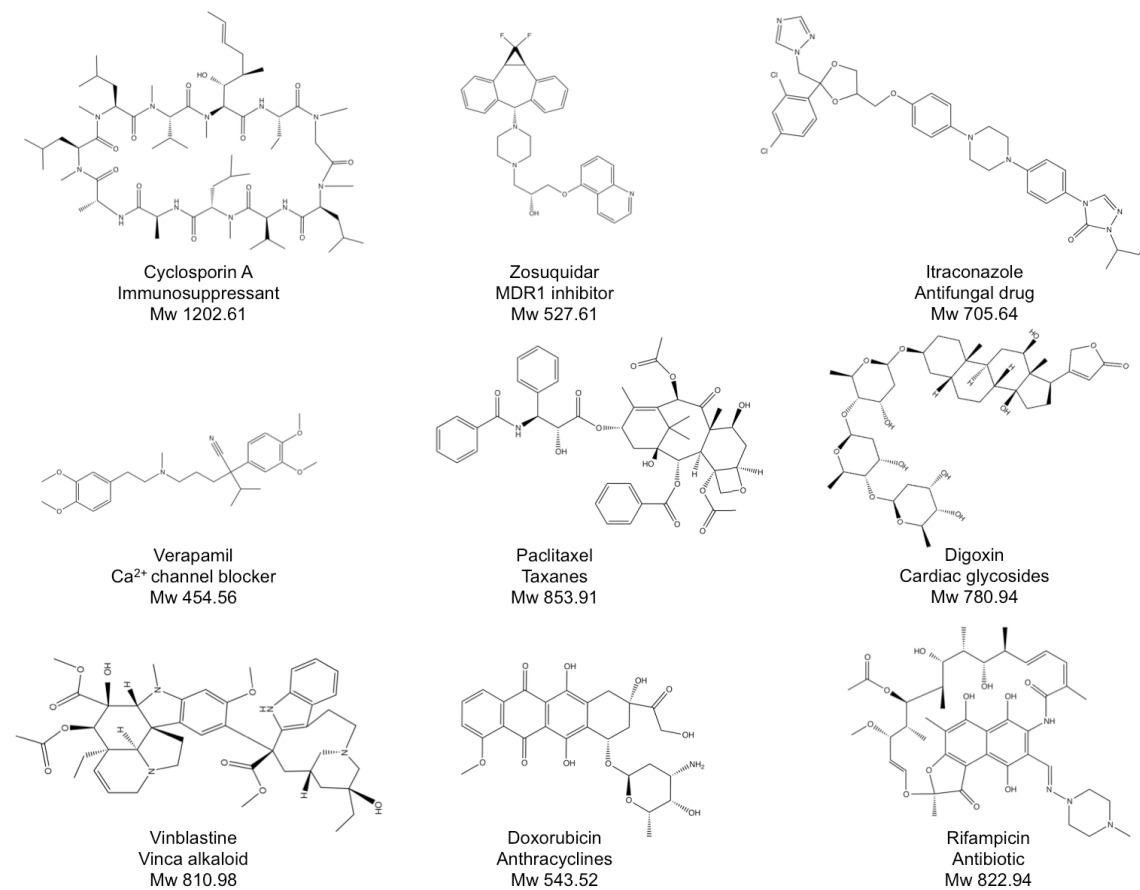


Figure 2



Drug-modulated ATPase activity of MDR3

Figure 3

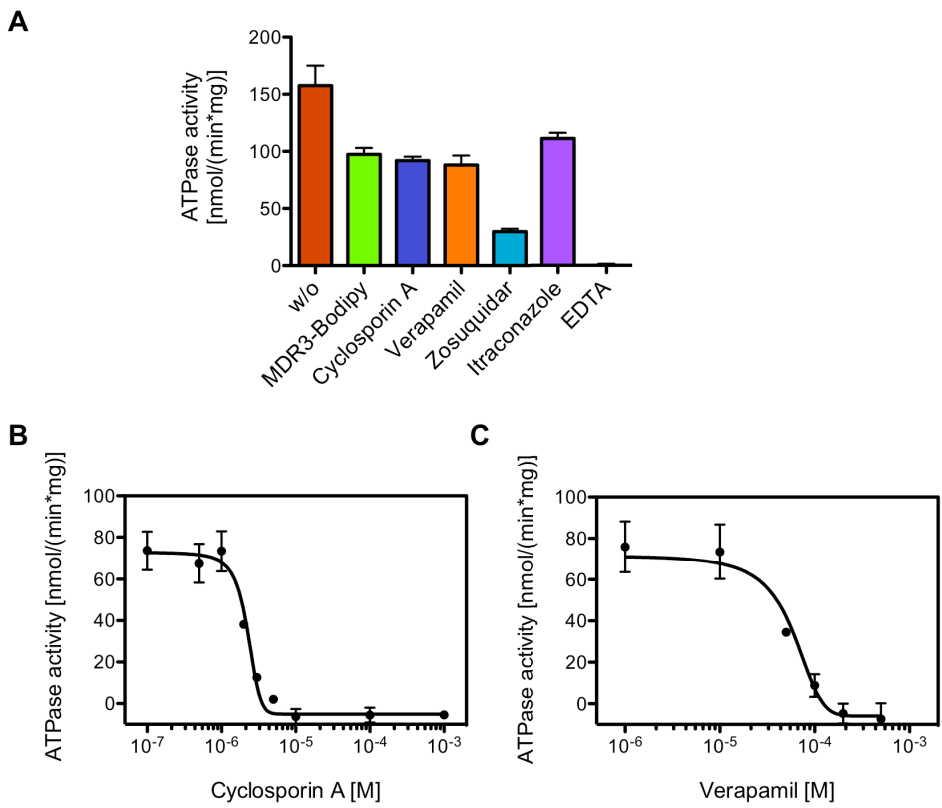




Figure 4

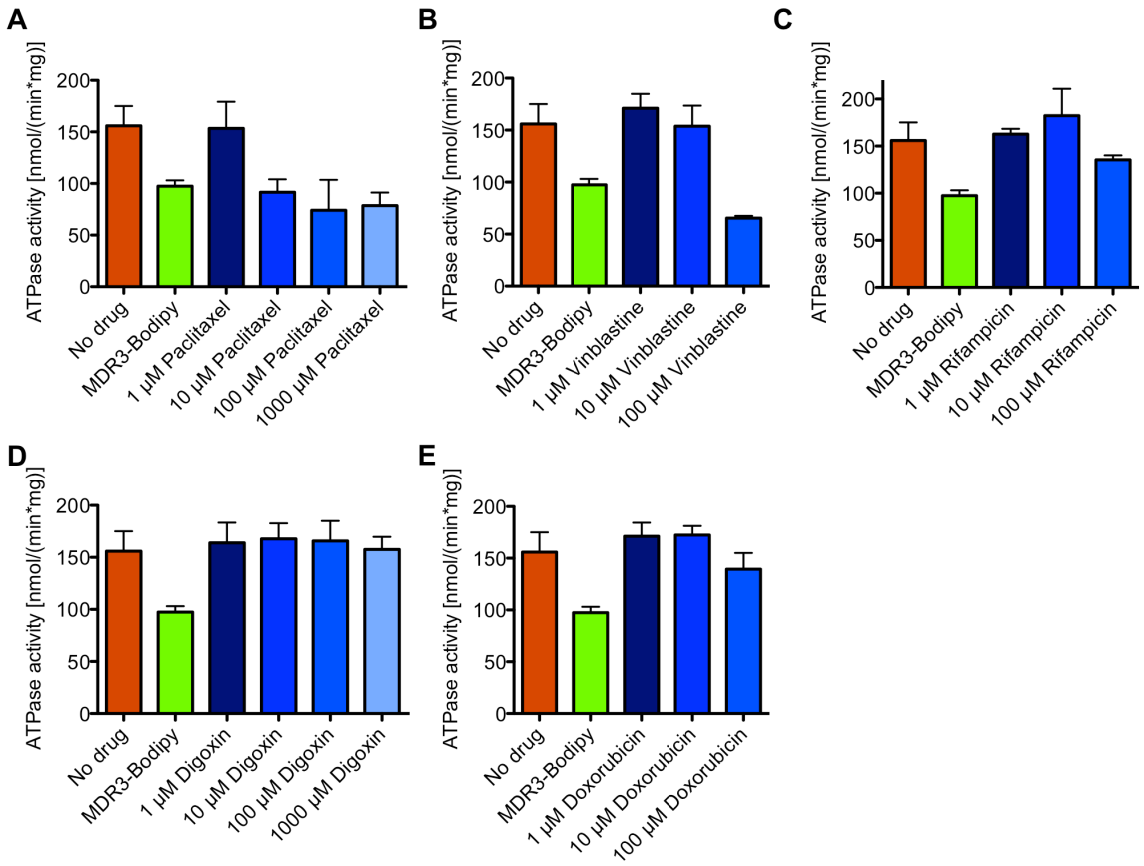
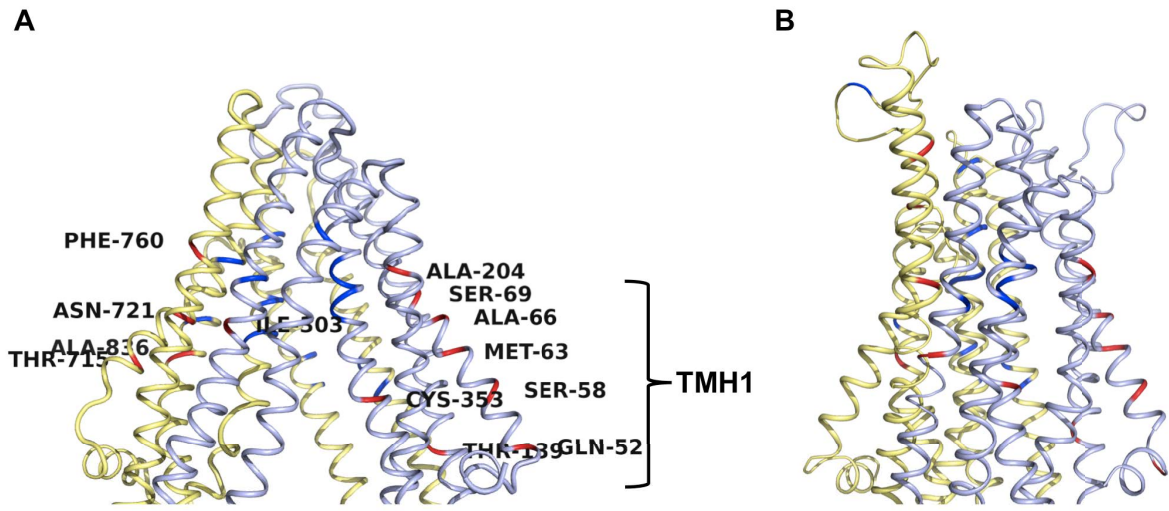


Figure 5



## Supplementary Figure S1

**Figure S1.** Primary sequence alignment of **(A)** TMD1 and **(B)** TMD2 of human MDR3, mouse Mdr2, human MDR1 and mouse Mdr1a. TMDs are highlighted in green, intracellular loops in yellow and extracellular loops in blue. Non-conserved amino acids are framed in red and drug-interacting residues are shown in black.

[illegible]

**B**

MDR3_HUMAN	PNGWKSLFRHSTQ-KNLKNSQCQKSLDVETDGLLEANVPPVSFLKVLKLNKTEWPYFVV	713
MDR3_MOUSE	PNGWKARIFRNSTK-KSLKSPH--QNRLDEETNELDANVPPVSFLKVLKLNKTEWPYFVV	710
MDR1_HUMAN	SNDRSSLLIRKRSTRRSVRGSQ-AQDRKLSTKEALDESIPPVSFWIRMKLNLTWPYFVV	713
MDR1A_MOUSE	SKDSGSSLIRRRSTRKSICGPH-DQDRKLSTKEALDEDVPPASFWIRLKLNSTEWPYFVV	709
	: : :* : :: : * : :*: ** *:*** *****	
MDR3_HUMAN	GTVCAIANGGLQPAFSVIFSEIIAIFGPGDDA-VKQQCKNFISLFILFLGIISFFTFFLQ	772
MDR3_MOUSE	GTVCAIANGALQPAFSIILSEMIAIFGPGDDA-VKQQCKNMFSLVFLGLGVLSFFTFFLQ	769
MDR1_HUMAN	GVFCAIINGGLQPAPFAIIFSIIIGVFTRIDDPETKRQNSNFLSLLFLALGIISFITFFLQ	773
MDR1A_MOUSE	GIFCAIINGGLQPAFSVIFSIVGVGFVTNGGPPETQRQNSNFLSLLFLILGIISFITFFLQ	769
	* ** ** ***** :*:*:::* : :*:**:* *****:*****	
MDR3_HUMAN	GFTFGKAGEILTTRLRSMFAKMLRQDMSWFDHKNSTGALSTRLATDAAQVQGATGTRL	832
MDR3_MOUSE	GFTFGKAGEILTTRLRSMFAKMLRQDMSWFDHKNSTGALSTRLATDAAQVQGATGTRL	829
MDR1_HUMAN	GFTFGKAGEILTKRLRYMVFRSMLRQDVSWFDDPKNTTGALTTRLANDAAQVKGAIGSRL	833
MDR1A_MOUSE	GFTFGKAGEILTCLRVMVFKSMLRQDVSWFDDPKNTTGALTTRLANDAAQVKGATGSRL	829
	***** ** * : ***** ** * :*****:***** ** *	
MDR3_HUMAN	ALIAQNLIANGLTGIIISFIYGWQLTLLLLAVVPPIIAGVEMKLLAGNAKRDKKELEAA	892
MDR3_MOUSE	ALIAQNTIANLGSGIIISFIYGWQLTLLLLSVVPPIIAGVEMKLLAGNAKRDKKEMEAA	889
MDR1_HUMAN	AVITQNLIANGLTGIIISFIYGWQLTLLLLAIVIPPIIAGVEMKMLSGQALKDKKELEGS	893
MDR1A_MOUSE	AVIFQNLIANGLTGIIISLIYGWQLTLLLLAIVIPPIIAGVEMKMLSGQALKDKKELEGS	889
	*:* ** ***** .*****:*****.*.:*****.**:*****:*	
MDR3_HUMAN	GKIATEAIENIRTVVSLTQERKFESMYVEKLYGPYRNSVQKAHIYGITFSISSAFMYFSY	952
MDR3_MOUSE	GKIATEAIENIRTVVSLTQERKFESMYVEKLHGYPYRNSVRKAHIYGITFSISSAFMYFSY	949
MDR1_HUMAN	GKIATEAIENFRTVVSLTQEQQFEHMYAQLQVPYRNSLRKAHIFGITFSIFTAMMYFSY	953
MDR1A_MOUSE	GKIATEAIENFRTVVSLTREQKFETMYAQLQIPYRNAMEKAHVFGITFSIFTAMMYFSY	949
	*****:*****:*:** ** :.* *****:*****:*****:*****	
MDR3_HUMAN	AGCFRFGAYLIVNGHMRFRDVIIVFSAIVFCVAVALGHASSFAPDYAKAKLSAAHLFMLFE	1012
MDR3_MOUSE	AGCFRFGSYLIVNGHMRFKDVIIVFSAIVLCVAVALGHASSFAPDYAKAKLSAAYLFSLFE	1009
MDR1_HUMAN	AGCFRFGAYLVAHKLMSFEDVLIIVFSADVFCAMAVGQVSSFAPDYAKAKISAHHIMIE	1013
MDR1A_MOUSE	AACFRFGAYLVTLMTFENVLIIVFSADVFCAMAVGQVSSFAPDYAKATVSASHIIRIE	1009
	* *****.* : * :*:*****:*****.*.:*****:***:*****	



## Chapter VI – Interactions of MDR3 with scaffold proteins

### Title:

**The human liver ABC transporter MDR3 (ABCB4) interacts with the N-terminal FERM domain of Radixin *in vitro***

Published in: *In Preparation*

Impact factor:

Own Proportion to this work: 70 %

Expression and Purification of human MDR3

Expression and Purification of the scaffold proteins

Pull-down Assays

Writing of the manuscript

## **The human liver ABC transporter ABCB4 (MDR3) interacts with the N-terminal FERM domain of radixin *in vitro***

Marianne Kluth, Katja Döhl, Susanne Przybylla and Lutz Schmitt<sup>#</sup>

From the Institute of Biochemistry, Heinrich Heine University, Düsseldorf, Germany

<sup>#</sup>To whom correspondence should be addressed

### **Affiliation:**

Institute of Biochemistry  
Heinrich Heine University Düsseldorf  
Universitätsstr. 1  
40225 Düsseldorf  
Germany

Phone: +49-211-81-10773

Fax: +49-211-81-15310

E-Mail: Lutz.Schmitt@hhu.de

**Keywords:** ABC transporter, radixin, NHERF-1, RACK1, MDR3, ABCB4, PFIC-3

**Abbreviations:** ABC-ATP binding cassette; ATP-Adenosine-5'-triphosphate; BSEP-Bile Salt Export Pump; CBP-Calmodulin Binding Peptide; cDNA-complementary DNA; CFTR-; cmc-Critical Micellar Concentration; EBP50-Erzin binding phosphoprotein 50; ERM-Erzin/Radixin/Moesin; ICP-Intrahepatic Cholestasis of Pregnancy; IMAC-Immobilized Metal-Ion Chromatography; LPAC- Low-Phospholipid Associated Cholestasis; MDR3/1-Multidrug Resistance Protein 3/1; NBD-Nucleotide-Binding Domain; NHERF-1- $\text{Na}^+/\text{H}^+$  exchanger regulatory factor; PC-Phosphatidylcholine; PFIC-Progressive Familial Intrahepatic Cholestasis; RACK1-Receptor for activated C-kinase 1; SDS-PAGE- Sodium dodecyl sulphate polyacrylamide gel electrophoresis; TAP-Tandem Affinity Purification; TMD-Transmembrane Domain

## Abstract

The human multidrug resistance protein 3 (MDR3/ABCB4) is a member of the ubiquitous ATP-binding cassette (ABC) transporter family. ABCB4 is exclusively located in the canalicular membrane of hepatocytes and transports phosphatidylcholine (PC) lipids from the inner to the outer leaflet of the canalicular membrane in an ATP dependent manner. Mutations of *ABCB4* gene are associated with different kinds of hereditary liver diseases such as cholesterol gallstones, intrahepatic cholestasis of pregnancy (ICP) and progressive familial intrahepatic cholestasis type 3 (PFIC-3), respectively. Currently, it is not known how human ABCB4 is regulated in terms of trafficking to and insertion into as well as recycling from the canalicular membrane. To understand how cell surface expression of ABCB4 is regulated, we aimed to identify adaptor proteins of this transporter mediating the interaction with the cytoskeleton. For this purpose we expressed and purified human RACK1, NHERF-1 and the FERM domain of radixin and performed pull-down assays with purified ABCB4 and the potential adaptor proteins. We found that RACK1 binds purified full-length ABCB4, an interaction observed previously *in vivo*. To our knowledge a direct interaction of the FERM domain of radixin with ABCB4 was not demonstrated *in vitro* so far.



## Introduction

Several ATP-binding cassette (ABC) transporters are localized in the canalicular (apical) membrane of hepatocytes and are involved in bile formation. Among them, the human ATP-binding cassette subfamily B member 4 (ABCB4), previously called multidrug resistance protein 3 (MDR3), fulfills the ATP-dependent flip-flop of phosphatidylcholine (PC) lipids from the inner to the outer leaflet of the canalicular membrane (1-6). PC lipids are one major component of bile and are crucial to protect the biliary duct from bile salts, which are translocated by the bile salt export pump (BSEP/ABCB11) (7-10). Furthermore, these PC/bile salt micelles absorb cholesterol translocated by a heterodimer of ABCG5 and ABCG8 (11).

Different kinds of hereditary liver diseases ranging from cholesterol gallstones, intrahepatic cholestasis of pregnancy (ICP) to progressive familial intrahepatic cholestasis type 3 (PFIC-3) are caused by dysfunction of ABCB4 (12-15). A multitude of ABCB4 missense mutations result in lack of functional protein at the canalicular membrane suggesting defects of the targeting or retention of ABCB4 in the canalicular membrane (16-18). For example, the mutations G68R and D459H, which are identified in PFIC-3 patients, led to a retention in the endoplasmatic reticulum (ER) membrane (19). To provide further insights into the pathways and proteins involved in trafficking of ABCB4 to the canalicular membrane, this study focused on the identification of adaptor proteins, which mediate ABCB4-cytoskeletal interactions.

Several cytosolic adaptor proteins are involved in surface regulation of ABC transporters. The receptor for activated C-kinase 1 (RACK1) is a scaffold protein and binds to a large number of proteins (20-23). For example, RACK1 mediates the stable cell surface expression of the ABC transporter cystic fibrosis transmembrane conductance regulator (CFTR/ABCC7) (24) and of the G protein-coupled receptor for thromboxane A<sub>2</sub> (20). Ikebuchi *et al.* used a yeast-two hybrid screen with a cytoplasmatic linker region of ABCB4 and identified RACK1 as an adaptor protein (25). After down-regulation of endogenous RACK1 expression in HeLa cells, ABCB4 was localized in a cytosolic compartment and the ABCB4-mediated PC translocation was reduced, although co-immunoprecipitation revealed no interaction of full-length ABCB4 and RACK1 (25).

Furthermore, the Na<sup>+</sup>/H<sup>+</sup> exchange regulatory factor (NHERF-1), also referred to ezrin binding phosphoprotein 50 (EBP50), was identified to conduct intracellular trafficking of CFTR and the multidrug resistance-associated proteins 2 (MRP2/ABCC2) and 4 (MRP4/ABCC4) (26-29). NHERF-1 is a multidomain scaffolding protein and contains two N-terminal postsynaptic density 95/disc large/zona occludens (PDZ) domains and an ezrin-

radixin-moesin (ERM)-binding (EB) domain at the C-terminus (30). The PDZ domains bind the cytoplasmic domains of membrane proteins, while the EB domain interacts with a cytoskeleton linker protein such as radixin or directly with the apical actin cytoskeleton (31,32). For CFTR it was demonstrated that NHERF-1 binds the C-terminus of CFTR (33,34) and colocalized in the apical membranes of airway epithelial cells (35).

In addition, radixin as a member of the ERM protein family and is primary localized at the canaliculr membrane of hepatocytes (36,37). Their radixin is essential for maintain the structure of the canalicular membrane (38). The N-terminale FERM (4.1-protein, Erzin, Radixin, Moesin) domain of radixin was demonstrated to bind the C-terminus of ABCC2 (39,40), whereas the C-terminal domain interacts with actin filaments (41-43). Radixin is autoregulated by intramolecular interactions between the FERM domain and the C-terminal actin-binding domain and becomes activated by phosphorylation of the C-terminal domain (44-46). Furthermore, radixin supression in rat hepatocytes demonstrated the loss of Abcb11 and Abcb1 (Mdr1) from the canalicular membrane suggesting that radixin is also required for the targeting and/or retention of other canalicular transporters.

These findings suggest that radixin as well as NHERF-1 are potential adaptor proteins of ABCB4. To analyze such an interaction further, we expressed and purified StrepII tagged fusion proteins of RACK1, NHERF-1 and the FERM domain of radixin. Full-length MDR3 was expressed and purified in a functional state with respect to its capability to bind and hydrolyze ATP as described (47). This set-up allowed pull-down assays with ABCB4 and the potential adaptor proteins *in vitro*. Our results proved that RACK1 also binds full-length ABCB4 *in vitro*. For the first time, we demonstrated that the FERM domain of radixin interacts with ABCB4 suggesting a pivotol role of these proteins in the trafficking of ABCB4 to the canalicular membrane.

## Material and Methods

### Chemicals and Routine Procedures

Fos-choline 16 (FC-16) was obtained from Affymetrix. All other chemicals were from Sigma-Aldrich. Strep-Tactin Sepharose and desthiobiotin was purchased from IBA. The protein concentration was determined by a Bradford assay using the Coomassie Plus Assay (Pierce).

### Cloning of human MDR3 and expression screening

We cloned human wild type MDR3 (NCBI accession NM\_000443.3) as previously described (47). MDR3 expression constructs were transformed into electro-competent *P. pastoris* X33 cells (Invitrogen) using standard procedures and the expression level was analyzed as described in Ellinger *et al.* (47).

### Fermentation of MDR3 transformed *P. pastoris* cells

*P. pastoris* cells containing the chromosomal integrated wild type *MDR3* gene were fermented in a 15 liter table-top glass fermenter (Applikon Biotechnology) according to the Invitrogen *Pichia* fermentation guidelines and as reported in (47).

### Crude membrane preparation, Solubilization and Purification of MDR3

The membrane preparation, solubilization and purification of MDR3 was performed as described previously (47). In brief, crude membrane vesicles equivalent to 100 g wet cells were solubilized in 1% (w/v) of Fos-choline-16 (FC-16) for 1 h at 4°C. The solubilized fraction was centrifuged (125,000 xg, 1 h, 4°C), loaded onto a Ni<sup>2+</sup>-loaded HiTrap Chelating column (5 ml, GE Healthcare) and subsequently the eluate containing MDR3 was applied to a 4 mL calmodulin affinity resin. All procedures were carried out at 4°C and all buffers typically contained 0.026 mM FC-16. The purified protein was snap frozen in liquid nitrogen and stored at -80°C. Aliquots of the sample were analyzed by Coomassie blue stained SDS-PAGE and immunoblotting.

### Cloning of RACK1, the FERM domain of radixin and NHERF-1

The cDNA of human RACK1 (GenBank accession NM\_006098), NHERF-1 (NCBI accession NM\_004252), and Radixin (RDX) (NCBI accession NM\_001260492.1) was cloned into the *Escherichia coli* vector pET51b (Novagen) using restriction enzymes, yielding constructs with an N-terminal StrepII tag coding sequence. The coding sequences for RACK1 were PCR amplified with the primer pairs RACK1-for and RACK1-rev, radixin with RDX-for and RDX-rev and NHERF-1 with NHERF-for and NHERF-rev, respectively (Table 1). The FERM domain of radixin (amino acids 1 – 320) was obtained via deletion of the C-

terminal domain using the primer pair delRDX-C\_for and delRDX-C\_rev. The sequences of all constructs were verified by DNA sequencing (GATC Biotech).

### **Expression and Purification of human RACK1**

Protein expression was conducted as described in (48) with minor modifications. Two liter low salt LB media containing 100 µg/mL ampicillin was inoculated with *E. coli* Rosetta (DE3) pLys cells transformed with pET51b-RACK1 and cultured at 37°C and 180 rpm until OD<sub>600</sub> 0.8-1.0 was reached. The culture was kept 30 min on ice, subsequently temperature was increased to 18°C and protein expression was induced by the addition of isopropyl-β-D-1-thiogalactopyranoside (IPTG; Roth) to a final concentration of 500 µM. After overnight incubation, cells were harvested at 5000 xg, 4°C for 10 min, washed with 100 mM HEPES pH 8.0, snap frozen in liquid nitrogen and stored at -80°C. For purification, cells were thawed on ice, re-suspended in buffer A (100 mM HEPES pH 8.0, 500 mM NaCl) and disrupted by four passages through a pre-cooled TS Series Cell Disrupter (Constant Systems) at 2.6 kbar. After cell debris was spun down (125,000 xg, 4°C, 1 h), the supernatant was loaded onto a 1 mL StrepTrap HP column (GE Healthcare). Subsequently, the proteins were eluted using buffer A supplemented with 2.5 mM desthiobiotin. The elution fractions were analyzed by SDS-PAGE and concentrated with an Amicon Ultra Centrifugal Filter device (30 kDa molecular-weight cutoff, Millipore) to a final concentration of 4 mg mL<sup>-1</sup>. As a second purification step, size-exclusion chromatography (SEC) using a Superdex 200 10/30 column (GE Healthcare) was performed employing a buffer containing 20 mM HEPES pH 8.0, 300 mM NaCl and 10% (v/v) glycerol. Fractions were collected, analyzed by SDS-PAGE and used for pull-down assays.

### **Expression and Purification of the N-terminal FERM domain of radixin and NHERF-1**

A pre-culture of *E. coli* BL21 (DE3) transformed with pET51b-RDX\_FERMD or pET51b-NHERF-1 was used to inoculate 2 L LBN media (10 g/L Trypton, 2 g/L glucose, 29.2 g/L NaCl) and 2 L low salt LB media supplemented with 100 µg/mL ampicillin, respectively. The culture was cultivated at 37°C to an OD<sub>600</sub> of 0.6-0.8, cooled on ice for 30 min and induced with IPTG at a final concentration of 1 mM for the FERM domain of radixin or 200 µM IPTG in the case of NHERF-1 at 18°C. After overnight incubation, cells were harvested at 5000 xg, 4°C for 10 min, washed with buffer B (100 mM Tris-HCl pH 8.0, 150 mM NaCl), snap frozen in liquid nitrogen and stored at -80°C. The purification of the FERM domain of radixin or NHERF-1 was performed by StrepII-tag affinity chromatography using a 1 mL StrepTrap HP column (GE Healthcare). Generally, cells were thawed on ice, re-suspended in buffer B and

disrupted by four passages through a pre-cooled TS Series Cell Disrupter (Constant Systems) at 2.6 kbar. The supernatant (125,000  $\times g$ , 4°C, 1 h) was loaded onto the column and the proteins were eluted in one step with buffer B supplemented with 2.5 mM desthiobiotin. The elution fractions were analyzed by SDS-PAGE and concentrated with an Amicon Ultra Centrifugal Filter device (30 kDa molecular-weight cutoff, Millipore) to a final concentration of 5 mg mL<sup>-1</sup>. In the case of the FERM domain of radixin, SEC was performed using a Superose 12 10/30 column (GE Healthcare) and 50 mM Tris-HCl pH 7.5, 150 mM NaCl as described in (49). Fractions were collected, analyzed by SDS-PAGE and used for pull-down assays.

### **Pull-down Assay**

Fifty microliter Strep-Tactin sepharose were equilibrated one time with ddH<sub>2</sub>O and two times with binding buffer (100 mM Tris-HCl pH 8.0, 150 mM NaCl, 10% (v/v) glycerol, 0.026 mM (2.5x cmc) FC-16 and 15  $\mu$ g RACK1, the FERM domain of radixin and NHERF-1 were immobilized, respectively. In FC-16 solubilized and purified MDR3 (75  $\mu$ g) was added to the sepharose, gently mixed and incubated for 15 min at 4°C. subsequently, the sepharose was washed five times with 200  $\mu$ l of binding buffer and the proteins were eluted with binding buffer supplemented with 2.5 mM desthiobiotin. The same procedure was performed in the absence of RACK1, the FERM domain of radixin or NHERF-1 to monitor unspecific binding of MDR3 to the column material. The samples were analyzed by SDS-PAGE and immunoblotted using a tank blot system (Bio-Rad) and the monoclonal anti-P-gp C219 antibody (Merck) and anti-StrepII antibody (IBA) employing standard procedures.

## Results

### *Expression and Purification of RACK1, NHERF-1 and the FERM domain of radixin*

The purification and the crystal structures of RACK1, the PDZ domain of NHERF-1 and the FERM domain of radixin have been reported (48,50,51). Because of the inactive state of radixin in its dephosphorylated state by intra- and intermolecular interactions between the FERM domain and the C-terminal domain (44-46), we expressed only the isolated FERM domain to determine the interaction of ABCB4 with radixin. In this study, we cloned and expressed RACK1, NHERF-1 and the FERM domain of radixin fused to an N-terminal StrepII tag in *E. coli*. We purified the proteins via Strep-Tactin affinity chromatography and analyzed the purity of the adaptor proteins by CBB stained SDS gels (Figure 1 A). We obtained 10 mg of NHERF-1 per liter culture with adequate purity. In the case of RACK1 and FERM domain of radixin, we performed a two-step purification protocol containing an additional SEC step. Human RACK1 is a 36 kDa protein that is monomeric in solution (48). We observed a signal at 8 mL retention volume, which is likely due to aggregation and/or larger oligomeric species of Strep-tagged RACK1 caused by the formation of disulfide-bridges followed by impurities of unspecific proteins with higher molecular weight compared to RACK1 (Figure 1 B). After 16.5 mL retention volume the monomer of RACK1 was eluted with high purity (>90%). For the FERM domain of radixin, we obtained approximately 95% monodisperse protein indicated by SEC (Figure 1 C). The expression and purification of ABCB4 from *P. pastoris* in a functional state with respect to ATP binding and hydrolysis was been reported previously (47).

### *In vitro pull-down assays using purified RACK1, NHERF-1 and the FERM domain of radixin*

To identify whether RACK1, NHERF-1 and the FERM domain of radixin interact with full-length ABCB4 we performed pull-down assays of the purified adaptor proteins and detergent-soluble ABCB4. First, we immobilized ABCB4 through the His<sub>6</sub>-Tag or the CBP-Tag, but the adaptor proteins interacted with both matrixes used for immobilizing MDR3. Thus, we performed the pull-down assay vice versa. In brief, RACK1, NHERF-1 or the FERM domain of radixin was immobilized using a Strep-Tactin resin. Subsequently, detergent-soluble ABCB4 was added to the mixture to allow complex formation. After several washing steps the complex was eluted by competitive replacement of the StrepII tag of the adaptor protein (Figure 2 A). The interaction was verified by immunoblot analysis using an antibody against

the StrepII tag and the P-glycoprotein specific antibody C219. We analysed the interaction of ABCB4 with the used Strep-Tactin resin in the absence of any adaptor protein and observed no signal for MDR3 after the fifth washing step in the immunoblot indicating no unspecific binding of MDR3 to the matrix (Figure 2 B). Thus, this approach is feasible to analyze the interaction of detergent-soluble ABCB4 with purified RACK1, NHERF-1 and the FERM domain of radixin.

RACK1 is a 36 kDa cytosolic protein composed of seven Trp-Asp (WD) motifs and was identified as binding partner of ABCB4 in a yeast-two-hybrid screen (25). Furthermore, ABCB4 localization at the plasma membrane was RACK1-dependent suggesting that RACK1 regulates the membrane surface expression of ABCB4. However, the interaction of full-length MDR3 to RACK1 could not be demonstrated. Here, we observed marginal unspecific binding of ABCB4 to the matrix, but the interaction of MDR3 to RACK1 was drastically stronger (Figure 2 C). This result demonstrated that full-length ABCB4 binds RACK1, which extends the results of Ikebuchi *et al.*

NHERF-1 contains two PDZ domains, which bind to the cytoplasmic region of membrane proteins. The PDZ domains were shown to bind the C-terminus of CFTR, which is required for the localization of CFTR to the apical plasma membrane (26,31,33,52). The C-terminal canonical type I PDZ binding motif (acidic-polar-X-hydrophobic, where X can be any amino acid), are highly conserved across human ABC transporters. We analyzed the primary sequence of ABCB4 in terms of the PDZ binding motif and identified that the C-terminal nucleotide-binding domain (NBD) of ABCB4 contains this binding motif twice. In addition, the extreme C-terminus (TQNL) revealed a PDZ-like motif. Thus, it is likely that ABCB4 interacts with PDZ proteins. To identify whether NHERF-1 is an adaptor protein of human ABCB4 *in vitro* or not, we performed pull-down assay of the purified proteins (Figure 2 C). We detected ABCB4 in the washing fraction as well as in the elution fraction. This is due to the weak binding of NHERF-1, which was also detected in the washing fraction, to the resin. Thus, we cannot draw any conclusion whether NHERF-1 binds MDR3 or not. Further investigations are needed to determine the interaction of ABCB4 with NHERF-1.

Furthermore, we investigated whether radixin is an adaptor protein of ABCB4. In the pull-down assay of full-length ABCB4 and the FERM domain ABCB4 was exclusively detected in the elution fraction revealing an interaction of both proteins (Figure 2 C). These findings suggested an important role of radixin in the regulation of the cell surface expression of ABCB4 at the apical membrane.

## Discussion

The ATP binding cassette subfamily B member 4 (ABCB4) is exclusively located in the canalicular membrane of hepatocytes and transports phosphatidylcholine into bile to protect the biliary ducts against the deleterious action of bile salts (1-6). Dysfunction of ABCB4 caused by mutations lead to hereditary liver diseases such as PFIC-3 and is associated with the absence of the transporter at the canalicular membrane (16-19). Although the canalicular localization of ABCB4 is indispensable for its function, a potential interaction of ABCB4 and proteins of the cytoskeleton has not been extensively investigated.

There are evidences that the scaffold protein RACK1 regulates the apical membrane expression of ABCB4. RACK1 was identified in a yeast-two-hybrid screen to interact with a cytosolic linker region of ABCB4. However, co-immunoprecipitation revealed no interaction of RACK1 with full-length MDR3 (25). Previously, we demonstrated that purified ABCB4 mediated PC-induced ATPase activity ((47) and Chapter 4). In the present study, we used pull-down assay and demonstrated that full-length ABCB4 bound RACK1 *in vitro*. Our result confirmed the suggestion of Ikebuchi and co-workers that RACK1 is crucial for the apical localization of ABCB4. So far it was demonstrated that RACK1 interacts with more than 80 binding partners and acts as anchor and cellular shuttle for its binding partners as well as enzymatic cofactor (20,23,24,48,53). RACK1 furthermore upregulates the protein expression of ABCG2 in plasma membranes, although the mRNA level was not influenced (54). In addition, RACK1 regulates the apical localization of CFTR by binding to NHERF-1, which is known to be essential for the functional expression of CFTR at the apical membrane (24). In contrast, it was reported that the cellular localization of ABCB1 (MDR1 or P-glycoprotein) was not affected by RACK1 suppression, although ABCB1 shares above 85% amino acid sequence homology with ABCB4. This indicates that RACK1 is exclusively responsible for the canalicular localization of ABCB4 and not for ABCB1 (25).

To understand how ABCB4 is targeted and retained in the canalicular membrane, we focused on the identification of new adaptor proteins of ABCB4. Thus, we purified the scaffold proteins NHERF-1 and the FERM domain of radixin and used the pull-down assay to investigate potential protein-protein interactions. With the pull-down assay we could not prove the interaction of ABCB4 with NHERF-1. However, we speculate that the PDZ-like domain at the C-terminus of ABCB4 is essential for binding of NHERF-1 and for the cell surface expression of ABCB4 at the canalicular membrane as demonstrated for other ABC transporters like ABCC2, ABCC4, CFTR and ABCC6 (26-29,33,52,55). NHERF-1 is involved in apical membrane surface expression of ABCC4 in polarized kidney cells and



down-regulation of NHERF-1 increased expression and function of ABCC4 (27,28). Furthermore, NHERF-1 knock-out mice showed a decreased expression of ABCC2 in hepatocytes (29). The C-terminus of CFTR was described to be required for the binding of NHERF-1 and for the apical localization of CFTR (26,52). The deletion of the last six amino acids of ABCC6, which contains a PDZ-like binding motif, resulted in a decreased expression and stability of ABCC6 at the plasma membrane and a mislocalization in polarized cells (55). Thus, further investigations like mutational analysis of the C-terminus of ABCB4 have to be performed to prove this speculation.

For the first time, we demonstrated that the FERM domain of radixin binds ABCB4. This is in agreement with data obtained for ABCB1. ABCB1 co-localized and co-immunoprecipitated with ezrin, radixin and moesin in leukemia cells (56) and a knock-down of radixin in HepG2 cells and rat hepatocytes resulted in a decrease of ABCB1 at the plasma membrane and relocalization to the intracellular pool (38,57). In radixin knock-out mice, it was observed that radixin regulates the localization of ABCB1 in the small intestine (58). Additionally, these mice developed conjugated hyperbilirubinemia, because of their impaired ability to localize ABCC2 to the canalicular membrane (40). Hence, ABCC2 internalization into the canalicular membrane was dependent on radixin activity (59,60). Radixin is autoregulated by intramolecular interactions of the N-terminal FERM domain and the C-terminal domain and activated by phosphorylation. The phosphorylation status of radixin was demonstrated to regulate the canalicular localization of ABCC2 (59). Moreover, radixin is required for the localization of Bsep at the canalicular membrane and downregulation of radixin in rat hepatocytes lead to reduced Bsep-mediated bile salt excretion (38). This data indicate that radixin exhibit a general function for the regulation of the cell surface expression of human liver ABC transporter at the canalicular membrane by cross-linking the membrane protein to the cytoskeleton.

Taken together, we confirmed that RACK1 binds full-length ABCB4 suggesting that RACK1 is important for ABCB4 trafficking to the canalicular membrane and we demonstrated an interaction of the FERM domain of radixin with ABCB4 *in vitro*. We proposed that ABCB4 localization is highly regulated by a complex system, which ensures proper trafficking of ABCB4 to the canalicular membrane containing at least RACK1, NHERF-1 and radixin.

## Acknowledgements

We are indebt to Prof. Dr. Dieter Häussinger, Prof. Dr. Ralf Kubitz, Dr. Jan Stindt and Dr. Phillip Ellinger for support and stimulating discussions. We thank Dr. Diana Kleinschrodt and Iris Leuz (Protein Production Facility of the Heinrich Heine University Düsseldorf) for excellent support with the cloning procedure and Dr. Sander Smits for critical reading of this manuscript. This work was supported by the DFG through the Collaborative Research Center 974 (TP B3 to R.K. and L. S.).

## References

1. Smit, J. J., Schinkel, A. H., Oude Elferink, R. P., Groen, A. K., Wagenaar, E., van Deemter, L., Mol, C. A., Ottenhoff, R., van der Lugt, N. M., van Roon, M. A., and et al. (1993) Homozygous disruption of the murine *mdr2* P-glycoprotein gene leads to a complete absence of phospholipid from bile and to liver disease. *Cell* **75**, 451-462
2. Smith, A. J., Timmermans-Hereijgers, J. L., Roelofsen, B., Wirtz, K. W., van Blitterswijk, W. J., Smit, J. J., Schinkel, A. H., and Borst, P. (1994) The human MDR3 P-glycoprotein promotes translocation of phosphatidylcholine through the plasma membrane of fibroblasts from transgenic mice. *FEBS Lett.* **354**, 263-266
3. van Helvoort, A., Smith, A. J., Sprong, H., Fritzsche, I., Schinkel, A. H., Borst, P., and van Meer, G. (1996) MDR1 P-glycoprotein is a lipid translocase of broad specificity, while MDR3 P-glycoprotein specifically translocates phosphatidylcholine. *Cell* **87**, 507-517
4. Morita, S. Y., Kobayashi, A., Takanezawa, Y., Kioka, N., Handa, T., Arai, H., Matsuo, M., and Ueda, K. (2007) Bile salt-dependent efflux of cellular phospholipids mediated by ATP binding cassette protein B4. *Hepatology* **46**, 188-199
5. Oude Elferink, R. P., and Paulusma, C. C. (2007) Function and pathophysiological importance of ABCB4 (MDR3 P-glycoprotein). *Pflugers Arch - Eur J Physiol* **453**, 601-610
6. Smith, A. J., de Vree, J. M., Ottenhoff, R., Oude Elferink, R. P., Schinkel, A. H., and Borst, P. (1998) Hepatocyte-specific expression of the human MDR3 P-glycoprotein gene restores the biliary phosphatidylcholine excretion absent in *Mdr2* (-/-) mice. *Hepatology* **28**, 530-536
7. Meier, P. J., and Stieger, B. (2002) Bile salt transporters. *Annu. Rev. Physiol.* **64**, 635-661
8. Gerloff, T., Stieger, B., Hagenbuch, B., Madon, J., Landmann, L., Roth, J., Hofmann, A. F., and Meier, P. J. (1998) The sister of P-glycoprotein represents the canalicular bile salt export pump of mammalian liver. *J. Biol. Chem.* **273**, 10046-10050
9. Trauner, M., Fickert, P., Halilbasic, E., and Moustafa, T. (2008) Lessons from the toxic bile concept for the pathogenesis and treatment of cholestatic liver diseases. *Wien. Med. Wochenschr.* **158**, 542-548
10. Gerloff, T., Meier, P. J., and Stieger, B. (1998) Taurocholate induces preferential release of phosphatidylcholine from rat liver canalicular vesicles. *Liver* **18**, 306-312
11. Small, D. M. (2003) Role of ABC transporters in secretion of cholesterol from liver into bile. *Proc. Natl. Acad. Sci. U. S. A.* **100**, 4-6
12. Gonzales, E., Davit-Spraul, A., Baussan, C., Buffet, C., Maurice, M., and Jacquemin, E. (2009) Liver diseases related to MDR3 (ABCB4) gene deficiency. *Front. Biosci.* **14**, 4242-4256
13. Dzagania, T., Engelmann, G., Haussinger, D., Schmitt, L., Flechtenmacher, C., Rtskhiladze, I., and Kubitz, R. (2012) The histidine-loop is essential for transport activity of human MDR3. A novel mutation of MDR3 in a patient with progressive familial intrahepatic cholestasis type 3. *Gene* **506**, 141-145
14. Andress, E. J., Nicolaou, M., Romero, M. R., Naik, S., Dixon, P. H., Williamson, C., and Linton, K. J. (2014) Molecular mechanistic explanation for the spectrum of cholestatic disease caused by the S320F variant of ABCB4. *Hepatology* **59**, 1921-1931

15. Trauner, M., Fickert, P., and Wagner, M. (2007) MDR3 (ABCB4) defects: a paradigm for the genetics of adult cholestatic syndromes. *Semin. Liver Dis.* **27**, 77-98
16. Jacquemin, E., De Vree, J. M., Cresteil, D., Sokal, E. M., Sturm, E., Dumont, M., Scheffer, G. L., Paul, M., Burdelski, M., Bosma, P. J., Bernard, O., Hadchouel, M., and Elferink, R. P. (2001) The wide spectrum of multidrug resistance 3 deficiency: from neonatal cholestasis to cirrhosis of adulthood. *Gastroenterology* **120**, 1448-1458
17. Dixon, P. H., Weerasekera, N., Linton, K. J., Donaldson, O., Chambers, J., Egginton, E., Weaver, J., Nelson-Piercy, C., de Swiet, M., Warnes, G., Elias, E., Higgins, C. F., Johnston, D. G., McCarthy, M. I., and Williamson, C. (2000) Heterozygous MDR3 missense mutation associated with intrahepatic cholestasis of pregnancy: evidence for a defect in protein trafficking. *Hum. Mol. Genet.* **9**, 1209-1217
18. de Vree, J. M., Jacquemin, E., Sturm, E., Cresteil, D., Bosma, P. J., Aten, J., Deleuze, J. F., Desrochers, M., Burdelski, M., Bernard, O., Oude Elferink, R. P., and Hadchouel, M. (1998) Mutations in the MDR3 gene cause progressive familial intrahepatic cholestasis. *Proc. Natl. Acad. Sci. U. S. A.* **95**, 282-287
19. Gordo-Gilart, R., Andueza, S., Hierro, L., Martinez-Fernandez, P., D'Agostino, D., Jara, P., and Alvarez, L. (2014) Functional analysis of ABCB4 mutations relates clinical outcomes of progressive familial intrahepatic cholestasis type 3 to the degree of MDR3 floppase activity. *Gut*
20. Parent, A., Laroche, G., Hamelin, E., and Parent, J. L. (2008) RACK1 regulates the cell surface expression of the G protein-coupled receptor for thromboxane A(2). *Traffic* **9**, 394-407
21. Neer, E. J., Schmidt, C. J., Nambudripad, R., and Smith, T. F. (1994) The ancient regulatory-protein family of WD-repeat proteins. *Nature* **371**, 297-300
22. Ron, D., Chen, C. H., Caldwell, J., Jamieson, L., Orr, E., and Mochly-Rosen, D. (1994) Cloning of an intracellular receptor for protein kinase C: a homolog of the beta subunit of G proteins. *Proc. Natl. Acad. Sci. U. S. A.* **91**, 839-843
23. Ohgaki, R., Fukura, N., Matsushita, M., Mitsui, K., and Kanazawa, H. (2008) Cell surface levels of organellar Na<sup>+</sup>/H<sup>+</sup> exchanger isoform 6 are regulated by interaction with RACK1. *J. Biol. Chem.* **283**, 4417-4429
24. Auerbach, M., and Liedtke, C. M. (2007) Role of the scaffold protein RACK1 in apical expression of CFTR. *Am J Physiol Cell Physiol* **293**, C294-304
25. Ikebuchi, Y., Takada, T., Ito, K., Yoshikado, T., Anzai, N., Kanai, Y., and Suzuki, H. (2009) Receptor for activated C-kinase 1 regulates the cellular localization and function of ABCB4. *Hepatol Res* **39**, 1091-1107
26. Wang, S., Raab, R. W., Schatz, P. J., Guggino, W. B., and Li, M. (1998) Peptide binding consensus of the NHE-RF-PDZ1 domain matches the C-terminal sequence of cystic fibrosis transmembrane conductance regulator (CFTR). *FEBS Lett.* **427**, 103-108
27. Hoque, M. T., Conseil, G., and Cole, S. P. (2009) Involvement of NHERF1 in apical membrane localization of MRP4 in polarized kidney cells. *Biochem. Biophys. Res. Commun.* **379**, 60-64
28. Hoque, M. T., and Cole, S. P. (2008) Down-regulation of Na<sup>+</sup>/H<sup>+</sup> exchanger regulatory factor 1 increases expression and function of multidrug resistance protein 4. *Cancer Res.* **68**, 4802-4809
29. Li, M., Wang, W., Soroka, C. J., Mennone, A., Harry, K., Weinman, E. J., and Boyer, J. L. (2010) NHERF-1 binds to Mrp2 and regulates hepatic Mrp2 expression and function. *J. Biol. Chem.* **285**, 19299-19307
30. Bhattacharya, S., Dai, Z., Li, J., Baxter, S., Callaway, D. J., Cowburn, D., and Bu, Z. (2010) A conformational switch in the scaffolding protein NHERF1 controls autoinhibition and complex formation. *J. Biol. Chem.* **285**, 9981-9994
31. Hall, R. A., Ostedgaard, L. S., Premont, R. T., Blitzer, J. T., Rahman, N., Welsh, M. J., and Lefkowitz, R. J. (1998) A C-terminal motif found in the beta2-adrenergic receptor, P2Y1 receptor and cystic fibrosis transmembrane conductance regulator determines binding to the Na<sup>+</sup>/H<sup>+</sup> exchanger regulatory factor family of PDZ proteins. *Proc. Natl. Acad. Sci. U. S. A.* **95**, 8496-8501

32. Swiatecka-Urban, A., Duhaime, M., Coutermarsh, B., Karlson, K. H., Collawn, J., Milewski, M., Cutting, G. R., Guggino, W. B., Langford, G., and Stanton, B. A. (2002) PDZ domain interaction controls the endocytic recycling of the cystic fibrosis transmembrane conductance regulator. *J. Biol. Chem.* **277**, 40099-40105
33. Moyer, B. D., Duhaime, M., Shaw, C., Denton, J., Reynolds, D., Karlson, K. H., Pfeiffer, J., Wang, S., Mickle, J. E., Milewski, M., Cutting, G. R., Guggino, W. B., Li, M., and Stanton, B. A. (2000) The PDZ-interacting domain of cystic fibrosis transmembrane conductance regulator is required for functional expression in the apical plasma membrane. *J. Biol. Chem.* **275**, 27069-27074
34. Sun, F., Hug, M. J., Bradbury, N. A., and Frizzell, R. A. (2000) Protein kinase A associates with cystic fibrosis transmembrane conductance regulator via an interaction with ezrin. *J. Biol. Chem.* **275**, 14360-14366
35. Short, D. B., Trotter, K. W., Reczek, D., Kreda, S. M., Bretscher, A., Boucher, R. C., Stutts, M. J., and Milgram, S. L. (1998) An apical PDZ protein anchors the cystic fibrosis transmembrane conductance regulator to the cytoskeleton. *J. Biol. Chem.* **273**, 19797-19801
36. Fouassier, L., Duan, C. Y., Feranchak, A. P., Yun, C. H., Sutherland, E., Simon, F., Fitz, J. G., and Doctor, R. B. (2001) Ezrin-radixin-moesin-binding phosphoprotein 50 is expressed at the apical membrane of rat liver epithelia. *Hepatology* **33**, 166-176
37. Amieva, M. R., Wilgenbus, K. K., and Furthmayr, H. (1994) Radixin is a component of hepatocyte microvilli in situ. *Exp. Cell Res.* **210**, 140-144
38. Wang, W., Soroka, C. J., Mennone, A., Rahner, C., Harry, K., Pypaert, M., and Boyer, J. L. (2006) Radixin is required to maintain apical canalicular membrane structure and function in rat hepatocytes. *Gastroenterology* **131**, 878-884
39. Saeki, J., Sekine, S., and Horie, T. (2011) LPS-induced dissociation of multidrug resistance-associated protein 2 (Mrp2) and radixin is associated with Mrp2 selective internalization in rats. *Biochem. Pharmacol.* **81**, 178-184
40. Kikuchi, S., Hata, M., Fukumoto, K., Yamane, Y., Matsui, T., Tamura, A., Yonemura, S., Yamagishi, H., Keppler, D., and Tsukita, S. (2002) Radixin deficiency causes conjugated hyperbilirubinemia with loss of Mrp2 from bile canalicular membranes. *Nat. Genet.* **31**, 320-325
41. Arpin, M., Algrain, M., and Louvard, D. (1994) Membrane-actin microfilament connections: an increasing diversity of players related to band 4.1. *Curr. Opin. Cell Biol.* **6**, 136-141
42. Bretscher, A. (1999) Regulation of cortical structure by the ezrin-radixin-moesin protein family. *Curr. Opin. Cell Biol.* **11**, 109-116
43. Mangeat, P., Roy, C., and Martin, M. (1999) ERM proteins in cell adhesion and membrane dynamics: Authors' correction. *Trends Cell Biol.* **9**, 289
44. Algrain, M., Turunen, O., Vaheri, A., Louvard, D., and Arpin, M. (1993) Ezrin contains cytoskeleton and membrane binding domains accounting for its proposed role as a membrane-cytoskeletal linker. *J. Cell Biol.* **120**, 129-139
45. Gary, R., and Bretscher, A. (1995) Ezrin self-association involves binding of an N-terminal domain to a normally masked C-terminal domain that includes the F-actin binding site. *Mol. Biol. Cell* **6**, 1061-1075
46. Bretscher, A., Edwards, K., and Fehon, R. G. (2002) ERM proteins and merlin: integrators at the cell cortex. *Nat Rev Mol Cell Biol* **3**, 586-599
47. Ellinger, P., Kluth, M., Stindt, J., Smits, S. H., and Schmitt, L. (2013) Detergent screening and purification of the human liver ABC transporters BSEP (ABCB11) and MDR3 (ABCB4) expressed in the yeast *Pichia pastoris*. *PLoS One* **8**, e60620
48. Ruiz Carrillo, D., Chandrasekaran, R., Nilsson, M., Cornvik, T., Liew, C. W., Tan, S. M., and Lescar, J. (2012) Structure of human Rack1 protein at a resolution of 2.45 Å. *Acta Crystallogr Sect F Struct Biol Cryst Commun* **68**, 867-872
49. Hamada, K., Matsui, T., Tsukita, S., and Hakoshima, T. (2000) Crystallographic characterization of the membrane-binding domain of radixin. *Acta Crystallogr D Biol Crystallogr* **56**, 922-923
50. Hamada, K., Shimizu, T., Matsui, T., Tsukita, S., and Hakoshima, T. (2000) Structural basis of the membrane-targeting and unmasking mechanisms of the radixin FERM domain. *EMBO J.* **19**, 4449-4462

51. Karthikeyan, S., Leung, T., and Ladas, J. A. (2002) Structural determinants of the Na<sup>+</sup>/H<sup>+</sup> exchanger regulatory factor interaction with the beta 2 adrenergic and platelet-derived growth factor receptors. *J. Biol. Chem.* **277**, 18973-18978
52. Moyer, B. D., Denton, J., Karlson, K. H., Reynolds, D., Wang, S., Mickle, J. E., Milewski, M., Cutting, G. R., Guggino, W. B., Li, M., and Stanton, B. A. (1999) A PDZ-interacting domain in CFTR is an apical membrane polarization signal. *J. Clin. Invest.* **104**, 1353-1361
53. Ron, D., Jiang, Z., Yao, L., Vagts, A., Diamond, I., and Gordon, A. (1999) Coordinated movement of RACK1 with activated betaIIIPKC. *J. Biol. Chem.* **274**, 27039-27046
54. Ikebuchi, Y., Ito, K., Takada, T., Anzai, N., Kanai, Y., and Suzuki, H. (2010) Receptor for activated C-kinase 1 regulates the cell surface expression and function of ATP binding cassette G2. *Drug Metab. Dispos.* **38**, 2320-2328
55. Xue, P., Crum, C. M., and Thibodeau, P. H. (2014) Regulation of ABCC6 trafficking and stability by a conserved C-terminal PDZ-like sequence. *PLoS One* **9**, e97360
56. Luciani, F., Molinari, A., Lozupone, F., Calcabrini, A., Lugini, L., Stringaro, A., Puddu, P., Arancia, G., Cianfriglia, M., and Fais, S. (2002) P-glycoprotein-actin association through ERM family proteins: a role in P-glycoprotein function in human cells of lymphoid origin. *Blood* **99**, 641-648
57. Kano, T., Wada, S., Morimoto, K., Kato, Y., and Ogihara, T. (2011) Effect of knockdown of ezrin, radixin, and moesin on P-glycoprotein function in HepG2 cells. *J. Pharm. Sci.* **100**, 5308-5314
58. Yano, K., Tomono, T., Sakai, R., Kano, T., Morimoto, K., Kato, Y., and Ogihara, T. (2013) Contribution of radixin to P-glycoprotein expression and transport activity in mouse small intestine in vivo. *J. Pharm. Sci.* **102**, 2875-2881
59. Suda, J., Zhu, L., and Karvar, S. (2011) Phosphorylation of radixin regulates cell polarity and Mrp-2 distribution in hepatocytes. *Am J Physiol Cell Physiol* **300**, C416-424
60. Sekine, S., Ito, K., Saeki, J., and Horie, T. (2011) Interaction of Mrp2 with radixin causes reversible canalicular Mrp2 localization induced by intracellular redox status. *Biochim. Biophys. Acta* **1812**, 1427-1434

## Tables

**Table 1:** PCR oligonucleotides used in this study

Oligonucleotide	Sequence 5' → 3'
RACK1-for (SalI)	CGCCGTCGACATGACTGAGCAGATGAC
RACK1-rev (HindIII)	CTCTGCCATAAGCTTCTAGCGTGTGCCAATG
RDX-for (KpnI)	GGGTACCAATGCCGAAACCAATCAACG
RDX-rev	CAAGGTGGGATCCATTCC
delRDX-C_for	TGAGAGCTGTTATTTTGCATATATG
delRDX-C_rev	TTACAACCTGCTTCTGATGTTTCTC
NHERF-for (KpnI)	ACCCGTCGCAGGTACCGATGAGC
NHERF1-rev	GAATGCTGGATCCGCCCTGC

## FIGURES

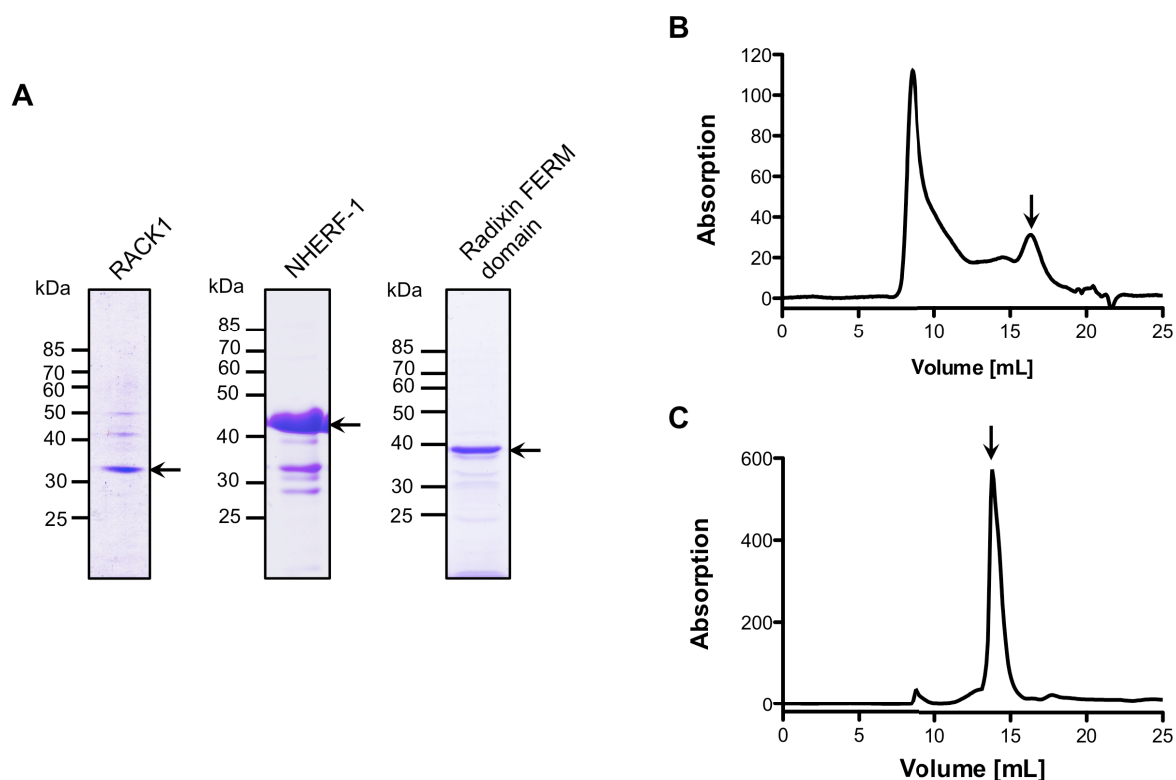


**Figure 1:** Purification of human RACK1, NHERF-1 and the FERM domain of radixin. The proteins were purified via Strep-tactin affinity chromatography and a subsequent SEC step for RACK1 and FERM domain of radixin. (A) The proteins were resolved on a 10% SDS-PAGE gel and stained with CBB. The arrows indicate the purified protein. Molecular weight markers are shown on the left. For the SEC chromatogram of (B) RACK1 and (C) the FERM domain of radixin the absorption at 280 nm in arbitrary units was plotted against the retention volume in millilitre.

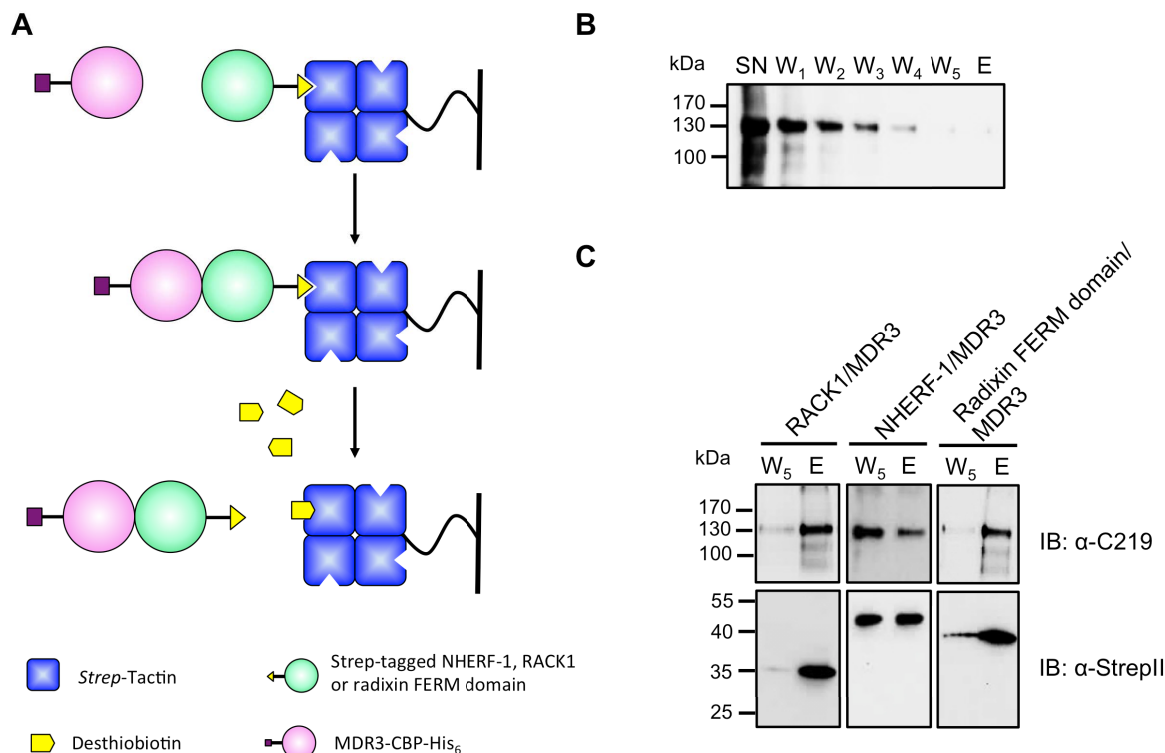


**Figure 2:** Pull-down assay of MDR3 and the scaffold proteins RACK1, the FERM domain of radixin and NHERF-1, respectively. **(A)** Scheme of the pull-down assay. In brief, the scaffold protein was immobilized on a Strep-Tactin sepharose resin and the complex was subsequently eluted with desthiobiotin. **(B)** Purified ABCB4 was used for control to estimate unspecific interactions of ABCB4 with the Strep-Tactin sepharose resin and the supernatant (SN), washing fractions (W) 1-5 and the elution fraction (E) was analyzed by SDS-PAGE and immunoblotting using C219 antibody. No ABCB4 was detected in the fourth washing (W<sub>4</sub>) and elution fraction (E). **(C)** Thus, the fifth washing fraction (W<sub>5</sub>) and the elution fraction (E) of the pull-down assays with MDR3 and RACK1, the FERM domain of radixin and NHERF-1 were analyzed by SDS-PAGE and immunoblotting using C219 antibody (upper panel) for ABCB4 and an antibody against the StrepII tag (lower panel) for the scaffold proteins.

## 4 General Discussion

The translocation of lipids from one leaflet to the other leaflet of a biological membrane is crucial for numerous cellular processes such as cell growth, cell morphology, signal transduction, apoptosis, vesicle formation in the secretory and endocytotic pathway and bile formation (9-15,134). For the secretion of bile into the biliary ducts three ATP-binding cassette (ABC) transporters are indispensable, the bile salt export pump (BSEP/ABCB11), the multidrug resistance protein 3 (MDR3/ABCB4) and the heterodimer ABCG5/G8. The main driving force of bile formation is the translocation of bile salts by BSEP (139,157). Bile salts excrete phosphatidylcholine (PC) lipids from the outer leaflet of the canalicular membrane and form mixed micelles together with cholesterol translocated by ABCG5/G8. PC lipids are translocated unidirectional from the cytoplasmic to exoplasmic leaflet of the canalicular membrane in an ATP-dependent manner by MDR3 (127,134,135,140,141). The main function of PC in bile is to reduce the detergent activity and cytotoxicity of the bile salts and consequently to protect the biliary ducts. Additionally, PC is important for cholesterol homeostasis and prevents cholesterol crystallization. Thus, dysfunction of MDR3 caused by mutations are related to different kinds of hereditary liver diseases from the range of cholesterol gallstone formation, intrahepatic cholestasis during pregnancy (ICP) to progressive intrahepatic familial cholestasis type 3 (PFIC-3) (145-148,150-152). To date, less is known about the impact of these mutations on the structure and function of MDR3. Furthermore, MDR3 shares 75% identity and more than 85% homology based on the amino acid sequences with the well-characterized multidrug resistance protein 1 (MDR1/ABCB1/P-glycoprotein) (138), but is not involved in MDR of cancer cells so far (120,181,182).

This doctoral thesis deals with the molecular *in vitro* analysis of human MDR3. First, this thesis addressed the question how lipid transport function with respect to the mechanism of the communication between the nucleotide-binding domains (NBDs) and the transmembrane domains (TMDs) and the influence of a clinical relevant mutation on a transmission interface. Secondly, the question arose whether the ATPase activity of MDR3 is modulated by the bile salt sodium taurocholate and MDR1 reversal agents, respectively. And thirdly new adaptor proteins should be identified, which are involved in the cell surface expression of MDR3. Thus, the first step was the heterologous expression of MDR3 with sufficient yields for purification and its subsequently biochemical analysis.



#### 4.1 Heterologous expression and purification of human MDR3

The main challenge to study human membrane proteins like MDR3 in its isolated form is the expression, solubilization and purification of the protein of interest in suitable amounts for structure-function analysis. In a previous doctoral thesis, it was shown that cloning and expression of *MDR3* gene in *E. coli* was not successful (163). The cDNA of *MDR3* and *BSEP* are described as unstable or toxic during cloning using conventional cloning in *E. coli* (163,183). Although *E. coli* is a well-established and widely used expression host yielding high yields of cytosolic proteins as well as membrane proteins, the expression of eukaryotic membrane proteins in a functional state is challenging due to the lack of a suitable protein processing machinery and codon usage (184-186). For example, the codon optimized gene of *BSEP* was cloned in *E. coli*, but no detectable expression was observed (187). In contrast, two human ABC transporters, MDR1 and ABCG2 (BCRP) was successfully expressed in *E. coli*, however the topology of MDR1 differed from the one expressed in cell culture systems (188,189) and ABCG2 was demonstrated to be inactive in inside-out membrane vesicles (190).

MDR3 was stably expressed in cell culture systems such as polarized pig kidney epithelial cells (LLC-PK1) and insect (*Sf9*) cells (127,143). On the contrary, Groen *et al.* reported an important cytotoxicity caused by overexpression of MDR3 in human embryonic kidney 293 cells (HEK293) and the toxicity was counteracted by coexpression of the P4-type ATPase ATP8B1-CDC50A complex (142). However, other groups did not observe this cytotoxicity (135,168). These cell culture systems have been extensively used to characterize wild type MDR3 and clinically relevant mutants with respect to *in vivo* processes like trafficking, localization and PC translocation. Although MDR1 containing membrane vesicles and purified MDR1 expressed in *Sf9* cells or HEK293 cells exhibited a significant ATPase activity, *in vitro* function of MDR3 was not observed in these systems (143,144). Furthermore, the big drawback by the use of cell culture systems is the low yield of purified protein insufficient to study the molecular mode of action of MDR3-mediated lipid translocation and ATPase activity.

An alternative to these systems is the use of yeast expression systems like *Saccharomyces cerevisiae* and *Pichia pastoris*, respectively. Yeast-based systems feature a well-established molecular biology and harbor a eukaryotic protein processing machinery. *S. cerevisiae* has been frequently used for eukaryotic membrane protein expression (191). For example, the overexpression of the pleiotropic drug resistance transporter Pdr5 and a number of membrane

proteins using the Pdr5 promotor of *S. cerevisiae* was demonstrated by our group revealing coomassie brilliant blue (CBB) stained amounts of functional protein (192).

*MDR3* was cloned via homologous recombination in *S. cerevisiae* (163), which is an efficient approach for general cloning of toxic or unstable genes of ABC transporters and was previously reported for *BSEP* (183). In addition, *MDR3* was expressed in *S. cerevisiae* to similar expression levels achieved for *MDR1* (see Chapter 2) (163,193,194). However, subcellular localization analysis showed that *MDR3* was localized not only at the plasma membrane, but also in every cell compartment of *S. cerevisiae* suggesting a mistargeting of *MDR3* caused by differences in regulation pathways of cell membrane surface expression, which results in the retention of this transporter in the ER (see Chapter 2; Figure 2). Furthermore, the purification of *MDR3* yielded 200 µg partial purified protein per litre cell culture (163). Because of the low yield of purified *MDR3*, the expression system was changed to the methylotrophic yeast *P. pastoris*. The expression rate was 10-fold higher in *P. pastoris* compared to *S. cerevisiae* (Chapter 2; Figure 1). Furthermore, the main advantage of *P.pastoris* is that it can be grown to high cell densities during fermentation yielding kilogram quantities of wet cell weights (wcw).

Chloupková *et al.* analysed 25 of 48 human ABC transporters for expression in *P. pastoris*, but *BSEP* and *MDR3* were not included in this study (195). Especially ABC transporters of the liver such as *MDR1*, *ABCG2*, *ABCG5/G8* and *ABCC1*, 3 and 6 (multidrug resistance related protein (MRP) 1, 3 and 6) could be expressed and partially purified with yields of about 1-6 mg per 100 g cells (96,195-199). Furthermore, the crystal structure of mouse *Mdr1a* was solved based on the expression in *P. pastoris* (96,136). Chapter 2 and chapter 3 of this doctoral thesis summarize the expression, localization and purification of human *MDR3*. *MDR3* was expressed in *P. pastoris* without visuable proteolytic degradation. The GFP-fusion protein of *MDR3* was properly localized at the plasma membrane suggesting that this transporter is correctly folded and targeted to the plasma membrane of *P. pastoris* (see Chapter 3; Figure 2). This result was confirmed by subcellular fractionation using wild type *MDR3* (Chapter 2; Figure 2).

The next step comprised the purification of *MDR3* in a functional state. Integral membrane proteins contain a hydrophobic transmembrane region to be located in the lipid bilayer. Thus, membrane proteins has to be extracted out of the lipid bilayer without destroying the protein structure by the use of detergents. Detergents are amphipatic molecules with a hydrophilic head group and a hydrophobic tail. The gernerall physical properties of detergents based on

the alkyl chain length, critical micellar concentration (cmc) and the charge of the polar hydrophilic head group. Detergents are classified into four main groups according to the charge of the head group: anionic, cationic, zwitterionic and neutral. Above their cmc detergents form micelles and destabilize membrane integrity. Membrane proteins can insert into these micelles by hydrophobic interaction allowing the membrane protein to be stable in the solvent environment. In detergent micelles membrane proteins adopt multiple conformations due to the divergent lateral pressure and relatively low structural order and tend to denature or lose their activity during solubilization process (200). Thus, the preservation of the native and functional membrane protein is a challenging process and there are no general rules for selection of an appropriate detergent.

High throughput screenings (HTS) have been developed in order to screen the influence of detergents on stability and monodispersity of the membrane protein (201-206). One of these methods is the fluorescence-detected size exclusion chromatography (FSEC), which based on the fluorescence of the green fluorescent protein (GFP) fused to the protein of interest (207). With FSEC the monodispersity of GFP-fusion membrane proteins in detergent solution can be observed without the need of purification. Over 100 different detergents were analyzed using dot blot technique with respect to extract MDR3 from membrane vesicles (Chapter 3; Figure 3). Unexpectedly, exclusively zwitterionic detergents of the fos-choline series with long acyl chains were able to solubilize MDR3 from *P. pastoris* membrane vesicles. This was also observed for numerous other membrane proteins where only fos-cholines facilitated the solubilization (208-210). For instance, the lipid floppase ABCA4 (ABCR) was only extracted from insect cell membranes by long-chain fos-cholines and in the presence of reducing agents (210). In contrast, MDR1 was solubilized from *P. pastoris* membranes in various detergents including  $\beta$ -DM,  $\beta$ -DDM, Lyso-PC, deoxycholic acid or Triton-X100 (96,199,211-213). The heterodimeric ABCG5/G8 as well as ABCG2 was solubilized in  $\beta$ -DDM, but ABCG2 could only be solubilized in fos-choline-16 (FC-16) when expressed in High Five insect cells (198,214,215).

FSEC analysis of the GFP-fusion protein of MDR3 solubilized in fos-choline series demonstrated an increased monodispersity, for longer the acyl chain and the best result in terms of monodispersity of MDR3 was obtained in fos-choline-16 (Chapter 2; Figure 4). Fos-choline-16 is a lipid-like zwitterionic detergents and were demonstrated to reduce the ATPase activity of the ABC transporter LmrA from *Lactococcus lactis* in contrast to  $\beta$ -DDM (216), which is a harm detergent and often used for crystallization. A disadvantage of FC-16 is that

it has a low cmc, which makes it difficult to be removed during reconstitution as it was observed for LmrA from *L. lactis* (216).

To date, a number of purification systems are available allowing the rapid and simple purification of proteins. The most common system is the affinity chromatography using affinity tags genetically fused to the protein of interest. After the successful extraction of MDR3 using FC-16, a tandem-affinity purification was established. The tandem affinity purification was composed of an immobilized metal ion affinity chromatography (IMAC) following by a calmodulin-binding peptide (CBP) affinity purification yielding amounts of approximately 6 mg wild type MDR3 per 100 g wet cell weight (wcw) with high homogeneity (>90%) (Chapter 3: Figure 5). The lower yield and purity of the MDR3 mutants generated in this thesis (Walker B mutant (EQ/EQ): 3.4 mg/100 g wcw; Q1174E mutant: 2.1 mg/100 g wcw) compared to the wild type floppase was due to the reduced expression levels of the mutants in *P. pastoris*, but lower integration numbers of the gene expression cassette into the target chromosome could not be excluded (Chapter 4; Figure 1 and Table 1). The tandem affinity purification was also applied for the purification of the human liver ABC transporters ABCG5/G8, ABCC3, MDR1 and BSEP resulting in similar yields of purified protein (187,195-199,217).

Beside the appropriate choice of detergent for solubilization, monodispersity of the purified protein is important to maintain a native and functional protein. To improve the monodispersity of MDR3 additives such as cyclodextrins and glycerol were tested during purification. The addition of cyclodextrins should remove excess of FC-16 bound to MDR3 resulting in an increased monodispersity of MDR3. However only slight improvement of the monodispersity was demonstrated (Chapter 2; Figure 7). The presence of glycerol generates a more native environment for membrane proteins by reducing the concentration of water and increasing the hydrophobicity (218) and increased the monodispersity of MDR3 (Chapter 2; Figure 5 B).

Taken together, for the first time the expression of human MDR3 in *P. pastoris* and its correct targeting to the plasma membrane was demonstrated. Subsequently, a purification procedure for MDR3 could be established yielding highly pure protein in amounts sufficient for the molecular analysis of MDR3.

## 4.2 Functional analysis of MDR3

The next step was the functional analysis of purified MDR3. Chapter 1 summarizes three different approaches to study protein-mediated lipid translocation across membranes based on short-chain lipids containing a spin-, fluorescent- or radiolabel. Briefly, short-chain lipids are integrated into the surface of the membrane and transport can be measured by chemically quenching of the label or extracted by use of bovine serum albumin (BSA) (127,219,220). In contrast, up to date a sensitive and easy-handle method to analyse the transport of endogenous lipids is not available. Giant unilamellar vesicles (GUVs) represents a potential tool for the visualization of lipid translocation and to determine kinetic parameters of the protein-mediated flip-flop (221-224). The flip-flop mediated by lipid translocators incorporated into GUVs lead to an insertion of the lipids in one of the leaflet generating an area difference between the two leaflets. The shape change in GUVs can be observed with an optical microscope. For the first time, this technique was used to demonstrate the flippase activity of yeast ER flippase (221). Recently, it was shown that the bacterial ABC transporter BmrC/BmrD transport drugs and encapsulated DNA incorporated into GUVs (225). These findings reveal GUVs as forward-looking tool to study the transport mechanism of ABC transporters.

ABC transporters are primary active transporters and exhibit besides the transport function an ATPase activity. The release of inorganic phosphate can be determined and correlates indirectly with substrate transport (see chapter 1). In ABC transporters, binding of the substrate to the TMD typically stimulates ATP hydrolysis at the NBDs and has been reported for several ABC transporters (113,195,197,214,226). In chapter 3, the substrate-induced ATPase activity of wild type MDR3 was shown for the first time. Since co-purified contaminating ATPases cannot be ruled out, an ATPase-deficient mutant (E558Q, E1207Q, further called EQ/EQ mutant) was generated by introducing two point mutations into the highly conserved Walker B motif. The exchange of Glu to Gln in the Walker B motif of MDR3 prevented ATP hydrolysis in both nucleotide-binding sites (NBS) and abolished MDR3-mediated PC translocation (142). The ATPase activity of MDR3 was approximately 2.5-fold stimulated in the presence PC lipids, while the EQ/EQ mutants exhibit not stimulation (Chapter 3; Figure 5). However, basal ATPase activity of MDR3 could not be observed due to co-purified contaminating ATPases. Thus, wild type MDR3 and mutants were crosslinked with the thiol-reactive fluorophore maleimide-bodipy. This abolished the basal and PC-induced ATPase activity of MDR3 as demonstrated for MDR1 (227-229) (Chapter 4; Figure 1). In addition, the FC-16 amount had a drastically effect on the ATPase

activity of MDR3 and the reduction of the FC-16 amount during purification increased the MDR3 ATPase activity sixfold (Chapter 4).

Chapter 4 of this thesis focused on the characterization of the ATPase activity of purified MDR3. In a first step, the Michaelis-Menten constant ( $K_M$ ) and the maximal ATPase activity ( $v_{max}$ ) of wild type MDR3 and labeled MDR3 were determined in the absence and presence of DOPC lipids (Chapter 4; Figure 1 and Table 1). The substrate-induced ATPase activity of MDR3 was about 9-fold lower than the ATPase activity of detergent-soluble mouse and human MDR in the presence of verapamil and lipids (199,226), but comparable to the substrate-induced ATPase activity of the chimera protein composed of MDR1 TMDs and MDR3 NBDs (MDR1/3) (144). Similar results were demonstrated for human ABCC3 and ABCG5/G8 (195,197). Although MDR1 and MDR3 exhibited different maximal ATPase activities in the presence of the substrate, both proteins have high  $K_M$  values for ATP, which were in a range typical for ABC transporters (195,197,226,230).

In a second step, an unspecific increase of ATPase activity caused by lipids was excluded and on the other hand the substrate spectrum of MDR3 was analyzed. Lipids led to a stabilizing effect on the conformation of the ABC transporter as shown for MDR1, ABCC3, TAP1/2 and ABCA4 (195,199,210,231,232). However, PC lipids specifically stimulated MDR3 ATPase activity, while brain PE, DOPE, PS and SM lipids did not induce any significant stimulation (Chapter 4: Figure 2). This led to the conclusion that MDR3 flops exclusively phospholipids with a choline head group, which is in good agreement with previous studies of MDR3 and the mouse homolog Mdr2 (127,135,140,141). For the first time, the kinetic parameters of the ATPase activity of MDR3 in dependence of liver PC and DOPC lipids was demonstrated (Chapter 4: Figure 2 and Table 2). Both kinds of lipids stimulated the ATPase activity in a concentration dependent manner with similar maximal ATPase activity and  $K_M$  values of  $109.8 \pm 5.9 \text{ nmol min}^{-1} \text{ mg}^{-1}$  and  $16.63 \pm 2.6 \text{ } \mu\text{M}$  for liver PC lipids and  $84.0 \pm 3.4 \text{ nmol min}^{-1} \text{ mg}^{-1}$  and  $11.97 \pm 1.6 \text{ } \mu\text{M}$  for DOPC lipids, respectively. The low turnover number and the low affinity of MDR3 ( $0.23 \pm 0.03 \text{ lipids per s}$ ) is consistent with the proposed model of Ishigami *et al.* (144). They demonstrated that MDR3 NBDs hydrolyze ATP more than 10-times slower than MDR1 NBDs using a purified chimera protein MDR1/3 and suggested that MDR3 is a low affinity transporter optimized for PC translocation (144).

In addition, the presence of the bile salt sodium taurocholate below the cmc (2.5 mM) induced a 7.5-fold stimulation of the ATPase activity of MDR3 (Chapter 5; Figure 1). Previous studies revealed that PC secretion by MDR3 was concentration-dependent on bile salts, while MDR1

was not affected (135). These results suggested that bile salts might assist PC translocation by directly acceptance of PC from MDR3 as proposed in the activated model for ABC transporter mediated lipid translocation (see Chapter 1.5) (233).

### **4.3 The X-loop of MDR3 – coupling the engine to the gate**

ABC transporters are composed of two domains, the nucleotide-binding domain (NBD) and the transmembrane domain (TMD). The NBDs were shown to convert the chemical energy of binding and hydrolysis of ATP to mechanical energy, whereas the TMDs form the translocation pathway and provide the substrate specificity (65,95-97). These two processes have to be coupled to facilitate substrate transport. Based on structural and biochemical analysis, it is known that ATP-induced dimerization of the NBDs generates a molecular motion (78,81,82), which is transmitted to the TMDs via non-covalent interactions (69,71,72). The TMD of ABC exporters contain two coupling helices. Because of the domain swapped arrangement of the TMD, each coupling helix interact with one NBD allowing a tight communication between NBDs and TMDs (71,72,96,98-100,136).

To date, two conserved motifs of the NBD are identified to be involved in the transmission interface, the Q-loop and the X-loop of ABC exporters (72,105,108,109). Mutational analysis and crosslinking studies of ABC importers and ABC exporters such as MaleFGK, CFTR and MDR1 demonstrated that the Q-loop interacts with the coupling helix, which are located in a groove of the NBD allowing the transmission of the conformational changes induced by ATP binding and hydrolysis to the TMD (106-108,234). In contrast, only ABC exporters contain a structurally diverse region (SDR) comprising the X-loop (TEVGERG), which is located in direct proximity of the ABC signature motif (C-loop) (71,72,78).

In chapter 4 the molecular function of the extended X-loop mutation Q1174E of NBD2, which was identified in a patient with PFIC-3 (235), was investigated. Immunostaining of the patient's liver biopsy and MDR3-transfected HEK293 cells showed that the Q1174E mutant was properly folded and localized at the canalicular and plasma membrane, respectively (Chapter 4; Figure 4). This indicated a drastic functional defect of MDR3. The Q1174E mutant was expressed in *P. pastoris* and purified with the same procedure as reported for wild type MDR3. The detergent-soluble Q1174E mutant exhibited no PC-induced, but basal ATPase activity (Chapter 4; Figure 6) suggesting that NBDs were uncoupled from TMDs in this mutated floppase.

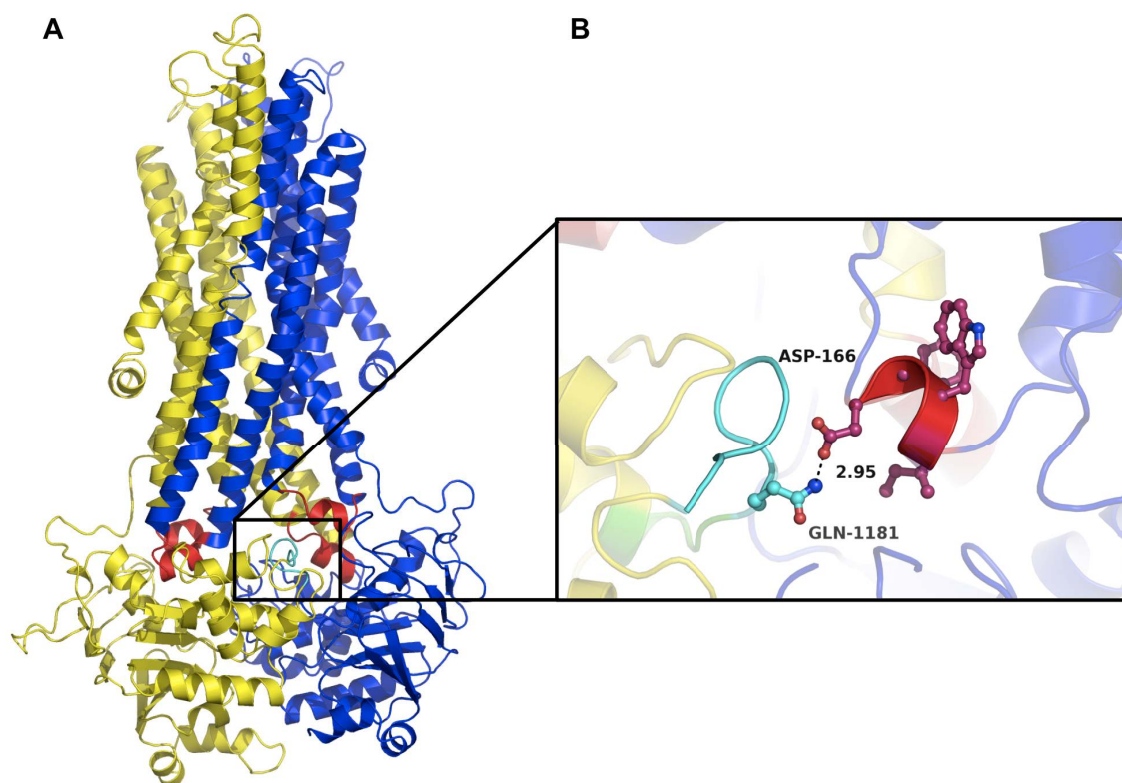


**Figure 13** Transmission interface of MDR3. **A)** Model of human MDR3 based on the structure of Sav1866 (PDB entry 2HYD) (72) and the amino acid sequence of isoform B of MDR3 (145). One transporter half is shown in blue and the second in yellow. The coupling helices are highlighted in red and the X-loop is colored in cyan. **B)** Close up view of the interface between TMD1 and NBD2. Gln1174 of the isoform A (Gln1181 of the isoform B) is shown in stick representation (cyan). Figure adapted from chapter 4.

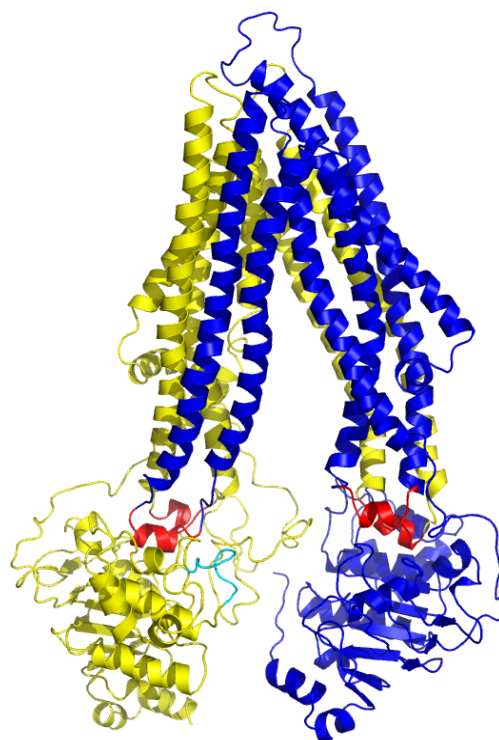


**Figure 14** Model of human MDR3 based on the structure of mouse Mdr1a (PDB entry 4M1M) (96,136) and the amino acid sequence of isoform B of MDR3. The structure is colored as described in figure legend 13.



A homology model of wild type MDR3 and the Q1174E mutant was generated based on the structure of the MDR-mediating transporter Sav1866 (72) and the isoform B of MDR3 (Figure 13). The isoform B contains seven additional amino acids within the NBD2 compared to the major isoform A, which was used in the experiments. The glutamine of isoform A at position 1174 and of isoform B at position 1181 did not differ in the homology model of NBD2 (Chapter 4; Figure 5). More considerable the glutamine at position 1174 (1181 in isoform B) of NBD2, which is located next to the leucine of the ABC signature motif, contacts the aspartate 166 of the first intracellular loop (ICL1) of the opposing TMD (Figure 13). No high conformational rearrangement was observed for the substitution of the glutamine to glutamate within the homology model of MDR3, but the amino acid change would prohibit the hydrogen bonding between Gln1174 and Asp166. Thus, it is likely that the conformational changes by binding the substrate to the TMD was not transmitted to the ABC signature motif of NBD2 suggesting a pivotal role of Glu1174 in communication between NBD and TMD. Furthermore, this interaction occurs only in the outward-facing conformation of MDR3 indicating that the X-loop plays an important role in the formation of the outward-facing conformation of human MDR3 (Figure 14).

This is in good agreement with structural and biochemical analysis of Sav1866 from *S. aureus*, human TAP1/2 (ABCB2/B3) and CFTR (ABCC7) (72,109,110) and molecular dynamics (MD) simulation of human MDR1 (236). The substitution of the conserved glutamate (E602) of the X-loop of TAP1/2 did not effect peptide binding, however transport activity was reduced from 20% for the E602D mutant to complete disruption for the E602R mutant. In addition, cross-linking studies of CFTR identified that the coupling helices of the TMDs contacts the X-loops and the Q-loops of the NBDs and were involved in channel gating (110). Chang *et al.* modeled the structure of human MDR1A based on mouse Mdr1a and investigated the transmission interface between NBDs and TMDs (236). They demonstrated that the amino acid residue Q1175 of NBD2, which is identical to Q1174 in MDR3, hydrogen bond with D164 (D166 in MDR3) of the ICL1 and identified this residue pair D164-Q1175 as key residue pair in the transmission interface (236).

In conclusion, these data strongly suggest that the Q1174E mutation severely impaired the crosstalk between the extended X-loop of NBD2 and the coupling helix of TMD1 resulting in a nonfunctional transporter.

#### 4.4 MDR3 – a multidrug pump?

MDR3 was classified as multidrug resistance (MDR) transport on the basis of the amino acid sequence similarity of 86% to the MDR-mediating transporter MDR1 (138). However, initial studies with MDR3-transfected cells showed no MDR phenotype (138,181,237). Recently, MDR3 gene products were found in paclitaxel-, doxorubicin- and vincristine-resistant cell lines, indicating that MDR3 might be involved in multidrug resistance (238). Although the transport rate was low for most MDR1 reversal agents, Smith *et al.* demonstrated directional transport of digoxin, paclitaxel, daunorubicin, ivermectin and vinblastine through MDR3-transfected LLC-PK1 cells (143). No significant transport of other MDR1 substrates, such as cyclosporin A and dexamethasone, was shown.

Chapter 5 of this thesis studied the modulation of the ATPase activity of MDR3 by MDR1 reversal agents. None of the tested drugs stimulated the ATPase activity of MDR3. Contrary, itraconazole, zosuquidar, cyclosporin A, verapamil and paclitaxel completely abolished the ATPase activity of detergent-soluble MDR3 in the micromolar range (Chapter 5; Figure 3 and Figure 4). The ATPase activity of MDR3 was only slightly inhibited in the presence of vinblastine and rifampicin and no change of ATP hydrolysis was demonstrated for digoxin. These data are in agreement with vanadate-dependent ATP trapping of MDR3 expressed in *Sf9* cells. Paclitaxel, vinblastine, verapamil, cyclosporin A and valspodar abolished vanadate-dependent ATP trapping, while ATP trapping of MDR1 was greatly stimulated (143). Several studies demonstrated that the MDR3-mediated translocation of endogenous PC, fluorescently-labeled short-chain PC (C<sub>6</sub>-NBD-PC) or digoxin was inhibited by itraconazole, cyclosporin A and verapamil (127,135,143,146,220,239). Consistently, the substrate-induced and the basal ATPase activity of MDR1 was inhibited by cyclosporin A (240-243) and bile salt translocation in *Sf9* membrane vesicles mediated by BSEP was inhibited by cyclosporin A with an IC<sub>50</sub> value of  $4.6 \pm 1.2 \mu\text{M}$  (244), which is similar to that demonstrated for MDR3 (Chapter 5; Table 1).

Furthermore, the amino acid residues, which form the drug-binding site (245-251), was conserved between MDR1 and MDR3 suggesting that both transporter contain similar substrate-binding sites and recognize similar substrates. However, ATPase activity of human MDR1 was 30-fold stimulated in the presence of verapamil indicating that verapamil is a MDR1 substrate, but an inhibitor of MDR3. The most divergent residues were located in TMH1 at the border of the cytosolic leaflet of the membrane, which might be involved in the interaction of the polar head group of the preferred substrate PC. These results suggest that

MDR3 is not specific for PC and binds various typical MDR1 reversal as well. However, why does drug binding inhibited ATPase activity, while the ATPase activity of MDR1 was stimulated? Currently, there is no satisfactory explanation. The cholesterol fill-in theory tries to explain how an ABC transporter can transport various distinct substrates with the same binding site by the use of cholesterol (252). Cholesterol binds to various ABC transporter (253,254). For example, for MDR1 the binding affinity of small substrates ranging from a molecular weight of 350 to 500 was increased in the presence of 20% cholesterol, while the binding affinity of substrates with a molecular weight between 800 and 900 was hardly affected by cholesterol (253). Furthermore, depletion of membrane cholesterol significantly reduced the MDR1-mediated transport activity (255,256). It was assumed that cholesterol fills the empty space in the binding cavity and forms the the substrate-binding site capable of binding individual substrates (252).

#### **4.5 Intracellular traffic and its role in MDR3 function**

Dysfunction of MDR3 are associated with different kinds of hereditary liver diseases from the range of cholesterol gallstone, low phospholipid associated cholelithiasis (LPAC) to progressive familial intrahepatic cholestasis type 3 (PFIC-3). Dysfunction are caused by three different kinds of MDR3 mutations resulting in truncated proteins by stop codon mutation, splicing mutations affecting the correct splicing (257) and missense mutations by amino acid substitution (139,146,151). On the one hand missense mutations within the *MDR3* gene can abolish the ATPase activity or PC transport due to amino acid substitution in structural essential sequences. For example, the mutations of the H-loop of NBD2 is suggested to be crucial for ATPase activity and leads to PFIC-3 in patients (145). On the other hand defects of the regulation pathway results in a non-functional transporter by improper targeting to the canalicular membrane. Phosphorylation appear to be one regulation mechanism of MDR3 function. The mutation T34M and R47G impaired MDR3 phosphorylation and reduce the PC translocation, while the mutants were proper localized at the plasma membrane (168). Not only truncated proteins but also missense mutations of MDR3 are associated with the absence of MDR3 at the canalicular membrane and lead to the retention of MDR3 in the ER (258,259). For example, the S320F translocated PC comparable to wild type MDR3, but expression at the plasma membrane was reduced to 50%, which could be rescued with the chemical chaperone cyclosporin A (146). Thus, the canalicular localization of MDR3 is indispensable for executing its function.

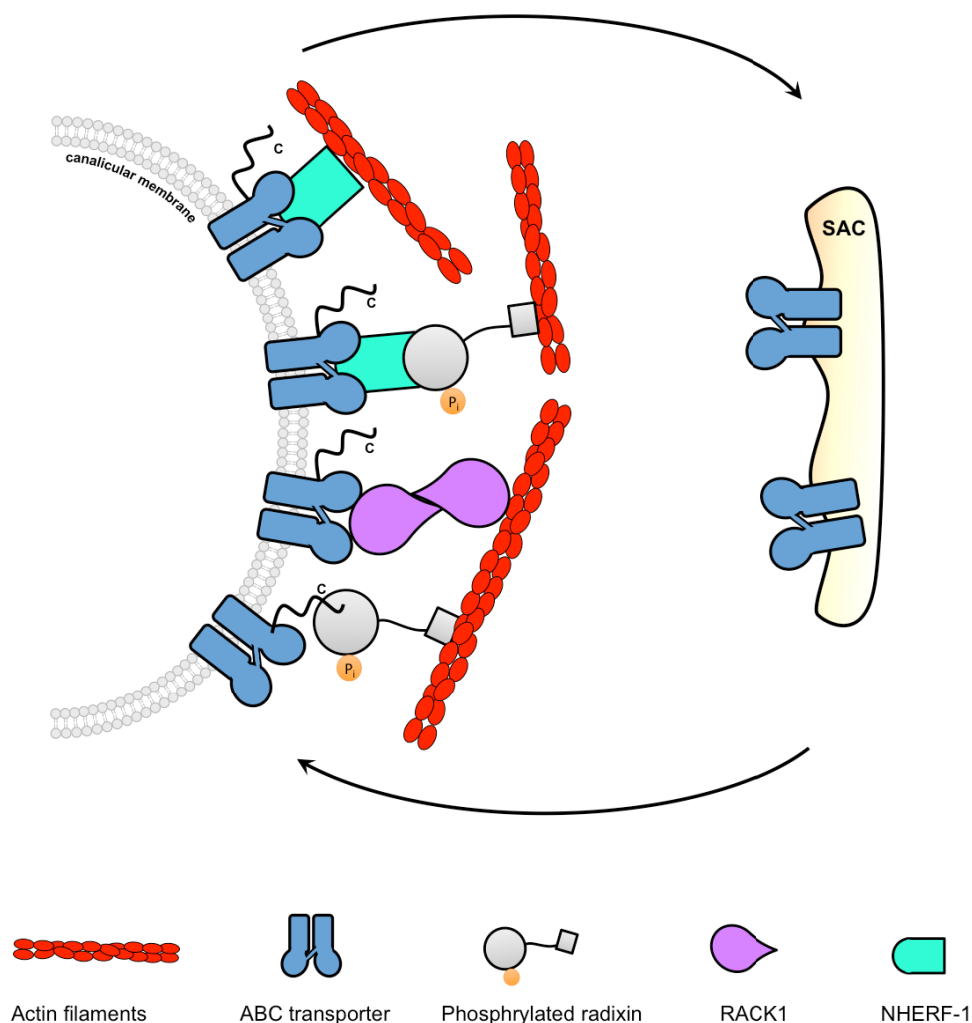


**Figure 15** Adapter proteins of MDR3 mediating the interaction of MDR3 with the cytoskeleton. SAC = subapical compartment.

Previously, the receptor for activated C-kinase 1 (RACK1) was demonstrated to mediate the stable expression of MDR3 at the plasma membrane and down-regulation reduced MDR3-mediated PC translocation (260), however no interaction of full-length MDR3 and RACK1 by co-immunoprecipitation was obtained. For the first time, the interaction of functionally full-length MDR3 and RACK1 was demonstrated using *in vitro* pull down assay (Chapter 5; Figure 2). In chapter 5 of this doctoral thesis radixin was identified as new adapter protein of human MDR3 and were suggested to facilitate MDR3-cytoskeletal interaction. Based on the evidences obtained in this doctoral thesis and for the ABC transporters CFTR, ABCC2 (MRP2), ABCC4 (MRP4), ABCG2 and MDR1 (ABCB1) a scheme of MDR3 cell surface expression at the canalicular membrane was proposed (Figure 15). To date, it has been elucidated that RACK1 mediates the stable expression of MDR3, ABCG2 and CFTR at the

canalicular membrane (260-262), but the cellular localization of the highly homologous MDR1 was not affected by RACK1 (260). This suggested that MDR3 and MDR1 possess different mechanism of cell surface expression.

The PDZ domain of NHERF-1 was demonstrated to recognize the last three amino acids of the C-terminus of CFTR, which is crucial for CFTR localization (263-266), while the ezrin-radixin-moesin (ERM)-binding (EB) domain interacts with the cytoskeleton linker protein such as radixin or directly with the apical cytoskeleton. Recently, it was shown that the PDZ-like motif at the C-terminus of ABCC6 is essential for trafficking and localization of ABCC6 (267). The C-terminus of MDR3 ends by a PDZ-like binding motif. Thus, it would be likely that NHERF-1 interact with these motif. However, the binding site of NHERF-1 in MDR3 remains to be elucidated. Furthermore, the PDZ domain of the NHERF-1 binds the cytoplasmic domain of ABCC2 and ABCC4, (263,268-270). In NHERF-1 knock-out mice of, ABCC2 expression was reduced at the apical membrane of hepatocytes (270). In contrast, ABCC4 cell surface expression and function was increased in polarized kidney cells by down-regulation of NHERF-1 (268,269).

Radixin is mainly located at the canalicular membrane in hepatocytes and is essential for maintaining the polarized targeting and retention of ABC transporters localized at the canalicular membrane (271). Radixin was shown to bind MDR1 and to be crucial for the retention of MDR1 at the plasma membrane (272). The down-regulation of radixin in HepG2 cells lead to an decrease of MDR1 at the plasma membrane with consistent expression in whole cell lysate (273) and in radixin knock-out mice, radixin regulates the localization of MDR1 in the small intestine (274). Furthermore, these mice develop conjugated hyperbilirubinemia because of their impaired ability to localize ABCC2 at the canalicular membrane (275). It was demonstrated that the phosphorylation status of radixin regulates the canalicular ABCC2 localization (276). Radixin is activated by phosphorylation at the C-terminal domain by the protein kinase C (PKC) (277,278).

In conclusion, RACK1 and the FERM domain of radixin was demonstrated to interact with full-length MDR3 *in vitro*. This suggested that MDR3 cell surface expression at the canalicular membrane is tightly regulated by a complex mechanism containing RACK1 and radixin. For the first time, this study might provide the foundation to investigate the regulation mechanism of MDR3 function and might facilitate new therapeutic perspectives.

## 5 Literature

1. Singer, S. J., and Nicolson, G. L. (1972) The fluid mosaic model of the structure of cell membranes. *Science* **175**, 720-731
2. Jain M. K., and Wagner R. C. (1988) Introduction to Biological Membranes, *Wiley*
3. Vereb, G., Szollosi, J., Matko, J., Nagy, P., Farkas, T., Vigh, L., Matyus, L., Waldmann, T. A., and Damjanovich, S. (2003) Dynamic, yet structured: The cell membrane three decades after the Singer-Nicolson model. *Proc. Natl. Acad. Sci. U. S. A.* **100**, 8053-8058
4. Pichler, H., and Riezman, H. (2004) Where sterols are required for endocytosis. *Biochim. Biophys. Acta* **1666**, 51-61
5. van Meer, G., Voelker, D. R., and Feigenson, G. W. (2008) Membrane lipids: where they are and how they behave. *Nat Rev Mol Cell Biol* **9**, 112-124
6. Devaux, P. F. (1991) Static and dynamic lipid asymmetry in cell membranes. *Biochemistry* **30**, 1163-1173
7. Bretscher, M. S. (1972) Asymmetrical lipid bilayer structure for biological membranes. *Nat New Biol* **236**, 11-12
8. Verkleij, A. J., Zwaal, R. F., Roelofsen, B., Comfurius, P., Kastelijn, D., and van Deenen, L. L. (1973) The asymmetric distribution of phospholipids in the human red cell membrane. A combined study using phospholipases and freeze-etch electron microscopy. *Biochim. Biophys. Acta* **323**, 178-193
9. Balasubramanian, K., and Schroit, A. J. (2003) Aminophospholipid asymmetry: A matter of life and death. *Annu. Rev. Physiol.* **65**, 701-734
10. Devaux, P. F. (2000) Is lipid translocation involved during endo- and exocytosis? *Biochimie* **82**, 497-509
11. Graham, T. R. (2004) Flippases and vesicle-mediated protein transport. *Trends Cell Biol.* **14**, 670-677
12. Verkleij, A. J., and Post, J. A. (2000) Membrane phospholipid asymmetry and signal transduction. *J. Membr. Biol.* **178**, 1-10
13. Sprong, H., van der Sluijs, P., and van Meer, G. (2001) How proteins move lipids and lipids move proteins. *Nat Rev Mol Cell Biol* **2**, 504-513
14. Bevers, E. M., Comfurius, P., and Zwaal, R. F. (1983) Changes in membrane phospholipid distribution during platelet activation. *Biochim. Biophys. Acta* **736**, 57-66
15. Krahling, S., Callahan, M. K., Williamson, P., and Schlegel, R. A. (1999) Exposure of phosphatidylserine is a general feature in the phagocytosis of apoptotic lymphocytes by macrophages. *Cell Death Differ.* **6**, 183-189
16. Berg J.M. , T. J. L., Stryer L. (2002) Lipids and Many Membrane Proteins Diffuse Rapidly in the Plane of the Membrane. in Biochemistry (WH, F. ed.), *Spectrum*
17. Edidin, M., Zuniga, M. C., and Sheetz, M. P. (1994) Truncation mutants define and locate cytoplasmic barriers to lateral mobility of membrane glycoproteins. *Proc. Natl. Acad. Sci. U. S. A.* **91**, 3378-3382
18. Jacobson, K., Elson, E., Koppel, D., and Webb, W. (1982) Fluorescence photobleaching in cell biology. *Nature* **295**, 283-284
19. Devaux, P., and McConnell, H. M. (1972) Lateral diffusion in spin-labeled phosphatidylcholine multilayers. *J. Am. Chem. Soc.* **94**, 4475-4481
20. Kornberg, R. D., and McConnell, H. M. (1971) Inside-outside transitions of phospholipids in vesicle membranes. *Biochemistry* **10**, 1111-1120

21. Morrot, G., Herve, P., Zachowski, A., Fellmann, P., and Devaux, P. F. (1989) Aminophospholipid translocase of human erythrocytes: phospholipid substrate specificity and effect of cholesterol. *Biochemistry* **28**, 3456-3462
22. Contreras, F. X., Sanchez-Magraner, L., Alonso, A., and Goni, F. M. (2010) Transbilayer (flip-flop) lipid motion and lipid scrambling in membranes. *FEBS Lett.* **584**, 1779-1786
23. Pohl, A., Devaux, P. F., and Herrmann, A. (2005) Function of prokaryotic and eukaryotic ABC proteins in lipid transport. *Biochim. Biophys. Acta* **1733**, 29-52
24. Pomorski, T., and Menon, A. K. (2006) Lipid flippases and their biological functions. *Cell, Mol. Life Sci.* **63**, 2908-2921
25. Chang, Q. L., Gummadi, S. N., and Menon, A. K. (2004) Chemical modification identifies two populations of glycerophospholipid flippase in rat liver ER. *Biochemistry* **43**, 10710-10718
26. Menon, A. K. (1995) Flippases. *Trends Cell Biol.* **5**, 355-360
27. Kol, M. A., de Kroon, A. I., Killian, J. A., and de Kruijff, B. (2004) Transbilayer movement of phospholipids in biogenic membranes. *Biochemistry* **43**, 2673-2681
28. Bishop, W. R., and Bell, R. M. (1985) Assembly of the endoplasmic reticulum phospholipid bilayer: the phosphatidylcholine transporter. *Cell* **42**, 51-60
29. Hrafnisdottir, S., Nichols, J. W., and Menon, A. K. (1997) Transbilayer movement of fluorescent phospholipids in *Bacillus megaterium* membrane vesicles. *Biochemistry* **36**, 4969-4978
30. Hrafnisdottir, S., and Menon, A. K. (2000) Reconstitution and partial characterization of phospholipid flippase activity from detergent extracts of the *Bacillus subtilis* cell membrane. *J. Bacteriol.* **182**, 4198-4206
31. Buton, X., Herve, P., Kubelt, J., Tannert, A., Burger, K. N., Fellmann, P., Muller, P., Herrmann, A., Seigneuret, M., and Devaux, P. F. (2002) Transbilayer movement of monohexosylsphingolipids in endoplasmic reticulum and Golgi membranes. *Biochemistry* **41**, 13106-13115
32. Gummadi, S. N., and Menon, A. K. (2002) Transbilayer movement of dipalmitoylphosphatidylcholine in proteoliposomes reconstituted from detergent extracts of endoplasmic reticulum. Kinetics of transbilayer transport mediated by a single flippase and identification of protein fractions enriched in flippase activity. *J. Biol. Chem.* **277**, 25337-25343
33. Sahu, S. K., Gummadi, S. N., Manoj, N., and Aradhyam, G. K. (2007) Phospholipid scramblases: an overview. *Arch. Biochem. Biophys.* **462**, 103-114
34. Smeets, E. F., Comfurius, P., Bevers, E. M., and Zwaal, R. F. (1994) Calcium-induced transbilayer scrambling of fluorescent phospholipid analogs in platelets and erythrocytes. *Biochim. Biophys. Acta* **1195**, 281-286
35. Williamson, P., Bevers, E. M., Smeets, E. F., Comfurius, P., Schlegel, R. A., and Zwaal, R. F. (1995) Continuous analysis of the mechanism of activated transbilayer lipid movement in platelets. *Biochemistry* **34**, 10448-10455
36. Axelsen, K. B., and Palmgren, M. G. (1998) Evolution of substrate specificities in the P-type ATPase superfamily. *J. Mol. Evol.* **46**, 84-101
37. Palmgren, M. G., and Nissen, P. (2011) P-type ATPases. *Annu Rev Biophys* **40**, 243-266
38. Lopez-Marques, R. L., Poulsen, L. R., Bailly, A., Geisler, M., Pomorski, T. G., and Palmgren, M. G. (2014) Structure and mechanism of ATP-dependent phospholipid transporters. *Biochim. Biophys. Acta*
39. Paulusma, C. C., Folmer, D. E., Ho-Mok, K. S., de Waart, D. R., Hilarius, P. M., Verhoeven, A. J., and Oude Elferink, R. P. (2008) ATP8B1 requires an accessory

- protein for endoplasmic reticulum exit and plasma membrane lipid flippase activity. *Hepatology* **47**, 268-278
40. Noji, T., Yamamoto, T., Saito, K., Fujimura-Kamada, K., Kondo, S., and Tanaka, K. (2006) Mutational analysis of the Lem3p-Dnf1p putative phospholipid-translocating P-type ATPase reveals novel regulatory roles for Lem3p and a carboxyl-terminal region of Dnf1p independent of the phospholipid-translocating activity of Dnf1p in yeast. *Biochem. Biophys. Res. Commun.* **344**, 323-331
  41. Saito, K., Fujimura-Kamada, K., Furuta, N., Kato, U., Umeda, M., and Tanaka, K. (2004) Cdc50p, a protein required for polarized growth, associates with the Drs2p P-type ATPase implicated in phospholipid translocation in *Saccharomyces cerevisiae*. *Mol. Biol. Cell* **15**, 3418-3432
  42. Ujhazy, P., Ortiz, D., Misra, S., Li, S., Moseley, J., Jones, H., and Arias, I. M. (2001) Familial intrahepatic cholestasis 1: studies of localization and function. *Hepatology* **34**, 768-775
  43. Bull, L. N., van Eijk, M. J., Pawlikowska, L., DeYoung, J. A., Juijn, J. A., Liao, M., Klomp, L. W., Lomri, N., Berger, R., Scharschmidt, B. F., Knisely, A. S., Houwen, R. H., and Freimer, N. B. (1998) A gene encoding a P-type ATPase mutated in two forms of hereditary cholestasis. *Nat. Genet.* **18**, 219-224
  44. Klomp, L. W., Vargas, J. C., van Mil, S. W., Pawlikowska, L., Strautnieks, S. S., van Eijk, M. J., Juijn, J. A., Pabon-Pena, C., Smith, L. B., DeYoung, J. A., Byrne, J. A., Gombert, J., van der Brugge, G., Berger, R., Jankowska, I., Pawlowska, J., Villa, E., Knisely, A. S., Thompson, R. J., Freimer, N. B., Houwen, R. H., and Bull, L. N. (2004) Characterization of mutations in ATP8B1 associated with hereditary cholestasis. *Hepatology* **40**, 27-38
  45. Paulusma, C. C., Groen, A., Kunne, C., Ho-Mok, K. S., Spijkerboer, A. L., Rudi de Waart, D., Hoek, F. J., Vreeling, H., Hoeven, K. A., van Marle, J., Pawlikowska, L., Bull, L. N., Hofmann, A. F., Knisely, A. S., and Oude Elferink, R. P. (2006) Atp8b1 deficiency in mice reduces resistance of the canalicular membrane to hydrophobic bile salts and impairs bile salt transport. *Hepatology* **44**, 195-204
  46. Vazquez de Aldana, C. R., Marton, M. J., and Hinnebusch, A. G. (1995) GCN20, a novel ATP binding cassette protein, and GCN1 reside in a complex that mediates activation of the eIF-2 alpha kinase GCN2 in amino acid-starved cells. *EMBO J.* **14**, 3184-3199
  47. Hirano, T. (2006) At the heart of the chromosome: SMC proteins in action. *Nat Rev Mol Cell Biol* **7**, 311-322
  48. Hopfner, K. P., Karcher, A., Shin, D. S., Craig, L., Arthur, L. M., Carney, J. P., and Tainer, J. A. (2000) Structural biology of Rad50 ATPase: ATP-driven conformational control in DNA double-strand break repair and the ABC-ATPase superfamily. *Cell* **101**, 789-800
  49. Doolittle, R. F., Johnson, M. S., Husain, I., Van Houten, B., Thomas, D. C., and Sancar, A. (1986) Domainal evolution of a prokaryotic DNA repair protein and its relationship to active-transport proteins. *Nature* **323**, 451-453
  50. Higgins, C. F., Hiles, I. D., Salmond, G. P., Gill, D. R., Downie, J. A., Evans, I. J., Holland, I. B., Gray, L., Buckel, S. D., Bell, A. W., and et al. (1986) A family of related ATP-binding subunits coupled to many distinct biological processes in bacteria. *Nature* **323**, 448-450
  51. Kozak, L., Gopal, G., Yoon, J. H., Sauna, Z. E., Ambudkar, S. V., Thakurta, A. G., and Dhar, R. (2002) Elf1p, a member of the ABC class of ATPases, functions as a mRNA export factor in *Schizosaccharomyces pombe*. *J. Biol. Chem.* **277**, 33580-33589
  52. Linton, K. J., and Higgins, C. F. (1998) The *Escherichia coli* ATP-binding cassette (ABC) proteins. *Mol. Microbiol.* **28**, 5-13



53. Moussatova, A., Kandt, C., O'Mara, M. L., and Tieleman, D. P. (2008) ATP-binding cassette transporters in *Escherichia coli*. *Biochim. Biophys. Acta* **1778**, 1757-1771
54. Bauer, B. E., Wolfger, H., and Kuchler, K. (1999) Inventory and function of yeast ABC proteins: about sex, stress, pleiotropic drug and heavy metal resistance. *Biochim. Biophys. Acta* **1461**, 217-236
55. Dean, M., Rzhetsky, A., and Allikmets, R. (2001) The human ATP-binding cassette (ABC) transporter superfamily. *Genome Res.* **11**, 1156-1166
56. Holland I. B, Cole S.P.C, and Kuchler K. and C. F. Higgins. (2003) *ABC proteins: From bacteria to man*, Academic Press London
57. Borst, P., and Elferink, R. O. (2002) Mammalian ABC transporters in health and disease. *Annu. Rev. Biochem.* **71**, 537-592
58. Rees, D. C., Johnson, E., and Lewinson, O. (2009) ABC transporters: the power to change. *Nat Rev Mol Cell Biol* **10**, 218-227
59. Tabcharani, J. A., Chang, X. B., Riordan, J. R., and Hanrahan, J. W. (1991) Phosphorylation-regulated Cl<sup>-</sup> channel in CHO cells stably expressing the cystic fibrosis gene. *Nature* **352**, 628-631
60. Martinez-Mir, A., Paloma, E., Allikmets, R., Ayuso, C., del Rio, T., Dean, M., Vilageliu, L., Gonzalez-Duarte, R., and Balcells, S. (1998) Retinitis pigmentosa caused by a homozygous mutation in the Stargardt disease gene ABCR. *Nat. Genet.* **18**, 11-12
61. Jacquemin, E. (2000) Progressive familial intrahepatic cholestasis. Genetic basis and treatment. *Clin Liver Dis* **4**, 753-763
62. Deeley, R. G., Westlake, C., and Cole, S. P. (2006) Transmembrane transport of endo- and xenobiotics by mammalian ATP-binding cassette multidrug resistance proteins. *Physiol. Rev.* **86**, 849-899
63. Biemans-Oldehinkel, E., Doeven, M. K., and Poolman, B. (2006) ABC transporter architecture and regulatory roles of accessory domains. *FEBS Lett.* **580**, 1023-1035
64. Oldham, M. L., and Chen, J. (2011) Snapshots of the maltose transporter during ATP hydrolysis. *Proc. Natl. Acad. Sci. U. S. A.* **108**, 15152-15156
65. Oldham, M. L., Khare, D., Quijcho, F. A., Davidson, A. L., and Chen, J. (2007) Crystal structure of a catalytic intermediate of the maltose transporter. *Nature* **450**, 515-521
66. Chen, S., Oldham, M. L., Davidson, A. L., and Chen, J. (2013) Carbon catabolite repression of the maltose transporter revealed by X-ray crystallography. *Nature* **499**, 364-368
67. Locher, K. P., Lee, A. T., and Rees, D. C. (2002) The *E. coli* BtuCD structure: a framework for ABC transporter architecture and mechanism. *Science* **296**, 1091-1098
68. Hvorup, R. N., Goetz, B. A., Niederer, M., Hollenstein, K., Perozo, E., and Locher, K. P. (2007) Asymmetry in the structure of the ABC transporter-binding protein complex BtuCD-BtuF. *Science* **317**, 1387-1390
69. Korkhov, V. M., Mireku, S. A., and Locher, K. P. (2012) Structure of AMP-PNP-bound vitamin B12 transporter BtuCD-F. *Nature* **490**, 367-372
70. Xu, K., Zhang, M., Zhao, Q., Yu, F., Guo, H., Wang, C., He, F., Ding, J., and Zhang, P. (2013) Crystal structure of a folate energy-coupling factor transporter from *Lactobacillus brevis*. *Nature* **497**, 268-271
71. Dawson, R. J., and Locher, K. P. (2007) Structure of the multidrug ABC transporter Sav1866 from *Staphylococcus aureus* in complex with AMP-PNP. *FEBS Lett.* **581**, 935-938
72. Dawson, R. J., and Locher, K. P. (2006) Structure of a bacterial multidrug ABC transporter. *Nature* **443**, 180-185

73. Slotboom, D. J. (2014) Structural and mechanistic insights into prokaryotic energy-coupling factor transporters. *Nat Rev Microbiol* **12**, 79-87
74. Zolnerciks, J. K., Address, E. J., Nicolaou, M., and Linton, K. J. (2011) Structure of ABC transporters. *Essays Biochem.* **50**, 43-61
75. Rodionov, D. A., Hebbeln, P., Eudes, A., ter Beek, J., Rodionova, I. A., Erkens, G. B., Slotboom, D. J., Gelfand, M. S., Osterman, A. L., Hanson, A. D., and Eitinger, T. (2009) A novel class of modular transporters for vitamins in prokaryotes. *J. Bacteriol.* **191**, 42-51
76. Karpowich, N. K., and Wang, D. N. (2013) Assembly and mechanism of a group II ECF transporter. *Proc. Natl. Acad. Sci. U. S. A.* **110**, 2534-2539
77. Hung, L. W., Wang, I. X., Nikaido, K., Liu, P. Q., Ames, G. F., and Kim, S. H. (1998) Crystal structure of the ATP-binding subunit of an ABC transporter. *Nature* **396**, 703-707
78. Schmitt, L., Benabdelhak, H., Blight, M. A., Holland, I. B., and Stubbs, M. T. (2003) Crystal structure of the nucleotide-binding domain of the ABC-transporter haemolysin B: identification of a variable region within ABC helical domains. *J. Mol. Biol.* **330**, 333-342
79. Vetter, I. R., and Wittinghofer, A. (1999) Nucleoside triphosphate-binding proteins: different scaffolds to achieve phosphoryl transfer. *Q. Rev. Biophys.* **32**, 1-56
80. Zaitseva, J., Jenewein, S., Jumpertz, T., Holland, I. B., and Schmitt, L. (2005) H662 is the linchpin of ATP hydrolysis in the nucleotide-binding domain of the ABC transporter HlyB. *EMBO J.* **24**, 1901-1910
81. Zaitseva, J., Jenewein, S., Oswald, C., Jumpertz, T., Holland, I. B., and Schmitt, L. (2005) A molecular understanding of the catalytic cycle of the nucleotide-binding domain of the ABC transporter HlyB. *Biochem. Soc. Trans.* **33**, 990-995
82. Zaitseva, J., Jenewein, S., Wiedenmann, A., Benabdelhak, H., Holland, I. B., and Schmitt, L. (2005) Functional characterization and ATP-induced dimerization of the isolated ABC-domain of the haemolysin B transporter. *Biochemistry* **44**, 9680-9690
83. Smith, P. C., Karpowich, N., Millen, L., Moody, J. E., Rosen, J., Thomas, P. J., and Hunt, J. F. (2002) ATP binding to the motor domain from an ABC transporter drives formation of a nucleotide sandwich dimer. *Mol. Cell* **10**, 139-149
84. Chen, J., Lu, G., Lin, J., Davidson, A. L., and Quirocho, F. A. (2003) A tweezers-like motion of the ATP-binding cassette dimer in an ABC transport cycle. *Mol. Cell* **12**, 651-661
85. Orelle, C., Dalmas, O., Gros, P., Di Pietro, A., and Jault, J. M. (2003) The conserved glutamate residue adjacent to the Walker-B motif is the catalytic base for ATP hydrolysis in the ATP-binding cassette transporter BmrA. *J. Biol. Chem.* **278**, 47002-47008
86. Moody, J. E., Millen, L., Binns, D., Hunt, J. F., and Thomas, P. J. (2002) Cooperative, ATP-dependent association of the nucleotide binding cassettes during the catalytic cycle of ATP-binding cassette transporters. *J. Biol. Chem.* **277**, 21111-21114
87. van der Does, C., and Tampe, R. (2004) How do ABC transporters drive transport? *Biol. Chem.* **385**, 927-933
88. Janas, E., Hofacker, M., Chen, M., Gompf, S., van der Does, C., and Tampe, R. (2003) The ATP hydrolysis cycle of the nucleotide-binding domain of the mitochondrial ATP-binding cassette transporter Mdl1p. *J. Biol. Chem.* **278**, 26862-26869
89. Senior, A. E., al-Shawi, M. K., and Urbatsch, I. L. (1995) The catalytic cycle of P-glycoprotein. *FEBS Lett.* **377**, 285-289

90. Urbatsch, I. L., Sankaran, B., Bhagat, S., and Senior, A. E. (1995) Both P-glycoprotein nucleotide-binding sites are catalytically active. *J. Biol. Chem.* **270**, 26956-26961
91. Gupta, R. P., Kueppers, P., Hanekop, N., and Schmitt, L. (2014) Generating symmetry in the asymmetric ABC transporter Pdr5 from *Saccharomyces cerevisiae*. *J. Biol. Chem.*
92. Tsai, M. F., Li, M., and Hwang, T. C. (2010) Stable ATP binding mediated by a partial NBD dimer of the CFTR chloride channel. *J. Gen. Physiol.* **135**, 399-414
93. Ernst, R., Koch, J., Horn, C., Tampe, R., and Schmitt, L. (2006) Engineering ATPase activity in the isolated ABC cassette of human TAP1. *J. Biol. Chem.* **281**, 27471-27480
94. Patzlaff, J. S., van der Heide, T., and Poolman, B. (2003) The ATP/substrate stoichiometry of the ATP-binding cassette (ABC) transporter OpuA. *J. Biol. Chem.* **278**, 29546-29551
95. Linton, K. J. (2007) Structure and function of ABC transporters. *Physiology* **22**, 122-130
96. Aller, S. G., Yu, J., Ward, A., Weng, Y., Chittaboina, S., Zhuo, R., Harrell, P. M., Trinh, Y. T., Zhang, Q., Urbatsch, I. L., and Chang, G. (2009) Structure of P-glycoprotein reveals a molecular basis for poly-specific drug binding. *Science* **323**, 1718-1722
97. Hollenstein, K., Dawson, R. J., and Locher, K. P. (2007) Structure and mechanism of ABC transporter proteins. *Curr. Opin. Struct. Biol.* **17**, 412-418
98. Jin, M. S., Oldham, M. L., Zhang, Q., and Chen, J. (2012) Crystal structure of the multidrug transporter P-glycoprotein from *Caenorhabditis elegans*. *Nature* **490**, 566-569
99. Kodan, A., Yamaguchi, T., Nakatsu, T., Sakiyama, K., Hipolito, C. J., Fujioka, A., Hirokane, R., Ikeguchi, K., Watanabe, B., Hiratake, J., Kimura, Y., Suga, H., Ueda, K., and Kato, H. (2014) Structural basis for gating mechanisms of a eukaryotic P-glycoprotein homolog. *Proc. Natl. Acad. Sci. U. S. A.*
100. Shintre, C. A., Pike, A. C., Li, Q., Kim, J. I., Barr, A. J., Goubin, S., Shrestha, L., Yang, J., Berridge, G., Ross, J., Stansfeld, P. J., Sansom, M. S., Edwards, A. M., Bountra, C., Marsden, B. D., von Delft, F., Bullock, A. N., Gileadi, O., Burgess-Brown, N. A., and Carpenter, E. P. (2013) Structures of ABCB10, a human ATP-binding cassette transporter in apo- and nucleotide-bound states. *Proc. Natl. Acad. Sci. U. S. A.* **110**, 9710-9715
101. Srinivasan, V., Pierik, A. J., and Lill, R. (2014) Crystal structures of nucleotide-free and glutathione-bound mitochondrial ABC transporter Atm1. *Science* **343**, 1137-1140
102. Stenham, D. R., Campbell, J. D., Sansom, M. S., Higgins, C. F., Kerr, I. D., and Linton, K. J. (2003) An atomic detail model for the human ATP binding cassette transporter P-glycoprotein derived from disulfide cross-linking and homology modeling. *FASEB J* **17**, 2287-2289
103. Al-Shawi, M. K. (2011) Catalytic and transport cycles of ABC exporters. *Essays Biochem.* **50**, 63-83
104. Mourez, M., Hofnung, M., and Dassa, E. (1997) Subunit interactions in ABC transporters: a conserved sequence in hydrophobic membrane proteins of periplasmic permeases defines an important site of interaction with the ATPase subunits. *EMBO J.* **16**, 3066-3077
105. Jones, P. M., and George, A. M. (2002) Mechanism of ABC transporters: a molecular dynamics simulation of a well characterized nucleotide-binding subunit. *Proc. Natl. Acad. Sci. U. S. A.* **99**, 12639-12644

106. Cotten, J. F., Ostedgaard, L. S., Carson, M. R., and Welsh, M. J. (1996) Effect of cystic fibrosis-associated mutations in the fourth intracellular loop of cystic fibrosis transmembrane conductance regulator. *J. Biol. Chem.* **271**, 21279-21284
107. Loo, T. W., and Clarke, D. M. (2014) Locking intracellular helices 2 and 3 together inactivates human P-glycoprotein. *J. Biol. Chem.* **289**, 229-236
108. Wen, P. C., and Tajkhorshid, E. (2011) Conformational coupling of the nucleotide-binding and the transmembrane domains in ABC transporters. *Biophys. J.* **101**, 680-690
109. Oancea, G., O'Mara, M. L., Bennett, W. F., Tieleman, D. P., Abele, R., and Tampe, R. (2009) Structural arrangement of the transmission interface in the antigen ABC transport complex TAP. *Proc. Natl. Acad. Sci. U. S. A.* **106**, 5551-5556
110. He, L., Aleksandrov, A. A., Serohijos, A. W., Hegedus, T., Aleksandrov, L. A., Cui, L., Dokholyan, N. V., and Riordan, J. R. (2008) Multiple membrane-cytoplasmic domain contacts in the cystic fibrosis transmembrane conductance regulator (CFTR) mediate regulation of channel gating. *J. Biol. Chem.* **283**, 26383-26390
111. Dean, M., Hamon, Y., and Chimini, G. (2001) The human ATP-binding cassette (ABC) transporter superfamily. *J. Lipid Res.* **42**, 1007-1017
112. Mosser, J., Douar, A. M., Sarde, C. O., Kioschis, P., Feil, R., Moser, H., Poustka, A. M., Mandel, J. L., and Aubourg, P. (1993) Putative X-linked adrenoleukodystrophy gene shares unexpected homology with ABC transporters. *Nature* **361**, 726-730
113. Takahashi, K., Kimura, Y., Kioka, N., Matsuo, M., and Ueda, K. (2006) Purification and ATPase activity of human ABCA1. *J. Biol. Chem.* **281**, 10760-10768
114. Pollock, N. L., and Callaghan, R. (2011) The lipid translocase, ABCA4: seeing is believing. *Febs J* **278**, 3204-3214
115. Kartner, N., Riordan, J. R., and Ling, V. (1983) Cell surface P-glycoprotein associated with multidrug resistance in mammalian cell lines. *Science* **221**, 1285-1288
116. Didier, A. D., and Loor, F. (1995) Decreased biotolerability for ivermectin and cyclosporin A in mice exposed to potent P-glycoprotein inhibitors. *Int. J. Cancer* **63**, 263-267
117. Ambudkar, S. V., Kimchi-Sarfaty, C., Sauna, Z. E., and Gottesman, M. M. (2003) P-glycoprotein: from genomics to mechanism. *Oncogene* **22**, 7468-7485
118. Cordon-Cardo, C., O'Brien, J. P., Boccia, J., Casals, D., Bertino, J. R., and Melamed, M. R. (1990) Expression of the multidrug resistance gene product (P-glycoprotein) in human normal and tumor tissues. *J. Histochem. Cytochem.* **38**, 1277-1287
119. Tanigawara, Y., Okamura, N., Hirai, M., Yasuhara, M., Ueda, K., Kioka, N., Komano, T., and Hori, R. (1992) Transport of digoxin by human P-glycoprotein expressed in a porcine kidney epithelial cell line (LLC-PK1). *J. pharm. Exp. Ther.* **263**, 840-845
120. Gottesman, M. M., Fojo, T., and Bates, S. E. (2002) Multidrug resistance in cancer: role of ATP-dependent transporters. *Nat Rev Cancer* **2**, 48-58
121. Borst, P., Schinkel, A. H., Smit, J. J., Wagenaar, E., Van Deemter, L., Smith, A. J., Eijdens, E. W., Baas, F., and Zaman, G. J. (1993) Classical and novel forms of multidrug resistance and the physiological functions of P-glycoproteins in mammals. *Pharmacol. Ther.* **60**, 289-299
122. Doran, A., Obach, R. S., Smith, B. J., Hosea, N. A., Becker, S., Callegari, E., Chen, C., Chen, X., Choo, E., Cianfroga, J., Cox, L. M., Gibbs, J. P., Gibbs, M. A., Hatch, H., Hop, C. E., Kasman, I. N., Laperle, J., Liu, J., Liu, X., Logman, M., Maclin, D., Nedza, F. M., Nelson, F., Olson, E., Rahematpura, S., Raunig, D., Rogers, S., Schmidt, K., Spracklin, D. K., Szewc, M., Troutman, M., Tseng, E., Tu, M., Van Deusen, J. W., Venkatakrishnan, K., Walens, G., Wang, E. Q., Wong, D., Yasgar, A. S., and Zhang, C. (2005) The impact of P-glycoprotein on the disposition of drugs

- targeted for indications of the central nervous system: evaluation using the MDR1A/1B knockout mouse model. *Drug Metab. Dispos.* **33**, 165-174
123. Schinkel, A. H. (1999) P-Glycoprotein, a gatekeeper in the blood-brain barrier. *Adv. Drug Del. Rev.* **36**, 179-194
124. Fromm, M. F. (2004) Importance of P-glycoprotein at blood-tissue barriers. *Trends Pharmacol. Sci.* **25**, 423-429
125. Ford, J. M., and Hait, W. N. (1990) Pharmacology of drugs that alter multidrug resistance in cancer. *Pharmacol. Rev.* **42**, 155-199
126. Ueda, K., Okamura, N., Hirai, M., Tanigawara, Y., Saeki, T., Kioka, N., Komano, T., and Hori, R. (1992) Human P-glycoprotein transports cortisol, aldosterone, and dexamethasone, but not progesterone. *J. Biol. Chem.* **267**, 24248-24252
127. van Helvoort, A., Smith, A. J., Sprong, H., Fritzsche, I., Schinkel, A. H., Borst, P., and van Meer, G. (1996) MDR1 P-glycoprotein is a lipid translocase of broad specificity, while MDR3 P-glycoprotein specifically translocates phosphatidylcholine. *Cell* **87**, 507-517
128. Bosch, I., Dunussi-Joannopoulos, K., Wu, R. L., Furlong, S. T., and Croop, J. (1997) Phosphatidylcholine and phosphatidylethanolamine behave as substrates of the human MDR1 P-glycoprotein. *Biochemistry* **36**, 5685-5694
129. Romsicki, Y., and Sharom, F. J. (2001) Phospholipid flippase activity of the reconstituted P-glycoprotein multidrug transporter. *Biochemistry* **40**, 6937-6947
130. Eckford, P. D., and Sharom, F. J. (2005) The reconstituted P-glycoprotein multidrug transporter is a flippase for glucosylceramide and other simple glycosphingolipids. *Biochem. J.* **389**, 517-526
131. Pohl, A., Lage, H., Muller, P., Pomorski, T., and Herrmann, A. (2002) Transport of phosphatidylserine via MDR1 (multidrug resistance 1)P-glycoprotein in a human gastric carcinoma cell line. *Biochem. J.* **365**, 259-268
132. Rothnie, A., Theron, D., Soceneantu, L., Martin, C., Traikia, M., Berridge, G., Higgins, C. F., Devaux, P. F., and Callaghan, R. (2001) The importance of cholesterol in maintenance of P-glycoprotein activity and its membrane perturbing influence. *Eur. Biophys. J.* **30**, 430-442
133. Sharom, F. J., Lugo, M. R., and Eckford, P. D. (2005) New insights into the drug binding, transport and lipid flippase activities of the p-glycoprotein multidrug transporter. *J. Bioenerg. Biomembr.* **37**, 481-487
134. Smit, J. J., Schinkel, A. H., Oude Elferink, R. P., Groen, A. K., Wagenaar, E., van Deemter, L., Mol, C. A., Ottenhoff, R., van der Lugt, N. M., van Roon, M. A., and et al. (1993) Homozygous disruption of the murine *mdr2* P-glycoprotein gene leads to a complete absence of phospholipid from bile and to liver disease. *Cell* **75**, 451-462
135. Morita, S. Y., Kobayashi, A., Takanezawa, Y., Kioka, N., Handa, T., Arai, H., Matsuo, M., and Ueda, K. (2007) Bile salt-dependent efflux of cellular phospholipids mediated by ATP binding cassette protein B4. *Hepatology* **46**, 188-199
136. Li, J., Jaimes, K. F., and Aller, S. G. (2014) Refined structures of mouse P-glycoprotein. *Protein Sci.* **23**, 34-46
137. Kimura, Y., Morita, S. Y., Matsuo, M., and Ueda, K. (2007) Mechanism of multidrug recognition by MDR1/ABCB1. *Cancer Sci.* **98**, 1303-1310
138. van der Bliek, A. M., Kooiman, P. M., Schneider, C., and Borst, P. (1988) Sequence of *mdr3* cDNA encoding a human P-glycoprotein. *Gene* **71**, 401-411
139. Oude Elferink, R. P., and Paulusma, C. C. (2007) Function and pathophysiological importance of ABCB4 (MDR3 P-glycoprotein). *Pflugers Arch - Eur J Physiol* **453**, 601-610
140. Smith, A. J., de Vree, J. M., Ottenhoff, R., Oude Elferink, R. P., Schinkel, A. H., and Borst, P. (1998) Hepatocyte-specific expression of the human MDR3 P-glycoprotein

- gene restores the biliary phosphatidylcholine excretion absent in Mdr2 (-/-) mice. *Hepatology* **28**, 530-536
141. Smith, A. J., Timmermans-Hereijgers, J. L., Roelofsen, B., Wirtz, K. W., van Blitterswijk, W. J., Smit, J. J., Schinkel, A. H., and Borst, P. (1994) The human MDR3 P-glycoprotein promotes translocation of phosphatidylcholine through the plasma membrane of fibroblasts from transgenic mice. *FEBS Lett.* **354**, 263-266
  142. Groen, A., Romero, M. R., Kunne, C., Hoosdally, S. J., Dixon, P. H., Wooding, C., Williamson, C., Seppen, J., Van den Oever, K., Mok, K. S., Paulusma, C. C., Linton, K. J., and Oude Elferink, R. P. (2011) Complementary functions of the flippase ATP8B1 and the floppase ABCB4 in maintaining canalicular membrane integrity. *Gastroenterology* **141**, 1927-1937 e1921-1924
  143. Smith, A. J., van Helvoort, A., van Meer, G., Szabo, K., Welker, E., Szakacs, G., Varadi, A., Sarkadi, B., and Borst, P. (2000) MDR3 P-glycoprotein, a phosphatidylcholine translocase, transports several cytotoxic drugs and directly interacts with drugs as judged by interference with nucleotide trapping. *J. Biol. Chem.* **275**, 23530-23539
  144. Ishigami, M., Tominaga, Y., Nagao, K., Kimura, Y., Matsuo, M., Kioka, N., and Ueda, K. (2013) ATPase activity of nucleotide binding domains of human MDR3 in the context of MDR1. *Biochim. Biophys. Acta* **1831**, 683-690
  145. Dzagania, T., Engelmann, G., Haussinger, D., Schmitt, L., Flechtenmacher, C., Rtskhiladze, I., and Kubitz, R. (2012) The histidine-loop is essential for transport activity of human MDR3. A novel mutation of MDR3 in a patient with progressive familial intrahepatic cholestasis type 3. *Gene* **506**, 141-145
  146. Andress, E. J., Nicolaou, M., Romero, M. R., Naik, S., Dixon, P. H., Williamson, C., and Linton, K. J. (2014) Molecular mechanistic explanation for the spectrum of cholestatic disease caused by the S320F variant of ABCB4. *Hepatology* **59**, 1921-1931
  147. Trauner, M., Fickert, P., and Wagner, M. (2007) MDR3 (ABCB4) defects: a paradigm for the genetics of adult cholestatic syndromes. *Semin. Liver Dis.* **27**, 77-98
  148. Gonzales, E., Davit-Spraul, A., Baussan, C., Buffet, C., Maurice, M., and Jacquemin, E. (2009) Liver diseases related to MDR3 (ABCB4) gene deficiency. *Front. Biosci.* **14**, 4242-4256
  149. Lazaridis, K. N., Gores, G. J., and Lindor, K. D. (2001) Ursodeoxycholic acid 'mechanisms of action and clinical use in hepatobiliary disorders'. *J. Hepatol.* **35**, 134-146
  150. Jacquemin, E. (2012) Progressive familial intrahepatic cholestasis. *Clin Res Hepatol Gastroenterol* **36 Suppl 1**, S26-35
  151. Nicolaou, M., Andress, E. J., Zolnericiks, J. K., Dixon, P. H., Williamson, C., and Linton, K. J. (2012) Canalicular ABC transporters and liver disease. *J. Phatol.* **226**, 300-315
  152. Mullenbach, R., Linton, K. J., Wiltshire, S., Weerasekera, N., Chambers, J., Elias, E., Higgins, C. F., Johnston, D. G., McCarthy, M. I., and Williamson, C. (2003) ABCB4 gene sequence variation in women with intrahepatic cholestasis of pregnancy. *J. Med. Genet.* **40**, e70
  153. Haussinger, D., Kubitz, R., Reinehr, R., Bode, J. G., and Schliess, F. (2004) Molecular aspects of medicine: from experimental to clinical hepatology. *Mol. Aspects Med.* **25**, 221-360
  154. Hofmann, A. F. (2009) Bile acids: trying to understand their chemistry and biology with the hope of helping patients. *Hepatology* **49**, 1403-1418
  155. Hofmann, A. F., and Hagey, L. R. (2008) Bile acids: chemistry, pathochemistry, biology, pathobiology, and therapeutics. *Cell. Mol. Life Sci.* **65**, 2461-2483

156. Meier, P. J., and Stieger, B. (2002) Bile salt transporters. *Annu. Rev. Physiol.* **64**, 635-661
157. Gerloff, T., Stieger, B., Hagenbuch, B., Madon, J., Landmann, L., Roth, J., Hofmann, A. F., and Meier, P. J. (1998) The sister of P-glycoprotein represents the canalicular bile salt export pump of mammalian liver. *J. Biol. Chem.* **273**, 10046-10050
158. Trauner, M., Fickert, P., Halilbasic, E., and Moustafa, T. (2008) Lessons from the toxic bile concept for the pathogenesis and treatment of cholestatic liver diseases. *Wien. Med. Wochenschr.* **158**, 542-548
159. Gerloff, T., Meier, P. J., and Stieger, B. (1998) Taurocholate induces preferential release of phosphatidylcholine from rat liver canalicular vesicles. *Liver* **18**, 306-312
160. Keitel, V., Burdelski, M., Warskulat, U., Kühlkamp, T., Keppler, D., Häussinger, D., and Kubitz, R. (2005) Expression and localization of hepatobiliary transport proteins in progressive familial intrahepatic cholestasis. *Hepatology* **41**, 1160-1172
161. Strautnieks, S. S., Byrne, J. A., Pawlikowska, L., Cebecauerova, D., Rayner, A., Dutton, L., Meier, Y., Antoniou, A., Stieger, B., Arnell, H., Ozcay, F., Al-Hussaini, H. F., Bassas, A. F., Verkade, H. J., Fischler, B., Nemeth, A., Kotalova, R., Shneider, B. L., Cielecka-Kuszyk, J., McClean, P., Whittington, P. F., Sokal, E., Jirsa, M., Wali, S. H., Jankowska, I., Pawlowska, J., Mieli-Vergani, G., Knisely, A. S., Bull, L. N., and Thompson, R. J. (2008) Severe bile salt export pump deficiency: 82 different ABCB11 mutations in 109 families. *Gastroenterology* **134**, 1203-1214
162. Small, D. M. (2003) Role of ABC transporters in secretion of cholesterol from liver into bile. *Proc. Natl. Acad. Sci. U. S. A.* **100**, 4-6
163. Stindt, J. (2010) Studies on ABC Transporters from Human Liver in Heterologous Systems. *Dissertation, HHU Düsseldorf*
164. Davit-Spraul, A., Gonzales, E., Baussan, C., and Jacquemin, E. (2010) The spectrum of liver diseases related to ABCB4 gene mutations: pathophysiology and clinical aspects. *Semin. Liver Dis.* **30**, 134-146
165. Lew, J. L., Zhao, A., Yu, J., Huang, L., De Pedro, N., Pelaez, F., Wright, S. D., and Cui, J. (2004) The farnesoid X receptor controls gene expression in a ligand- and promoter-selective fashion. *J. Biol. Chem.* **279**, 8856-8861
166. Plass, J. R., Mol, O., Heegsma, J., Geuken, M., Faber, K. N., Jansen, P. L., and Muller, M. (2002) Farnesoid X receptor and bile salts are involved in transcriptional regulation of the gene encoding the human bile salt export pump. *Hepatology* **35**, 589-596
167. Eloranta, J. J., and Kullak-Ublick, G. A. (2008) The role of FXR in disorders of bile acid homeostasis. *Physiology* **23**, 286-295
168. Gautherot, J., Delautier, D., Maubert, M. A., Ait-Slimane, T., Bolbach, G., Delaunay, J. L., Durand-Schneider, A. M., Firrincieli, D., Barbu, V., Chignard, N., Housset, C., Maurice, M., and Falguieres, T. (2014) Phosphorylation of ABCB4 impacts its function: Insights from disease-causing mutations. *Hepatology*
169. Jardetzky, O. (1966) Simple allosteric model for membrane pumps. *Nature* **211**, 969-970
170. Higgins, C. F., and Linton, K. J. (2004) The ATP switch model for ABC transporters. *Nat. Struct. Mol. Biol.* **11**, 918-926
171. Martin, C., Higgins, C. F., and Callaghan, R. (2001) The vinblastine binding site adopts high- and low-affinity conformations during a transport cycle of P-glycoprotein. *Biochemistry* **40**, 15733-15742
172. Sauna, Z. E., and Ambudkar, S. V. (2000) Evidence for a requirement for ATP hydrolysis at two distinct steps during a single turnover of the catalytic cycle of human P-glycoprotein. *Proc. Natl. Acad. Sci. U. S. A.* **97**, 2515-2520

173. Neumann, L., Abele, R., and Tampe, R. (2002) Thermodynamics of peptide binding to the transporter associated with antigen processing (TAP). *J. Mol. Biol.* **324**, 965-973
174. Qu, Q., Russell, P. L., and Sharom, F. J. (2003) Stoichiometry and affinity of nucleotide binding to P-glycoprotein during the catalytic cycle. *Biochemistry* **42**, 1170-1177
175. Higgins, C. F., and Gottesman, M. M. (1992) Is the multidrug transporter a flippase? *Trends Biochem. Sci.* **17**, 18-21
176. Rosenberg, M. F., Kamis, A. B., Callaghan, R., Higgins, C. F., and Ford, R. C. (2003) Three-dimensional structures of the mammalian multidrug resistance P-glycoprotein demonstrate major conformational changes in the transmembrane domains upon nucleotide binding. *J. Biol. Chem.* **278**, 8294-8299
177. Rosenberg, M. F., Velarde, G., Ford, R. C., Martin, C., Berridge, G., Kerr, I. D., Callaghan, R., Schmidlin, A., Wooding, C., Linton, K. J., and Higgins, C. F. (2001) Repacking of the transmembrane domains of P-glycoprotein during the transport ATPase cycle. *EMBO J.* **20**, 5615-5625
178. van Meer, G., Halter, D., Sprong, H., Somerharju, P., and Egmond, M. R. (2006) ABC lipid transporters: extruders, flippases, or floppless activators? *FEBS Lett.* **580**, 1171-1177
179. Abreu, M. S., Moreno, M. J., and Vaz, W. L. (2004) Kinetics and thermodynamics of association of a phospholipid derivative with lipid bilayers in liquid-disordered and liquid-ordered phases. *Biophys. J.* **87**, 353-365
180. Oude Elferink, R. P., and Groen, A. K. (2000) Mechanisms of biliary lipid secretion and their role in lipid homeostasis. *Semin. Liver Dis.* **20**, 293-305
181. Buschman, E., and Gros, P. (1994) The inability of the mouse *mdr2* gene to confer multidrug resistance is linked to reduced drug binding to the protein. *Cancer Res.* **54**, 4892-4898
182. Gros, P., and Buschman, E. (1993) The mouse multidrug resistance gene family: structural and functional analysis. *Int. Rev. Cytol.* **137C**, 169-197
183. Stindt, J., Ellinger, P., Stross, C., Keitel, V., Haussinger, D., Smits, S. H., Kubitz, R., and Schmitt, L. (2011) Heterologous overexpression and mutagenesis of the human bile salt export pump (ABCB11) using DREAM (Directed REcombination-Assisted Mutagenesis). *PLoS One* **6**, e20562
184. Terpe, K. (2006) Overview of bacterial expression systems for heterologous protein production: from molecular and biochemical fundamentals to commercial systems. *Appl. Microbiol. Biotechnol.* **72**, 211-222
185. Wagner, S., Bader, M. L., Drew, D., and de Gier, J. W. (2006) Rationalizing membrane protein overexpression. *Trends Biotechnol.* **24**, 364-371
186. Midgett, C. R., and Madden, D. R. (2007) Breaking the bottleneck: eukaryotic membrane protein expression for high-resolution structural studies. *J. Struct. Biol.* **160**, 265-274
187. Ellinger, P. (2013) P-loop ATPases – Csn2 from *Streptococcus agalactiae* and the human liver ABC transporter BSEP. *Dissertation, HHU Düsseldorf*
188. Bibi, E., Gros, P., and Kaback, H. R. (1993) Functional expression of mouse *mdr1* in *Escherichia coli*. *Proc. Natl. Acad. Sci. U. S. A.* **90**, 9209-9213
189. Linton, K. J., and Higgins, C. F. (2002) P-glycoprotein misfolds in *Escherichia coli*: evidence against alternating-topology models of the transport cycle. *Mol. Membr. Biol.* **19**, 51-58
190. Pozza, A., Perez-Victoria, J. M., and Di Pietro, A. (2010) Insect cell versus bacterial overexpressed membrane proteins: an example, the human ABCG2 transporter. *Methods Mol. Biol.* **654**, 47-75



191. Junge, F., Schneider, B., Reckel, S., Schwarz, D., Dotsch, V., and Bernhard, F. (2008) Large-scale production of functional membrane proteins. *Cell. Mol. Life Sci.* **65**, 1729-1755
192. Gupta, R. P. (2014) Biochemical studies on Pdr5 – an ABC transporter from *Saccharomyces cerevisiae*. *Dissertation, HHU Düsseldorf*
193. Figler, R. A., Omote, H., Nakamoto, R. K., and Al-Shawi, M. K. (2000) Use of chemical chaperones in the yeast *Saccharomyces cerevisiae* to enhance heterologous membrane protein expression: high-yield expression and purification of human P-glycoprotein. *Arch. Biochem. Biophys.* **376**, 34-46
194. Mao, Q., and Scarborough, G. A. (1997) Purification of functional human P-glycoprotein expressed in *Saccharomyces cerevisiae*. *Biochim. Biophys. Acta* **1327**, 107-118
195. Chloupkova, M., Pickert, A., Lee, J. Y., Souza, S., Trinh, Y. T., Connelly, S. M., Dumont, M. E., Dean, M., and Urbatsch, I. L. (2007) Expression of 25 human ABC transporters in the yeast *Pichia pastoris* and characterization of the purified ABCC3 ATPase activity. *Biochemistry* **46**, 7992-8003
196. Zehnpfennig, B., Urbatsch, I. L., and Galla, H. J. (2009) Functional reconstitution of human ABCC3 into proteoliposomes reveals a transport mechanism with positive cooperativity. *Biochemistry* **48**, 4423-4430
197. Johnson, B. J., Lee, J. Y., Pickert, A., and Urbatsch, I. L. (2010) Bile acids stimulate ATP hydrolysis in the purified cholesterol transporter ABCG5/G8. *Biochemistry* **49**, 3403-3411
198. Wang, Z., Stalcup, L. D., Harvey, B. J., Weber, J., Chloupkova, M., Dumont, M. E., Dean, M., and Urbatsch, I. L. (2006) Purification and ATP hydrolysis of the putative cholesterol transporters ABCG5 and ABCG8. *Biochemistry* **45**, 9929-9939
199. Lerner-Marmarosh, N., Gimi, K., Urbatsch, I. L., Gros, P., and Senior, A. E. (1999) Large scale purification of detergent-soluble P-glycoprotein from *Pichia pastoris* cells and characterization of nucleotide binding properties of wild-type, Walker A, and Walker B mutant proteins. *J. Biol. Chem.* **274**, 34711-34718
200. Prive, G. G. (2007) Detergents for the stabilization and crystallization of membrane proteins. *Methods* **41**, 388-397
201. Zeder-Lutz, G., Cherouati, N., Reinhart, C., Pattus, F., and Wagner, R. (2006) Dot-blot immunodetection as a versatile and high-throughput assay to evaluate recombinant GPCRs produced in the yeast *Pichia pastoris*. *Protein Expression Purif.* **50**, 118-127
202. Newstead, S., Kim, H., von Heijne, G., Iwata, S., and Drew, D. (2007) High-throughput fluorescent-based optimization of eukaryotic membrane protein overexpression and purification in *Saccharomyces cerevisiae*. *Proc. Natl. Acad. Sci. U. S. A.* **104**, 13936-13941
203. Mizutani, K., Yoshioka, S., Mizutani, Y., Iwata, S., and Mikami, B. (2011) High-throughput construction of expression system using yeast *Pichia pastoris*, and its application to membrane proteins. *Protein Expression Purif.* **77**, 1-8
204. Drew, D., Newstead, S., Sonoda, Y., Kim, H., von Heijne, G., and Iwata, S. (2008) GFP-based optimization scheme for the overexpression and purification of eukaryotic membrane proteins in *Saccharomyces cerevisiae*. *Nat Protoc* **3**, 784-798
205. Eshaghi, S. (2009) High-throughput expression and detergent screening of integral membrane proteins. *Methods Mol. Biol.* **498**, 265-271
206. Vergis, J. M., Purdy, M. D., and Wiener, M. C. (2010) A high-throughput differential filtration assay to screen and select detergents for membrane proteins. *Anal. Biochem.* **407**, 1-11

207. Hattori, M., Hibbs, R. E., and Gouaux, E. (2012) A fluorescence-detection size-exclusion chromatography-based thermostability assay for membrane protein precrystallization screening. *Structure* **20**, 1293-1299
208. Arachea, B. T., Sun, Z., Potente, N., Malik, R., Isailovic, D., and Viola, R. E. (2012) Detergent selection for enhanced extraction of membrane proteins. *Protein Expression Purif.* **86**, 12-20
209. Curnow, P., Senior, L., Knight, M. J., Thamatrakoln, K., Hildebrand, M., and Booth, P. J. (2012) Expression, purification, and reconstitution of a diatom silicon transporter. *Biochemistry* **51**, 3776-3785
210. Pollock, N. L., McDevitt, C. A., Collins, R., Niesten, P. H., Prince, S., Kerr, I. D., Ford, R. C., and Callaghan, R. (2014) Improving the stability and function of purified ABCB1 and ABCA4: the influence of membrane lipids. *Biochim. Biophys. Acta* **1838**, 134-147
211. Urbatsch, I. L., Beaudet, L., Carrier, I., and Gros, P. (1998) Mutations in either nucleotide-binding site of P-glycoprotein (Mdr3) prevent vanadate trapping of nucleotide at both sites. *Biochemistry* **37**, 4592-4602
212. Beaudet, L., Urbatsch, I. L., and Gros, P. (1998) High-level expression of mouse Mdr3 P-glycoprotein in yeast *Pichia pastoris* and characterization of ATPase activity. *Methods Enzymol.* **292**, 397-413
213. Bai, J., Swartz, D. J., Protasevich, II, Brouillette, C. G., Harrell, P. M., Hildebrandt, E., Gasser, B., Mattanovich, D., Ward, A., Chang, G., and Urbatsch, I. L. (2011) A gene optimization strategy that enhances production of fully functional P-glycoprotein in *Pichia pastoris*. *PLoS One* **6**, e22577
214. McDevitt, C. A., Collins, R., Kerr, I. D., and Callaghan, R. (2009) Purification and structural analyses of ABCG2. *Adv. Drug Del. Rev.* **61**, 57-65
215. Rosenberg, M. F., Bikadi, Z., Chan, J., Liu, X., Ni, Z., Cai, X., Ford, R. C., and Mao, Q. (2010) The human breast cancer resistance protein (BCRP/ABCG2) shows conformational changes with mitoxantrone. *Structure* **18**, 482-493
216. Infed, N., Hanekop, N., Driessen, A. J., Smits, S. H., and Schmitt, L. (2011) Influence of detergents on the activity of the ABC transporter LmrA. *Biochim. Biophys. Acta* **1808**, 2313-2321
217. Ellinger, P., Kluth, M., Stindt, J., Smits, S. H., and Schmitt, L. (2013) Detergent screening and purification of the human liver ABC transporters BSEP (ABCB11) and MDR3 (ABCB4) expressed in the yeast *Pichia pastoris*. *PLoS One* **8**, e60620
218. Arnold, T., and Linke, D. (2008) The use of detergents to purify membrane proteins. *Current protocols in protein science / editorial board, John E. Coligan ... [et al.]* **Chapter 4**, Unit 4 8 1-4 8 30
219. Sleight, R. G., and Pagano, R. E. (1985) Transbilayer movement of a fluorescent phosphatidylethanolamine analogue across the plasma membranes of cultured mammalian cells. *J. Biol. Chem.* **260**, 1146-1154
220. Ruetz, S., and Gros, P. (1994) Phosphatidylcholine translocase: a physiological role for the *mdr2* gene. *Cell* **77**, 1071-1081
221. Papadopoulos, A., Vehring, S., Lopez-Montero, I., Kutschenko, L., Stockl, M., Devaux, P. F., Kozlov, M., Pomorski, T., and Herrmann, A. (2007) Flippase activity detected with unlabeled lipids by shape changes of giant unilamellar vesicles. *J. Biol. Chem.* **282**, 15559-15568
222. Kahya, N., Scherfeld, D., Bacia, K., and Schwille, P. (2004) Lipid domain formation and dynamics in giant unilamellar vesicles explored by fluorescence correlation spectroscopy. *J. Struct. Biol.* **147**, 77-89

223. Robinson, T., Kuhn, P., Eyer, K., and Dittrich, P. S. (2013) Microfluidic trapping of giant unilamellar vesicles to study transport through a membrane pore. *Biomicrofluidics* **7**, 44105
224. Stachowiak, J. C., Richmond, D. L., Li, T. H., Liu, A. P., Parekh, S. H., and Fletcher, D. A. (2008) Unilamellar vesicle formation and encapsulation by microfluidic jetting. *Proc. Natl. Acad. Sci. U. S. A.* **105**, 4697-4702
225. Dezi, M., Di Cicco, A., Bassereau, P., and Levy, D. (2013) Detergent-mediated incorporation of transmembrane proteins in giant unilamellar vesicles with controlled physiological contents. *Proc. Natl. Acad. Sci. U. S. A.* **110**, 7276-7281
226. Urbatsch, I. L., Wilke-Mounts, S., Gimi, K., and Senior, A. E. (2001) Purification and characterization of N-glycosylation mutant mouse and human P-glycoproteins expressed in *Pichia pastoris* cells. *Arch. Biochem. Biophys.* **388**, 171-177
227. Loo, T. W., and Clarke, D. M. (1995) Covalent modification of human P-glycoprotein mutants containing a single cysteine in either nucleotide-binding fold abolishes drug-stimulated ATPase activity. *J. Biol. Chem.* **270**, 22957-22961
228. Loo, T. W., and Clarke, D. M. (1999) Determining the structure and mechanism of the human multidrug resistance P-glycoprotein using cysteine-scanning mutagenesis and thiol-modification techniques. *Biochim. Biophys. Acta* **1461**, 315-325
229. Gabriel, M. P., Storm, J., Rothnie, A., Taylor, A. M., Linton, K. J., Kerr, I. D., and Callaghan, R. (2003) Communication between the nucleotide binding domains of P-glycoprotein occurs via conformational changes that involve residue 508. *Biochemistry* **42**, 7780-7789
230. Pozza, A., Perez-Victoria, J. M., Sardo, A., Ahmed-Belkacem, A., and Di Pietro, A. (2006) Purification of breast cancer resistance protein ABCG2 and role of arginine-482. *Cell. Mol. Life Sci.* **63**, 1912-1922
231. Urbatsch, I. L., Gimi, K., Wilke-Mounts, S., Lerner-Marmarosh, N., Rousseau, M. E., Gros, P., and Senior, A. E. (2001) Cysteines 431 and 1074 are responsible for inhibitory disulfide cross-linking between the two nucleotide-binding sites in human P-glycoprotein. *J. Biol. Chem.* **276**, 26980-26987
232. Scholz, C., Parcej, D., Ejlsing, C. S., Robenek, H., Urbatsch, I. L., and Tampe, R. (2011) Specific lipids modulate the transporter associated with antigen processing (TAP). *J. Biol. Chem.* **286**, 13346-13356
233. Morita, S. Y., and Terada, T. (2014) Molecular mechanisms for biliary phospholipid and drug efflux mediated by ABCB4 and bile salts. *BioMed research international* **2014**, 954781
234. Zolnerciks, J. K., Akkaya, B. G., Snippe, M., Chiba, P., Seelig, A., and Linton, K. J. (2014) The Q loops of the human multidrug resistance transporter ABCB1 are necessary to couple drug binding to the ATP catalytic cycle. *FASEB J.* **28**, 4335-4346
235. Kubitz, R., Bode, J., Erhardt, A., Graf, D., Kircheis, G., Muller-Stover, I., Reinehr, R., Reuter, S., Richter, J., Sagir, A., Schmitt, M., and Donner, M. (2011) Cholestatic liver diseases from child to adult: the diversity of MDR3 disease. *Z. Gastroenterol.* **49**, 728-736
236. Chang, S. Y., Liu, F. F., Dong, X. Y., and Sun, Y. (2013) Molecular insight into conformational transmission of human P-glycoprotein. *J. Chem. Phys.* **139**, 225102
237. Buschman, E., and Gros, P. (1991) Functional analysis of chimeric genes obtained by exchanging homologous domains of the mouse *mdr1* and *mdr2* genes. *Mol. Cell. Biol.* **11**, 595-603
238. Januchowski, R., Wojtowicz, K., Andrzejewska, M., and Zabel, M. (2014) Expression of MDR1 and MDR3 gene products in paclitaxel-, doxorubicin- and vincristine-resistant cell lines. *Biomedicine & pharmacotherapy* **68**, 111-117

- 
239. Yoshikado, T., Takada, T., Yamamoto, T., Yamaji, H., Ito, K., Santa, T., Yokota, H., Yatom, Y., Yoshida, H., Goto, J., Tsuji, S., and Suzuki, H. (2011) Itraconazole-induced cholestasis: involvement of the inhibition of bile canalicular phospholipid translocator MDR3/ABCB4. *Mol. Pharmacol.* **79**, 241-250
240. Tamai, I., and Safa, A. R. (1990) Competitive interaction of cyclosporins with the Vinca alkaloid-binding site of P-glycoprotein in multidrug-resistant cells. *J. Biol. Chem.* **265**, 16509-16513
241. Sarkadi, B., Muller, M., Homolya, L., Hollo, Z., Seprodi, J., Germann, U. A., Gottesman, M. M., Price, E. M., and Boucher, R. C. (1994) Interaction of bioactive hydrophobic peptides with the human multidrug transporter. *FASEB J.* **8**, 766-770
242. Sharom, F. J., DiDiodato, G., Yu, X., and Ashbourne, K. J. (1995) Interaction of the P-glycoprotein multidrug transporter with peptides and ionophores. *J. Biol. Chem.* **270**, 10334-10341
243. Rao, U. S., and Scarborough, G. A. (1994) Direct demonstration of high affinity interactions of immunosuppressant drugs with the drug binding site of the human P-glycoprotein. *Mol. Pharmacol.* **45**, 773-776
244. Stieger, B., Fattinger, K., Madon, J., Kullak-Ublick, G. A., and Meier, P. J. (2000) Drug- and estrogen-induced cholestasis through inhibition of the hepatocellular bile salt export pump (Bsep) of rat liver. *Gastroenterology* **118**, 422-430
245. Loo, T. W., Bartlett, M. C., and Clarke, D. M. (2006) Transmembrane segment 7 of human P-glycoprotein forms part of the drug-binding pocket. *Biochem. J.* **399**, 351-359
246. Loo, T. W., Bartlett, M. C., and Clarke, D. M. (2006) Transmembrane segment 1 of human P-glycoprotein contributes to the drug-binding pocket. *Biochem. J.* **396**, 537-545
247. Loo, T. W., Bartlett, M. C., and Clarke, D. M. (2007) Suppressor mutations in the transmembrane segments of P-glycoprotein promote maturation of processing mutants and disrupt a subset of drug-binding sites. *J. Biol. Chem.* **282**, 32043-32052
248. Loo, T. W., Bartlett, M. C., and Clarke, D. M. (2003) Methanethiosulfonate derivatives of rhodamine and verapamil activate human P-glycoprotein at different sites. *J. Biol. Chem.* **278**, 50136-50141
249. Loo, T. W., and Clarke, D. M. (2005) Do drug substrates enter the common drug-binding pocket of P-glycoprotein through "gates"? *Biochem. Biophys. Res. Commun.* **329**, 419-422
250. Loo, T. W., and Clarke, D. M. (1997) Identification of residues in the drug-binding site of human P-glycoprotein using a thiol-reactive substrate. *J. Biol. Chem.* **272**, 31945-31948
251. Taguchi, Y., Morishima, M., Komano, T., and Ueda, K. (1997) Amino acid substitutions in the first transmembrane domain (TM1) of P-glycoprotein that alter substrate specificity. *FEBS Lett.* **413**, 142-146
252. Kimura, Y., Kodan, A., Matsuo, M., and Ueda, K. (2007) Cholesterol fill-in model: mechanism for substrate recognition by ABC proteins. *J. Bioenerg. Biomembr.* **39**, 447-452
253. Kimura, Y., Kioka, N., Kato, H., Matsuo, M., and Ueda, K. (2007) Modulation of drug-stimulated ATPase activity of human MDR1/P-glycoprotein by cholesterol. *Biochem. J.* **401**, 597-605
254. Kis, E., Ioja, E., Nagy, T., Szente, L., Heredi-Szabo, K., and Krajcsi, P. (2009) Effect of membrane cholesterol on BSEP/Bsep activity: species specificity studies for substrates and inhibitors. *Drug Metab. Dispos.* **37**, 1878-1886
255. Gayet, L., Dayan, G., Barakat, S., Labialle, S., Michaud, M., Cogne, S., Mazane, A., Coleman, A. W., Rigal, D., and Baggetto, L. G. (2005) Control of P-glycoprotein

- activity by membrane cholesterol amounts and their relation to multidrug resistance in human CEM leukemia cells. *Biochemistry* **44**, 4499-4509
256. Bucher, K., Belli, S., Wunderli-Allenspach, H., and Kramer, S. D. (2007) P-glycoprotein in proteoliposomes with low residual detergent: the effects of cholesterol. *Pharm. Res.* **24**, 1993-2004
257. Tavian, D., Degiorgio, D., Roncaglia, N., Vergani, P., Cameroni, I., Colombo, R., and Coviello, D. A. (2009) A new splicing site mutation of the ABCB4 gene in intrahepatic cholestasis of pregnancy with raised serum gamma-GT. *Dig Liver Dis* **41**, 671-675
258. Dixon, P. H., Weerasekera, N., Linton, K. J., Donaldson, O., Chambers, J., Egginton, E., Weaver, J., Nelson-Piercy, C., de Swiet, M., Warnes, G., Elias, E., Higgins, C. F., Johnston, D. G., McCarthy, M. I., and Williamson, C. (2000) Heterozygous MDR3 missense mutation associated with intrahepatic cholestasis of pregnancy: evidence for a defect in protein trafficking. *Hum. Mol. Genet.* **9**, 1209-1217
259. Gautherot, J., Durand-Schneider, A. M., Delautier, D., Delaunay, J. L., Rada, A., Gabillet, J., Housset, C., Maurice, M., and Ait-Slimane, T. (2012) Effects of cellular, chemical, and pharmacological chaperones on the rescue of a trafficking-defective mutant of the ATP-binding cassette transporter proteins ABCB1/ABCB4. *J. Biol. Chem.* **287**, 5070-5078
260. Ikebuchi, Y., Takada, T., Ito, K., Yoshikado, T., Anzai, N., Kanai, Y., and Suzuki, H. (2009) Receptor for activated C-kinase 1 regulates the cellular localization and function of ABCB4. *Hepatol Res* **39**, 1091-1107
261. Ikebuchi, Y., Ito, K., Takada, T., Anzai, N., Kanai, Y., and Suzuki, H. (2010) Receptor for activated C-kinase 1 regulates the cell surface expression and function of ATP binding cassette G2. *Drug Metab Dispos.* **38**, 2320-2328
262. Auerbach, M., and Liedtke, C. M. (2007) Role of the scaffold protein RACK1 in apical expression of CFTR. *Am J Physiol Cell Physiol* **293**, C294-304
263. Wang, S., Raab, R. W., Schatz, P. J., Guggino, W. B., and Li, M. (1998) Peptide binding consensus of the NHE-RF-PDZ1 domain matches the C-terminal sequence of cystic fibrosis transmembrane conductance regulator (CFTR). *FEBS Lett.* **427**, 103-108
264. Moyer, B. D., Duhaime, M., Shaw, C., Denton, J., Reynolds, D., Karlson, K. H., Pfeiffer, J., Wang, S., Mickle, J. E., Milewski, M., Cutting, G. R., Guggino, W. B., Li, M., and Stanton, B. A. (2000) The PDZ-interacting domain of cystic fibrosis transmembrane conductance regulator is required for functional expression in the apical plasma membrane. *J. Biol. Chem.* **275**, 27069-27074
265. Moyer, B. D., Denton, J., Karlson, K. H., Reynolds, D., Wang, S., Mickle, J. E., Milewski, M., Cutting, G. R., Guggino, W. B., Li, M., and Stanton, B. A. (1999) A PDZ-interacting domain in CFTR is an apical membrane polarization signal. *J. Clin. Invest.* **104**, 1353-1361
266. Hall, R. A., Ostedgaard, L. S., Premont, R. T., Blitzer, J. T., Rahman, N., Welsh, M. J., and Lefkowitz, R. J. (1998) A C-terminal motif found in the beta2-adrenergic receptor, P2Y1 receptor and cystic fibrosis transmembrane conductance regulator determines binding to the Na<sup>+</sup>/H<sup>+</sup> exchanger regulatory factor family of PDZ proteins. *Proc. Natl. Acad. Sci. U. S. A.* **95**, 8496-8501
267. Xue, P., Crum, C. M., and Thibodeau, P. H. (2014) Regulation of ABCC6 trafficking and stability by a conserved C-terminal PDZ-like sequence. *PLoS One* **9**, e97360
268. Hoque, M. T., Conseil, G., and Cole, S. P. (2009) Involvement of NHERF1 in apical membrane localization of MRP4 in polarized kidney cells. *Biochem. Biophys. Res. Commun.* **379**, 60-64

- 
269. Hoque, M. T., and Cole, S. P. (2008) Down-regulation of Na<sup>+</sup>/H<sup>+</sup> exchanger regulatory factor 1 increases expression and function of multidrug resistance protein 4. *Cancer Res.* **68**, 4802-4809
270. Li, M., Wang, W., Soroka, C. J., Mennone, A., Harry, K., Weinman, E. J., and Boyer, J. L. (2010) NHERF-1 binds to Mrp2 and regulates hepatic Mrp2 expression and function. *J. Biol. Chem.* **285**, 19299-19307
271. Wang, W., Soroka, C. J., Mennone, A., Rahner, C., Harry, K., Pypaert, M., and Boyer, J. L. (2006) Radixin is required to maintain apical canalicular membrane structure and function in rat hepatocytes. *Gastroenterology* **131**, 878-884
272. Luciani, F., Molinari, A., Lozupone, F., Calcabrini, A., Lugini, L., Stringaro, A., Puddu, P., Arancia, G., Cianfriglia, M., and Fais, S. (2002) P-glycoprotein-actin association through ERM family proteins: a role in P-glycoprotein function in human cells of lymphoid origin. *Blood* **99**, 641-648
273. Kano, T., Wada, S., Morimoto, K., Kato, Y., and Ogihara, T. (2011) Effect of knockdown of ezrin, radixin, and moesin on P-glycoprotein function in HepG2 cells. *J. Pharm. Sci.* **100**, 5308-5314
274. Yano, K., Tomono, T., Sakai, R., Kano, T., Morimoto, K., Kato, Y., and Ogihara, T. (2013) Contribution of radixin to P-glycoprotein expression and transport activity in mouse small intestine in vivo. *J. Pharm. Sci.* **102**, 2875-2881
275. Kikuchi, S., Hata, M., Fukumoto, K., Yamane, Y., Matsui, T., Tamura, A., Yonemura, S., Yamagishi, H., Keppler, D., and Tsukita, S. (2002) Radixin deficiency causes conjugated hyperbilirubinemia with loss of Mrp2 from bile canalicular membranes. *Nat. Genet.* **31**, 320-325
276. Suda, J., Zhu, L., and Karvar, S. (2011) Phosphorylation of radixin regulates cell polarity and Mrp-2 distribution in hepatocytes. *Am J Physiol Cell Physiol* **300**, C416-424
277. Bretscher, A., Edwards, K., and Fehon, R. G. (2002) ERM proteins and merlin: integrators at the cell cortex. *Nat Rev Mol Cell Biol* **3**, 586-599
278. Algrain, M., Turunen, O., Vaheri, A., Louvard, D., and Arpin, M. (1993) Ezrin contains cytoskeleton and membrane binding domains accounting for its proposed role as a membrane-cytoskeletal linker. *J. Cell Biol.* **120**, 129-139



## 6 Acknowledgment / Danksagung

Lutz: Danke, dass du einem vermittelst, vieles erreichen zu können und auch mal von Cell, Science und Nature zu träumen. Vielen Dank für deinen unglaublichen Optimismus für das Projekt und die großzügigen Möglichkeiten bei meiner Arbeit immer freie Hand zu haben.

Frau PD Dr. med. Verena Keitel-Anselmino möchte ich für die freundliche Übernahme des Korreferats danken. Ich möchte Dr. med. Ralf Kubitz für die erfolgreiche Kooperation innerhalb der klinischen Forschergruppe 217 und des Sonderforschungsbereichs 974 danken.

Sander: Vielen Dank für Dein Bemühen, dass alle vorwärts kommen, deine Anstöße auch mal nachzudenken und dafür, dass du immer ein Ansprechpartner im Institut bist.

PD. Dr. Ulrich Schulte: Danke für die tolle Betreuung während des Biochemie-Studiums.

Iris, du bist nicht nur eine Labor-Kollegin für mich, sondern auch eine liebgewonnene Freundin. Danke für deine Unterstützung, deine Aufmunterungen und den ein oder anderen Anschubser besonders in der Endphase dieser Arbeit.

Britta: Danke, dass Du immer da warst, wenn man Hilfe brauchte, einen Motivationsschub, oder auch einfach eine pragmatische Lösung auch nach deiner Zeit im Institut.

Nils & Philipp, meine Unterstützung beim MDR Meeting. Nils, dich kann ich mit Fug und Recht als konstante Größe in meiner Zeit bei Lutz bezeichnen und ich bin immer wieder beeindruckt, woher Du auf so viele Dinge quasi aus dem Nichts eine Antwort zauberst. Philipp, es hat mir sehr viel Spaß bereitet mit dir auf den Leber ABC-Transportern zu arbeiten, du hast so manche Frustration mit mir geteilt.

Andre, Miro & Christian: Danke für eine tolle Zeit im Büro, für mein erstes Fußballspiel im Stadion, gemeinsames Grillen und das eine oder andere Bier. Auch meinen neuen Büro-Kolleginnen Kerstin, Kalpana, Katharina, Sakshi und Sandra möchte ich danken. Eine bessere Arbeitsatmosphäre hätte ich mir nicht vorstellen können.



Martina, Isa & Ricarda: Danke, für eine sehr schöne Zeit zusammen. Es war eine Freude mit euch zusammen zu Arbeiten. Ich wünsche euch alles Gute für eure Zukunft.

Petra, Patrick, Jan & Nacera: Ich möchte euch herzlich für die Aufnahme in die Arbeitsgruppe danken. Ich habe während meines Studiums und auch danach sehr viel von euch lernen können.

Liebe Katja und Susanne, euch beiden wünsche ich viel Erfolg bei den human Leber ABC Transportern.

Frau Blum & Frau Rasid: vielen Dank dafür, dass sie sich um alles gekümmert haben, mit dem ich am liebsten nichts zu tun haben möchte. Zwar auf ganz unterschiedliche Art und Weise, aber es hat die Arbeit sehr viel entspannter gemacht.

Allen jetzigen Mitarbeiter danke ich für die tolle Atmosphäre, gemeinsamen Kuchen- & Eis-Pausen und die vielen Gespräche: Sven, Michael, Sabrina, Diana, Iris (Leuz), Rakesh, Jens, Marcel, Elenor & Manuel.

**Meiner Familie & meinen Freunden: DANKE!!!**

Diese Arbeit wurde im Rahmen der klinischen Forschergruppe 217 (KFO 217) und des Sonderforschungsbereichs 974 (SFB 974) der Heinrich-Heine Universität Düsseldorf gefördert.

## 7 Curriculum vitae

### Personal Data

---

Date of Birth	9th February 1986 in Neuss, Germany
Nationality	German

### Work Experience

---

since Jan 2011	<b>Ph.D. student</b> at the Institute of Biochemistry with Prof. Dr. Lutz Schmitt, Heinrich Heine University Düsseldorf
March 2006	<b>Internship</b> at SCHWARZ BIOSCIENCE GmbH in the Pharmaceutical Development Group, Monheim am Rhein

### Academic Education

---

Oct 2008 – Aug 2010	Master studies in Biochemistry at the Heinrich Heine University Düsseldorf Degree: <b><i>Master of Science in Biochemistry</i></b>
Oct 2005 – Sep 2008	Bachelor studies in Biochemistry at the Heinrich Heine University Düsseldorf Degree: <b><i>Bachelor of Science in Biochemistry</i></b>

### School Education

---

Aug 1992 – Jul 2005	Elementary and secondary school in Grevenbroich, Germany Degree: Abitur
---------------------	--

### Stipends and Awards

---

Jul 2005	<b>School prize in chemistry</b> of the Entrepreneurship Chemistry Niederrhein e.V.
Oct 2009 – Sep 2010	<b>Stipend of the Dr. Jost Henkel Foundation</b>
Jun 2011	<b>Master prize</b> of the German Society for Biochemistry and Molecular Biology (GBM) e.V.

### Further Training and Commitments

---

since Jan 2011	Member of the graduate school iGRAD
since Oct 2013	Member of the integrated graduate school iGK974 of the CRC974

## List of Publications

---

Mansurova M, Scheercousse P, Simon J, **Kluth M**, Gärtner W. Chromophore exchange in the blue light-sensitive photoreceptor YtvA from *Bacillus subtilis*. *Chembiochem* (2011) 7;12(4):641-6. doi: 10.1002/cbic.201000515.

Ellinger P, **Kluth M**, Przybylla S, Smits SH, Schmitt L. Structure and function of hepatic ABC-transporters. In: Hepatobiliary Transport in Health and Disease (2012) Eds. Häussinger D, Kubitz R, Keitel V), *de Gruyter*, Berlin, 23-41.

Ellinger P<sup>#</sup>, **Kluth M**<sup>#</sup>, Stindt J, Smits SH, Schmitt L. Detergent Screening and Purification of the Human Liver ABC Transporters BSEP (ABCB11) and MDR3 (ABCB4) expressed in the yeast *Pichia pastoris*. *PLoS ONE*. (2013); 8(4):e60620.

**Kluth M**, Döhl K, Ellinger P, Przybylla S, Smits SH, Schmitt L. Identification of new interaction partners of the human ABC transporter MDR3. *Eur. J. Med. Res.* (2014); 19(Suppl 1):S19. doi: 10.1186/2047-783X-19-S1-S19.

**Kluth M**, Stindt J, Dröge C, Linnemann D, Kubitz R, Schmitt L. A mutation within the extended X loop abolished substrate-induced ATPase activity of the human liver ABC Transporter MDR3. *J Biol Chem*. In press.

<sup>#</sup> equally contributed

## **8 Erklärung zur Dissertation**

Ich versichere an Eides Statt, dass die vorliegende Dissertation von mir selbstständig und ohne unzulässige fremde Hilfe unter Beachtung der Grundsätze zur Sicherung guter wissenschaftlicher Praxis an der Heinrich-Heine-Universität Düsseldorf verfasst worden ist. Die Dissertation wurde in der vorgelegten oder in ähnlicher Form noch bei keiner anderen Institution eingereicht. Ich habe bisher keine erfolglosen Promotionsversuche unternommen.

Düsseldorf, den

---

Marianne Kluth